# DIRECT ESTIMATION OF GAS RESERVES

# USING PRODUCTION DATA

A Thesis

by

IBRAHIM MUHAMMAD BUBA

Submitted to the Office of Graduate Studies of
Texas A&M University
in partial fulfillment of the requirements for the degree of

MASTER OF SCIENCE

August 2003

Major Subject: Petroleum Engineering

# DIRECT ESTIMATION OF GAS RESERVES

# USING PRODUCTION DATA

A Thesis

by

IBRAHIM MUHAMMAD BUBA

Submitted to the Office of Graduate Studies of
Texas A&M University
in partial fulfillment of the requirements for the degree of

MASTER OF SCIENCE

Approved as to style and content by:

| | |
|---|---|
| _____ | _____ |
| Thomas A. Blasingame<br>(Chair of Committee) | Daulat D. Mamora<br>(Member) |
| _____ | _____ |
| Robert R. Berg<br>(Member) | Hans C. Juvkam-Wold<br>(Interim Head of Department) |

August 2003

Major Subject: Petroleum Engineering

# ABSTRACT

Direct Estimation of Gas Reserves Using Production Data. (August 2003)
Ibrahim Muhammad Buba, B.Eng., University of Bath (U.K.)
Chair of Advisory Committee: Dr. Thomas A. Blasingame

This thesis presents the development of a semi-analytical technique that can be used to estimate the gas-in-place for volumetric gas reservoirs. This new methodology utilizes plotting functions, plots, extrapolations, etc. — where all analyses are based on the following governing identity:

$$q_g = q_{gi} - \frac{2q_{gi}}{\left[1-\left[\frac{p_{wf}/z_{wf}}{p_i/z_i}\right]^2\right]G}G_p + \frac{q_{gi}}{\left[1-\left[\frac{p_{wf}/z_{wf}}{p_i/z_i}\right]^2\right]G^2}G_p^2$$

The "governing identity" is derived and validated by others for $p_i$<6000 psia. We have reproduced the derivation of this result and we provide validation using numerical simulation for cases where $p_i$>6000 psia.

The relevance of this work is straightforward — using a simple governing relation, we provide a series of plotting functions which can be used to extrapolate or interpret an estimate of gas-in-place — using only production data ($q_g$ and $G_p$). The proposed methodology does not require a prior knowledge of formation and/or fluid compressibility data, nor does it require average reservoir pressure. In fact, no formation or fluid properties are directly required for this analysis and interpretation approach. The new methodology is validated/demonstrated using results from numerical simulation (*i.e.*, cases where we know the exact answer), as well as for a number of field cases.

Perhaps the most valuable component of this work is our development of a "spreadsheet" approach in which we perform multiple analyses/interpretations simultaneously using MS Excel. This allows us to visualize all data plots simultaneously — and to "link" the analyses to a common set of parameters. While this "simultaneous" analysis approach may seem rudimentary (or even obvious), it provides the critical (and necessary) "visualization" that makes the technique functional. The base relation (given above) renders different behavior for different plotting functions, and we must have a "linkage" that forces all analyses to "connect" to one another. The proposed multiplot spreadsheet approach provides just such a connection.

# DEDICATION

*In the Name of Allah, the Most Gracious the Most Merciful.*
*All Praise be to Allah, Cherisher and Sustainer of the Worlds.*
*The Most Gracious, the Most Merciful.*
*Master* (*and only Judge*) *of the Day of Recompense.*
*You alone we worship and You alone we ask for help.*
*Guide us to the Right Path.*
*The path of those on whom You have bestowed Your Grace,*
*not (the path) of those who have earned Your anger,*
*nor those that have gone astray.* (*Noble Qur'an*, 1:1-7*)*
Ameen.

*Allah! None has the right to be worshipped but He, the Ever Living,*
*the One Who sustains and protects all that exists.*
*Neither slumber, nor sleep overtakes Him.*
*To Him belongs whatever is in the heavens and whatever is on earth.*
*Who is he that can intercede with Him except by His Permission?*
*He knows what happens to them* (*His creatures*) *in this world,*
*and what will happen to them in the Hereafter.*
*And they will never compass anything of His Knowledge except that which He wills.*
*His Throne extends over the heavens and the earth,*
*and He feels no fatigue in guarding and preserving them.*
*And He is the Most High, the Most Great.* (*Noble Qur'an,* 2:255)

To my parents, their forbearers, and to those who took the responsibility for their upbringing.

# ACKNOWLEDGEMENTS

I would like to express my sincere gratitude and deepest appreciation to the following:

Dr. Tom Blasingame, chair of my advisory committee — for his valuable guidance, intellectual contributions, his patience and tenacity in helping me bring this research to completion.

Drs. Daulat Mamora and Bob Berg for serving as members of my advisory committee.

Dr. Rosalind Archer for her valuable advice and assistance with my research — you are that shining star in Auckland. I wish you all the best.

Dr. Wayne Ahr for his input during the final examination.

Finally, I want to thank the faculty and staff of the Department of Petroleum Engineering at Texas A&M University and all my colleagues for a memorable experience.

# TABLE OF CONTENTS

Page

# LIST OF FIGURES

FIGURE Page

# LIST OF TABLES

# CHAPTER I
# INTRODUCTION

A primary objective of reservoir engineering is the estimation of the original volume of in-place fluids. Obviously the phase behavior of the fluids (PVT) and the pore space itself govern the storage of in-place fluids. In a traditional sense, the estimation of in-place fluids is based in large part on the concept of a material balance — *i.e.*, a mass balance performed on the reservoir system, which is typically formulated as a volume balance (using appropriate mass references). Such balances include the production, injection, and generation terms (for most applications only the production term is relevant), as well as a fundamental linkage to pressure (as a surrogate for reservoir energy). The proposed work begins with a relationship derived for a volumetric dry gas reservoir system being produced at pseudosteady-state flow conditions. Most importantly, the material balance is rigorously maintained in this solution, although we note that a semi-analytical "flow relation" is used to represent the production rate based on the difference between the flowing wellbore pressure and the average wellbore pressure. This result is an appropriate governing relation — provided that the conditions of its derivation are recognized (most notably, a constant flowing wellbore pressure is assumed and the initial reservoir pressure is presumed to be less than 6000 psia).

At issue is the estimation of gas reserves (*i.e.*, in-place fluids) using minimal data — in our case the rate-time and cumulative production data. It is imperative for operators to generate reasonable estimates of original gas-in-place as early in the life of a reservoir as possible in order to provide economic development and exploitation plans for such reservoirs. We will not address the issue of "early" estimates of gas-in-place, but rather, we will focus on the development and implementation of techniques that clearly identify the volumetric behavior of the gas reservoir system — and in doing so we implicitly address the issue of the appropriate quantity of data (*i.e.,* time duration of production) that is required to obtain an accurate estimate of gas-in-place.

As noted above, this work introduces a new semi-analytical method for the estimation of original gas-in-place for a volumetric gas reservoir where this new approach requires only time and flowrate data (and cumulative production by integration). This approach is <u>independent</u> of the many requirements associated with the material balance techniques currently in use — particularly requirements for reservoir and fluid properties, as well as the requirement of average reservoir pressure. In this thesis we summarize the development, application, and viability of our new method — as well as demonstrate its utility as a mechanism for estimating original gas-in-place.

---

This thesis follows the style of the *SPE Journal*.

### 1.1 Research Problem

The methods presently used for the estimation of original gas-in-place for a volumetric dry-gas reservoir may require prior knowledge of formation, well, and fluid properties which can be inaccurate — and these requirements may cause a particular technique to yield erroneous results. Additional data which are typically required, *a priori* include: statistical averages or approximations of reservoir properties (*e.g.*, porosity, net pay thickness, permeability), as well as estimates of these properties based on correlations, analogs, etc. Such data often include inconsistencies and uncertainties, which will amplify inadvertent errors associated with the estimation of original gas-in-place.

The challenge of such analyses is to provide a simple analysis — *e.g.*, an extrapolation function where the gas-in-place is determined as the *x*- or *y*-intercept of a particular plot or other such simple graphical analyses. However, such analyses should be as rigorous as possible, without requiring data beyond that of the plotting functions. For instance, the familiar material balance plot of $(\overline{p}/\overline{z})$ versus $G_p$ matches our criteria — but, we cannot (and do not) presume the availability of average pressure data $(\overline{p})$ in this work.

Our goal is to develop plotting functions which form a linear trend from which we can estimate the gas-in-place. We will impose that these functions use only $q_g$-$G_p$ data, and by manipulation of the algebraic model, we develop "linear" plotting functions (*i.e.*, functions which when plotted on a Cartesian axis yield a straight-line trend). We expect that such functions would not distort the character of the data, and that any/all analyses revert to a linear form ($y=ax+b$). As an example, the exponential and hyperbolic rate decline models can be written as linear forms — but, as in the case of the hyperbolic decline case, the derivative of the rate function is required as a data function in the linearization of the plotting function and we note that the derivative of production data is generally far too distorted to be of any practical use.

Another issue to be considered is the typical requirement of fluid properties, well, and reservoir parameters for production data analysis. Such parameters may be dynamic (*i.e.*, continuously changing with reservoir pressure), while other parameters remain constant throughout the producing life of the reservoir (*e.g.*, porosity, net pay thickness, etc.). The difficulty with production data analysis methods which require dynamic properties is that reservoir pressure must be incorporated into the analysis approach (which is at best tedious and at worst impossible). Not only are the associated calculations tedious, but since it is very rare that we would have access to regular estimates of average reservoir pressure (and flowing well pressures), such methods may not be well-suited for general use. We will note that all of our efforts deal with a single well in a closed reservoir — multiwell cases would compound the data requirements.

As we have discussed the problems associated with current methods for estimating gas-in-place, let us now reflect on what we expect as the products of this work — specifically, plotting function(s) which predict an estimate of gas-in-place as the intercept of a particular plot.

### 1.2 Objectives

The objectives of the research being proposed are:

- Development of a novel technique for the direct estimation of the reserves ($G$) for a volumetric dry-gas reservoir using only production data. Specifically, we use the quadratic $q_g$ — $G_p$ model and its auxiliary relations in order to develop a variety of data plotting functions.
- Development of a "rate-cumulative production" decline type curve based on the quadratic $q_g$ — $G_p$ model. This type curve approach is used to orient and verify our primary analysis of rate-cumulative production data based on plotting functions derived from the quadratic $q_g$ — $G_p$ model.

### 1.3 Deliverables

The expected deliverables of the research are:

- Presentation of a straightforward technique for the estimation of ultimate recovery of normally pressured dry-gas reservoirs using a relation derived via combination of the pseudosteady-state gas flow equation and the gas material balance expression. The solution to this problem will be obtained graphically, as the result of a specialized plotting function. Several different plotting functions may evolve from this work.
- Verification/comparison of our new method(s) for estimating gas reserves using only production data with existing methods. Such verification will assess the accuracy and reliability of the new methods relative to existing methods for production data analysis.
- A thorough evaluation/examination of the proposed methods using both field and numerical simulation data.

### 1.4 Summary of Results

This report presents semi-analytical techniques for the estimation of gas reserves that is both accurate and robust. This new approach was verified using synthetic data of varying initial reservoir pressures and varying flowing bottomhole pressures. Our validation using synthetic data was extended using field production data both from the petroleum literature and industrial case histories.

In this work we present methods which utilize only production data as the input for estimating the original gas-in-place for a volumetric dry gas reservoir. In particular, we present several plotting functions which are developed from the quadratic rate-cumulative production relation and plotted on the vertical axis of a Cartesian plot with the cumulative gas production plotted on the horizontal axis. For reference, the "quadratic rate-cumulative production" relation is given by: (derived from results in ref. 1)

$$q_g = q_{gi} - \frac{2q_{gi}}{\left[1-\left[\frac{p_{wf}/z_{wf}}{p_i/z_i}\right]^2\right]G}G_p + \frac{q_{gi}}{\left[1-\left[\frac{p_{wf}/z_{wf}}{p_i/z_i}\right]^2\right]G^2}G_p^2 \quad \text{.....(1.1)}$$

Using a "shorthand" notation for Eq. 1.1, we have:

$$q_g = q_{gi} - D_i G_p + \frac{1}{2}\frac{D_i}{G} G_p^{\,2} \quad \text{.....(1.2)}$$

Where the "decline constant" ($D_i$) for the gas case is defined as follows:

$$D_i = \frac{2q_{gi}}{\left[1 - \left[\frac{p_{wf}/z_{wf}}{p_i/z_i}\right]^2\right] G} \quad \text{.....(1.3)}$$

Eq. 1.1 serves as the starting point for our work — in particular, we utilize this base relation to define a family of auxiliary functions, as well as to generate plotting functions for data analysis.

For convenience, we further "lump" the $(p_{wf}/z_{wf})/(p_i/z_i)$ term (in Eqs. 1.1 and 1.3) into a single variable ($p_{wD}$) as follows:

$$p_{wD} = \left[\frac{p_{wf}/z_{wf}}{p_i/z_i}\right] \quad \text{.....(1.4)}$$

Where Eq. 1.3 becomes:

$$D_i = \frac{2q_{gi}}{(1 - p_{wD}^{\,2})\, G} \quad \text{.....(1.5)}$$

For the purposes of our work, one of the most important aspects of Eq. 1.2 is to recognize that we can reduce this relation to 3 distinct parameters ($q_{gi}$, $D_i$, and $G$) — although we note that we have implemented the analysis sequence using the variables $q_{gi}$, $D_i$, and $p_{wD}$ ($G$ is calculated with Eq. 1.5 using the current estimates of the $q_{gi}$, $D_i$, and $p_{wD}$ parameters). This approach (*i.e.*, using Eqs. 1.2 and 1.5 with variable estimates of the $q_{gi}$, $D_i$, and $p_{wD}$ parameters) allows us to compare our results (*i.e.*, $G$) against other analyses (*e.g.*, material balance, simplified decline curves and decline type curves).

The viability of our new methodology was assessed and validated using results from numerical simulation — where the reservoir model was chosen to represent a single layer dry gas reservoir. The analysis methodology was also demonstrated using production data from the petroleum literature, as well as a number of field data cases obtained from industry sources. In all field cases the new methodology was shown to yield results comparable to other methods (*i.e.*, material balance, simplified decline curves and decline type curves) — and the new approach was also found to be generally more "error tolerant" than the other techniques. We will give the caveat that our analysis had the benefit of being implemented as a "spreadsheet," so all analysis plots were linked, and the analyses were performed simultaneously across all plots (*e.g.*, the quadratic plots (2), the extrapolation plotting function graphs (3), the rate-time plot (1), and the proposed "rate-cumulative" decline type curves (2) — which yields 8 (eight) plots/analyses being performed simultaneously).

The limitations of the new methods are analyzed critically (particularly the requirements of a constant bottomhole flowing pressure and an initial reservoir pressure less than 6000 psia). and practical considerations associated with field and reservoir conditions are discussed to ensure that the proposed methods are properly applied to field data. We will comment that we found no significant limitations with regard to the bottomhole flowing pressure nor the initial reservoir pressure — it appears that methodology is tolerant of significant violations with regard to these presumed conditions.

**1.5 Outline of Thesis**

The outline of the proposed research thesis is as follows:

- Chapter I — Introduction
  - Research problem
  - Research objectives
  - Summary of results
- Chapter II — Literature Review
  - Material balance methods
  - Decline curve analysis
  - Semi-analytical methods
- Chapter III — Development of The New Semi-Analytical Method for The Analysis of Production Data From Gas Wells
  - Development of the "rate-cumulative production" relation
  - Development of analysis methods using the "rate-cumulative production" relation
  - Validation using synthetic data
- Chapter IV — Field Applications of The New Semi-Analytical Method for The Analysis of Production Data From Gas Wells
  - Field examples — petroleum literature and industry sources
  - Practical considerations — guidelines for applications
  - Closure — limitations of the new methodology
- Chapter V — Summary, Conclusions, and Recommendations for Future Work
  - Summary
  - Conclusions
  - Recommendations for future work
- Nomenclature
- References
- Appendices
  - Appendix A — Analysis of Simulated Well Performance Cases
  - Appendix B — Analysis of Field Examples obtained from the Petroleum Literature and Industry Sources
  - Appendix C — Derivation of the "Quadratic" Plotting Functions for the Analysis of Production Data

# CHAPTER II
# LITERATURE REVIEW

Using currently accepted methods for analysis, the estimation of original gas-in-place may require several iterations and/or secondary calculations, as well as other reservoir or well parameters. These methods can be time consuming, tedious, and are susceptible to errors — for example, an incorrect value of any of the primary parameters will propagate the errors in the sequence of calculations. As mentioned earlier, this research presents a direct method for the estimation of original gas-in-place for the case of a volumetric dry gas reservoir using only rate-time (and rate-cumulative) data. This new approach significantly reduces the secondary calculations requirements and iterations. The proposed methods require minimal data — however, the characteristic behavior of pseudosteady-state (or boundary-dominated flow) must be exhibited.

The reserve estimation methods discussed in this section are primarily those methods typically applied to volumetric dry-gas reservoirs. In such cases gas expansion is the only drive mechanism — no external source(s) of energy are considered. All of these methods (including our own) presume that the entire reservoir is being characterized by performance from a single well — which is obviously not the case. However, in the case of moderate to low permeability reservoirs we can analyze data on a "per well" basis as each well drains its own particular volume, and does not interfere with other wells in the system. This is probably the most limiting assumption in general for the analysis of well performance data, but we recognize that violations of this assumption are generally observed as "leakage" or loss of performance in one or more wells when another well is put on production.

## 2.1 Material Balance Methods

The material balance method was developed after the volumetric method (i.e., estimates base on porosity, thickness, areal extent) and material balance has evolved to become the most popular mechanism for estimating reserves. In 1941, Schilthius[1,2] presented a general form of material balance equation derived using a volumetric balance (as a surrogate for a mass balance) on a hydrocarbon fluid system. Material balances typically assume that the reservoir pore volume remains unchanged or it changes in a consistent manner with respect to reservoir pressure. The data required for material balance calculations include: fluid production data, reservoir temperature, reservoir pressure data, reservoir fluid properties, and core data. The material balance equation for a volumetric dry gas reservoir system presented by Schilthius (which neglects water drive and interstitial water production) is given as

$$GB_{gi} = (G - G_p)B_g \quad \text{.....(2.1)}$$

Where $GB_{gi}$ is the reservoir volume occupied by gas at the initial reservoir pressure, $p_i$, and, on the right hand side, $(G\text{-}G_p)\ B_g$ is the reservoir volume occupied by gas after gas production at any pressure below the initial pressure. Schilthius used the principle of conservation of mass to calculate remaining gas-in-place. In volumetric terms, the statement of the material balance equation is that remaining reserves are the initial reserves less the produced reserves[3]. In this case, the simplest form of the material balance equa-tion for a volumetric dry-gas reservoir is

Initial Volume = Volume Remaining + Volume Removed .....(2.2)

The material balance equation was simplified and represented graphically and, in particular, a plot of $\overline{p}/\overline{z}$ versus $G_p$ will yield a straight-line trend requiring only an extrapolation of the $\overline{p}/\overline{z}$ trend to the $G_p$-axis, which yields the estimated ultimate gas produced, or the gas reserves. This relation is given by:

$$\frac{p}{z}=\frac{p_i}{z_i}\left[1-\frac{G_p}{G}\right]=\frac{p_i}{z_i}-\frac{p_i}{z_i G}G_p \quad \text{.....(2.3)}$$

The material balance method can be applied for production at constant rate or constant bottomhole flowing pressure — or any variable-rate/variable-pressure condition. An advantage of the $\overline{p}/\overline{z}$ versus $G_p$ plot is that it can be applied at any period of reservoir development. Most importantly, the material balance method gives a good estimate of recoverable gas-in-place as it reports on only the volumes which are in pressure communication. We note that material balance methods are developed in terms of cumulative fluid production and changes in reservoir pressure, and therefore require accurate measurements of both quantities.

The material balance plot (*i.e.*, the $\overline{p}/\overline{z}$ versus $G_p$ plot) has historically been used to provide an indication of the reservoir drive mechanism from the shape of the $\overline{p}/\overline{z}$ trend. A consistent deviation of data from the straight line trend can indicate external source(s) of energy or a secondary drive mechanism. We note that this is not an objective of the present work, and we will not address cases other than the case of a volumetric dry gas reservoir system.

It is important to note that material balance methods require a sufficient duration of the production history in order to yield accurate results — typically 10 percent of the estimated reserves must be produced to provide a reliable estimate of gas reserves. Due to the sensitivity of the material balance methods to both data quantity and quality, one may rely on the volumetric method for reserve estimation in the early stages of production, and then use the material balance methods to refine the reserves estimation when sufficient data are available.

The complexity associated with the material balance method for reserve estimation is linked to the availability of average and initial reservoir pressure data. Recall that the pressure dependent parameters in the material balance equation are evaluated at the average reservoir pressure. The average reservoir

pressure remains the reference point for all parameters throughout the producing life of the reservoir; and therefore its importance in the material balance method cannot be overstated.

In obtaining the average reservoir pressure estimates, most operators use a pressure build-up test which can be costly, particularly for tight (or low permeability) gas reservoirs. Pressure build-up tests for gas wells require long-shut-in periods for the reservoir pressure profile to stabilize. This practice is simply uneconomical for many low permeability reservoirs. Sullivan, *et al.*[4] present a technique that uses short-term pressure build-up tests for tight gas reservoirs as a mechanism for estimating average reservoir pressures and presented an extrapolation technique for the non-stabilized data points shown on the $\overline{p}/\overline{z}$ versus $G_p$ plot.

**2.2 Decline Curve Analysis**

The analysis of production decline curve data can provide estimates of original gas-in-place, gas reserves, drainage area, future expected production rate and the remaining productive life of the well. As with other methods, the decline curve technique is dependent on the quantity and quality of data. The basis for the decline curve methods vary from empirical relations (*e.g.*, the exponential and hyperbolic relations) to semi-analytical relations derived using material balance and pseudosteady-state flow relations. The calculated reserves are considered to be the hydrocarbons in communication with a particular producing well.

The use of production data as a forecasting tool dates back to 1918 when Lewis and Beal[5] presented the consistent shape of the production decline curve as a mathematical tool which may be used to forecast future production. Lewis and Beal observed that the production decline on a Cartesian plot of rate against time has a "power law" behavior (actually a straight-line trend on a log-log plot), and using the model trend or the calculated coefficients, a forecast of future production can be projected.

Production data analysis became a popular reserve forecasting tool in the 1940's when Arps[6] presented his harmonic, exponential, and hyperbolic decline relations (each of which where empirically based). This technique, developed by Arps, although well received in the industry, was used only for prediction and interpretation of production rate decline — not for the estimation of in-place fluid reserves or formation properties.

Arps[7] later expanded the use of decline curve analysis to provide the prediction of primary reserves. This approach involved the extrapolation of rate-time data using hyperbolic and exponential decline data models. For reference, the Arps relations for flowrate and cumulative production are given in table 2.1 below

**Table 2.1 – Summary of the "Arps Analysis" relations.**

*Arps Flowrate Relations*:

| Case | Rate Relation |
|---|---|
| *Exponential*: ($b$=0) | $q(t) = q_i \exp(-D_{Arps} t)$ ..... (2.4) |
| *Hyperbolic*: (0<$b$<1) | $q(t) = \dfrac{q_i}{\left[1 + bD_{Arps} t\right]^{\frac{1}{b}}}$ ..... (2.5) |
| *Harmonic*: ($b$=1) | $q(t) = \dfrac{q_i}{\left[1 + D_{Arps} t\right]}$ ..... (2.6) |

*Arps Cumulative Production Relations*:

| Case | Cumulative Relation |
|---|---|
| *Exponential*: ($b$=0) | $N_p(t) = \dfrac{q_i}{D_{Arps}} \left[1 - \exp(-D_{Arps} t)\right]$ ..... (2.7) |
| *Hyperbolic*: (0<$b$<1) | $N_p(t) = \dfrac{q_i}{(1-b) D_{Arps}} \left[1 - (1 + bD_{Arps}\, t)^{1 - 1/b}\right]$ ..... (2.8) |
| *Harmonic*: ($b$=1) | $N_p(t) = \dfrac{q_i}{D_{Arps}} \ln(1 + D_{Arps}\, t)$ ..... (2.9) |

And we also reference Arps' observations regarding the "decline curve exponent," $b$ — for solution gas-drive reservoir systems:

- $b = 0$ — Reservoir is highly undersaturated.
- $b = 0$ — Dominant producing mechanism is due to gravity drainage and no free surface.
- $b = 0.5$ — Gravity drainage with free surface.
- $b = 0.667$ — Solution gas-drive reservoir, when average reservoir pressure, $\bar{p}$ *versus* cumulative oil, $N_p$ is linear.
- $b = 0.333$ — Solution gas-drive reservoir, when average reservoir pressure squared, $\bar{p}^2$ *versus* cumulative oil, $N_p$ is linear.

We do not confirm nor endorse the "Arps conditions" given above, we simply provide these comments from Arps as a guide for those readers who may be curious as to the physical condition represented by the decline curve exponent ($b$).

In the early 1970's Fetkovich[7] proposed a substantial improvement in decline curve analysis by suggesting the matching production data onto specialized "type curves" (analogous to the analysis of well test data). Fetkovich[7] presented the "unified" exponential decline type curve (which is the analytical solution for the case of a single well in a bounded symmetric reservoir) and coupled this data with the with Arps[6] hyperbolic rate relations (given in terms of specialized dimensionless rate and time function) to create what has become know as the "Fetkovich Decline Type Curve" (or simply the "Fetkovich Type Curve"). The Fetkovich type curve is the most familiar and widely accepted type curve for the analysis of production data.

Regarding the hyperbolic "stems" on the Fetkovich type curve, these trends are thought to account for "non-ideal" reservoir behavior such as: changes in mobility, reservoir heterogeneity and layering — but we note that even thirty years later, the hyperbolic stems remain largely attributed to "unknown" mechanisms (*i.e.*, whatever phenomena cause "hyperbolic" behavior in production data remain more or less unknown in the context of reservoir and fluid properties). We also note that the "early time" portion of the Fetkovich decline type curve is utilized much the same as type curve analysis for well test data (as we would suspect, as these are also transient performance data). We will comment that the analysis of early time production data using the Fetkovich decline type curve is often problematic — the quantity and quality of these data may prevent a unique analysis from being achieved.

Fetkovich and coworkers[7,8] combined the appropriate material balance and pseudosteady-state flowrate equations to develop explicit rate-time decline equations for single-phase flow behavior in both oil and gas reservoir systems. This work was seen as a theoretical attempt to justify the Arps empirical equations which Fetkovich had used as the foundation to develop the unified type-curves. Our only comment is that the result that Fetkovich proposed in ref. 7 for the rate-time behavior of a gas reservoir system is generally not accurate for long periods of time (if at all).

Fetkovich *et al*[8] advise that reservoir volume and volume-related flow characteristics should not be estimated using decline type curve analyses prior to the full development of boundary dominated flow behavior. . The reported use of decline curve analyses on several field cases in ref. 8 illustrates the versatility and utility of the decline type curve analysis concept.

Al-Hussainy, *et al.*[9] presented a new mechanism for addressing the effects of pressure-dependent gas properties. The new concept was that of a "pseudopressure" as a variable that could be used to partially linearize the gas diffusivity equation. The definition of pseudopressure as given by the authors is

$$m(p) = 2\int_{p_{base}}^{p} \frac{p}{\mu_g(p)\, z(p)} dp \qquad \text{.....(2.10)}$$

The first comprehensive attempt to linearize entire the gas flow equation was by Agarwal.[10] Agarwal presented a pseudotime function for a real gas that incorporates changes in gas viscosity and total compressibility as a function of time. The pseudotime function as proposed by Agarwal is given as

$$t_a(t) = \int_0^t \frac{1}{\mu_g(p)\, c_t(p)}\, dt \qquad \text{.....(2.11)}$$

Another type curve solution for analysis of gas flow systems was presented by Carter[11] who correlated the case of a gas well produced at a constant bottomhole pressure using specialized dimensionless variables. As expected, this type curve clearly exhibits the influence of the pressure drawdown (*i.e.*, $p_i$-$p_{wf}$) on the gas

flowrate behavior. In theory, the "Carter type curve" addresses the issue of the compressibility-viscosity product (as a function of the average reservoir pressure) — however, we must note that the controlling factor on the Carter formulation is the assumption of the constant bottomhole pressure condition.

Carter used a the $\lambda$-variable to reflect the magnitude of pressure drawdown and the influence of pressure drawdown on the compressibility-gas viscosity product. For example, the $\lambda$=1 case corresponds to the exponential decline curve exponent (*i.e.*, $b$=0) — that is, the equivalent liquid case. Large pressure drawdown cases yield $\lambda$-values as low as 0.75 (or lower). As noted, the Carter type curve was developed as a solution to boundary dominated radial gas flow equations for production at constant bottomhole pressure — where these conditions make the Carter type curve the appropriate choice for the estimation of gas well reserves (for the case of gas flowrate-time analysis). The Carter $\lambda$-variable is given as:

$$\lambda = \frac{\mu_{gi} c_{ti}}{\mu_g c_t} \quad \text{.....(2.12)}$$

The Fetkovich decline type curve with all its innovation in the improvement of production data analyses is not without its limitations. Doublet, *et al.*[12] reported the limitations of Fetkovich decline type curve analysis are largely due to non-compatibility with field operations and reservoir inconsistencies that distort the production data (in particular, the variable rate/pressure histories common in practice as well as the analysis of gas reservoir systems). These issues are significantly and often render the original "Fetkovich" analysis approach untenable.

Another issue associated with the Fetkovich decline type curve approach is the oversimplification of the gas flow solution. The (liquid) solution presented by Fetkovich is only applicable for gas flow cases during transient flow and for (very) small pressure drawdowns. These small drawdowns assume gas properties remain constant or change only slightly with changing pressures. For large drawdown cases the liquid case can not be used to represent the gas flow case.

The pseudopressure and pseudotime functions are shown to linearize[13] the gas diffusivity equation and thus, permit us to use liquid flow solutions as a basis (*e.g.*, the Fetkovich type curve) for the analyses of gas production data — provided that the pseudopressure and pseudotime functions are appropriately defined and computed for the case of boundary-dominated gas flow behavior.

In 1987, Fraim and Wattenbarger[14] modified the Agarwal definition of the pseudotime function to yield a "normalized" formulation and proposed to use this form to account for the non-linear product of total compressibility and gas viscosity using the average reservoir pressure as the reference pressure in the pseudotime integral. The normalized pseudopressure and pseudotime functions are shown to linearize[14] the gas diffusivity equation (*i.e.*, create an "equivalent liquid" response) — and, as such, allows for the use of liquid flow solutions for the analyses of gas production data. Although the Fraim and Wattenbarger

pseudopressure and pseudotime formulations can be directly incorporated into decline type curve analysis, we still require estimates of the average reservoir pressure to compute the normalized pseudotime function. The Fraim and Wattenbarger approach provides a direct mechanism to address the variation in pressure dependent properties for the gas flow case — however, this approach does not address the variable-rate/pressure-drop case.

Blasingame and Lee[15] introduced a new concept for addressing the issue of variable-rate and variable pressure production data — in particular, how to analyze such data to provide estimates of drainage area and reservoir shape. This work was not applied to type curve matching — however, it was clear from the conclusions that the proposed concepts would be useful in decline curve analysis.

In 1993, Palacio and Blasingame[16] proposed a rigorous approach for the analysis of variable-rate and variable bottomhole pressure data using a modified pseudotime function (where this result was a combination of the Fraim and Wattenbarger pseudotime relation (for gas) and the Blasingame and Lee variable-rate/variable pressure drop relation. The approach was both straightforward and stable, and was a significant improvement over work presented by McCray, *et al.*[17] — where the objective of McCray, *et al.* was to establish a constant pressure production analog. As such, Palacio and Blasingame proposed a constant rate analog where $q_g/\Delta p_p$ data were plotted against a pseudotime function, and, based on theory, the data trend was matched onto the Arps harmonic stem ($b$=1) on the Fetkovich decline type curve.

In 1995, Callard and Scheneweck[18] presented a simplified approach for well performance using a "combined type curve" analysis. Callard and Scheneweck provided a method for the pressure normalization of cumulative production in decline curve analysis. Variations in the bottomhole flowing pressures were addressed by dividing the cumulative production by the pressure difference between initial and bottomhole pressures

In 1998 Agarwal, *et al*.[19] presented a combined package of decline type curve analysis using the work of Palacio and Blasingame (ref. 16), Carter (ref. 11), and Cullard and Scheneweck (ref. 18). Agarwal, *et al*. also presented a "Rate-Cumulative Production Decline Type Curve" which is a plot of normalized gas flowrate as a function of cumulative production. The proposed type curve approach is a more robust version of the Cullard-Scheneweck work (ref. 18) and Agarwal, *et al*. used this method to estimate gas-in-place and to differentiate between transient and pseudosteady-state flow behavior. Another contribution of this work is the "Cumulative Production-Time Decline Type Curve" created for both radial and vertically fractured wells — where this is seen as an extension to the earlier work by Cullard and Scheneweck.

**2.3 Semi-Analytical Methods**

The concept of using rate versus cumulative production to forecast future production has been revisited a number of times since Lewis and Beal[5] proposed such a forecast in 1918. The popularity of this and other

semi-analytical approaches has grown steadily along with decline type curve analysis, particularly in recent years. A semi-analytical method is typically derived from a combination of the pseudosteady-state flow equation and the material balance equation for a particular case. Generally speaking, one should not "cheat" or "adjust" the material balance equation in the combining process as this makes the final result less accurate (and sometimes unpredictable). It is also worth making a general comments that semi-analytical techniques are limited to the analysis of production data experiencing boundary-dominated (or pseudosteady-state flow conditions).

In 1935, Rawlins and Schellhardt[20] presented an empirical result for relating gas flowrate and flowing bottomhole pressure that is most frequently used in deliverability test analysis. This empirical gas flow result is given by:

$$q_g = C(\bar{p}^{\,2} - p_{wf}^{\,2})^n \quad \text{.....(2.13)}$$

We do note that a similar form as Eq. 2.13 (for $n$=1) can be derived using Darcy's law (steady-state relation) and the assumption that the $\mu_g z$-product is constant — but we are quick to comment that the form of the result is similar, but does not necessarily have the same terms which are in Eq. 2.13. In fact, Eq. 2.13 (again, for $n$=1) can be derived for pseudosteady-state flow conditions, but this is more by analogy than direct derivation. Using the normalized pseudopressure, we can derive the pseudosteady-state form of Eq. 2.13 (again, for $n$=1) — this result is given by:

$$q_g = C(p_p(\bar{p}) - p_p(p_{wf}))^n \quad \text{.....(2.14)}$$

A semi-analytical approach for the analysis of production data from a solution gas-drive oil reservoir system at pressures above the bubblepoint is derived by using a rigorous coupling of the material balance equation and the pseudosteady-state flow equation. Doublet, *et al.*[12] present the following general result:

$$\frac{(p_i - p_{wf})}{q} = b_{pss} + \frac{1}{N c_t}\frac{B_o}{B_{oi}}\frac{N_p}{q} \qquad (\Delta p/q \text{ versus } N_p/q) \quad \text{.....(2.15)}$$

And, assuming a <u>constant</u> bottomhole flowing pressure, $p_{wf}$, we have:

$$q = \frac{1}{b_{pss}}(p_i - p_{wf}) - \frac{1}{N c_t}\frac{B_o}{B_{oi}}\frac{1}{b_{pss}}N_p \quad (q \text{ versus } N_p \ (p_{wf} \text{ is constant})) \quad \text{.....(2.16)}$$

Or, assuming a <u>variable</u> bottomhole flowing pressure, $p_{wf}$, we have:

$$\frac{q}{(p_i - p_{wf})} = \frac{1}{b_{pss}} - \frac{1}{N c_t}\frac{B_o}{B_{oi}}\frac{1}{b_{pss}}\frac{N_p}{(p_i - p_{wf})} \qquad (q/\Delta p \text{ versus } N_p/\Delta p \text{ (variable } p_{wf} \text{ result)}) \quad \text{.....(2.17)}$$

Eqs. 2.15-2.17 can be used to estimate the oil-in-place, $N$, and Eqs. 2.16 can be used to estimate the recoverable oil (or oil reserves), $N_{p,max}$, by extrapolation to $q$=0. Eq. 2.15 is the most versatile relation for the general case of variable-rate/variable pressure drop production (we note that Eq. 2.17 is an auxiliary relation, but it is unlikely that this will evolve into as popular a form as that given by Eq. 2.15).

Knowles[1] and Ansah, *et al*.[21] present new approaches for developing linearized (or semi-analytical) gas flow equations using the rigorous gas material balance relation and an approximate gas flow relation (*i.e.*, the pseudosteady-state flow equation). Specifically, Knowles introduced a linearization scheme in the form of a first order polynomial function. This resulted in the need for a gas flow relation in terms of $(\overline{p}/\overline{z})^2$ — as we noted, this is an approximation — but generally a very accurate formulation (particularly for $p_i$<6000 psia). Ansah, *et al*. provide additional formulations (including details for the original Knowles formulation) — however, it is the Knowles rate-cumulative result that is of primary relevance to the present work and this is the topic of our focus (see relations below).

*Knowles "Pressure" Result*:

$$\frac{\overline{p}/\overline{z}}{p_i/z_i}=\frac{p_{wf}/z_{wf}}{p_i/z_i}\frac{\left[1+\frac{\left[1-\frac{p_{wf}/z_{wf}}{p_i/z_i}\right]}{\left[1+\frac{p_{wf}/z_{wf}}{p_i/z_i}\right]}\exp\left[-\frac{2q_{gi}}{G}\frac{p_{wf}/z_{wf}}{p_i/z_i}\frac{1}{\left[1-\left[\frac{p_{wf}/z_{wf}}{p_i/z_i}\right]^2\right]}t\right]\right]}{\left[1-\frac{\left[1-\frac{p_{wf}/z_{wf}}{p_i/z_i}\right]}{\left[1+\frac{p_{wf}/z_{wf}}{p_i/z_i}\right]}\exp\left[-\frac{2q_{gi}}{G}\frac{p_{wf}/z_{wf}}{p_i/z_i}\frac{1}{\left[1-\left[\frac{p_{wf}/z_{wf}}{p_i/z_i}\right]^2\right]}t\right]\right]} \quad \text{..... (2.18)}$$

*Knowles "Rate" Result*:

$$q_g(t)=q_{gi}\frac{\left[\frac{p_{wf}/z_{wf}}{p_i/z_i}\right]^2}{\left[1-\left[\frac{p_{wf}/z_{wf}}{p_i/z_i}\right]^2\right]}\left[\left[\frac{1+\frac{\left[1-\frac{p_{wf}/z_{wf}}{p_i/z_i}\right]}{\left[1+\frac{p_{wf}/z_{wf}}{p_i/z_i}\right]}\exp\left[-\frac{2q_{gi}}{G}\frac{p_{wf}/z_{wf}}{p_i/z_i}\frac{1}{\left[1-\left[\frac{p_{wf}/z_{wf}}{p_i/z_i}\right]^2\right]}t\right]}{1-\frac{\left[1-\frac{p_{wf}/z_{wf}}{p_i/z_i}\right]}{\left[1+\frac{p_{wf}/z_{wf}}{p_i/z_i}\right]}\exp\left[-\frac{2q_{gi}}{G}\frac{p_{wf}/z_{wf}}{p_i/z_i}\frac{1}{\left[1-\left[\frac{p_{wf}/z_{wf}}{p_i/z_i}\right]^2\right]}t\right]}\right]^2-1\right] \quad \text{....(2.19)}$$

*Knowles "Rate-Cumulative" Result*:

$$q_g = q_{gi} - \frac{2q_{gi}}{\left[1-\left[\frac{p_{wf}/z_{wf}}{p_i/z_i}\right]^2\right]G}G_p + \frac{q_{gi}}{\left[1-\left[\frac{p_{wf}/z_{wf}}{p_i/z_i}\right]^2\right]G^2}G_p^2 \quad \text{.....(1.1)}$$

We note that, other that to generate our base relation (*i.e.*, Eq. 1.1), Eqs. 2.18 and 2.19 are only used in the spreadsheet analysis implementation of this work, we have not attempted to use these results for "direct" analysis (*i.e.*, a straight-line trend or some other graphical analysis technique). We note that Eq. 1.1 is obtained using Eqs. 2.18 and 2.19, and is an expression which is independent of reservoir parameters, average reservoir pressure, etc. In addition, the simple form presented by Eq. 1.1 yields the basis for a sequence of auxiliary functions and graphical plotting functions.

Application techniques for the quadratic gas rate model have been developed and successfully applied to both synthetic and field data.[22] We will also present a detailed validation of these relations and their utility as mechanisms for the analysis of production data obtained from gas wells.

# CHAPTER III
# DEVELOPMENT OF THE NEW SEMI-ANALYTICAL METHOD FOR THE ANALYSIS OF PRODUCTION DATA FROM GAS WELLS

In this chapter we present the development of the "quadratic cumulative production relation" and the corresponding linearized "quadratic" plotting functions. For orientation to the graphical nature of Eq. 1 we consider a Cartesian plot of gas production rate ($q_g$) versus cumulative gas production ($G_p$) — see **Fig. 3.1** (below):

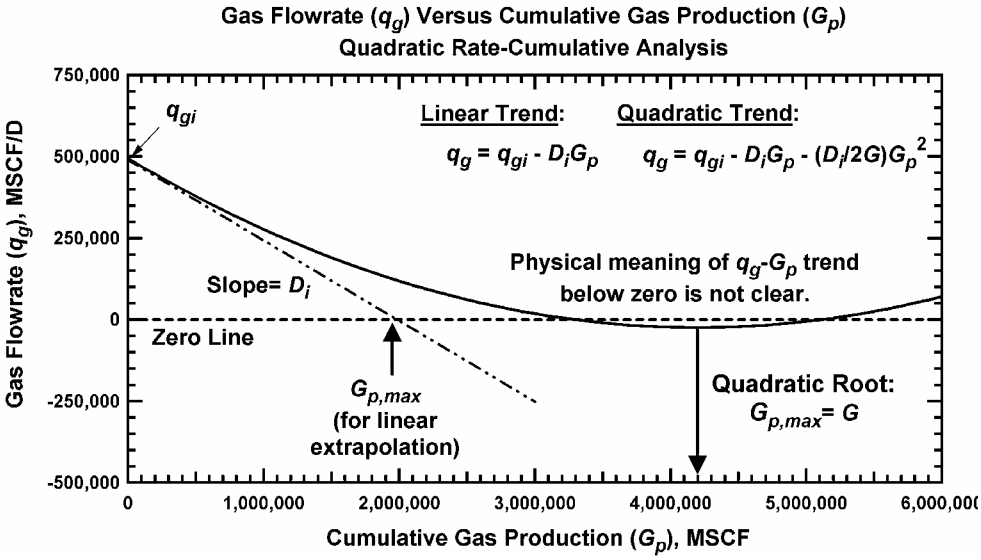


**Figure 3.1 – Schematic Behavior: $q_g$ versus $G_p$ (introductory plot).**

From **Fig. 3.1** we note that the $q_g$-$G_p$ profile does have an apparent linear regime (analogous to the liquid case), but then the trend deviates from the apparent linear trend in a quadratic fashion and actually *increases* at large values of cumulative gas production. It is straightforward to prove that the minimum point in the $q_g$-$G_p$ profile (i.e., the root) is actually the gas-in-place ($G$). What is not clear from **Fig. 3.1** is how one would actually estimate the gas-in-place using a data plot (which would obviously not trend to below zero and "curl" back up. This is a point for consideration and discussion — can we use Eq. 1.1 to develop one or more direct extrapolation techniques for estimating the gas-in-place?

We will address the details of the function plotted in **Fig. 3.1** later in this chapter, but we do note the relevance (and convenience) of this approach — we only require a simple set of rate-time data (from which the cumulative production and other auxiliary functions can be computed).

We do not require specialized PVT or reservoir properties, nor do we require pressure data (initial, average, or otherwise). The can be considered to be a simplified approach that has a rigorous basis in theory. The most relevant issue at present is the development of auxiliary plotting functions that we can utilize to estimate the parameters in Eq. 1.1. Recalling Eq. 1.1 for illustrative purposes, we have.

$$q_g = q_{gi} - \frac{2q_{gi}}{\left[1-\left[\frac{p_{wf}/z_{wf}}{p_i/z_i}\right]^2\right]G}G_p + \frac{q_{gi}}{\left[1-\left[\frac{p_{wf}/z_{wf}}{p_i/z_i}\right]^2\right]G^2}G_p^2 \quad \text{.....(1.1)}$$

In considering Eq. 1.1, one should not be tempted to simply use statistical regression techniques to fit Eq. 1.1 to production data — regardless of the care used in this effort, the result will not be representative in terms of the parameters obtained. This observation may seem overly cautious as the underlying relation in Eq. 1.1 is simply a quadratic — it can easily be fitted to production data using a variety of tools, and we can even factor the result to yield the quadratic roots. However, the $q_g$-$G_p$ profile for the case of a gas well produced at a constant bottomhole flowing pressure in a closed reservoir simply is not a perfect quadratic — it is close, even indiscernible from a quadratic in most cases, but ultimately the $q_g$-$G_p$ profile is not a perfect quadratic function. The result of fitting a quadratic function to essentially quadratic data (neglecting random errors for the moment) will yield parameters which may not (and in fact, will not) be representative. While tempting, we strongly recommend against using a regression scheme to fit Eq. 1.1 to production data. We committed considerable time and effort to this activity in the early stages of this research and virtually every attempt (even for "perfect" data (*i.e.*, results of numerical simulation)) yielded results which were in substantial error.

Instead of utilizing regression, we have pursued a concept of using multiple plotting functions to allow the data profile (*i.e.*, $q_g$-$G_p$ data) to provide a "characterization" of Eq. 1. By using graphical techniques (rather than regression) to resolve the parameters in Eq. 1 we provide a direct linkage between the influence of individual parameters and the model (Eq. 1.1). Ultimately this yields a much more robust analysis/interpretation, and we use the data (rather than statistics) to drive the analysis process.

As a validation of the proposed analysis procedure we provide a suite of 19 numerical simulation cases (for a variety of initial and bottomhole flowing pressures) — the analysis results for these simulation cases are presented in Appendix A (in addition, a summaries of the analyses/interpretations performed for the field cases considered in this work are provided in Appendix B). As we noted earlier, Knowles[1] and Ansah, *et al*,[2] give a constraint of "medium to low pressure reservoirs" (*i.e.*, $p_i$< 6000 psi) for the relations used to derive Eq. 1.1, we successfully applied the proposed analysis techniques to simulated reservoir performance data for cases where the initial reservoir pressures ranged from 1000 to 10,000 psia.

### 3.1 Characteristics of the Reservoir Model

The following conditions/constraints are imposed on the reservoir and fluid properties for the reservoir model used in this work:

Reservoir Properties:

- The reservoir is a closed, volumetric dry-gas reservoir.
- The reservoir is an isothermal system.
- At initial conditions (*i.e.*, time zero) the reservoir pressure is assumed to be uniform throughout the reservoir, although the actual value of the initial reservoir pressure is not of interest.

Fluid and Rock-Fluid Properties:

- The reservoir acts as an isothermal system.
- Dry-gas is the only mobile fluid in the reservoir.
- Changes in volumetric gas properties are characterized by the real gas law, changes in transport properties (viscosity) are characterized by Newtonian fluid flow.
- The effects of formation and water compressibility are neglected.
- Gravity and capillary pressure effects are assumed to be negligible.

Production/Injection/Influx Conditions:

- A single well exists in this reservoir and is produced at a constant bottomhole flowing pressure.
- Aquifer or water influx effects are assumed to be negligible.

The reservoir/well model solutions are taken from Knowles[1] and Ansah, *et al.*[21] — with Eq. 1.1 being proposed in this work (see Appendix C).

### 3.2 Development of Quadratic Cumulative Production Relation

In Appendix C we present the development of the quadratic $q_g$-$G_p$ model as well as the auxiliary and plotting functions. As discussed earlier, the base relations for this work are given by:

$$q_g = q_{gi} - \frac{2q_{gi}}{\left[1-\left[\frac{p_{wf}/z_{wf}}{p_i/z_i}\right]^2\right]G}G_p + \frac{q_{gi}}{\left[1-\left[\frac{p_{wf}/z_{wf}}{p_i/z_i}\right]^2\right]G^2}G_p^2 \quad \text{.....(1.1)}$$

Where we note that Eq. 1.1 is obtained using results from Knowles[1] and Ansah, *et al.*[21] as shown in Appendix C. The "shorthand" form of Eq. 1.1 is given as:

$$q_g = q_{gi} - D_i G_p + \frac{1}{2}\frac{D_i}{G}G_p^2 \quad \text{.....(1.2)}$$

Where the "decline constant" ($D_i$) for this case is defined as:

$$D_i = \frac{2q_{gi}}{\left[1-\left[\frac{p_{wf}/z_{wf}}{p_i/z_i}\right]^2\right]G} \quad \text{.....(1.3)}$$

"Lumping" the $(p_{wf}/z_{wf})/(p_i/z_i)$ term (in Eqs. 1.1 and 1.3) into a single variable ($p_{wD}$), we obtain the following "dimensionless" pressure function ($p_{wD}$), which is defined as:

$$p_{wD} = \left[ \frac{p_{wf}/z_{wf}}{p_i/z_i} \right] \quad \text{.....(1.4)}$$

Substituting the definition given by Eq. 1.4 into. Eq. 1.3 yields:

$$D_i = \frac{2q_{gi}}{(1 - p_{wD}{}^2)\, G} \quad \text{.....(1.5)}$$

The form given by Eq. 1.2 is the starting point for our development of the auxiliary and plotting functions to be used in this work. As noted earlier, although the form given by Eq. 1.2 is tempting as a regression model, we strongly discourage its use in that capacity. We

### 3.3 New Methods for the Analysis of $q_g$-$G_p$ Data

The plotting functions for this work are derived in Appendix C — and the relevant governing relations and plotting functions are summarized in this section as needed. As noted earlier in this work, the primary result for modelling the gas rate-cumulative gas production behavior is given by:

$$q_g = q_{gi} - \frac{2q_{gi}}{\left[1 - \left[\frac{p_{wf}/z_{wf}}{p_i/z_i}\right]^2\right] G} G_p + \frac{q_{gi}}{\left[1 - \left[\frac{p_{wf}/z_{wf}}{p_i/z_i}\right]^2\right] G^2} G_p^{\,2} \quad \text{.....(1.1)}$$

And the "shorthand" form of Eq. 1.1 is given as:

$$q_g = q_{gi} - D_i G_p + \frac{1}{2}\frac{D_i}{G} G_p{}^2 \quad \text{.....(1.2)}$$

Where the "decline constant" ($D_i$) for the gas case is defined as follows:

$$D_i = \frac{2q_{gi}}{\left[1 - \left[\frac{p_{wf}/z_{wf}}{p_i/z_i}\right]^2\right] G} \quad \text{.....(1.3)}$$

Or, in its alternate form as:

$$D_i = \frac{2q_{gi}}{(1 - p_{wD}{}^2)\, G} \quad \text{.....(1.5)}$$

At this point, few functional definitions are in order — summarizing the auxiliary functions presented in Appendix C, we have the definition of the "cumulative averaged rate" function:

$$(q_g)_{i,Gp} \equiv \frac{1}{G_p} \int_0^{G_p} q_g \, dG_p \quad \text{.....(3.1)}$$

And the substitution of Eq. 1.2 into Eq. 3.1 yields our working relation for the "cumulative averaged rate" function:

$$(q_g)_{i,Gp} \equiv q_{gi} - \frac{D_i}{2} G_p + \frac{1}{6}\frac{D_i}{G} G_p^{\,2} \quad \text{.....(3.2)}$$

Having Eqs. 1.1 and 3.2 in hand, we present the "plotting functions" derived for the analysis of rate-cumulative data from gas wells (all relations are derived in Appendix C). In particular, we have:

$$\frac{q_{gi} - q_g}{G_p} = D_i - \frac{1}{2}\frac{D_i}{G} G_p \quad \text{.....(3.3)}$$

$$\frac{(q_g)_{i,Gp} - q_{gi}}{G_p} = \frac{1}{2} D_i - \frac{1}{6}\frac{D_i}{G} G_p \quad \text{.....(3.4)}$$

$$\frac{(q_g)_{i,Gp} - q_g}{G_p} = \frac{1}{2} D_i - \frac{1}{3}\frac{D_i}{G} G_p \quad \text{.....(3.5)}$$

For orientation, we illustrate the use of each "working relation" and "plotting function" in a series of schematic plots. These schematic plots illustrate the characteristic behavior of each data function, and provide guidance on how to analyze and interpret data on a given plot (a summary is given in **Table 3.1**).

**Table 3.1 – Summary of the "Quadratic Analysis" relations.**

| Case | Plotting Functions | Root/Intercept | **Fig.** |
|---|---|---|---|
| Eq. 1.1 | $q_g$ vs. $G_p$ | $\underset{Root}{Quadratic} = G$ | **3.2** |
| Eq. 3.2 | $(q_g)_{i,Gp}$ vs. $G_p$ | $\underset{Root}{Quadratic} = \frac{3}{2} G$ | **3.3** |
| Eq. 3.3 | $(PF_1)$ $\frac{q_{gi} - q_g}{G_p}$ vs. $G_p$ | $G_{p,\max} = 2G$ | **3.4** |
| Eq.3.4 | $(PF_2)$ $\frac{(q_g)_{i,Gp} - q_{gi}}{G_p}$ vs. $G_p$ | $G_{p,\max} = 3G$ | **3.5** |
| Eq. 3.5 | $(PF_3)$ $\frac{(q_g)_{i,Gp} - q_g}{G_p}$ vs. $G_p$ | $G_{p,\max} = \frac{3}{2} G$ | **3.6** |

In **Fig. 3.2** we note two strong characteristics of the rate-cumulative plot — first, the quadratic trend can have a region of *negative behavior* (which is simply a behavior of the model, and is not defined physically). Second, we note that the minimum value in the $q_g$-$G_p$ trend actually *defines* the location of the maximum gas production (or the gas-in-place, $G$).

The derivation of this "root" is relative simple — we can differentiate the governing equation (Eq. 1.1) with respect to the cumulative gas production ($G_p$), which yields:

$$\frac{d}{dG_p}\left[q_g\right] = -D_i + \frac{D_i}{G} G_p \quad \text{.....(3.6)}$$

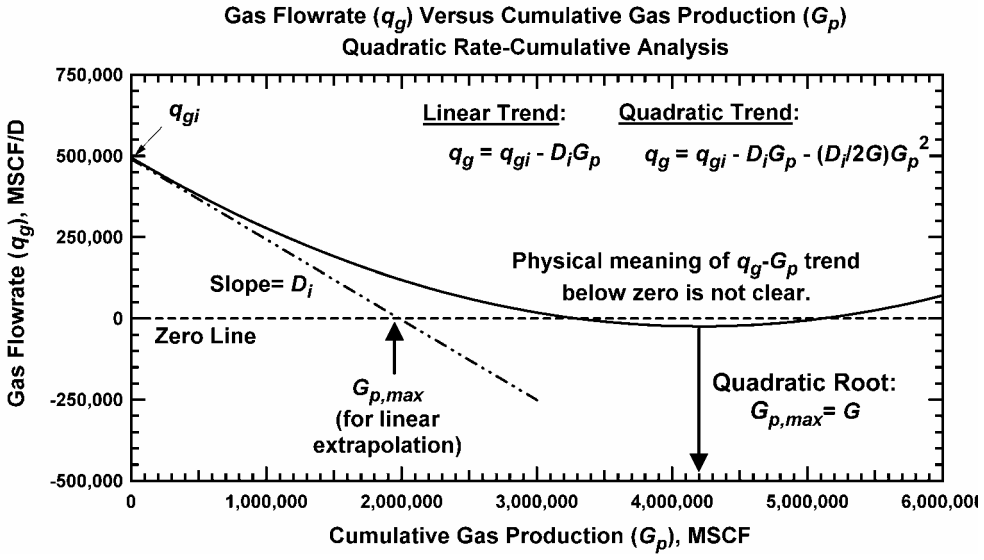


**Figure 3.2 – Schematic Behavior: $q_g$ versus $G_p$.**

Setting Eq. 3.6 equal to zero (*i.e,* the point at which the $q_g$ function experiences a minimum), then solving for $G_p$ gives the location of the "maximum" cumulative gas production ($G_{p.max}$). This action reduces to the following expression:

$$G_{p,\max} = G \quad \text{.....(3.7)}$$

In our work we have used the concept of a "spreadsheet"-type solution where Eq. 1.1 is used as the basis for the reservoir model. In our approach, the model parameters are modified in a systematic manner in order to match the model function to the data.

From the calculations provided for the gas-in-place, $G$ (in the spreadsheet), the model parameters, $q_{gi}$, $D_i$, and $p_{wD}$ (Eq. 1.4)) are adjusted continuously to update the estimate of the gas-in-place, $G$. Specifically, we use the definition of $D_i$ (Eq. 1.5) to estimate/verify the gas-in-place.

$$G = \frac{2q_{gi}}{(1-p_{wD}{}^2)D_i} \text{ where } p_{wD} = \left[\frac{p_{wf}/z_{wf}}{p_i/z_i}\right] \quad \text{.....(3.8)}$$

Again, our approach is an "active analysis" which utilizes the model and data functions interactively — using a spreadsheet mechanism with a graphical display of the model and the data. It is important to note that all of our analyses are linked in this spreadsheet approach — in particular, the methods defined by Eqs. 1.1, 3.2-3.5. Each relation is linked by a common set of model parameters.

The "cumulative averaged rate" analysis defined using Eq. 3.2 has many similar traits to the rate-cumulative production analysis described above. In this case we consider the behavior of the "cumulative averaged rate" function ($(q_g)_{i,Gp}$) as a function of the cumulative gas production ($G_p$).

The schematic behavior of $q_{gi,Gp}$ versus $G_p$ is shown in **Fig. 3.3**. We note that the $q_{gi,Gp}$-$G_p$ trend does not appear to drift into negative values, and the interpretation of the "root" is based on Eq. 3.2 (rather than Eq. 1.1 (or Eq. 3.7), where Eq. 3.2 yields a root of $G_{p,max}$ =3/2 $G$ for $q_{gi,Gp}$=0.

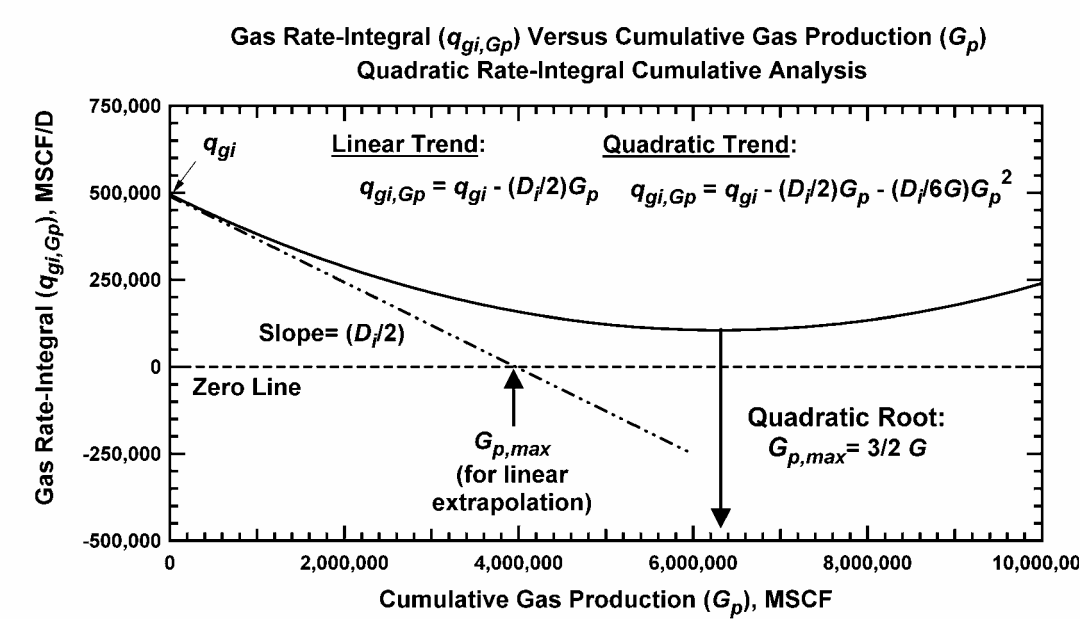


**Figure 3.3 – Schematic Behavior: $q_{gi,Gp}$ versus $G_p$.**

Our new plotting functions are constructed in such a fashion that we achieve a straight-line trend for each function, where the slope, the $y$-axis intercept, and the $x$-axis intercepts each include a component of the solution/model (*e.g.*, the $D_i$ or $G$ variables). In order to distinguish the plotting functions in a practical manner, we have elected to use a naming convention as shown in **Table 3.2**:

**Table 3.2 – Name convention for the "Quadratic Analysis" plotting functions.**

| Case | Name | Plotting Function | Root/Intercept |
|---|---|---|---|
| Eq. 3.3 | ($PF_1$) | $\frac{q_{gi}-q_g}{G_p}$ vs. $G_p$ | $G_{p,\max}=2G$ |
| Eq. 3.4 | ($PF_2$) | $\frac{(q_g)_{i,Gp}-q_{gi}}{G_p}$ vs. $G_p$ | $G_{p,\max}=3G$ |
| Eq. 3.5 | ($PF_3$) | $\frac{(q_g)_{i,Gp}-q_g}{G_p}$ vs. $G_p$ | $G_{p,\max}=\frac{3}{2}G$ |

In **Table 3.2** the "*PF*" variables denote "plotting functions." The most straightforward approach to explain these functions is to recognize that the functions ($PF_1$ to $PF_3$) increase in complexity as we progress from $PF_1$ to $PF_3$. For example, $PF_1$ is simply an algebraic rearrangement of Eq. 1.1, and as such, is relatively easy to construct and is generally well-behaved.

In **Fig. 3.4** we present a schematic plot of $PF_1$, and we are quick to note that this function yields an easy to visualize analysis — *i.e.*, the straight-line constructed on **Fig. 3.4**.

As we noted in an earlier section, our analyses are "linked" in a spreadsheet approach and for the case of all of the plotting functions, the most difficult variable to assess is the initial gas flowrate ($q_{gi}$). As such, we have utilized "high," low," and "correct" estimates of the $q_{gi}$ variable (in our case we use $0.9q_{gi}$, $q_{gi}$, $1.1q_{gi}$ (*i.e.*, a 10 percent high/low spread)). This methodology is coupled with our "linked" analysis and we provide the calculated production data functions trends for matching against the appropriate model function. This procedure will be illustrated in a demonstration example provided later in this chapter.

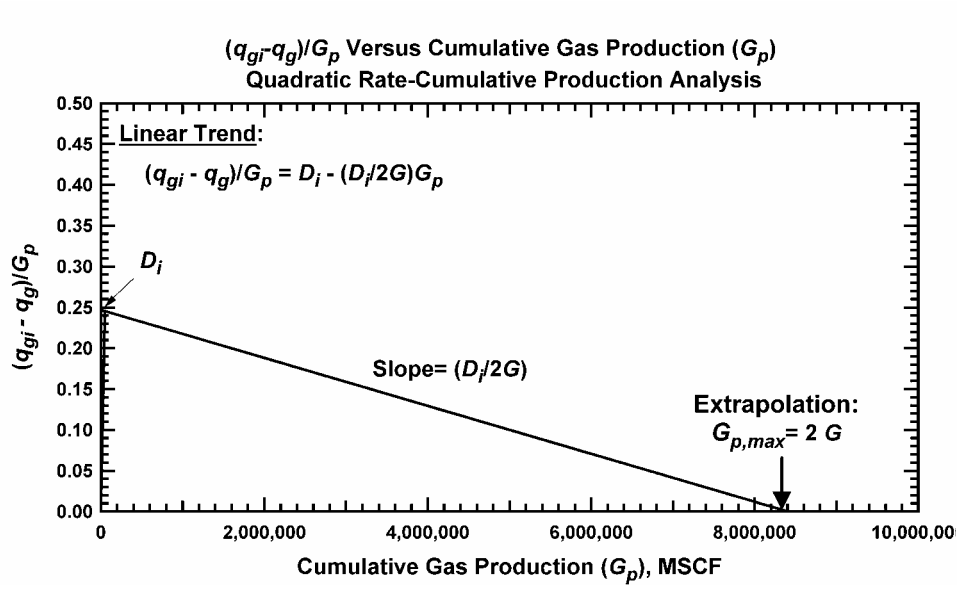


**Figure 3.4 – Schematic Behavior: $(q_{gi} - q_g)/G_p$ versus $G_p$ ($PF_1$).**

The construction of $PF_2$ is similar to that for $PF_1$ in that we simply rearrange Eq. 3.2 into a linear form (*i.e.,* Eq. 3.4). In **Fig. 3.5** we illustrate $PF_2$ and we note its similarity in form and function to $PF_1$. We also utilize the $0.9q_{gi}$, $q_{gi}$, $1.1q_{gi}$ approach in generating production data functions for analysis. The data functions generated using $PF_2$ are generally "smoother" than those generated using $PF_1$ (the averaging process provides an "integral smoothing" of the production data).

The definition and structure of $PF_3$ is a combination of $PF_1$ and $PF_2$ — which should (logically) provide the benefits of each component function (*i.e.*, $PF_1$ and $PF_2$). While this is true, and we expect $PF_3$ to be the most "mature" of the proposed plotting functions, this function does suffer from irregular behavior in the data. Specifically, the use of both the $q_g$ and $(q_g)_{i,Gp}$ functions amplifies distortions in the data, as well as any behavior that may not be represented by the base model. Put simply, $PF_3$ is the most sensitive of the plotting functions, and it must be recognized as such. A schematic plot of $PF_3$ is shown in **Fig. 3.6**.

For reference, we do not utilize the $0.9q_{gi}$, $q_{gi}$, $1.1q_{gi}$ values in our analysis procedure as the $q_{gi}$ parameter is not used in $PF_3$.

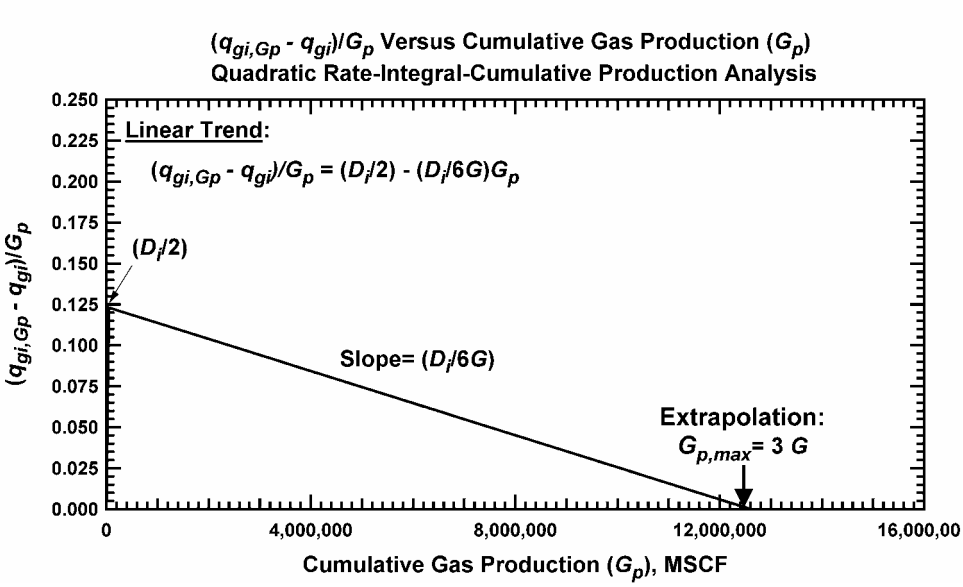


**Figure 3.5 – Schematic Behavior: $(q_{gi,Gp} - q_{gi})/G_p$ versus $G_p$ ($PF_2$).**

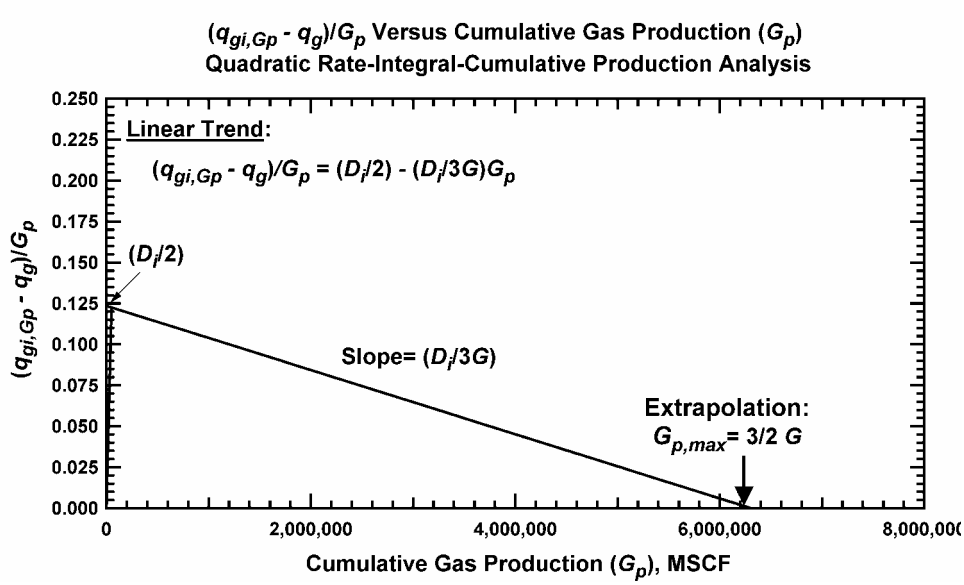


**Figure 3.6 – Schematic Behavior: $(q_{gi,Gp} - q_g)/G_p$ versus $G_p$ ($PF_3$).**

### 3.4 Validation and Illustrative Analyses — Synthetic Data

As a mechanism for validation, we have generated and evaluated 19 cases of performance in a finite gas reservoir. In particular, 9 cases of performance at a constant bottomhole pres-sure of 1000 psia and 10 cases of production at a pressure of 500 psia. The initial reservoir pressures for these cases range from 1000 psia to 10,000 psia. The base data for the validation cases are inventoried as follows:

Reservoir Properties:

| | |
|---|---|
| Wellbore radius, $r_w$ | = 0.0745 ft |
| Average net pay thickness, $h$ | = 30 ft |
| Net pay thickness, $h$ | = 30 ft |
| Formation permeability, $k$ | = 100 md |
| Average porosity, $\phi$ | = 0.30 (fraction) |
| Nominal well spacing | = 40 acres |
| Initial reservoir pressure, $p_i$ | = 1000 to 10,000 psia |

Fluid properties:

| | |
|---|---|
| Gas specific gravity, $\gamma_g$ | = 0.6 (air=1.0) |
| Reservoir temperature, $T$ | = 200 deg F |

Production parameters:

| | |
|---|---|
| Constant bottomhole pressure, $p_{wf}$ | = 500 or 1000 psia |

For the purpose of demonstration, an "average" case was selected — in particular, the initial pressure ($p_i$) is 5000 psia and the flowing bottomhole pressure ($p_{wf}$) is 1000 psia. In this case the gas-in-place is 4.20 BSCF. In **Figs. 3.7-3.13** we present the analysis plots for this simulated gas well performance case. The inventory of analysis cases is given below in **Table 3.3**.

**Table 3.3 – Analysis plots for the simulated gas reservoir case.**

| Plotting Functions | **Fig.** |
|---|---|
| $q_g$ vs. $t$ (log-log plot) | **3.7** |
| $G_p$ vs. $t$ (log-log plot) | **3.8** |
| $q_g$ vs. $G_p$ | **3.9** |
| $(q_g)_{i,Gp}$ vs. $G_p$ | **3.10** |
| $(PF_1)\ \frac{q_{gi}-q_g}{G_p}$ vs. $G_p$ | **3.11** |
| $(PF_2)\ \frac{(q_g)_{i,Gp}-q_{gi}}{G_p}$ vs. $G_p$ | **3.12** |
| $(PF_3)\ \frac{(q_g)_{i,Gp}-q_g}{G_p}$ vs. $G_p$ | **3.13** |

The fist two plots, **Figs. 3.7 and 3.8** can be considered to be "summary" or "conventional" plots — we present these plots in log-log format to provide resolution for the entire range of data.

While we do not use these plots directly for analysis (recall that we use a "spreadsheet" of all plotting functions linked to a common set of reservoir properties), we note that **Figs. 3.7** and **3.8** do provide a "time-dependent" data perspective.

In particular we note that the data and the plotting functions match quite well — as we would expect for this case since this case fits our requisite condition (*i.e.*, $p_i$<6000 psia). Perhaps most importantly, there are no surprises — the boundary dominated flow behavior is accurately represented by the proposed reservoir model.

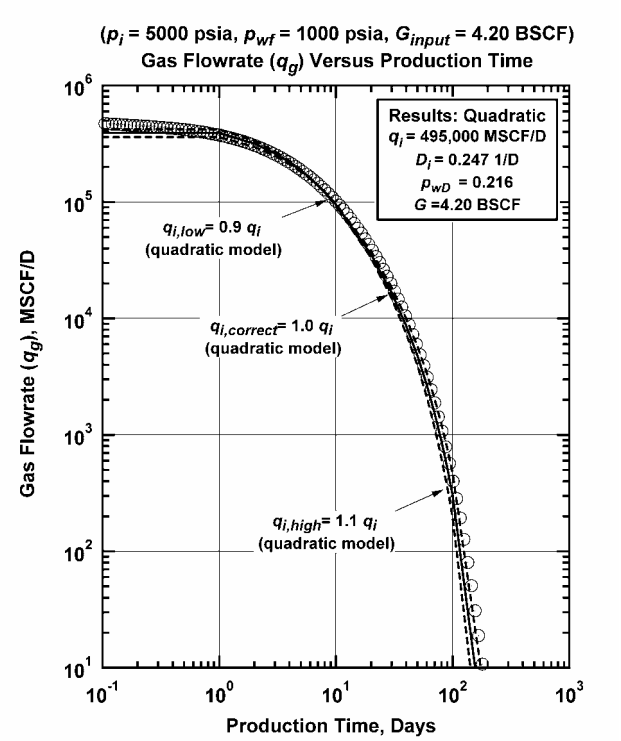


**Figure 3.7 – Simulated Performance Case: $q_g$ versus $t$ ($p_i$= 5000 psia, $p_{wf}$=1000 psia, $G_{input}$=4.20 BSCF).**

In **Figs. 3.9** and **3.10** we present the $q_g$-$G_p$ and $q_{gi,Gp}$-$G_p$ trends (respectively) — where our objective is to illustrate the behavior of these functions in a format where we can verify that the data and model functions yield appropriate agreement. We recall that in these plots we present each *model* function computed using the $0.9q_{gi}$, $q_{gi}$, and $1.1q_{gi}$ values in order to generate comparative trends. Each model trend is "live" and is "linked" to the common parameter values being estimated using a spreadsheet-based program module.

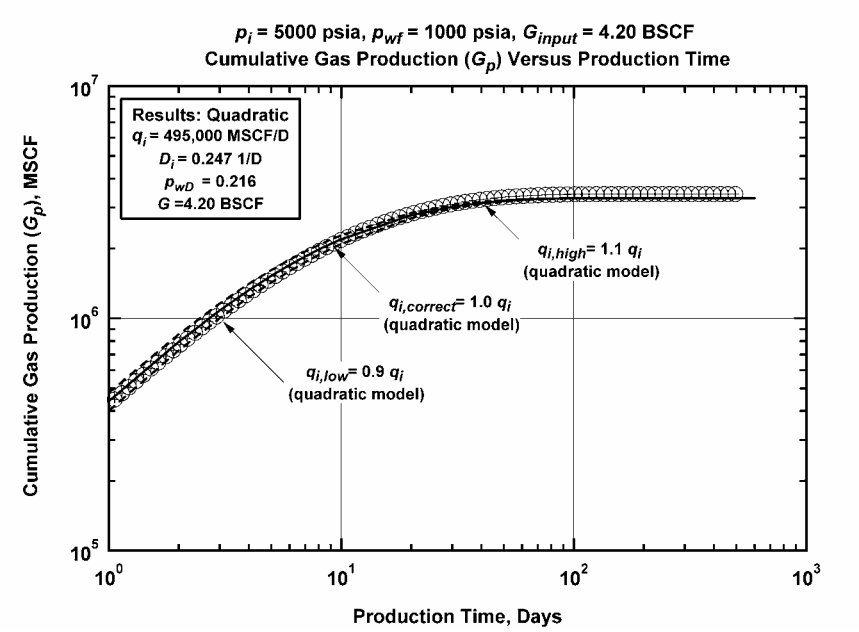


**Figure 3.8 – Simulated Performance Case: $G_g$ versus $t$ ($p_i$= 5000 psia, $p_{wf}$=1000 psia, $G_{input}$=4.20 BSCF).**

In **Figs. 3.9** and **3.10** we find (as expected) that the multiple model functions match the respective data function ($q_g$-$G_p$ or $q_{gi,Gp}$-$G_p$) quite well. We also note that each function ($q_g$-$G_p$ and $q_{gi,Gp}$-$G_p$) exhibits the expected "quadratic minimum," from which we can estimate the gas-in-place ($G$). We would designate this determination as "rough," and will comment that this estimate is used as a guide. We recall that the $q_g$-$G_p$ and $q_{gi,Gp}$-$G_p$ analyses are performed in conjunction with the analyses performed using the specialized plotting functions — where by the nature of the extrapolated trends generated by the specialized plotting functions, these results (*i.e.*, the results from **Figs. 3.11-3.13**) should be considered more precise than the results estimated from **Figs. 3.9** and **3.10**.

**Figs. 3.11-3.13** provide illustrations of the characteristic trends for the specialized plotting functions ($PF_1$-$PF_3$ (*i.e.*, Eqs. 19-21)). Specifically, we note that in this analysis approach we utilize the data and model functions for each plotting function, and we note the use of the $0.9q_{gi}$, $q_{gi}$, and $1.1q_{gi}$ values — which are used in generating the *model and data functions* in **Figs. 3.11** and **3.12**. Fig. **3.13** does not utilize this approach because the $q_{gi}$ variable is not used in the plotting function for this case.

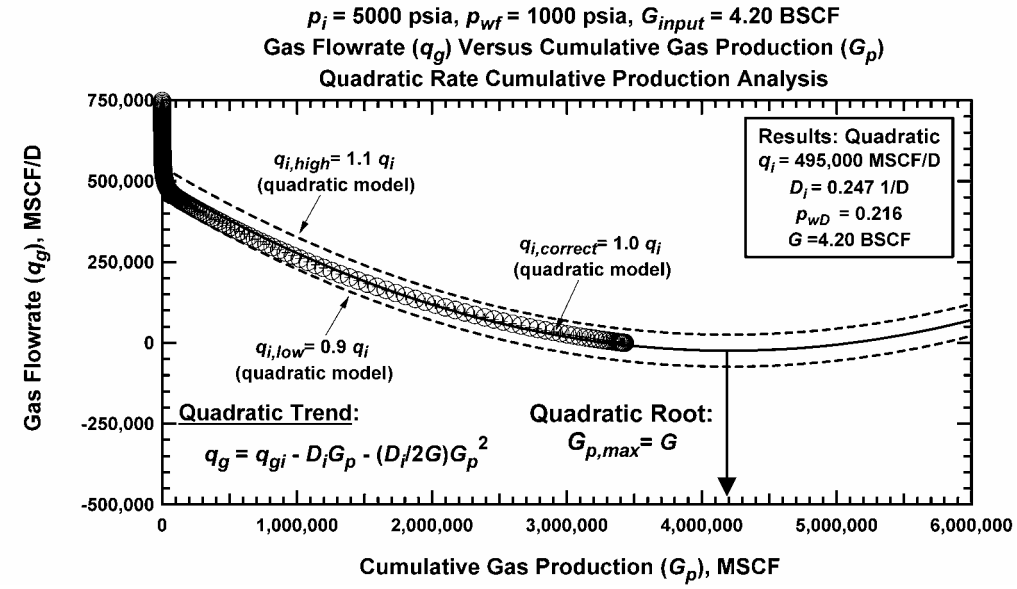


**Figure 3.9 – Simulated Performance Case: $q_g$ versus $G_p$ ($p_i$= 5000 psia, $p_{wf}$=1000 psia, $G_{input}$=4.20 BSCF).**

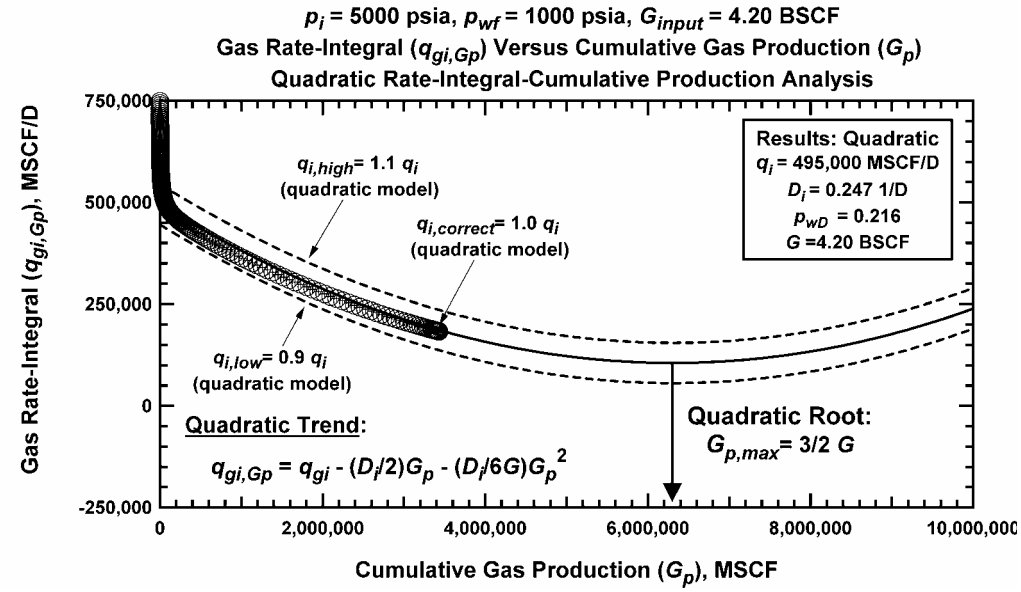


**Figure 3.10 – Simulated Performance Case: $q_{qi,Gp}$ versus $G_p$ ($p_i$= 5000 psia, $p_{wf}$=1000 psia, $G_{input}$=4.20 BSCF).**

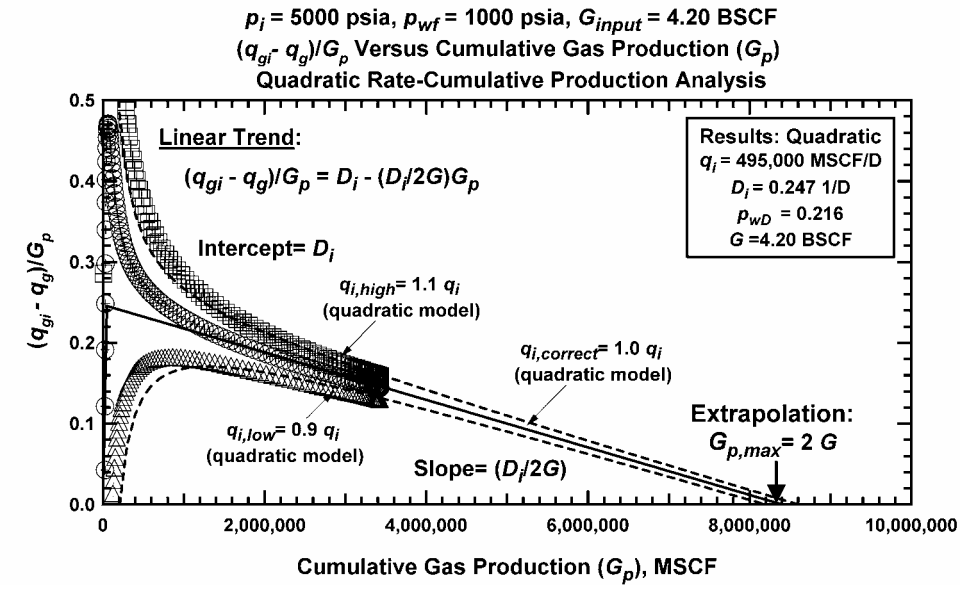


**Figure 3.11 – Simulated Performance Case: $(q_{qi}-q_q)/G_p$ versus $G_p$ ($p_i$= 5000 psia, $p_{wf}$=1000 psia, $G_{input}$=4.20 BSCF) (Plotting Function 1 ($PF_1$)).**

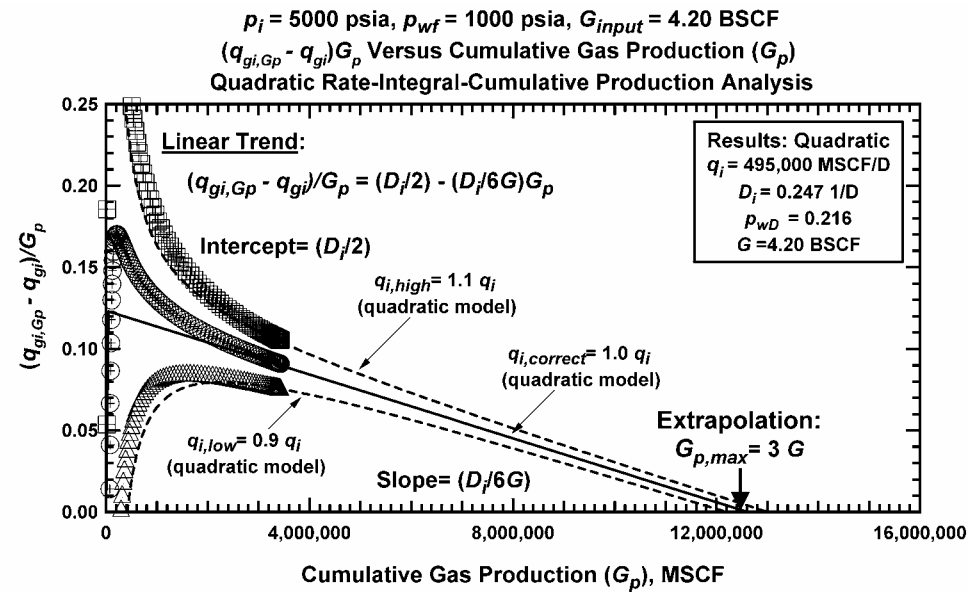


**Figure 3.12 – Simulated Performance Case: $(q_{qi,Gp}-q_{qi})/G_p$ versus $G_p$ ($p_i$= 5000 psia, $p_{wf}$=1000 psia, $G_{input}$=4.20 BSCF) (Plotting Function 2 ($PF_2$)).**

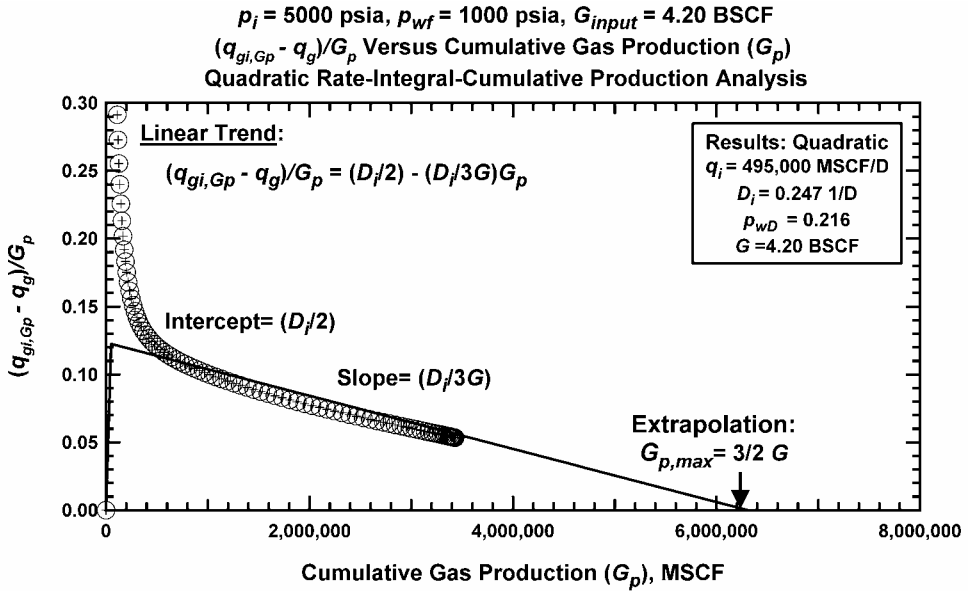


**Figure 3.13 – Simulated Performance Case: $(q_{qi,Gp}-q_q)/G_p$ versus $G_p$ ($p_i$= 5000 psia, $p_{wf}$=1000 psia, $G_{input}$=4.20 BSCF) (Plotting Function 3 ($PF_3$)).**

In **Fig. 3.11** we note that the model and data functions agree very well once boundary-dominated flow behavior has been established. Although the data for this case were simulated, the "convergence" of the $0.9q_{gi}$, $q_{gi}$, and $1.1q_{gi}$ trends is some-what universal in nature. In **Fig. 3.12** we utilize the $q_{gi,Gp}$ function — and we also note the characteristic behavior of both the data and model functions. As a comment, we note that the linear trends illustrated by the data functions in **Fig. 3.12** (based on $q_{gi,Gp}$) are delayed in comparison to their counterpart data functions in **Fig. 3.11** (which are based on $q_g$). This "delay" in the integral-type functions (*i.e.*, the $q_{gi,Gp}$) is quite common, and should not affect the overall analysis of the data in **Fig. 3.12**, although we do encourage that the use of **Figs. 3.11** and **3.12** be "coordinated" so as to perform the best match of all data and model functions.

As noted earlier, plotting function 3 (*i.e.*, $PF_3$) does not use the $q_{gi}$ variable — and, as such, we only use a single data and model function for this analysis. The illustrative plot for this case is shown in **Fig. 3.13**, and we note that an "apparent" linear trend does evolve. We recall that since all of our analyses are linked via the spreadsheet module, the model trend in **Fig. 3.13** is fixed. It appears that we could obtain a slightly better correlation of the model and data (*i.e.*, the model trend could be adjusted slightly to better agree with the data). However, this analysis is "fixed," by the linkage to all of the other analyses, and we believe that this is the appropriate match of the model and data functions.

The trends in **Fig. 3.13** accentuate the need to have a "linkage" mechanism through which all analyses are tied. Specifically, we might be tempted to make adjustments to individual analyses in order to obtain a better "local" match of the data and model — however, such an action would be at the cost of the rigor of

the analysis and would invalidate the "global" coordination of our data analysis. This point should not be underemphasized, the analysis approach proposed in this work — specifically the "global" linkage of all analyses using a spreadsheet module (or other, similar computer-aided mechanism) must be employed. *Failure to provide simultaneous analyses of all data/model functions will result in inconsistent results and, ultimately, a loss in the rigor and utility of this approach.*

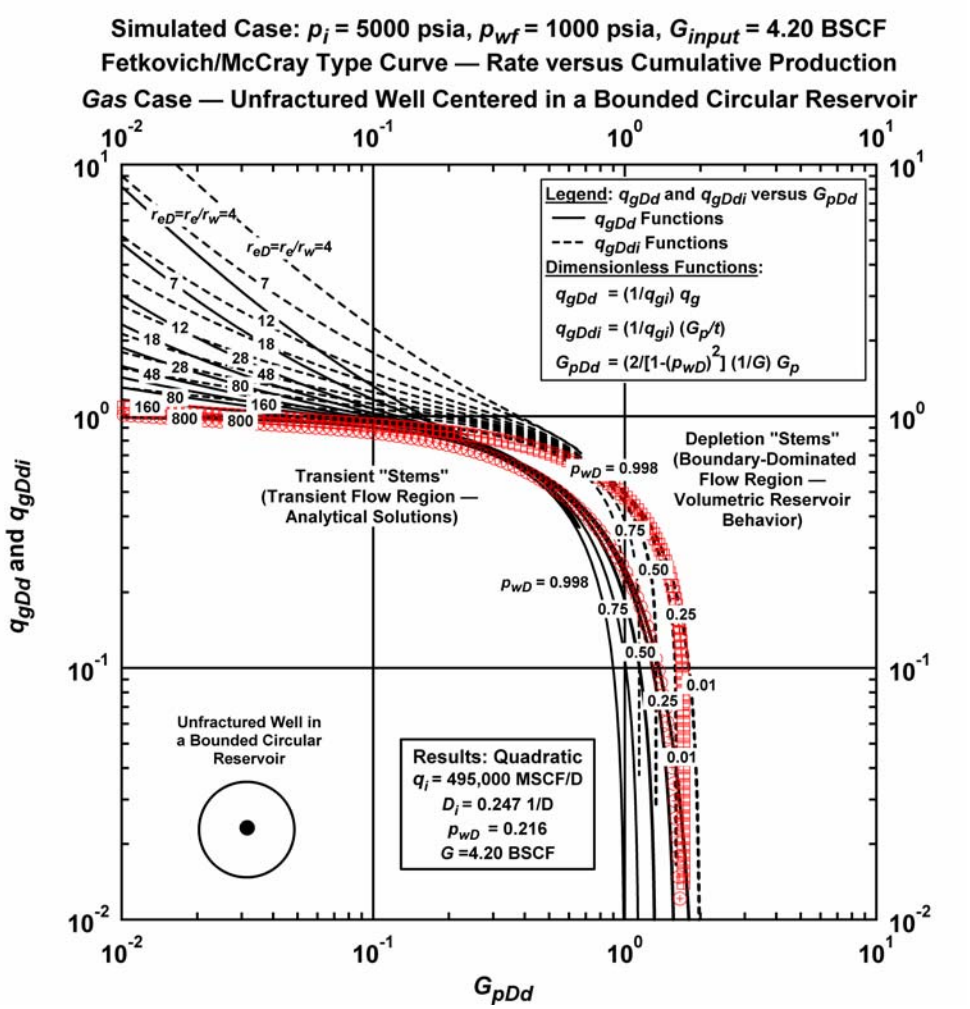


**Figure 3.14 – Simulated Performance Case: "Quadratic" Rate-Cumulative Decline Type Curve Analysis ($p_i$= 5000 psia, $p_{wf}$=1000 psia, $G_{quad}$=4.20 BSCF).**

**Figs. 3.14** and **3.15** show a comparison of the "quadratic" and "hyperbolic" rate-cumulative decline type curve analyses, respectively. The data match produced on the "quadratic" type curve can not be repeated on the hyperbolic type curve as the data functions cross over several hyperbolic type curve stems. We will also note that the hyperbolic method does not reproduce the input gas-in-place — this outcome further verifies the accuracy of the quadratic model over the hyperbolic model for representing gas flow behavior.

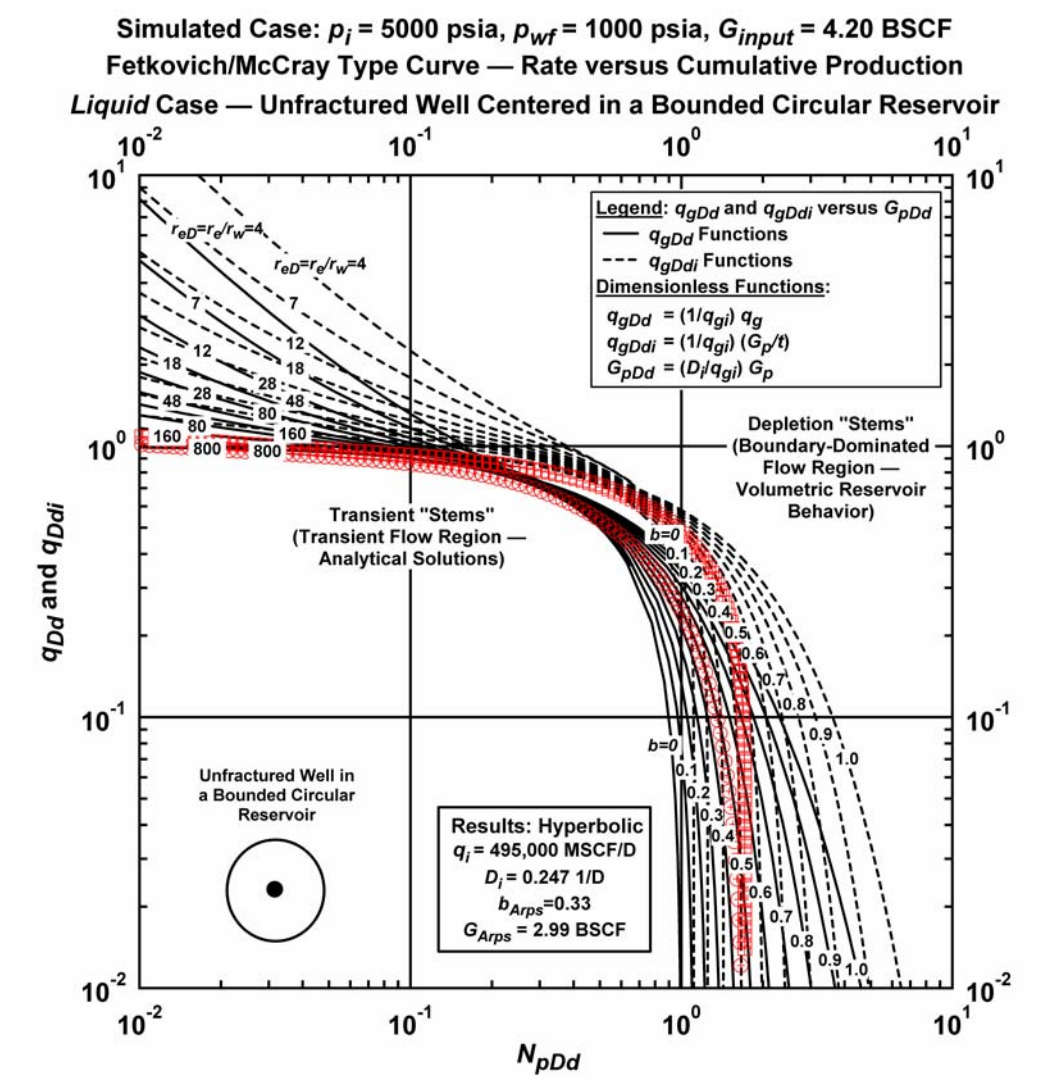


**Figure 3.15 – Simulated Performance Case: "Hyperbolic" Rate-Cumulative Decline Type Curve Analysis ($p_i$= 5000 psia, $p_{wf}$=1000 psia, $G_{quad}$=4.20 BSCF).**

In **Fig. 3.16** we present the analysis and interpretation of the simulated performance data using decline type curve analysis.[12,16] It is important to note that this approach is completely rigorous in the treatment of gas properties as functions of pressure and time (we have utilized the appropriate pseudopressure and pseudotime functions in this work). The decline type curve analysis yields essentially exact results for this case — *i.e.*, the input simulation parameters are reproduced from the analysis and interpretation of the performance data. In conclusion, the analysis illustrated by **Fig. 3.16** confirms the validity of the data and the decline type curve methodology.

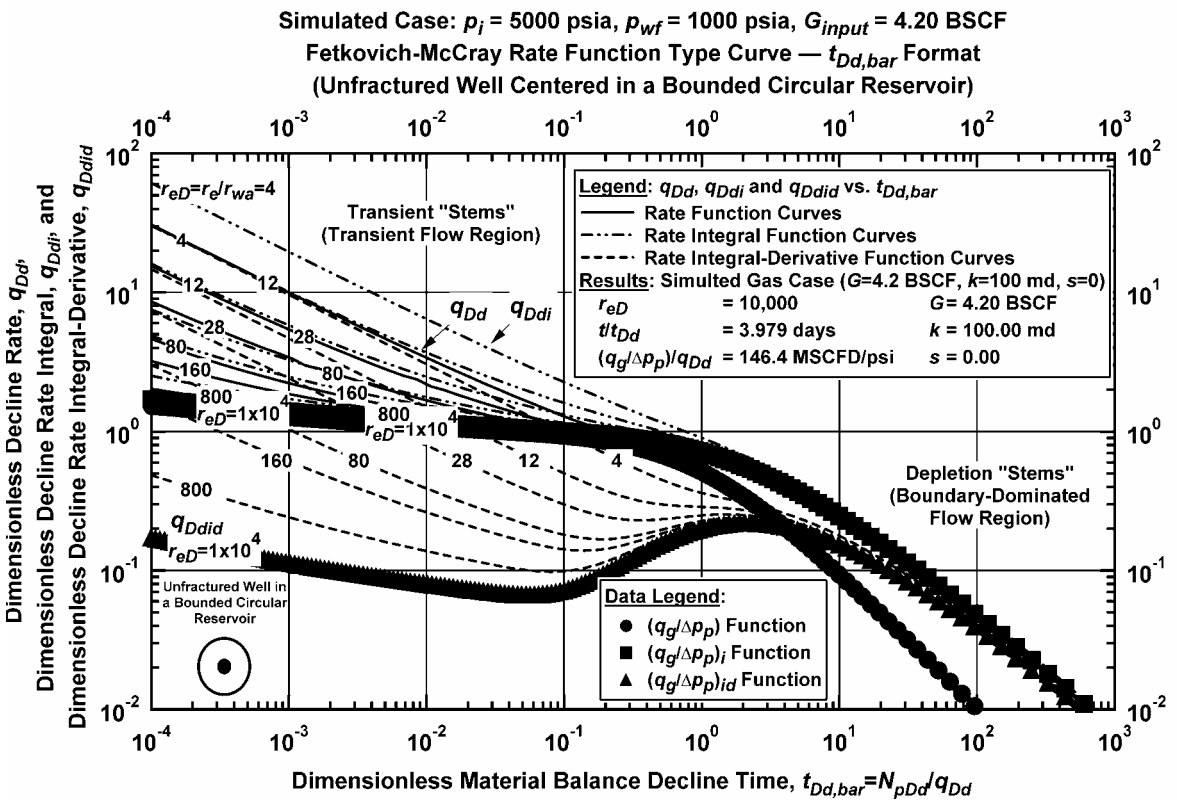


**Figure 3.16 – Simulated Performance Case: Decline Type Curve Analysis ($p_i$= 5000 psia, $p_{wf}$=1000 psia, $G_{input}$=4.20 BSCF).**

As a final commentary on this "validation" sequence, we will recall that 19 cases were utilized in this effort, and all cases were analyzed in exactly the same fashion — using a simultaneous analysis of all data for a particular case. In addition, all cases were validated — *i.e.*, we were able to reproduce the input values of the gas-in-place, *G*, using the analysis of the performance data for each case.

# CHAPTER IV
# EXAMPLE APPLICATION OF THE NEW SEMI-ANALYTICAL METHOD FOR THE ANALYSIS OF PRODUCTION DATA FROM GAS WELLS

In this chapter we will demonstrate the application of the proposed analysis methodology using a "standard" literature case (i.e., ref. 8). For reference, we provide the input data as well as the analysis and interpretation plots for this "literature" case and 8 other field cases in Appendix B. These cases are provided as a cross-section of potential field cases that a reservoir engineer might typically encounter

## 4.1 West Virginia Field, Well A (ref. 8)

*Description — West Virginia Field, Well A*

In this case the conditions of the well and reservoir are such that the well produces at a nearly constant bottomhole flowing pressure. This particular case has become a standard in the literature for the analysis of gas well performance. Perhaps most importantly, these data exhibit a near-perfect correlation with the proposed model — which suggests that that proposed methodology may be widely applicable.

The reservoir, fluid, and production parameters for this case are summarized below:

Reservoir Properties:

| | |
|---|---|
| Average net pay thickness, $h$ | = 70 ft |
| Average porosity, $\phi$ | = 0.06 (fraction) |
| Average formation permeability, $k$* | = 0.07 md |
| Irreducible water saturation, $S_{wi}$ | = 0.35 (fraction) |
| Initial reservoir pressure, $p_i$ | = 4175 psia |

Fluid properties:

| | |
|---|---|
| Gas specific gravity, $\gamma_g$ | = 0.57 (air=1) |
| Reservoir temperature, $T$ | = 160 deg F |

Production parameters:

| | |
|---|---|
| Bottomhole flowing pressure, $p_{wf}$ | = 710 psia |

* Permeability estimate obtained from pressure transient test analysis.

*Example Analysis — West Virginia Well A*

Fetkovich, *et.* al.[8] presented the analysis and interpretation for "West Virginia Well A" based on the application of the "Fetkovich" decline type curve (a precursor to the analysis we have employed for decline type curve analysis (refs. 12 and 16)). The analysis presented for this case by Fetkovich, *et al.* should be considered both accurate and relevant. In fact, this case is unusual in that regardless of the analysis method employed, the analysis results are comparable.

The analysis plots for this case are inventoried as given below in **Table 4.1**.

**Table 4.1 – Inventory of analysis plots for West Virginia Well A.**

| Plotting Functions | **Fig.** |
|---|---|
| $q_g$ vs. $t$ (log-log plot) | **4.1** |
| $q_g$ and $p_{wf}$ vs. $t$ (semilog plot (for $q_g$)) | **4.2** |
| $G_p$ vs. $t$ (log-log plot) | **4.3** |
| $q_g$ vs. $G_p$ (Cartesian plot) | **4.4** |
| $(q_g)_{i,Gp}$ vs. $G_p$ (Cartesian plot) | **4.5** |
| $(PF_1)\ \frac{q_{gi}-q_g}{G_p}$ vs. $G_p$ | **4.6** |
| $(PF_2)\ \frac{(q_g)_{i,Gp}-q_{gi}}{G_p}$ vs. $G_p$ | **4.7** |
| $(PF_3)\ \frac{(q_g)_{i,Gp}-q_g}{G_p}$ vs. $G_p$ | **4.8** |
| $q_g$ vs. $G_p$ (log-log type curve plot (quadratic model)) | **4.9** |
| $q_g$ vs. $G_p$ (log-log type curve plot (hyperbolic model)) | **4.10** |
| *WPA* Plot (log-log type curve plot (full reservoir model)) | **4.11** |

We present the production history in **Figs. 4.1-4.3** and in **Figs. 4.1** and **4.3** we note extraordinary matches of the model and the $q_g$ versus $t$ and $G_p$ versus $t$ data functions (respectively). We note that matches of this clarity are unusual in practice, but we recognize (and endorse) that vigilant data acquisition efforts can yield such cases. **Figure 4.2** may not seem to be of much use since the flowing bottomhole pressure is reported to be constant — however, we note that the rate-time data appear both consistent and unique in this semilog plot.

In **Figs. 4.4** and **4.5** we note similarly strong matches of the model and the $q_g$ versus $G_p$ and the $q_{gi,Gp}$ versus $G_p$ data functions (respectively). In particular, we note that the proposed model for each function matches the corresponding data function with clarity and uniqueness. As we noted earlier, all analyses are linked through the spreadsheet formulation, which yields a very consistent interpretation for this case.

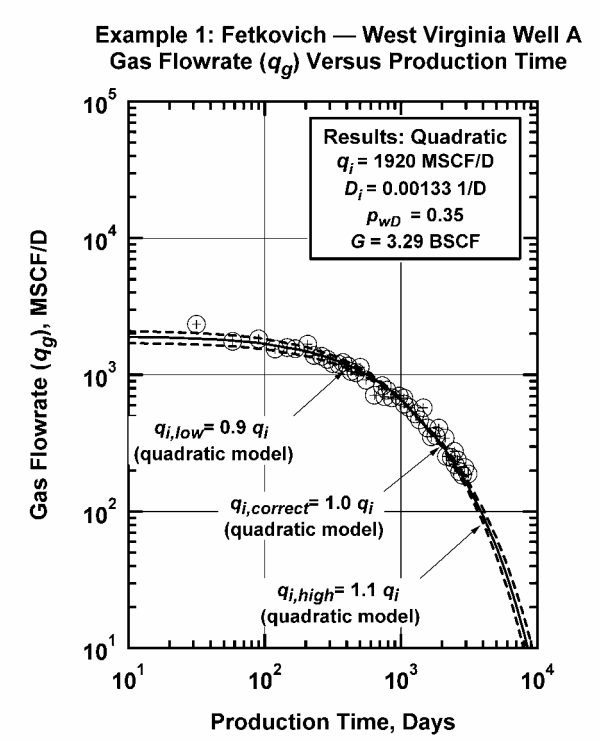


**Figure 4.1 – West Virginia Well A (Fetkovich, *et al.*[8]): $q_g$ versus $t$.**

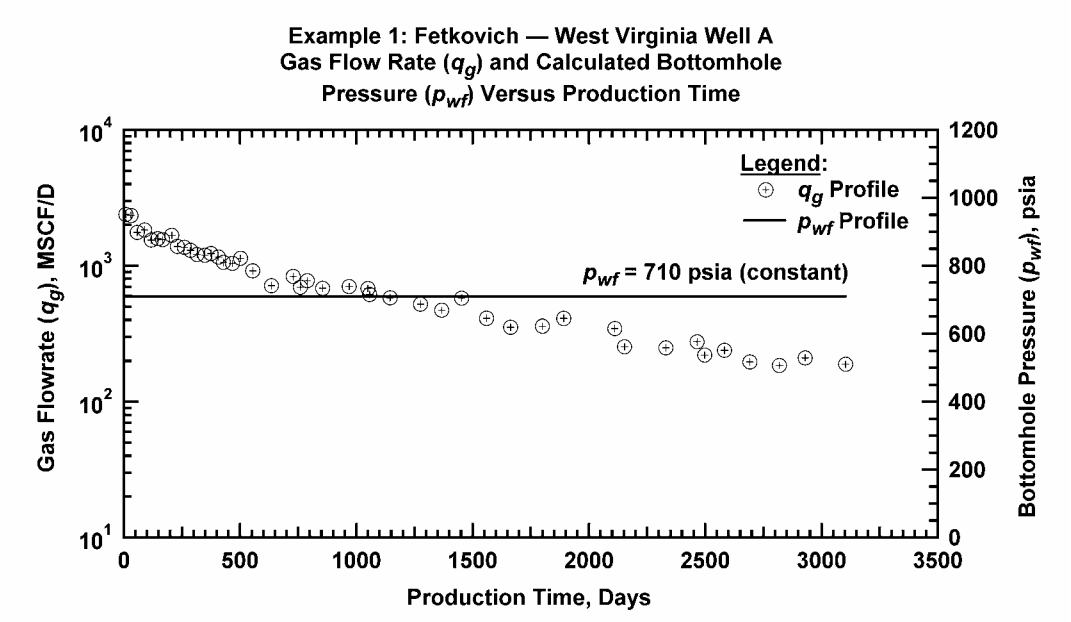


**Figure 4.2 – West Virginia Well A (Fetkovich, *et al.*[8]): $q_g$ versus $t$ and $p_{wf}$ versus $t$ — Production History Plot.**

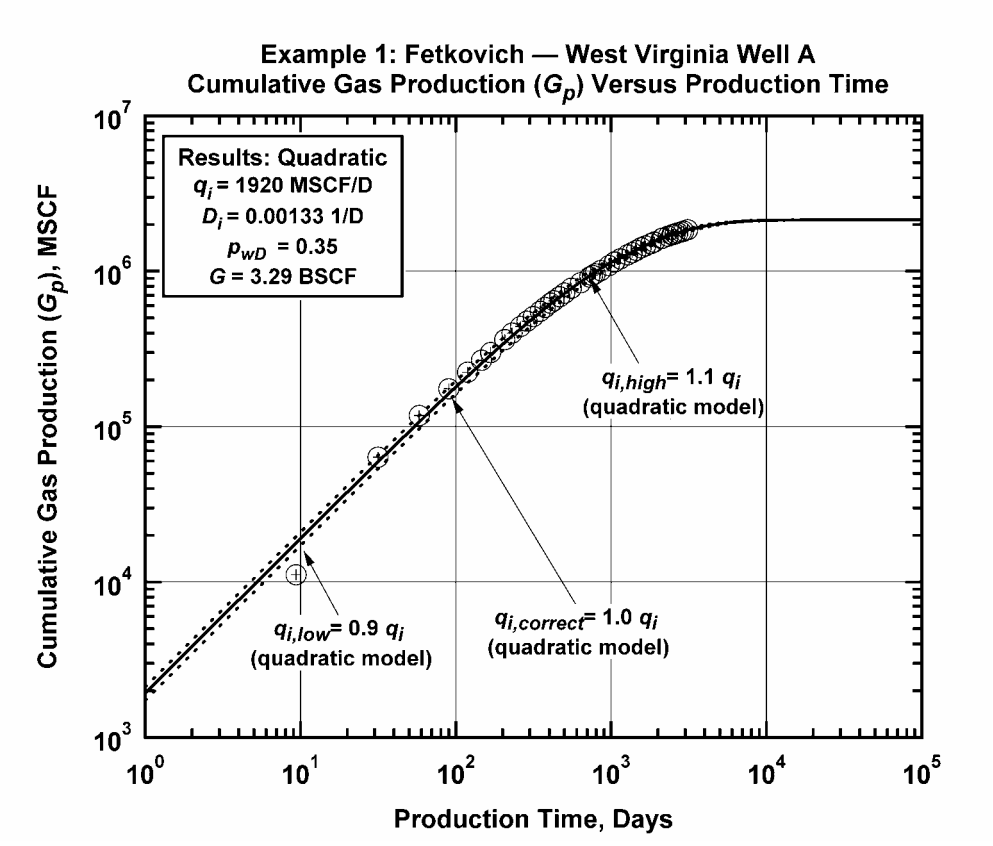


**Figure 4.3 – West Virginia Well A (Fetkovich, *et al.*[8]): $G_p$ versus *t*.**

In **Figs. 4.6-4.8** we present plotting functions $PF_1$, $PF_2$, and $PF_3$ (respectively). As in previous cases, we again present multiple and model functions (for $PF_1$ and $PF_2$) — and we note excellent "convergence" of these functions and the subsequent extrapolations to estimate the gas-in-place, $G$.

The rate-cumulative type curve analyses are presented in **Figs. 4.9** and **4.10**. Although the data trends are generally sparse, the data trends shown on the "quadratic" rate-cumulative type curve (**Fig. 4.9)** are be seen to be tied to a particular type curve stem (*i.e.*, match one of the quadratic solution cases). The same cannot be said of the data/model match on the "hyperbolic" type curve (**Fig. 4.10)**. Upon close investigation, we note that the data plotted on the "hyperbolic" type curve appear to cross multiple stems — as such, we suggest that the use of "hyperbolic" analysis for case of a gas well can be somewhat inconclusive (and possibly inaccurate).

**Figure 4.11** presents the material balance decline type curve analysis for this case (refs. 12 and 16). We note excellent agreement between the data and the model functions. Given the strength of the match shown in **Fig. 4.11** we believe that this analysis is both accurate and consistent.

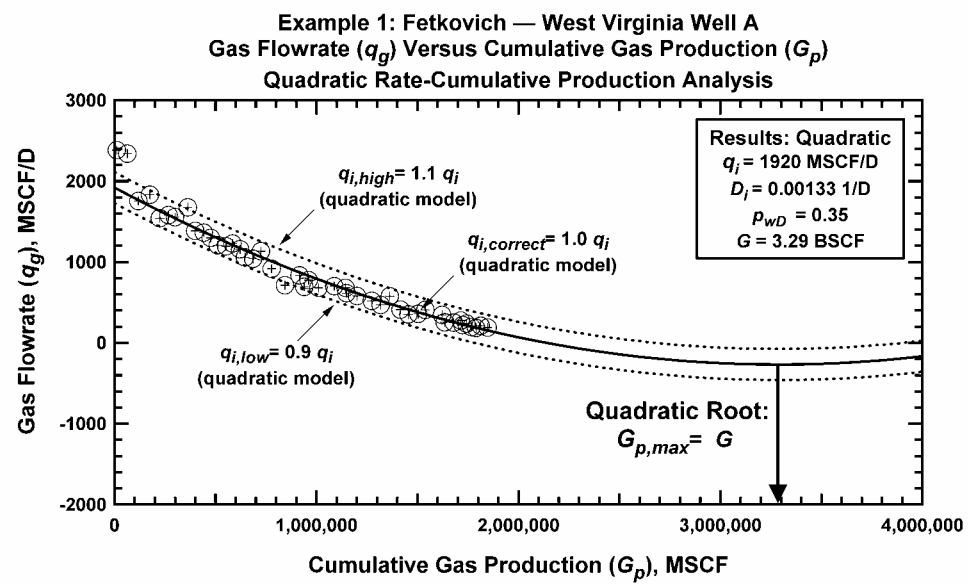


**Figure 4.4 – West Virginia Well A (Fetkovich, *et al.*[8]): $q_g$ versus $G_p$.**

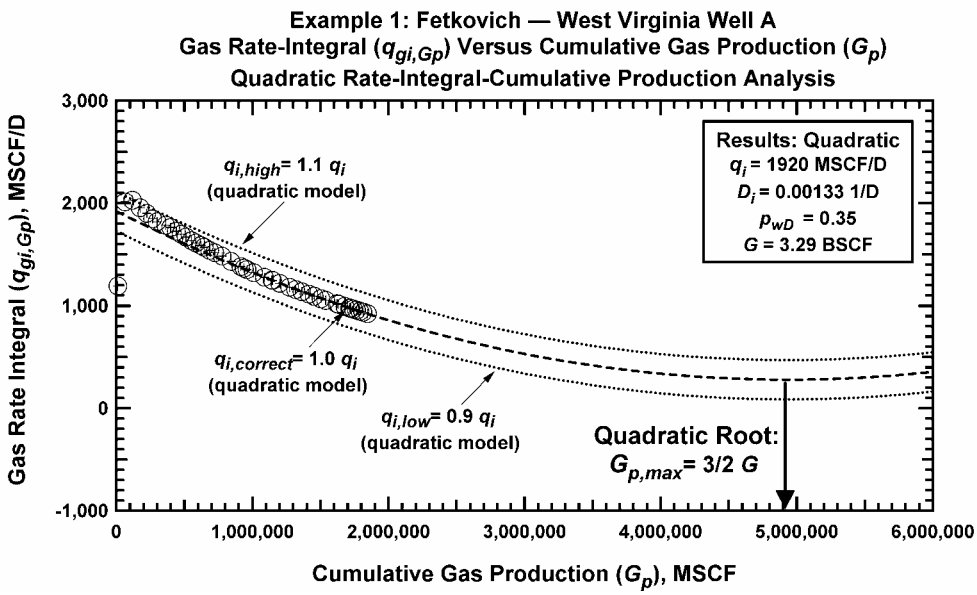


**Figure 4.5 – West Virginia Well A (Fetkovich, *et al.*[8]): $q_{qi,Gp}$ versus $G_p$.**

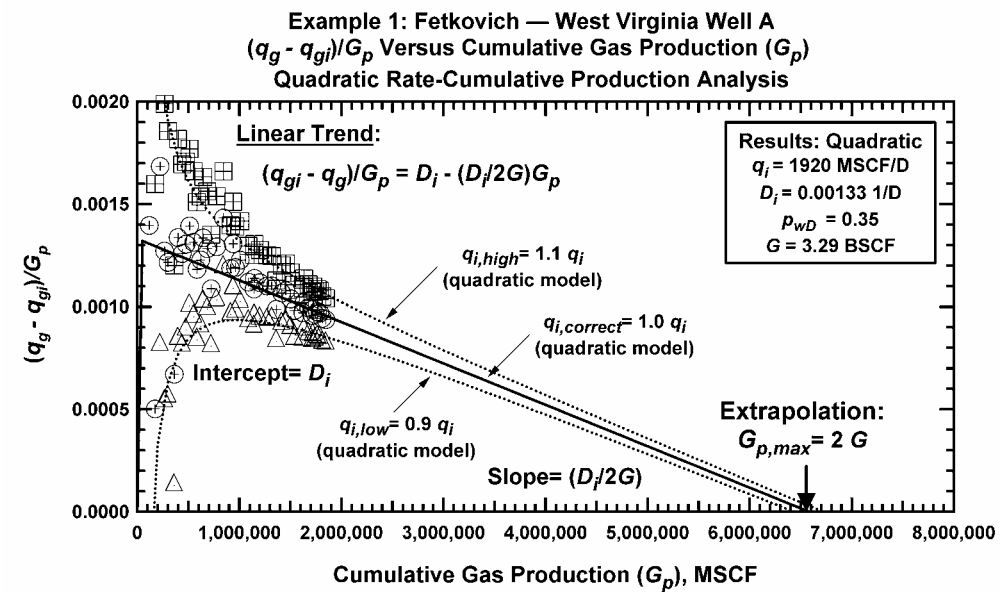


**Figure 4.6 – West Virginia Well A (Fetkovich, *et al.*[8]): $(q_{qi}-q_q)/G_p$ versus $G_p$ (Plotting Function 1 ($PF_1$)).**

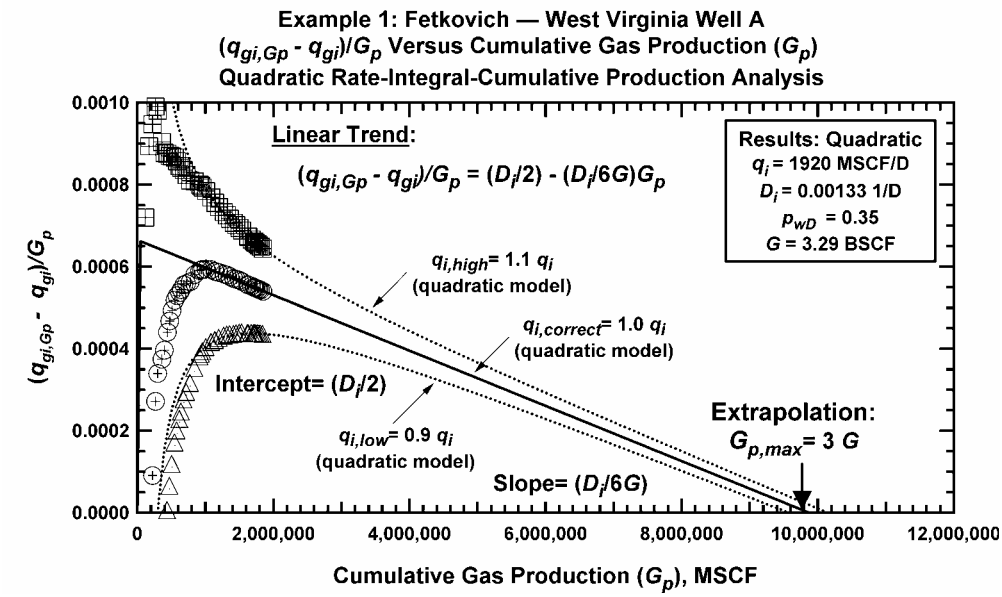


**Figure 4.7 – West Virginia Well A (Fetkovich, *et al.*[8]): $(q_{qi,Gp}-q_{qi})/G_p$ versus $G_p$ (Plotting Function 2 ($PF_2$)).**

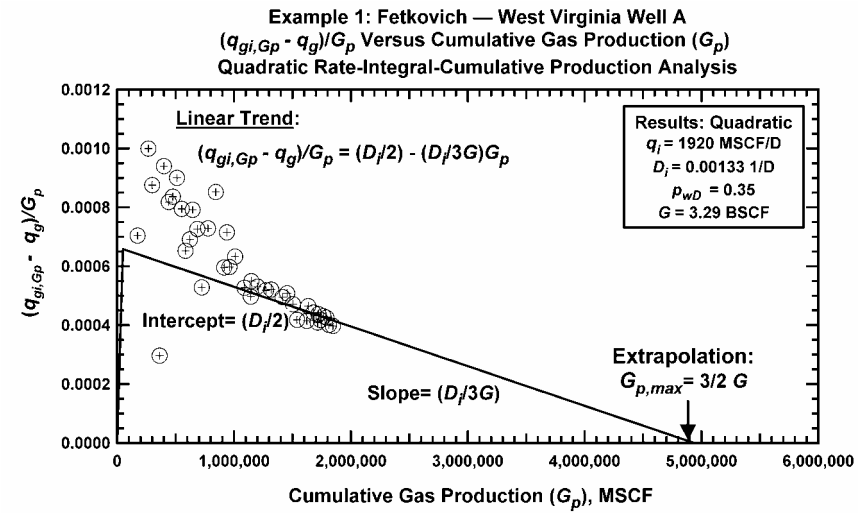


**Figure 4.8 – West Virginia Well A (Fetkovich, *et al.*[8]): $(q_{qi,Gp}-q_q)/G_p$ versus $G_p$ (Plotting Function 3 ($PF_3$)).**

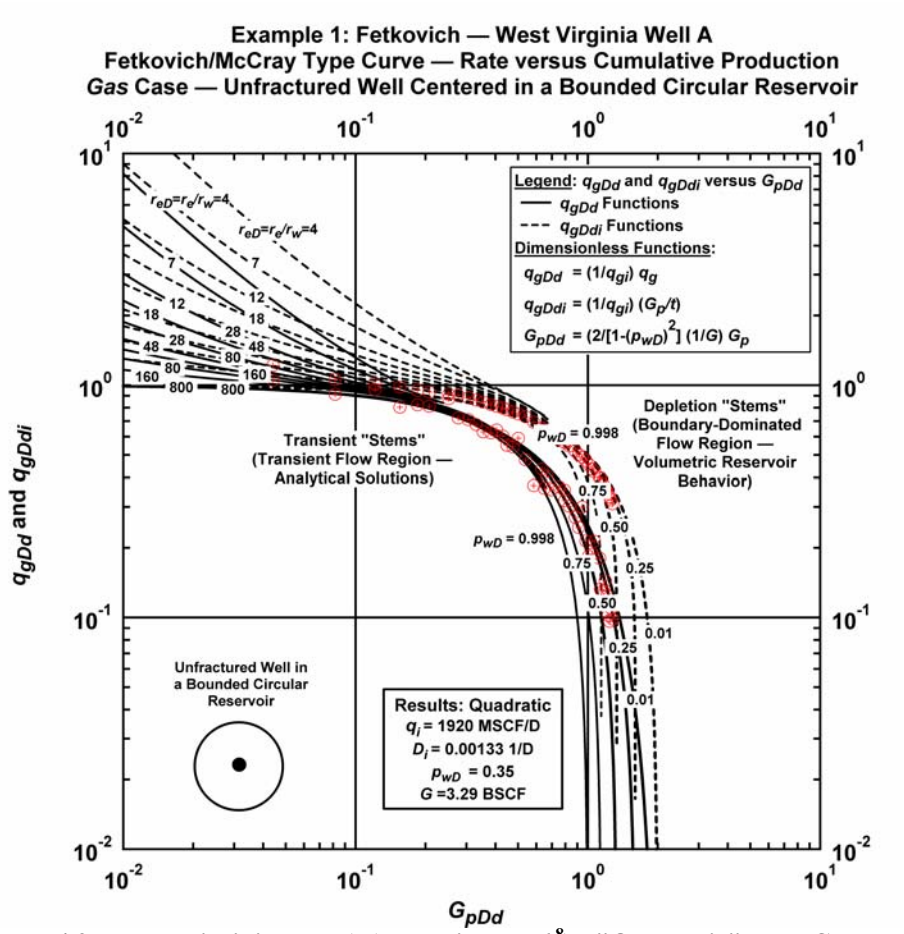


**Figure 4.9 – West Virginia Well A (Fetkovich, *et al.*[8]): "Quadratic" Rate-Cumulative Decline Type Curve Analysis.**

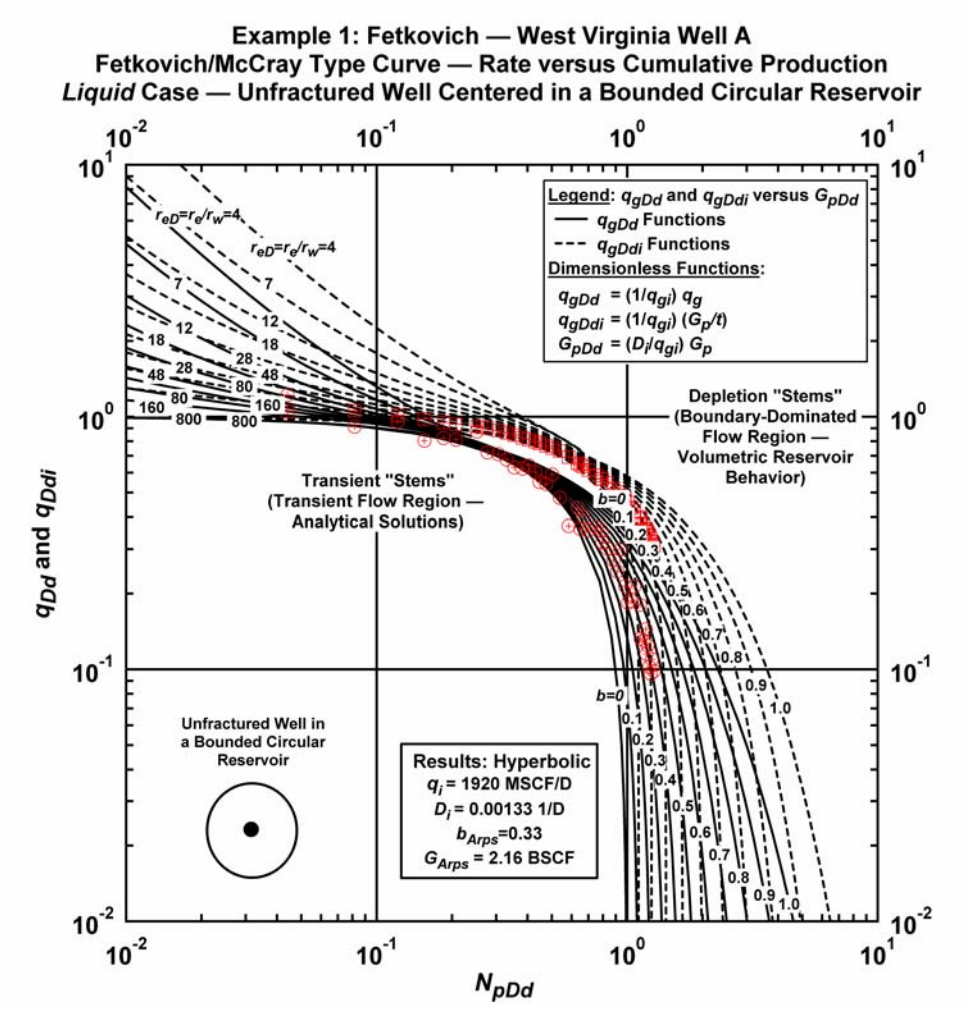


**Figure 4.10 – West Virginia Well A (Fetkovich, *et al.*[8]): "Hyperbolic" Rate-Cumulative Decline Type Curve Analysis.**

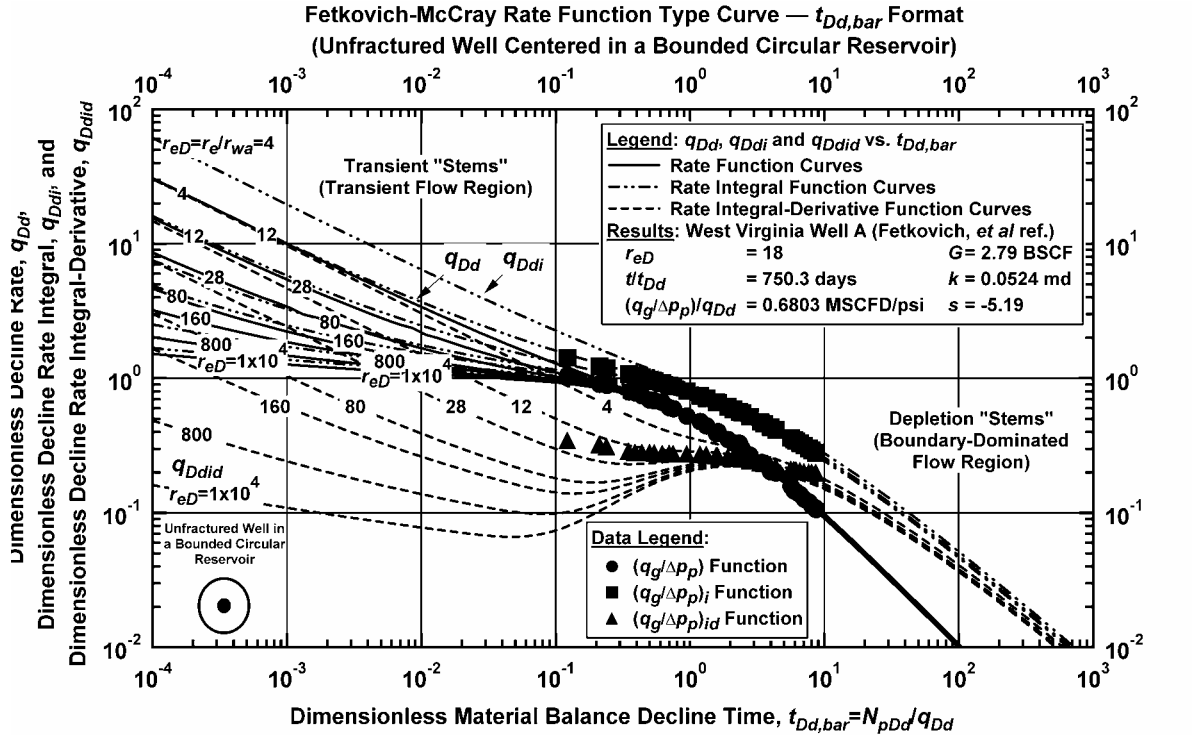


**Figure 4.11 – West Virginia Well A (Fetkovich, *et al.*[8]): Decline Type Curve Analysis.**

The results for this case are given below:

*Analysis Results*: West Virginia Well A

New "quadratic analysis" methods:

| | |
|---|---|
| Initial gas production rate, $q_{gi}$ | = 1920 MSCF/D |
| Decline constant, $D_i$ | = 0.00133 1/D |
| Dimensionless pressure, $p_{wD}$ | = 0.35 |
| Gas-in-place, $G$ | = 3.29 BSCF |

Material balance decline type curve analysis: (methods of ref. 12 and 16)

| | |
|---|---|
| Gas-in-place, $G$ | = 2.79 BSCF |
| Gas permeability, $k_g$ ($r_{eD}$=18) | = 0.0524 md |
| Near-well skin factor, $s$ ($r_{eD}$=18) | = -5.19 (dim-less) |

Fetkovich, *et al.*: (ref. 8)

| | |
|---|---|
| Gas-in-place, $G$ | = 3.36 BSCF |
| Gas permeability, $k_g$ ($r_{eD}$=20) | = 0.0524 md |
| Near-well skin factor, $s$ ($r_{eD}$=20) | = -5.17 (dim-less) |

Fraim and Wattenbarger: (ref. 14)

| | |
|---|---|
| Gas-in-place, $G$ | = 3.035 BSCF |
| Gas permeability, $k_g$ ($r_{eD}$=24) | = 0.077 md |
| Near-well skin factor, $s$ ($r_{eD}$=24) | = -5.08 (dim-less) |

McCray, *et al.*: (ref. 17)

| | |
|---|---|
| Gas-in-place, $G$ ($r_{eD}$=20) | = 2.62 BSCF |
| Gas permeability, $k_g$ ($r_{eD}$=20) | = 0.054 md |
| Near-well skin factor, $s$ ($r_{eD}$=20) | = -4.71 (dim-less) |

We recognize that there are differences in these analyses — in particular, our estimate of gas-in-place obtained using material balance decline type curve analysis are "conservative" (as well as the results from refs. 14 and 17 which were generated using similar theories). However, this observation of a "conservative" estimate of gas-in-place is consistent with other such experiences — and we do note that all of the methods used in this work give identical results in the case where we considered simulated well performance behavior. We suspect that the rigorous analyses (*e.g.*, decline type curve analysis) may require better estimates/knowledge of rock and fluid properties. Similarly, we believe that the "less rigorous" analyses simply do not require such accuracy in the fluid and rock property data. Regardless, we are satisfied that our analysis of the data for this case is both comprehensive and appropriate.

**4.2 Practical Limitations of the New Methodology**

In this section we briefly identify and discuss factors/issues that we perceive to be limitations as the implimentation of this new suite of analyses for production data obtained from gas wells.

Reservoir pressure: Recall that the base relations from which this methodology was derived presumes moderate to low pressure reservoir behavior (*i.e.*, $p_i$<6000 psia). Although we have validated this methodology using data from simulated cases at pressures of up to 10,000 psia and for field data at pressures greater than 12,000 psia, we recommend that the analyst keep this limitation in mind. While we would not suggest that applications for pressures greater than 6000 psia be avoided, we do urge that as many other analyses as possible be engaged to compliment our proposed methodology (*e.g.*, classic decline curve analysis, material balance, decline type curve analysis, etc.).

Bottomhole flowing pressure (constant): While this has (apparently) not proved to be a limitation for field cases we have considered where the pressure has varied substantially, we do note that there will be cases where the issue of variations in the bottomhole flowing pressure becomes significant. As earlier, we suggest the use of complimentary analyses to ensure proper results are obtained.

Flow regime: Although this methodology was derived assuming boundary-dominated (or pseudo-steady-state) flow behavior in the reservoir, it is inevitable that the methodology will be "accidentally" employed on data which lie in the transient or transition flow regimes. To this issue we advise vigilance — clearly this methodology (as would any technique) should not be applied outside the conditions for which it was derived. We urge that the methods in this work be performed simultaneously with other techniques to ensure that the appropriate conditions exist for the application of the proposed methodology.

Data quantity/quality: While we would describe this new method as "error tolerant," we recognize that some data simply do have sufficient quality to warrant certain applications. If there is a question of data quality, we encourage application of this methodology — it should be self-evident in the spreadsheet analysis format. On the other hand, the issue of data quantity is critical.

This methodology must only be performed on data experiencing boundary-dominated flow behavior (as noted above) — but we also note that in addition to the duration of the data (*i.e.*, into boundary-do-minated flow conditions) we must also recognize that the frequency of data acquisition is a major issue. Daily measurements are preferred and monthly measurements (or summaries) are most com-mon — but yearly estimates/measurements of production data may not be sufficient for a meaningful analysis to be achieved.

# CHAPTER V
# SUMMARY, CONCLUSIONS, AND RECOMMENDATIONS FOR FUTURE WORK

## 5.1 Summary

We have proposed a conceptual model for the simplified analysis of rate and cumulative production data for case of a volumetric dry gas reservoir produced at a constant bottomhole flowing pressure through a single well. This conceptual model was proposed using solutions provided by Knowles[1] and Ansah, *et al*.[21] — and we note that Knowles and Ansah, *et al*. were focused on forward modeling rather than analysis, so, to our knowledge, our proposal is unique.

Once we proposed the base model (Eq. 1.1), we proceeded to develop plots and plotting functions using this model — and in doing so we created a comprehensive analysis procedure using a "spreadsheet" approach where all analyses are linked to a common set of parameters. This analysis procedure (and the imbedded plotting functions) was validated using a large suite of numerical simulations as well as a wide variety of field data cases. We believe that the proposed analyses, plotting functions, and procedures are robust (and unique) and should be considered appropriate tools for the practical analysis of field data.

## 5.2 Conclusions

The following conclusions are made based on the results obtained from this work

1. Base Solution: (*i.e.,* the quadratic $q_g$-$G_p$ relation) The base $q_g$-$G_p$ result was proposed and effectively validated by Knowles[1] and Ansah, *et al*.[21] While neither Knowles nor Ansah, *et al.* developed analysis techniques based on the $q_g$-$G_p$ result (*i.e.*, Eq. 1.1), our present work validates the concept and application of the proposed "Knowles" model for the analysis and interpretation of field data. Recall that this rate-cumulative production model is given by:

$$q_g = q_{gi} - \frac{2q_{gi}}{\left[1-\left[\frac{p_{wf}/z_{wf}}{p_i/z_i}\right]^2\right]G}G_p + \frac{q_{gi}}{\left[1-\left[\frac{p_{wf}/z_{wf}}{p_i/z_i}\right]^2\right]G^2}G_p^2 \quad \text{.....(1.1)}$$

2. Rate-Cumulative Plots: We have proposed the use of the base "Knowles" relation as a plotting function (*i.e.*, $q_g$ versus $G_p$) and we find that, while the "root" for estimating the gas-in-place ($G$) is perhaps unwieldy using graphical plots, we also find that this function is quite useful for analysis. The auxiliary function $(q_g)_{i,Gp}$ is also plotted versus $G_p$ and we find that this function is generally much smoother than the $q_g$-$G_p$ trend. The simultaneous application of these plots has proved to be very useful.

For reference, we recall the definition of the auxiliary function $(q_g)_{i,Gp}$, which is given by:

$$(q_g)_{i,Gp} \equiv \frac{1}{G_p}\int_0^{G_p} q_g \, dG_p \quad \text{.....(3.1)}$$

3. Plotting Functions: The proposed plotting functions proposed in this work (*e.g.*, $PF_1$, $PF_2$, and $PF_3$) are shown to be very effective as analysis mechanisms — particularly in the ability of these functions to distinguish volumetric reservoir behavior. For $PF_1$ and $PF_2$ we consider not only the data and model functions for a presumed value of the initial rate, $q_i$, but we also provide "high" and "low" cases which vary by $1.1q_i$ and $0.9q_i$, respectively — this approach is particularly useful in the interpretation of the production performance. Recalling these plotting functions as $PF_1$, $PF_2$ and $PF_3$ respectively we have:

$$\frac{q_{gi} - q_g}{G_p} = D_i - \frac{1}{2}\frac{D_i}{G}G_p \quad \text{.....(3.3)}$$

$$\frac{(q_g)_{i,Gp} - q_{gi}}{G_p} = \frac{1}{2}D_i - \frac{1}{6}\frac{D_i}{G}G_p \quad \text{.....(3.4)}$$

$$\frac{(q_g)_{i,Gp} - q_g}{G_p} = \frac{1}{2}D_i - \frac{1}{3}\frac{D_i}{G}G_p \quad \text{.....(3.5)}$$

4. Data Analysis Approach: Perhaps the most significant observation that can be made regarding this work is that, despite the considerable variations in data quantity and quality in the field cases, we were able to obtain robust and representative analyses. We credit the "spreadsheet" approach where multiple analyses are performed simultaneously. The value of this analysis approach can not be overstated — we believe that the "spreadsheet" approach should be adapted to other reservoir engineering activities (*e.g.*, well test analysis, PVT data calibration (tuning), petrophysical data interpretation, etc.).

### 5.3 Recommendations for Future Work

We put forth the following recommendations as mechanisms to extend this research work

1. Abnormally Pressured Gas Reservoirs: Such a proposal may be seen as ambitious, but we believe it is important to design a technique to observe/account for the influence of abnormal pressure effects which are often observed in the production data obtained from gas reservoirs. However, it is *possible* that the methods proposed in this work could be extended or modified to account for abnormal reservoir pressure effects.

2. Integration with Decline Type Curve Analysis: While we did utilize the new "rate-cumulative" decline type curves proposed in this work as part of the "spreadsheet" analysis, we did not incorporate the conventional rate-time decline type curve analyses. Some (model) calculations may not be convenient for spreadsheet-type programs, but we believe that an integrated analysis package would be very useful.

We do not recommend the extension of the plotting functions proposed in this work to include derivative functions (in particular, the derivative of the flowrate function). We have formulated such functions and have consistently found that even "good" production data are unsuited for the calculation of the rate derivative function. Perhaps it is better to say that we encourage extension of the proposed plotting functions, but we do not expect the rate derivative function to be of much value in such extensions.

# NOMENCLATURE

Variables:

$A$ = Reservoir drainage area, ft$^2$

$b$ = Decline exponent, dim-less

$B_{oi}$ = Oil formation volume factor at initial reservoir pressure, RB/SCF

$B_o$ = Oil formation volume factor at current conditions, RB/SCF

$C$ = coefficient of the flow equation, MSCF/D-psia$^2$/cp

$c_f$ = Formation (rock) compressibility, psi$^{-1}$

$c_g$ = Gas compressibility, psi$^{-1}$

$c_t$ = Total system compressibility, psi$^{-1}$

$c_w$ = Water compressibility, psi$^{-1}$

$D_{Arps}$ = Arps decline rate constant, D$^{-1}$

$D_i$ = Decline rate constant (quadratic gas flow model), D$^{-1}$

$G$ = Original-gas-in-place, MSCF or BSCF

$G_p$ = Cumulative gas production, MSCF

$h$ = Reservoir (net pay) thickness, ft

$k$ = Formation permeability, md

$L$ = Tubing length, ft

$m(p)$ = Al-Hussainy real gas pseudopressure, psia

$N$ = Original-oil-in-place (OOIP), STB

$Np,max$ = Oil reserves, STB

$\bar{p}$ = Average reservoir pressure, psia

$p_{wD}$ = Dimensionless, pressure, dim-less

$p_i$ = Initial reservoir pressure, psia

$p_{wf}$ = Bottomhole flowing pressure, psia

$q_{Dd}$ = Dimensionless decline rate, dim-less

$q_g$ = Gas flowrate, MSCF/D

$r_{eD}$ = Dimensionless reservoir radius, dim-less

$r_e$ = Reservoir drainage radius, ft

$R_S$ = Solution gas-oil ratio, scf/scf

$r_w$ = Wellbore radius , ft

$r_{wa}$ = Apparent wellbore radius (including formation damage, *etc*.), ft

$s$ = Skin factor

$s_{avg}$ = Average skin factor

$S_g$ = Gas saturation, fraction

$S_{wi}$ = Irreducible (connate) water saturation, fraction

$t$ = Time, D

$t_a$ = Agarwal pseudotime, hr/(cp/psi) (generally used for well test analysis)

$\bar{t}$ = Material balance time, D

$T$ = Reservoir temperature, deg R ($T$ is also given in deg F, but deg R is used in calculations)

$t_{Dd}$ = Dimensionless "decline" time

$z$ = Gas compressibility factor

Subscripts:

$a$ = Pseudotime

$avg$ = Average

$base$ = Base (reference) conditions

$D$ = Dimensionless

$g$ = Gas

o = Oil

$i$ = Initial condition

$p$ = Pseudopressure

$wf$ = Wellbore flowing conditions

Greek Symbols:

$\beta$ = Correlating parameter as defined in Chapter 3

$\lambda$ = Correlating parameter as defined in Chapter 3

$K$ = Correlating parameter as defined in Chapter 3

$\phi$ = Porosity, fraction

$\gamma_g$ = Specific gravity (air=1)

$\mu$ = Fluid viscosity, cp

# REFERENCES


1. Knowles R.S.: "Development and Verification of New Semi-Analytical Methods for the Analysis and Prediction of Gas Well Performance," M.S Thesis, Texas A&M University, College Station, TX (1999).
2. Schilthius, R.J.: "Active Oil and Reservoir Energy," *Trans*., AIME (1936) **118**, 33-52.
3. Dake, L.P.: *Fundamentals of Reservoir Engineering*, Elsevier Scientific Publishing Company, New York (1978).
4. Sullivan, S.A., Poston, S.W. and Piper, L.D.: "Using Short-Term Pressure Buildup Tests for Gas Reserve Estimation in Tight Gas Reservoirs," paper SPE 17707 presented at the 1998 SPE Gas Technology Symposium, Dallas, TX. June 13-15
5. Lewis, J.O., and Beal, C.H.: "Some New Methods for Estimating the Future Productions of Oil Wells," *Trans*. AIME (1918) **59**, 492-525.
6. Arps, J.J: "Analysis of Decline Curves," *Trans*. AIME (1945) **160**, 228-247.
7. Fetkovich, M.J.: "Decline Curve Analysis Using Type Curves," *JPT* (March 1968) 1065-1077.
8. Fetkovich, M.J., Vienot, M.E., Bradley and M.D., Kiesow, U.G.: "Decline Curve Analysis Using Type Curves – Case Histories," *SPEFE* (Dec. 1987) 637-656.
9. Al-Hussainy, R., Ramey, H.J., Jr., and Crawford, P.B.: "The Flow of Real Gases Through Porous Media", *JPT* (May 1966) 30-42.
10. Agarwal, R.G.: "Real Gas Pseudo-Time — A New Function for Pressure Buildup Analysis of MHF Gas Wells," paper SPE 8279 presented at the 1979 SPE Annual Technical Conference and Exhibition, Las Vegas, NV, Sept. 23-26.
11. Carter, R.D.: "Type Curves for Finite Radial and Linear Gas Flow Systems: Constant-Terminal Pressure Case," *SPEJ* (Oct. 1985) 116-121.
12. Doublet, L.E., Pande, P.K., McCollum, T.J and Blasingame, T.A.: "Decline Curve Analysis Using Type Curves – Analysis of Well Production Data Using Material Balance Time: Application to Field Cases," paper SPE 28688 presented at the 1994 Petroleum Conference and Exhibition of Mexico. Veracruz, Mexico, Oct. 10-13.
13. Lee, W.J., and Wattenbarger, R.A..: *Gas Reservoir Engineering*, *SPE* Textbook Series, Dallas, Volume 5, 1996, 214-229.

14. Fraim, M.L. and Wattenbarger, R.A.: "Gas Reservoir Decline Curve Analysis Using Type Curves with Real-Gas Pseudopressure and Normalized Time," *SPEFE* (Dec. 1987) 671-682; *Trans.* AIME, **290**

15. Blasingame, T.A. and Lee, W.J.: "Variable-Rate Reservoir Limits Testing," paper SPE 15028 presented at the 1986 SPE Permian Basin Oil and Gas Recovery Conference, Midland, TX, March 13-14.

16. Palacio, J.C. and Blasingame, T.A.: "Decline Curve Analysis Using Type Curves: Analysis of Gas Well Production Data," paper SPE 25909 presented at the 1993 SPE Rocky Mountain Regional/Low Permeability Reservoirs Symposium, Denver, CO. April 12-14.

17. Blasingame, T.A., McCray, T.C. and Lee, W.J.: "Decline Curve Analysis for Variable Pressure Drop/Variable Flowrate Systems," paper SPE 21513 presented at the 1991 SPE Gas Technology Symposium, Houston, TX, Jan. 23-24.

18. Callard, J.G. and Schenewerk, P.A..: "Reservoir Performance History Matching Using Rate/ Cumulative Type Curves," paper SPE 30793 presented at the 1995 SPE Annual Technical Conference and Exhibition, Dallas, TX, Oct. 22-25

19. Agarwal, R.G., Gardner, D.C., Kleinsteiber, S.W. and Fussell, D.D.: "Analyzing Well Production Data Using Combined-Type-Curve and Decline-Curve Analysis Concepts," paper 57916 presented at the 1998 SPE Annual Technical Conference and Exhibition, New Orleans Sept.27-30.

20. Rawlins E.L and Schellhardt, M.A.: *Back Pressure Data on Natural Gas Wells and Their Application to Production Practices*, Monograph Series USBM (1935) **7**.

21. Ansah, J., Knowles, R.S., and Blasingame, T.A.: "A Semi-Analytic (*p/z*) Rate-Time Relation for the Analysis and Prediction of Gas Well Performance," paper SPE 35268 presented at the 1996 SPE Mid-Continent Gas Symposium, Amarillo, TX, Apr. 28-30.

22. Buba, I.M., and Blasingame, T.A.: "Direct Estimation of Gas Reserves Using Production Data," paper 2002 SPE 77550 presented at the SPE Annual Technical Conference and Exhibition, San Antonio, TX, Sept. 30 - Oct. 3 2002.

# APPENDIX A
# ANALYSIS OF SIMULATED WELL PERFORMANCE CASES

There are two parts to this Appendix — the first set of cases presents the analysis plots for the condition where $p_{wf}$ = 1000 psia — the second set of cases presents the analysis plots for the condition where $p_{wf}$ = 500 psia.

**Simulated Well Performance Cases: (inventory of simulation cases)**

| Case | $p_i$ (psia) | $p_{wf}$ (psia) | $G$ (BSCF) |
|---|---|---|---|
| 1 | 2000 | 1000 | 1.87 |
| 2 | 3000 | 1000 | 2.79 |
| 3 | 4000 | 1000 | 3.57 |
| 4 | 5000 | 1000 | 4.20 |
| 5 | 6000 | 1000 | 4.72 |
| 6 | 7000 | 1000 | 5.14 |
| 7 | 8000 | 1000 | 5.50 |
| 8 | 9000 | 1000 | 5.81 |
| 9 | 10,000 | 1000 | 6.09 |
| 10 | 1000 | 500 | 0.897 |
| 11 | 2000 | 500 | 1.87 |
| 12 | 3000 | 500 | 2.79 |
| 13 | 4000 | 500 | 3.57 |
| 14 | 5000 | 500 | 4.20 |
| 15 | 6000 | 500 | 4.72 |
| 16 | 7000 | 500 | 5.14 |
| 17 | 8000 | 500 | 5.50 |
| 18 | 9000 | 500 | 5.81 |
| 19 | 10,000 | 500 | 6.09 |

**Simulated Well Performance Cases: (input data)**

Reservoir Properties:

| | |
|---|---|
| Wellbore radius, $r_w$ | = 0.0745 ft |
| Average net pay thickness, $h$ | = 30 ft |
| Net pay thickness, $h$ | = 30 ft |
| Formation permeability, $k$ | = 100 md |
| Average porosity, $\phi$ | = 0.30 (fraction) |
| Nominal well spacing | = 40 acres |
| Initial reservoir pressure, $p_i$ | = 1000 to 10,000 psia |

Fluid properties:

| | |
|---|---|
| Gas specific gravity, $\gamma_g$ | = 0.6 (air=1.0) |
| Reservoir temperature, $T$ | = 200 deg F |

Production parameters:

| | |
|---|---|
| Constant bottomhole pressure, $p_{wf}$ | = 500 or 1000 psia |

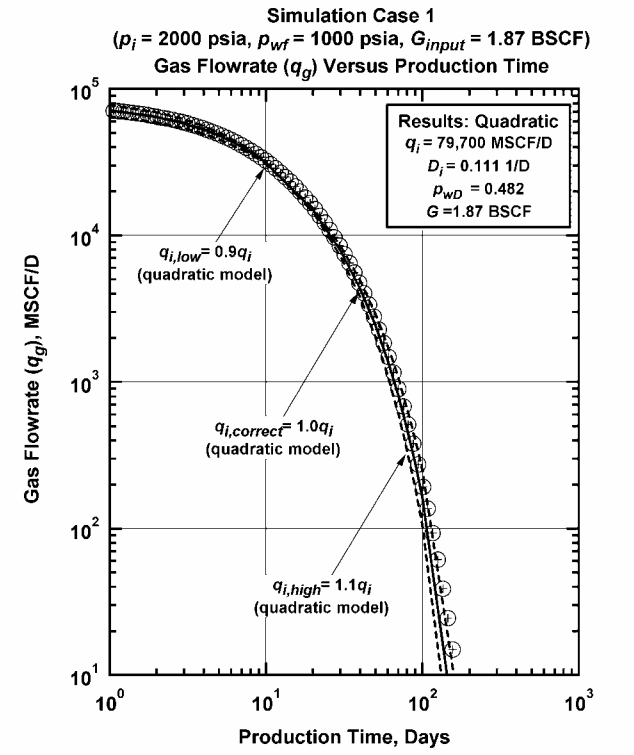


**Figure A-1 – Simulated Performance Case 1: $q_g$ versus $t$ ($p_i$=2000 psia, $p_{wf}$=1000 psia, $G_{input}$=1.87 BSCF).**

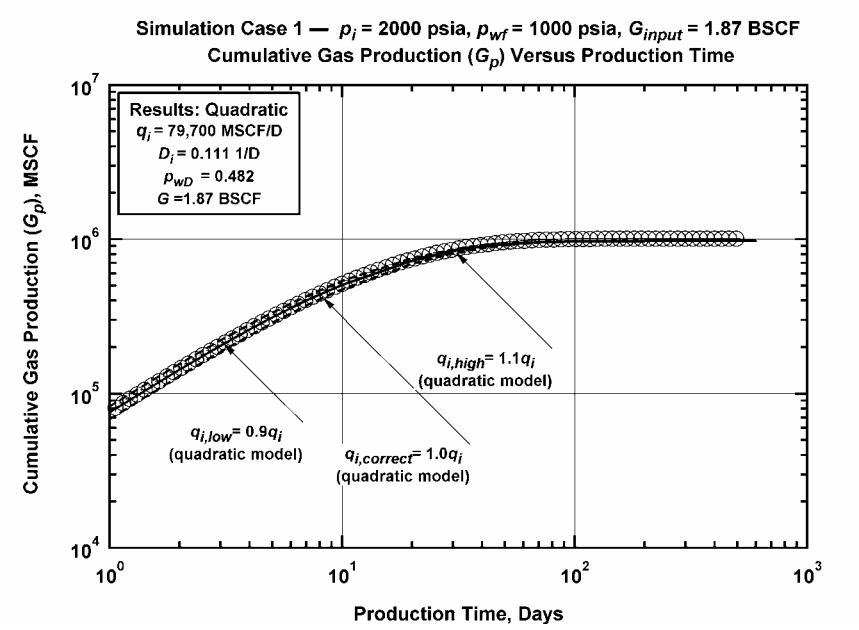


**Figure A-2 – Simulated Performance Case 1: $G_p$ versus $t$ ($p_i$=2000 psia, $p_{wf}$=1000 psia, $G_{input}$=1.87 BSCF).**

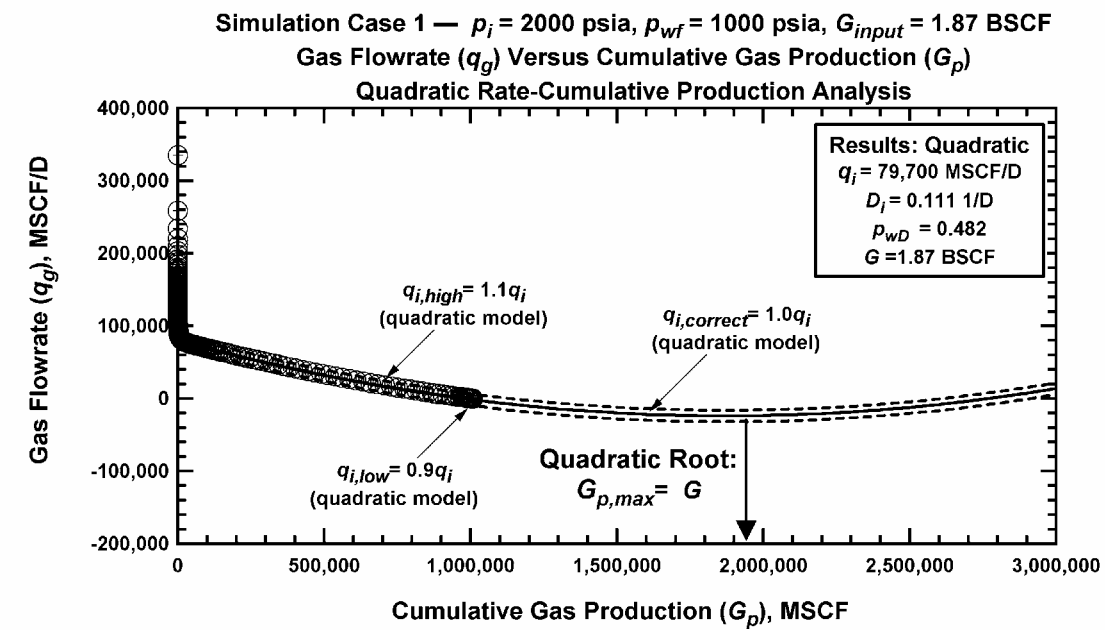


**Figure A-3 – Simulated Performance Case 1: $q_g$ versus $G_p$ ($p_i$=2000 psia, $p_{wf}$=1000 psia, $G_{input}$=1.87 BSCF).**

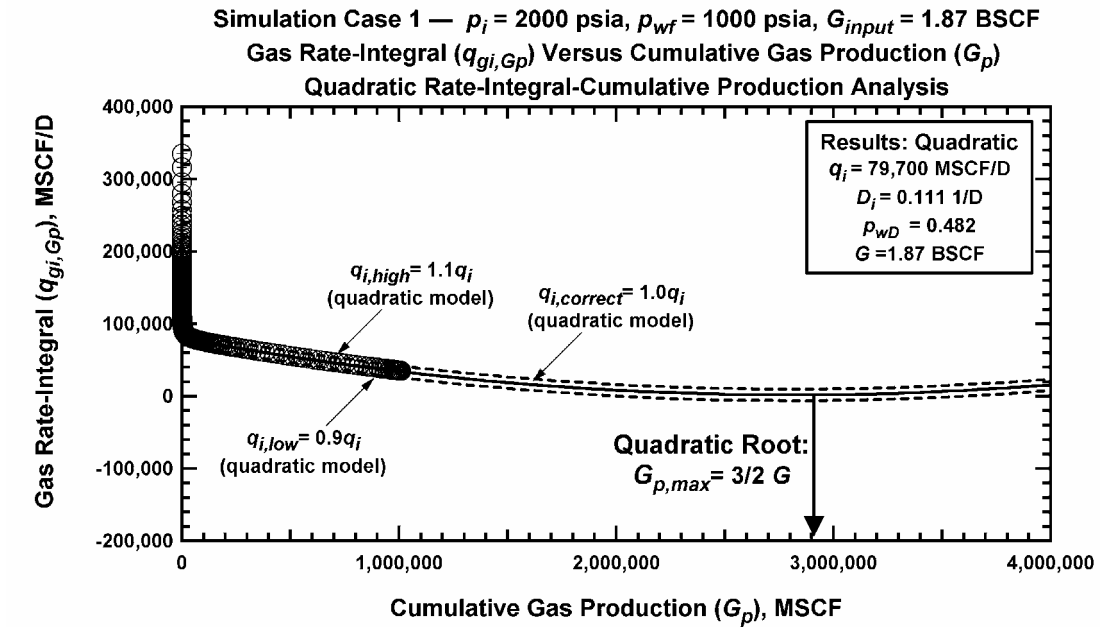


**Figure A-4 – Simulated Performance Case 1: $q_{qi,Gp}$ versus $G_p$ ($p_i$= 2000 psia, $p_{wf}$=1000 psia, $G_{input}$=1.87 BSCF).**

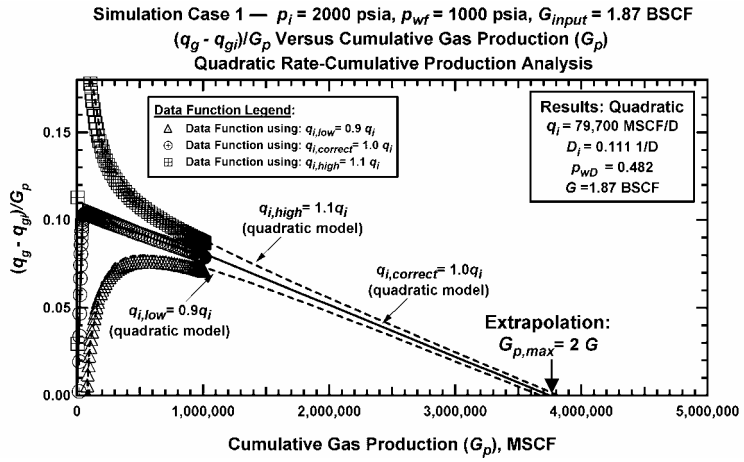


**Figure A-5 – Simulated Performance Case 1: $(q_{qi}-q_q)/G_p$ versus $G_p$ ($p_i$= 2000 psia, $p_{wf}$=1000 psia, $G_{input}$=1.87 BSCF) (Plotting Function 1 ($PF_1$)).**

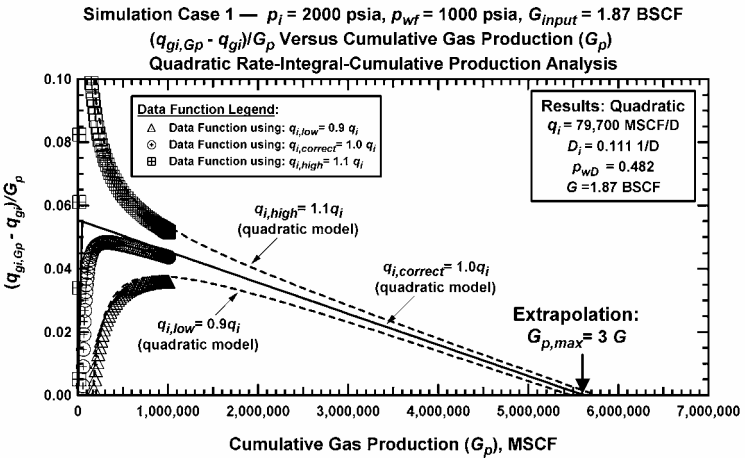


**Figure A-6 – Simulated Performance Case 1: $(q_{qi,Gp}-q_{qi})/G_p$ versus $G_p$ ($p_i$= 2000 psia, $p_{wf}$=1000 psia, $G_{input}$=1.87 BSCF) (Plotting Function 2 ($PF_2$)).**

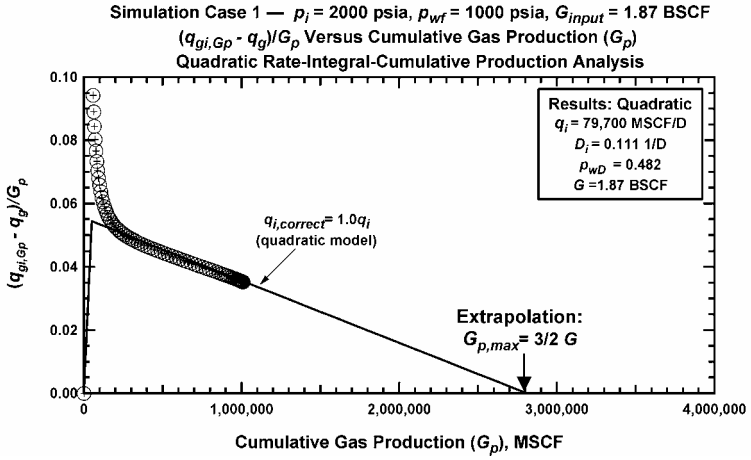


**Figure A-7 – Simulated Performance Case 1: $(q_{qi,Gp}-q_q)/G_p$ versus $G_p$ ($p_i$= 2000 psia, $p_{wf}$=1000 psia, $G_{input}$=4.20 BSCF) (Plotting Function 3 ($PF_3$)).**

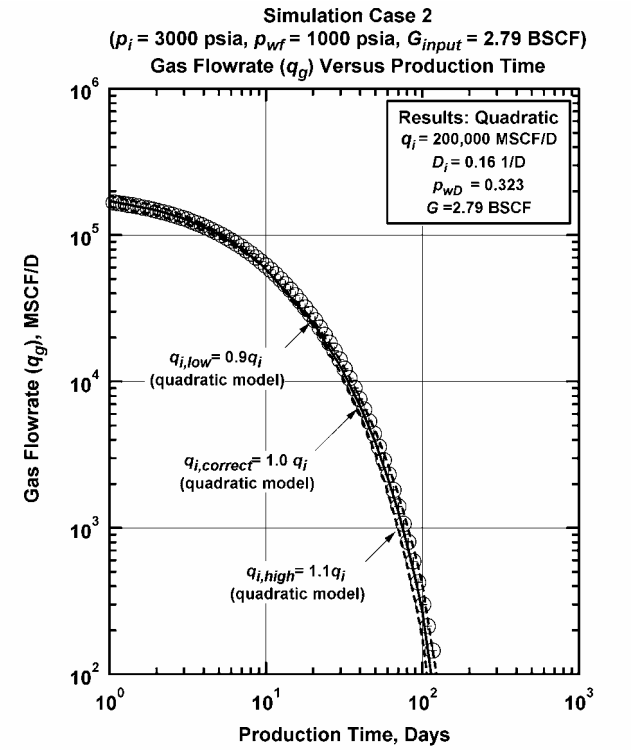


**Figure A-8 – Simulated Performance Case 2: $q_g$ versus $t$ ($p_i$=3000 psia, $p_{wf}$=1000 psia, $G_{input}$=2.79 BSCF).**

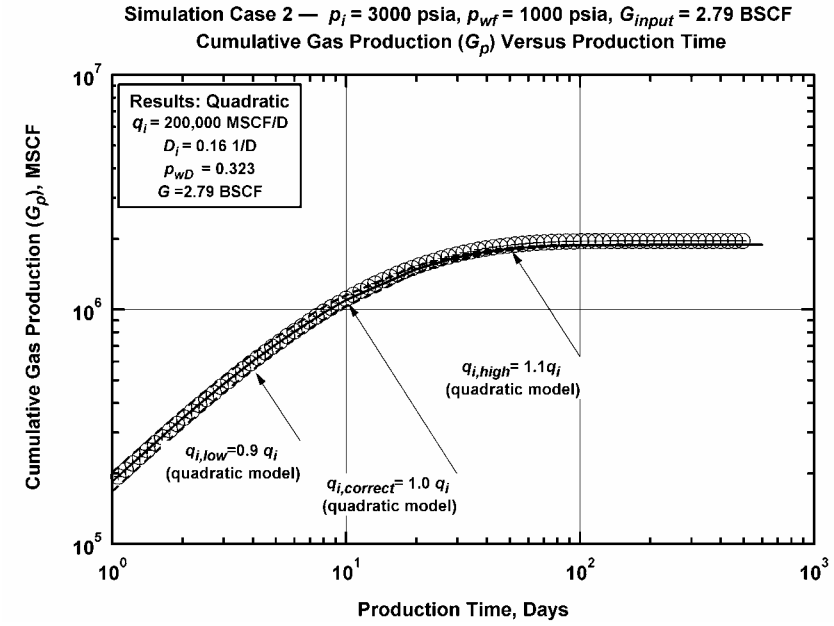


**Figure A-9 – Simulated Performance Case 2: $G_p$ versus $t$ ($p_i$=3000 psia, $p_{wf}$=1000 psia, $G_{input}$=2.79 BSCF).**

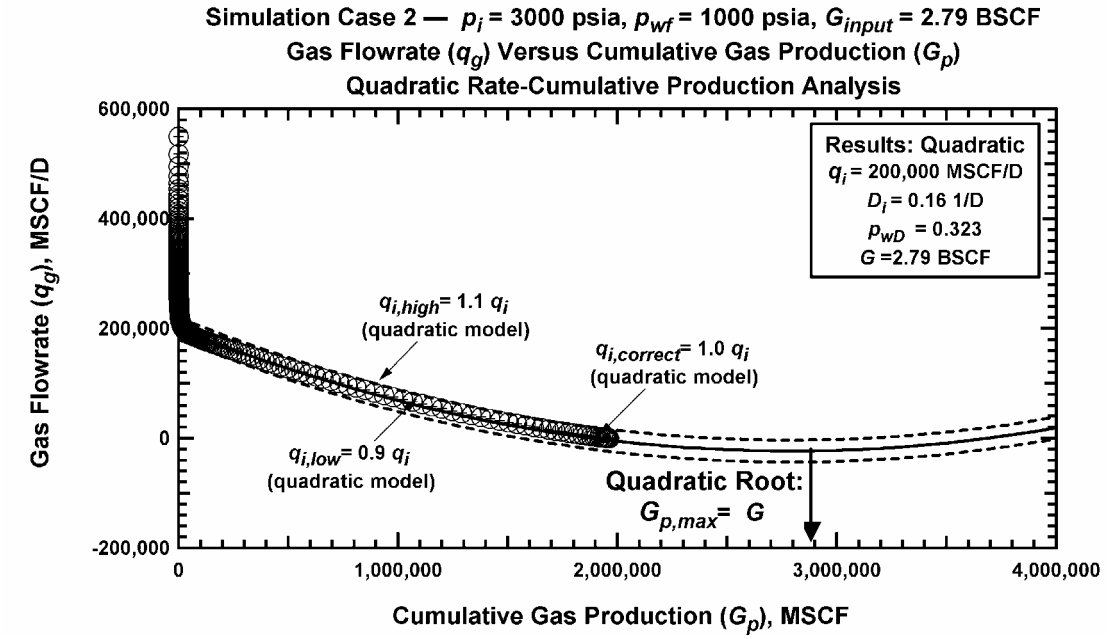


**Figure A-10 – Simulated Performance Case 2: $q_g$ versus $G_p$ ($p_i$=3000 psia, $p_{wf}$=1000 psia, $G_{input}$=2.79 BSCF).**

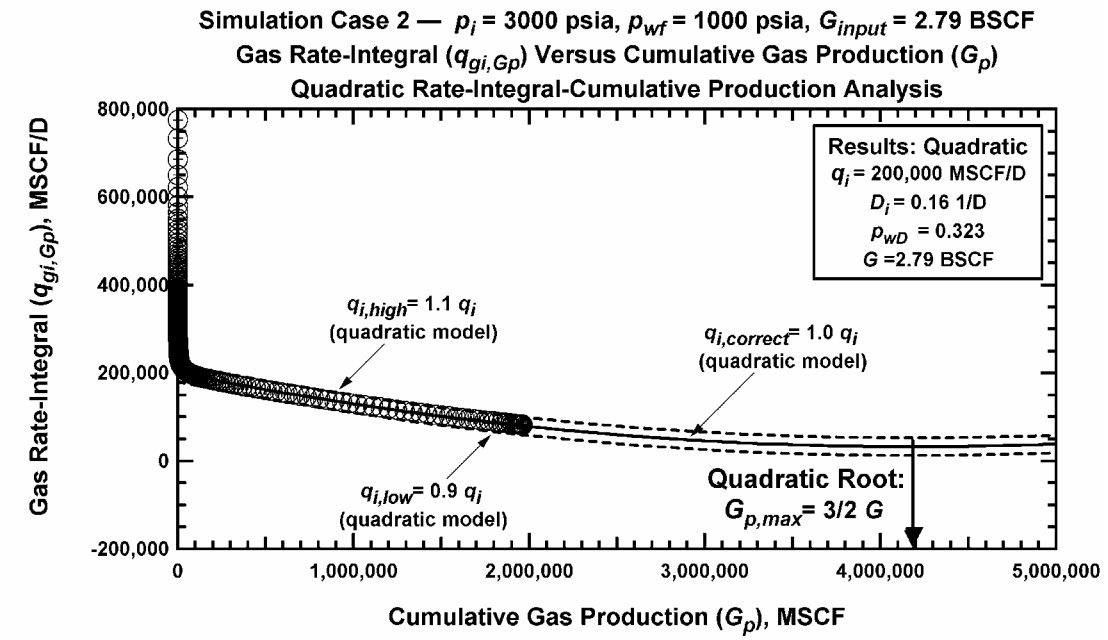


**Figure A-11 – Simulated Performance Case 2: $q_{qi,Gp}$ versus $G_p$ ($p_i$= 3000 psia, $p_{wf}$=1000 psia, $G_{input}$=2.79 BSCF).**

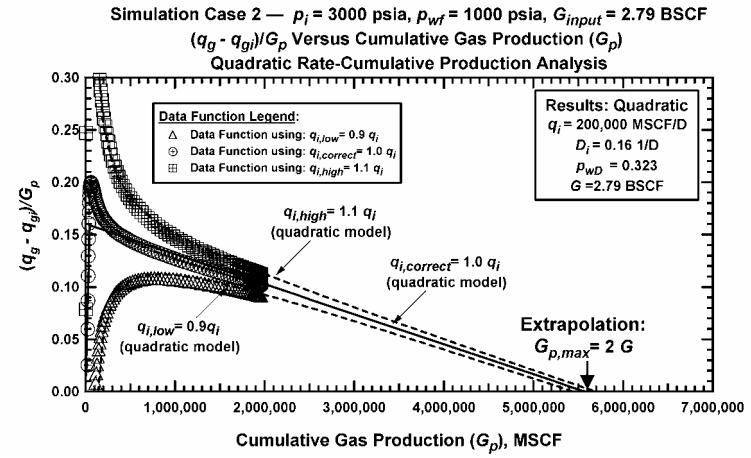


**Figure A-12 – Simulated Performance Case 2: $(q_{qi}-q_q)/G_p$ versus $G_p$ ($p_i$= 3000 psia, $p_{wf}$=1000 psia, $G_{input}$=2.79 BSCF) (Plotting Function 1 ($PF_1$)).**

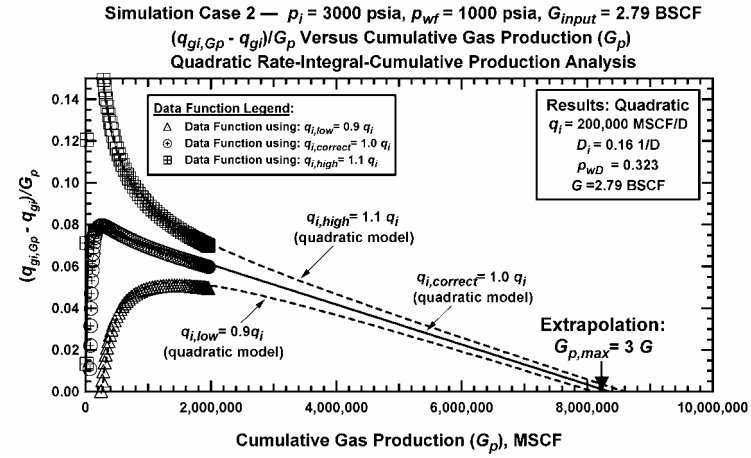


**Figure A-13 – Simulated Performance Case 2: $(q_{qi,Gp}-q_{qi})/G_p$ versus $G_p$ ($p_i$= 3000 psia, $p_{wf}$=1000 psia, $G_{input}$=2.79 BSCF) (Plotting Function 2 ($PF_2$)).**

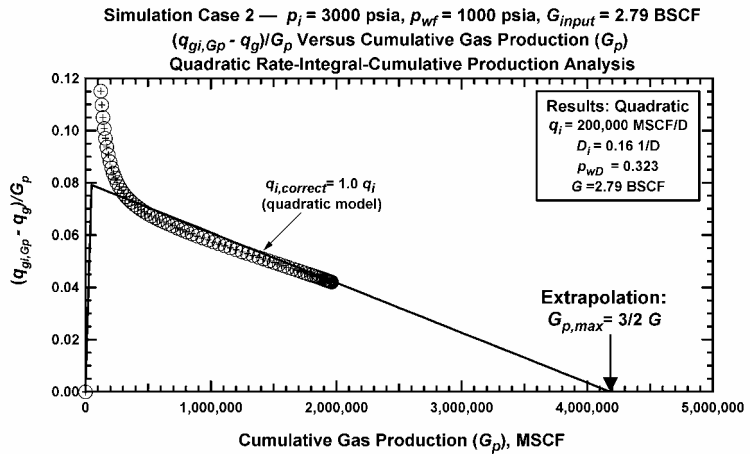


**Figure A-14 – Simulated Performance Case 2: $(q_{qi,Gp}-q_q)/G_p$ versus $G_p$ ($p_i$= 3000 psia, $p_{wf}$=1000 psia, $G_{input}$=2.79 BSCF) (Plotting Function 3 ($PF_3$)).**

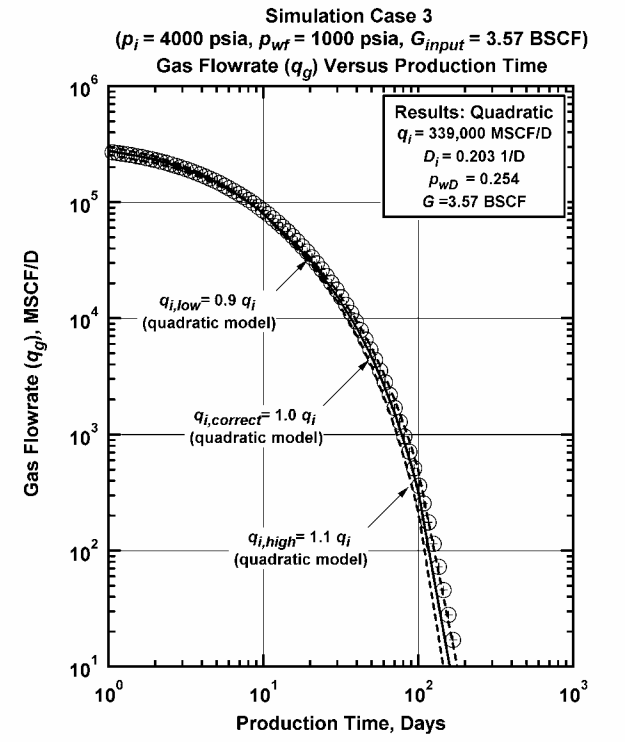


**Figure A-15 – Simulated Performance Case 3: $q_g$ versus $t$ ($p_i$=4000 psia, $p_{wf}$=1000 psia, $G_{input}$=3.57 BSCF).**

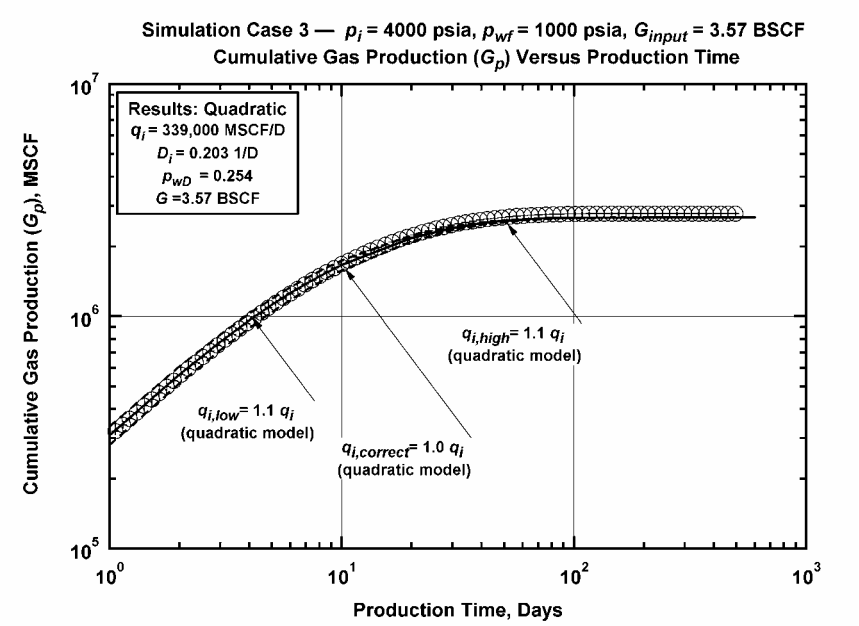


**Figure A-16 – Simulated Performance Case 3: $G_p$ versus $t$ ($p_i$=4000 psia, $p_{wf}$=1000 psia, $G_{input}$=3.57 BSCF).**

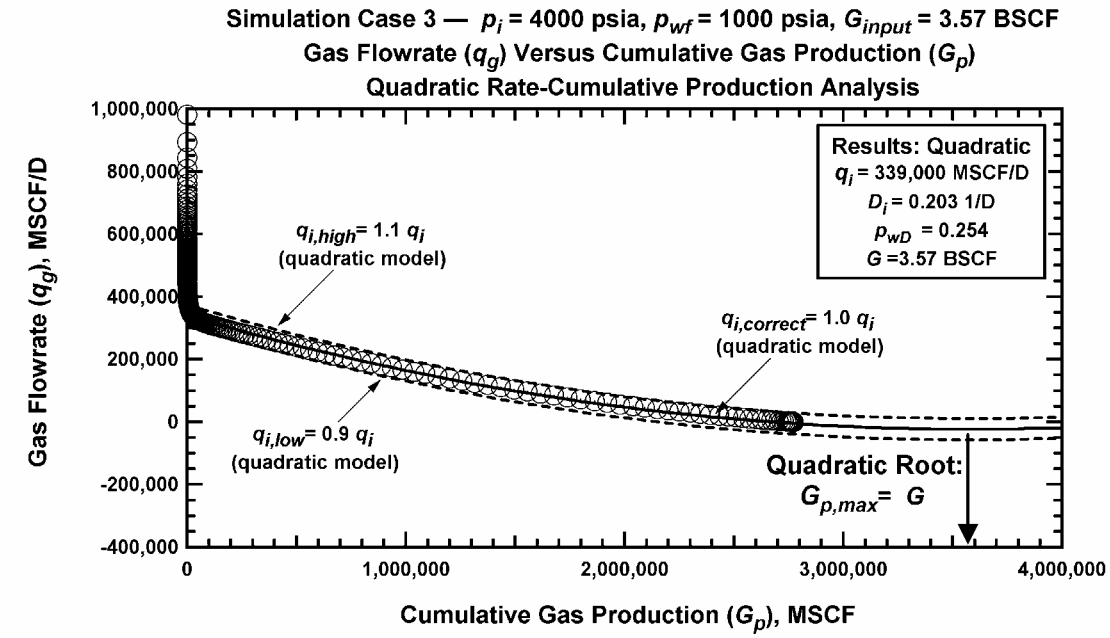


**Figure A-17 – Simulated Performance Case 3: $q_g$ versus $G_p$ ($p_i$=4000 psia, $p_{wf}$=1000 psia, $G_{input}$=3.57 BSCF).**

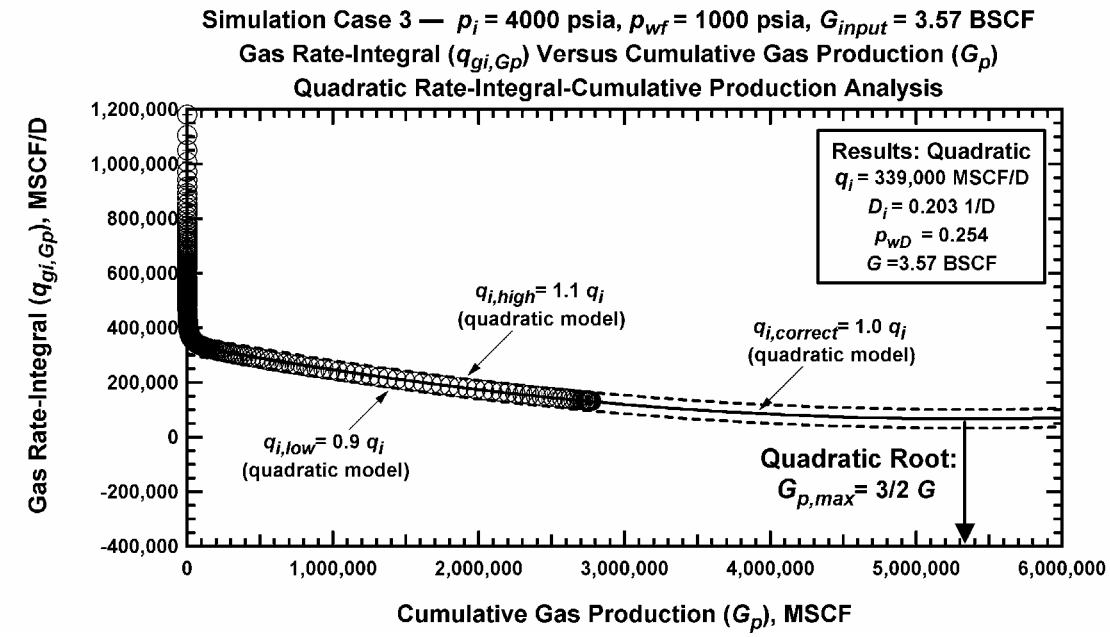


**Figure A-18 – Simulated Performance Case 3: $q_{qi,Gp}$ versus $G_p$ ($p_i$= 4000 psia, $p_{wf}$=1000 psia, $G_{input}$=3.57 BSCF).**

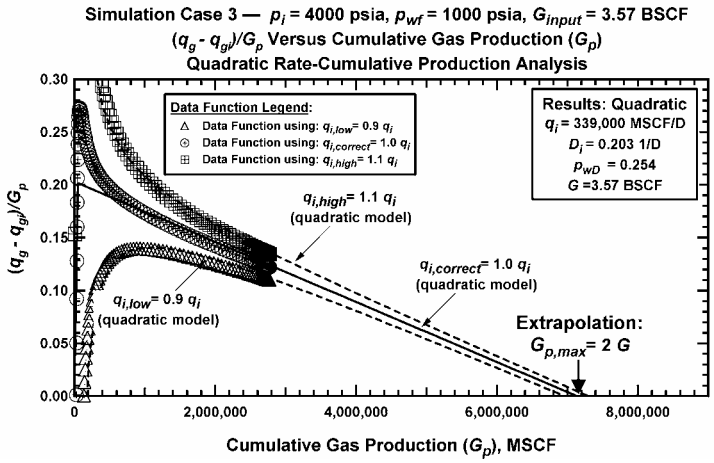


**Figure A-19 – Simulated Performance Case 3: $(q_{qi}-q_q)/G_p$ versus $G_p$ ($p_i$= 4000 psia, $p_{wf}$=1000 psia, $G_{input}$=3.57 BSCF) (Plotting Function 1 ($PF_1$)).**

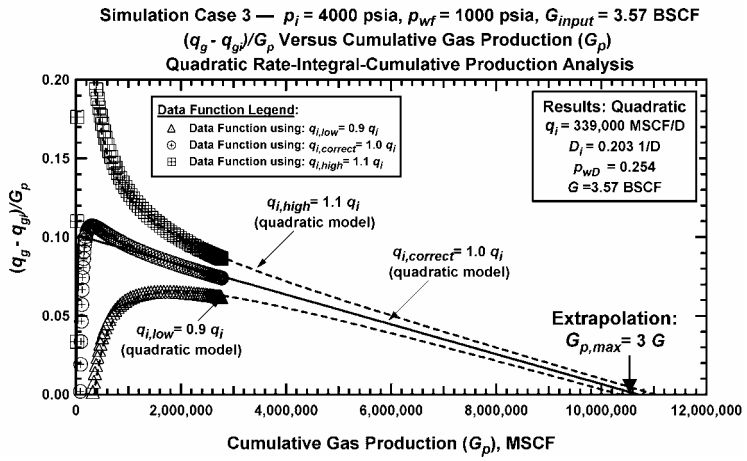


**Figure A-20 – Simulated Performance Case 3: $(q_{qi,Gp}-q_{qi})/G_p$ versus $G_p$ ($p_i$= 4000 psia, $p_{wf}$=1000 psia, $G_{input}$=3.57 BSCF) (Plotting Function 2 ($PF_2$)).**

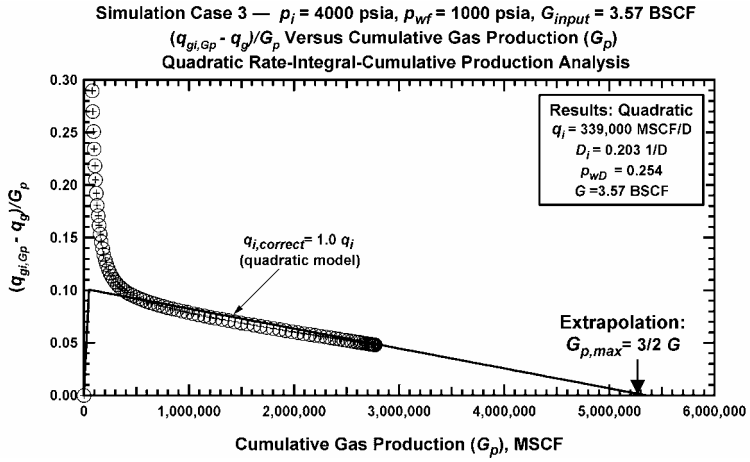


**Figure A-21 – Simulated Performance Case 3: $(q_{qi,Gp}-q_q)/G_p$ versus $G_p$ ($p_i$= 4000 psia, $p_{wf}$=1000 psia, $G_{input}$=3.57 BSCF) (Plotting Function 3 ($PF_3$)).**

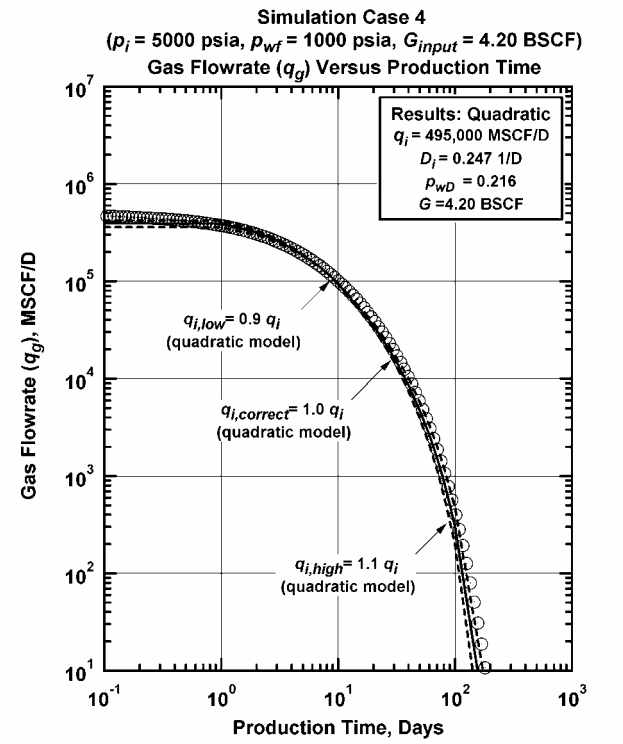


**Figure A-22 – Simulated Performance Case 4: $q_g$ versus $t$ ($p_i$=5000 psia, $p_{wf}$=1000 psia, $G_{input}$=4.20 BSCF).**

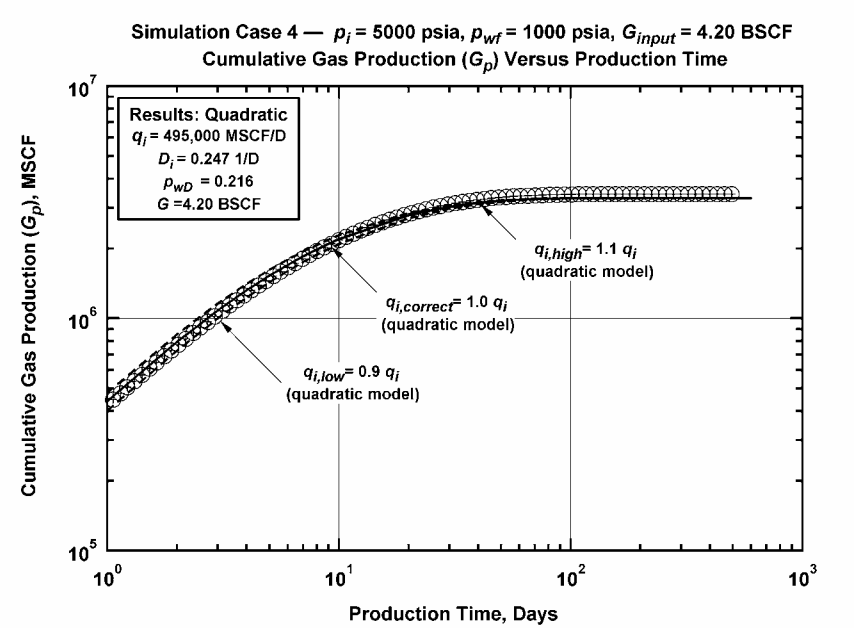


**Figure A-23 – Simulated Performance Case 4: $G_p$ versus $t$ ($p_i$=5000 psia, $p_{wf}$=1000 psia, $G_{input}$=4.20 BSCF).**

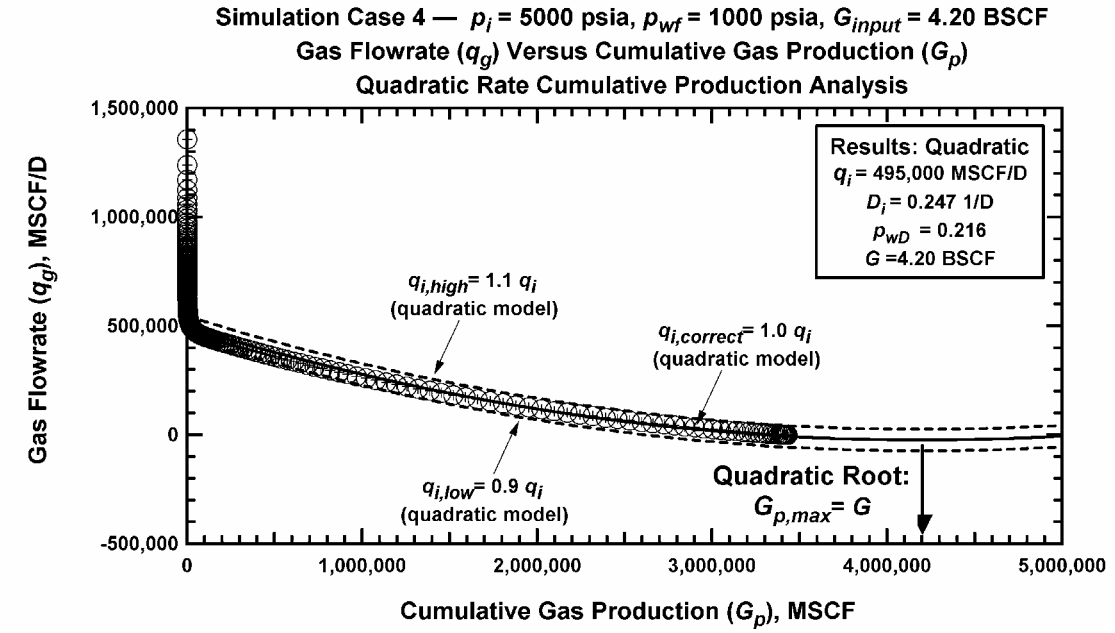


**Figure A-24 – Simulated Performance Case 4: $q_g$ versus $G_p$ ($p_i$=5000 psia, $p_{wf}$=1000 psia, $G_{input}$=4.20 BSCF).**

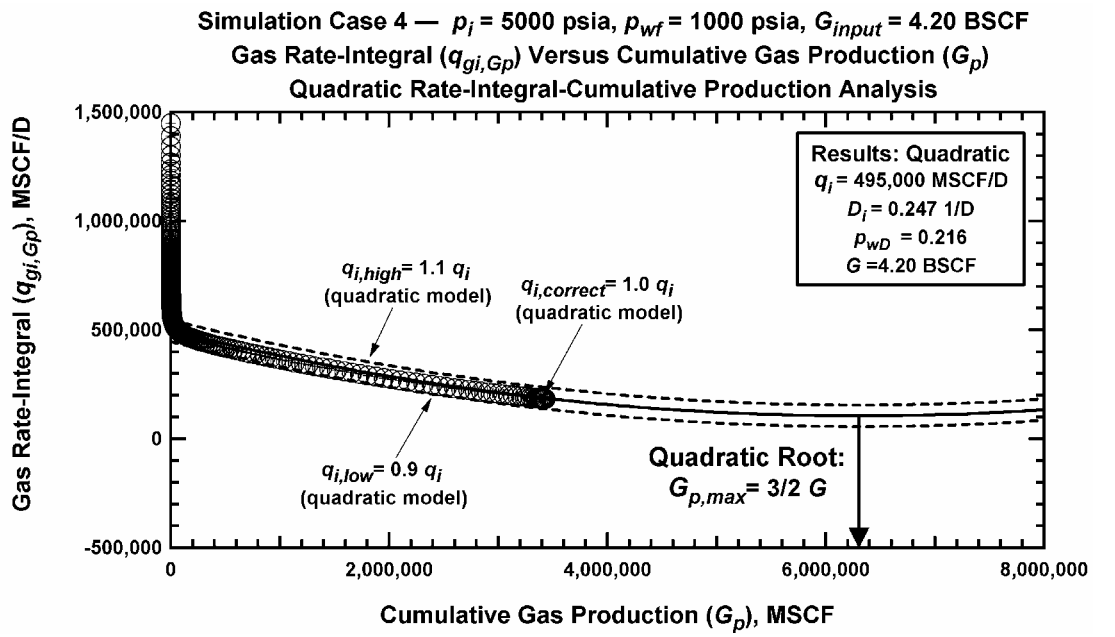


**Figure A-25 – Simulated Performance Case 4: $q_{qi,Gp}$ versus $G_p$ ($p_i$= 5000 psia, $p_{wf}$=1000 psia, $G_{input}$=4.20 BSCF).**

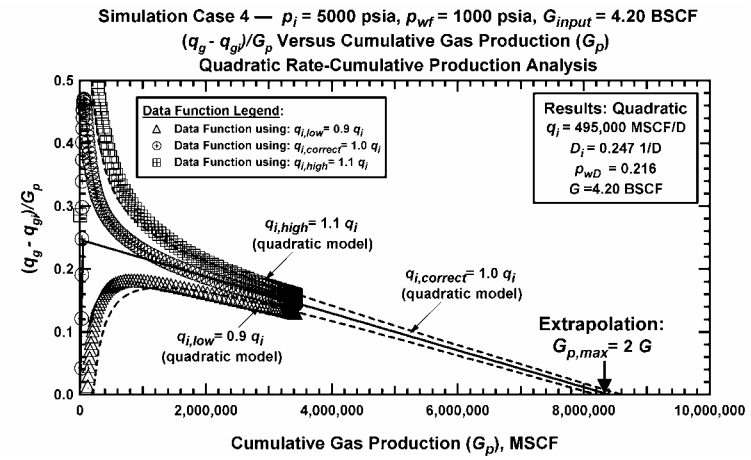


**Figure A-26 – Simulated Performance Case 4: $(q_{qi}-q_q)/G_p$ versus $G_p$ ($p_i$= 5000 psia, $p_{wf}$=1000 psia, $G_{input}$=4.20 BSCF) (Plotting Function 1 ($PF_1$)).**

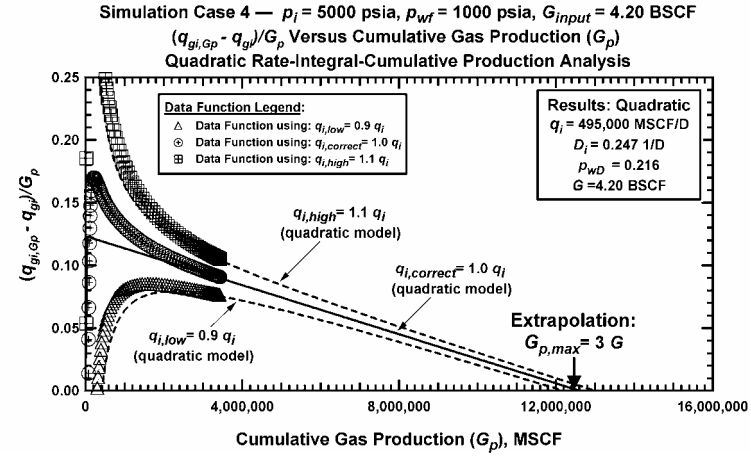


**Figure A-27 – Simulated Performance Case 4: $(q_{qi,Gp}-q_{qi})/G_p$ versus $G_p$ ($p_i$= 5000 psia, $p_{wf}$=1000 psia, $G_{input}$=4.20 BSCF) (Plotting Function 2 ($PF_2$)).**

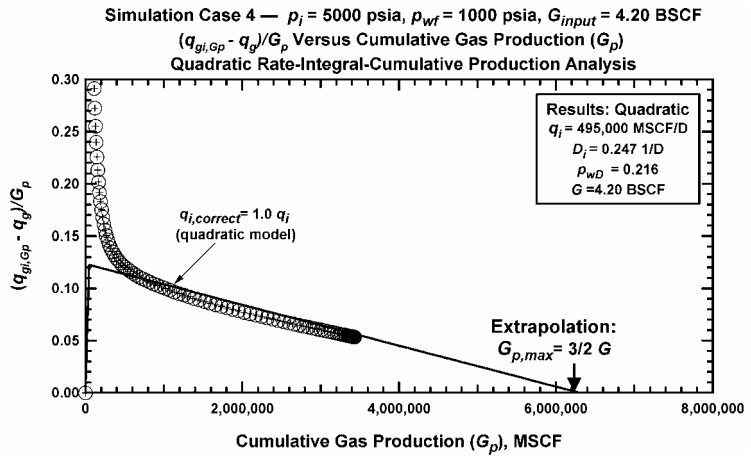


**Figure A-28 – Simulated Performance Case 4: $(q_{qi,Gp}-q_q)/G_p$ versus $G_p$ ($p_i$= 5000 psia, $p_{wf}$=1000 psia, $G_{input}$=4.20 BSCF) (Plotting Function 3 ($PF_3$)).**

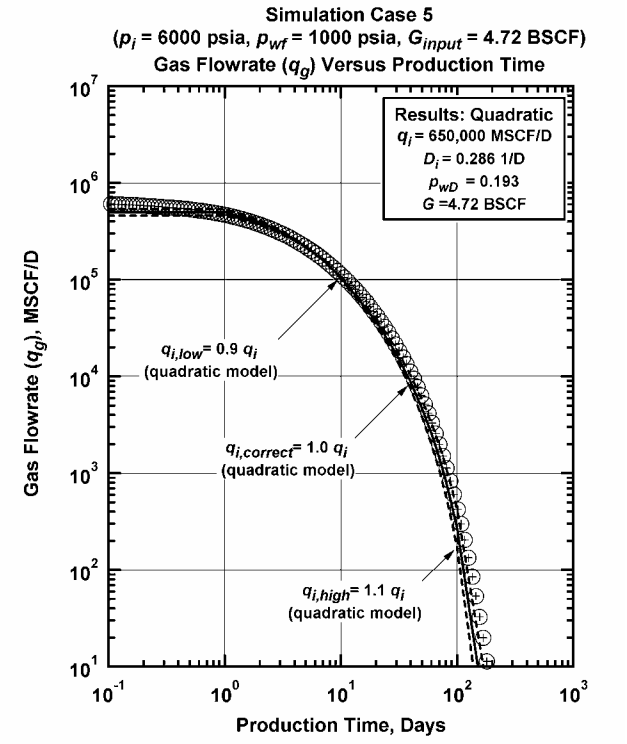


**Figure A-29 – Simulated Performance Case 5: $q_g$ versus $t$ ($p_i$=6000 psia, $p_{wf}$=1000 psia, $G_{input}$=4.72 BSCF).**

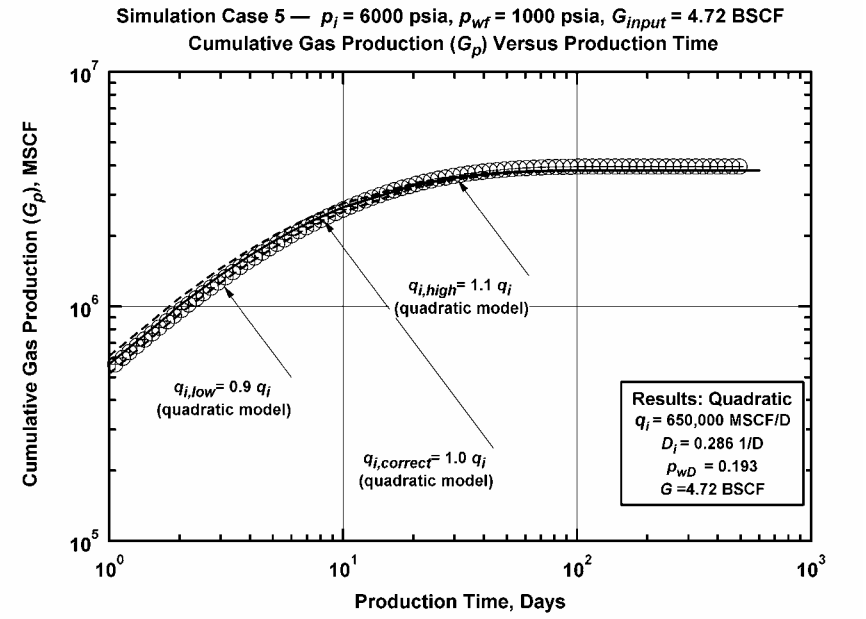


**Figure A-30 – Simulated Performance Case 5: $G_p$ versus $t$ ($p_i$=6000 psia, $p_{wf}$=1000 psia, $G_{input}$=4.72 BSCF).**

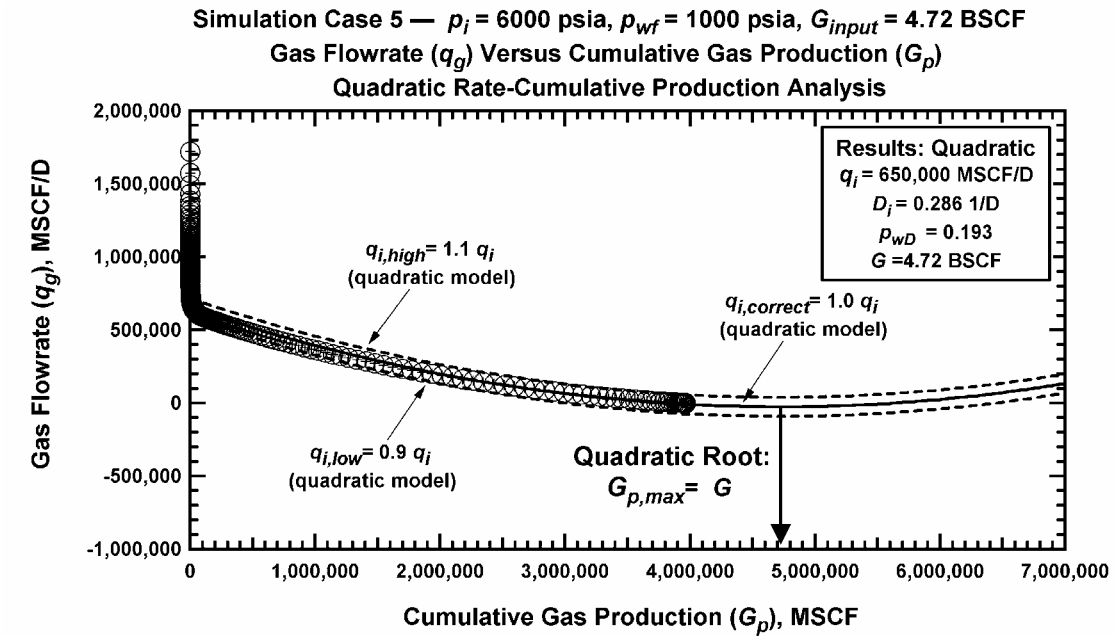


**Figure A-31 – Simulated Performance Case 5: $q_g$ versus $G_p$ ($p_i$=6000 psia, $p_{wf}$=1000 psia, $G_{input}$=4.72 BSCF).**

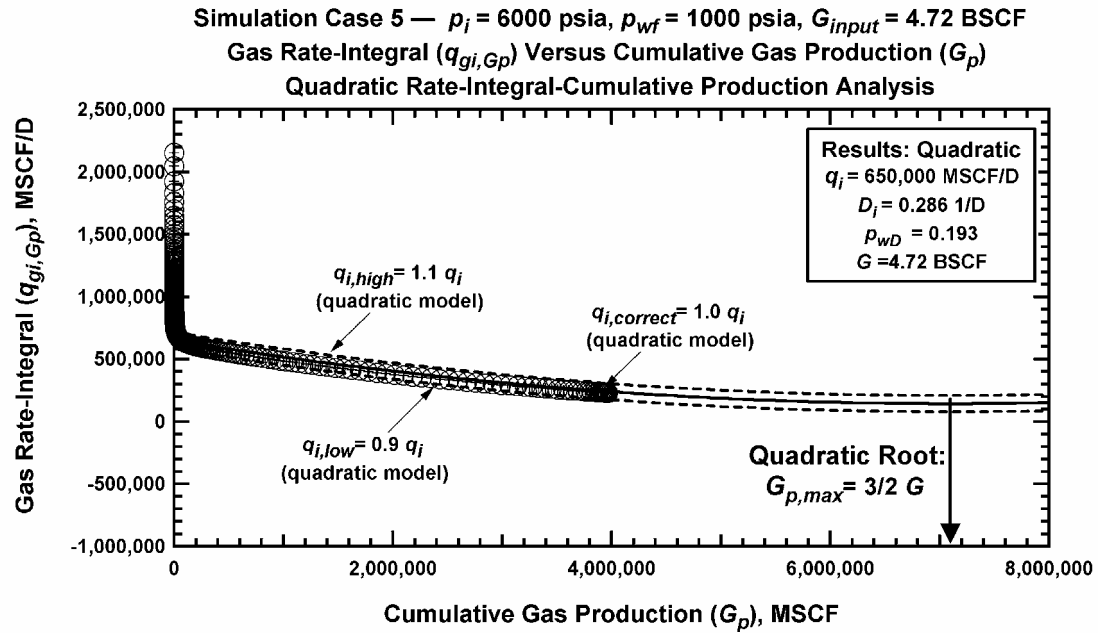


**Figure A-32 – Simulated Performance Case 5: $q_{qi,Gp}$ versus $G_p$ ($p_i$= 6000 psia, $p_{wf}$=1000 psia, $G_{input}$=4.72 BSCF).**

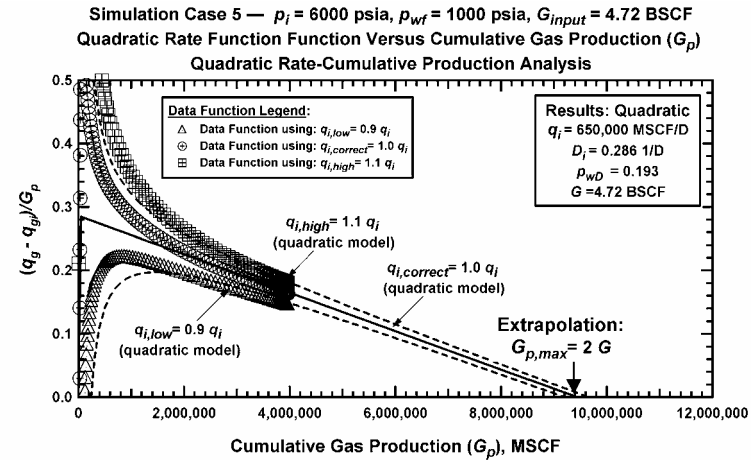


**Figure A-33 – Simulated Performance Case 5: $(q_{qi}-q_q)/G_p$ versus $G_p$ ($p_i$= 6000 psia, $p_{wf}$=1000 psia, $G_{input}$=4.72 BSCF) (Plotting Function 1 ($PF_1$)).**

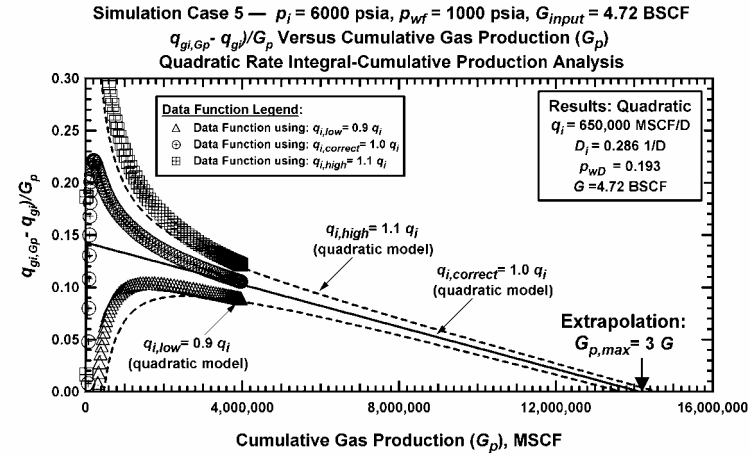


**Figure A-34 – Simulated Performance Case 5: $(q_{qi,Gp}-q_{qi})/G_p$ versus $G_p$ ($p_i$= 6000 psia, $p_{wf}$=1000 psia, $G_{input}$=4.72 BSCF) (Plotting Function 2 ($PF_2$)).**

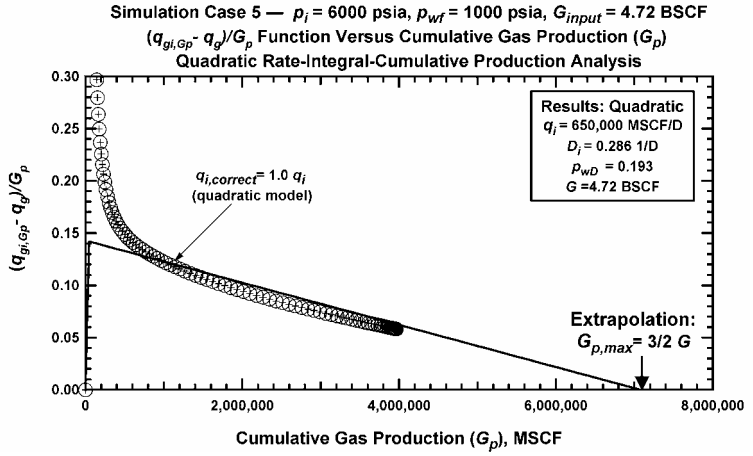


**Figure A-35 – Simulated Performance Case 5: $(q_{qi,Gp}-q_q)/G_p$ versus $G_p$ ($p_i$= 6000 psia, $p_{wf}$=1000 psia, $G_{input}$=4.72 BSCF) (Plotting Function 3 ($PF_3$)).**

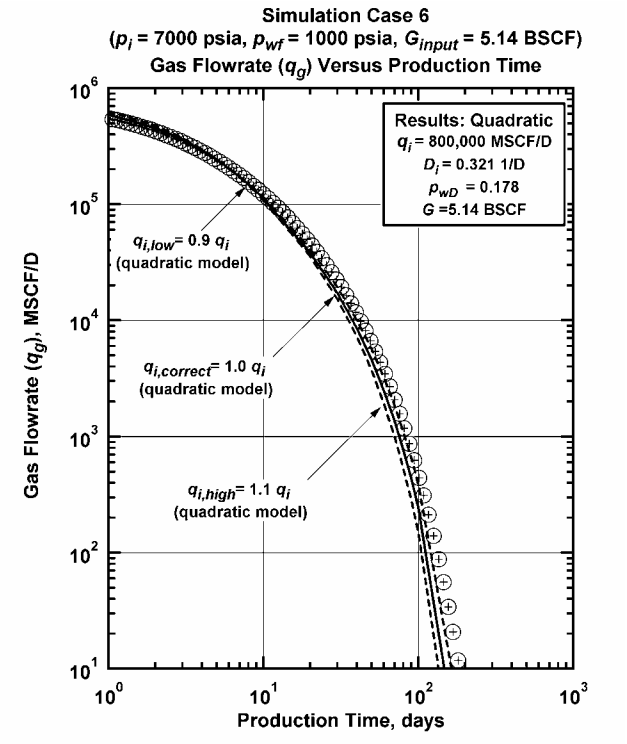


**Figure A-36 – Simulated Performance Case 6: $q_g$ versus $t$ ($p_i$=7000 psia, $p_{wf}$=1000 psia, $G_{input}$=5.14 BSCF).**

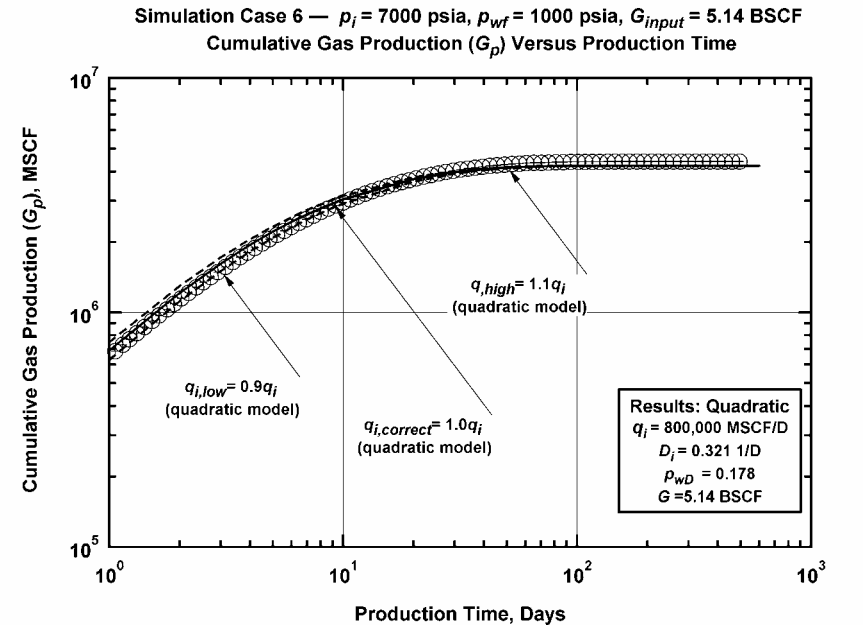


**Figure A-37 – Simulated Performance Case 6: $G_p$ versus $t$ ($p_i$=7000 psia, $p_{wf}$=1000 psia, $G_{input}$=5.14 BSCF).**

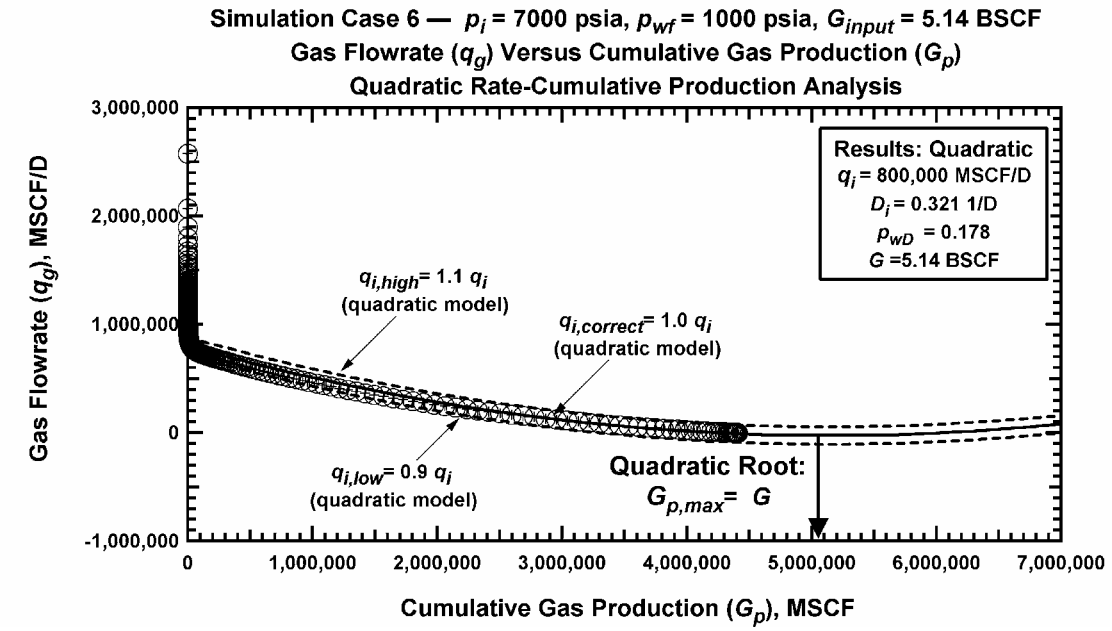


**Figure A-38 – Simulated Performance Case 6: $q_g$ versus $G_p$ ($p_i$=7000 psia, $p_{wf}$=1000 psia, $G_{input}$=5.14 BSCF).**

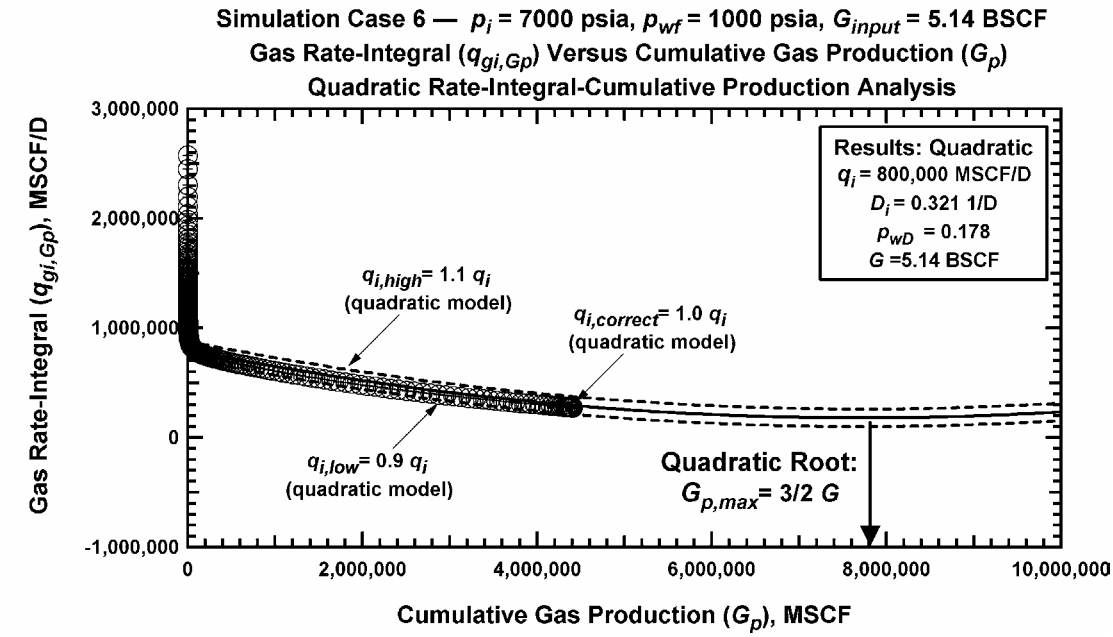


**Figure A-39 – Simulated Performance Case 6: $q_{qi,Gp}$ versus $G_p$ ($p_i$= 7000 psia, $p_{wf}$=1000 psia, $G_{input}$=5.14 BSCF).**

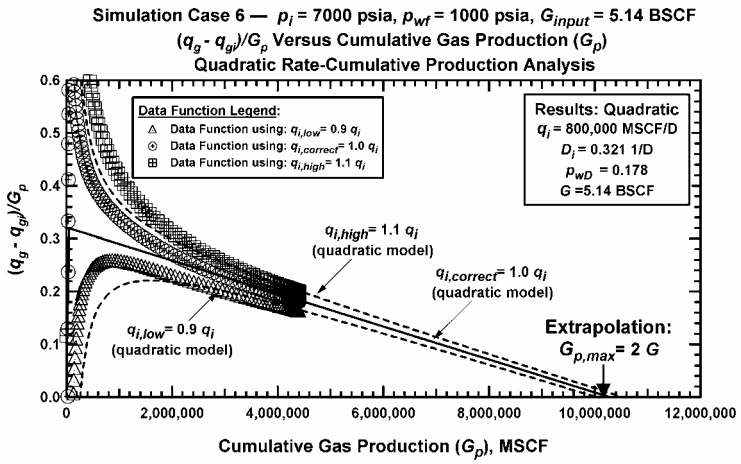


**Figure A-40 – Simulated Performance Case 6: $(q_{qi}-q_q)/G_p$ versus $G_p$ ($p_i$= 7000 psia, $p_{wf}$=1000 psia, $G_{input}$=5.14 BSCF) (Plotting Function 1 ($PF_1$)).**

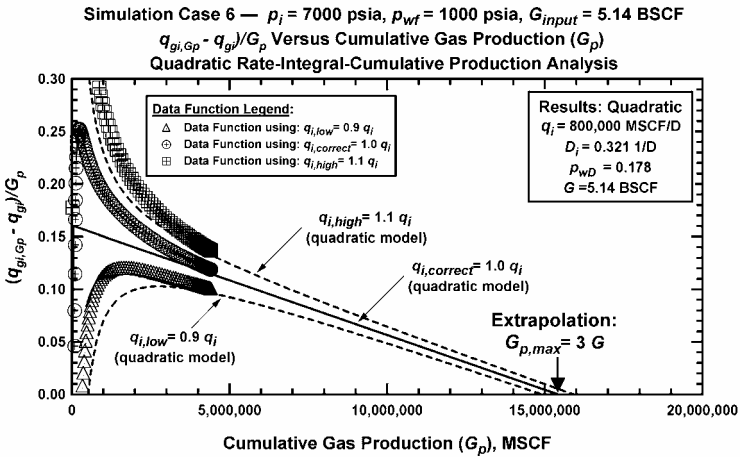


**Figure A-41 – Simulated Performance Case 6: $(q_{qi,Gp}-q_{qi})/G_p$ versus $G_p$ ($p_i$= 7000 psia, $p_{wf}$=1000 psia, $G_{input}$=5.14 BSCF) (Plotting Function 2 ($PF_2$)).**

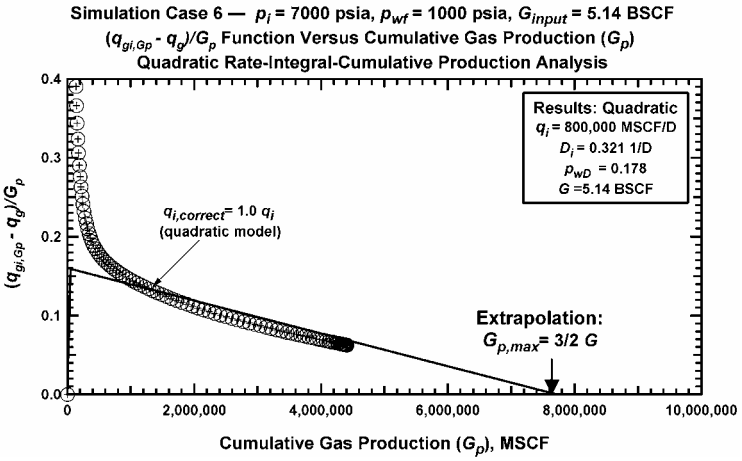


**Figure A-42 – Simulated Performance Case 6: $(q_{qi,Gp}-q_q)/G_p$ versus $G_p$ ($p_i$= 7000 psia, $p_{wf}$=1000 psia, $G_{input}$=5.14 BSCF) (Plotting Function 3 ($PF_3$)).**

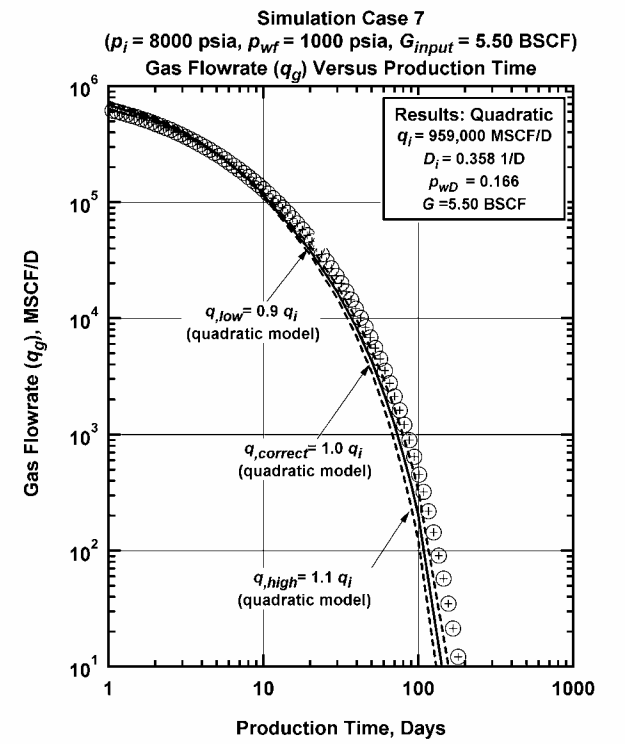


**Figure A-43 – Simulated Performance Case 7: $q_g$ versus $t$ ($p_i$=8000 psia, $p_{wf}$=1000 psia, $G_{input}$=5.50 BSCF).**

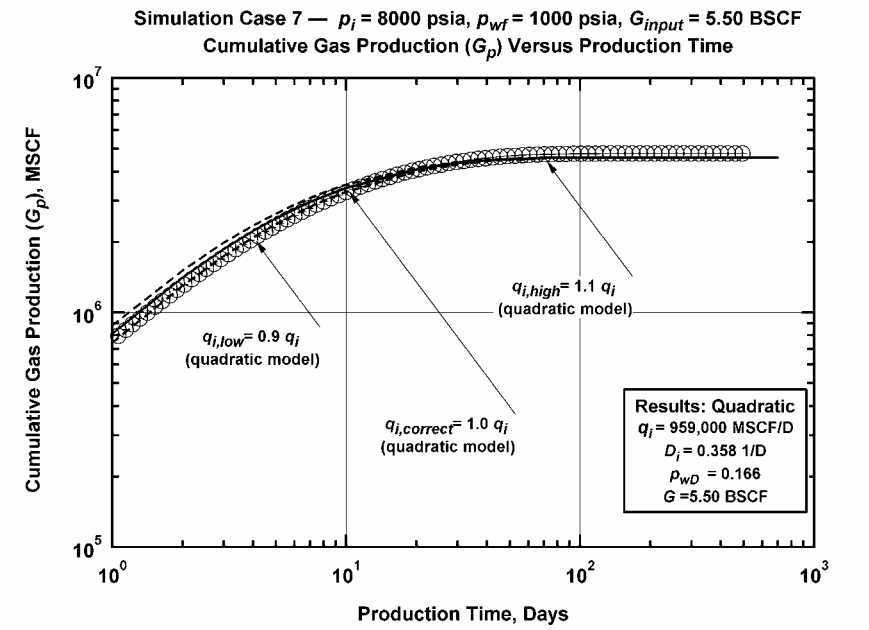


**Figure A-44 – Simulated Performance Case 7: $G_p$ versus $t$ ($p_i$=8000 psia, $p_{wf}$=1000 psia, $G_{input}$=5.50 BSCF).**

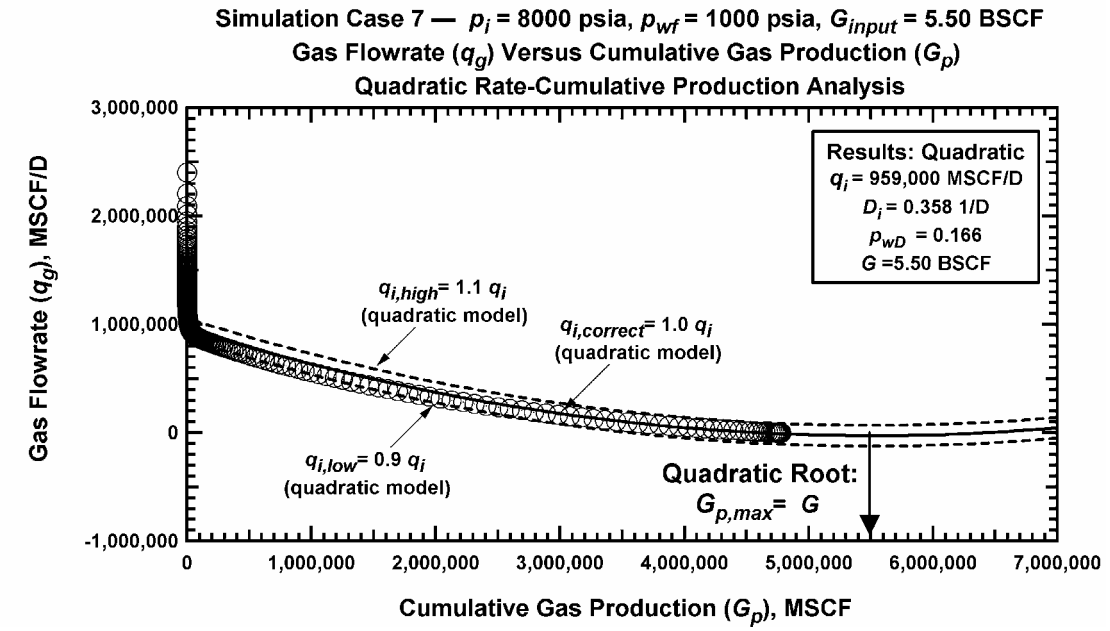


**Figure A-45 – Simulated Performance Case 7: $q_g$ versus $G_p$ ($p_i$=8000 psia, $p_{wf}$=1000 psia, $G_{input}$=5.50 BSCF).**

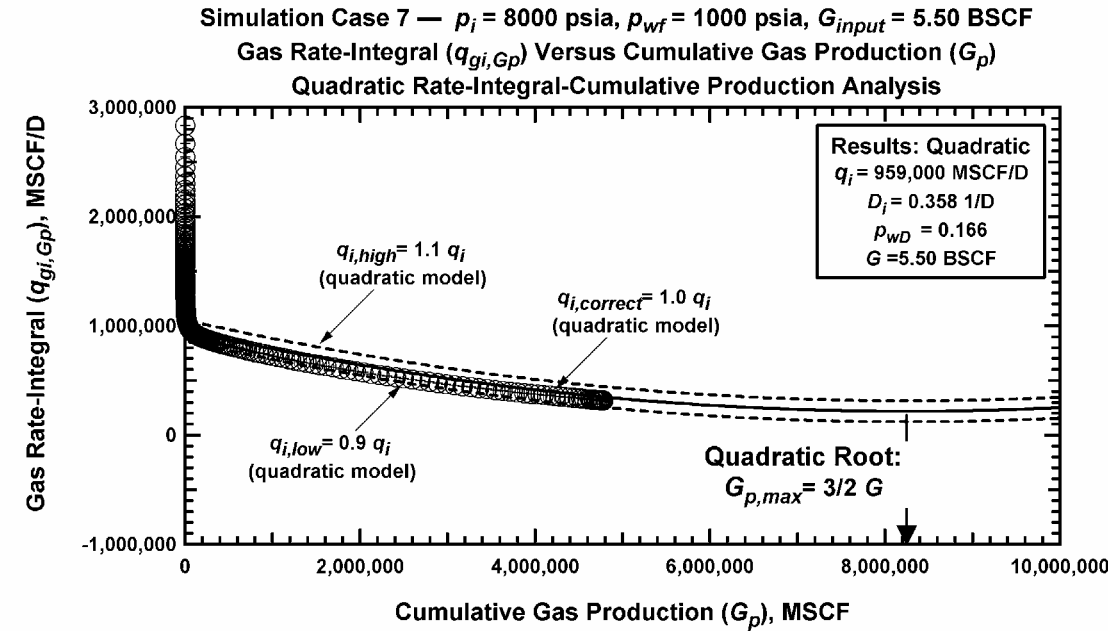


**Figure A-46 – Simulated Performance Case 7: $q_{qi,Gp}$ versus $G_p$ ($p_i$= 8000 psia, $p_{wf}$=1000 psia, $G_{input}$=5.50 BSCF).**

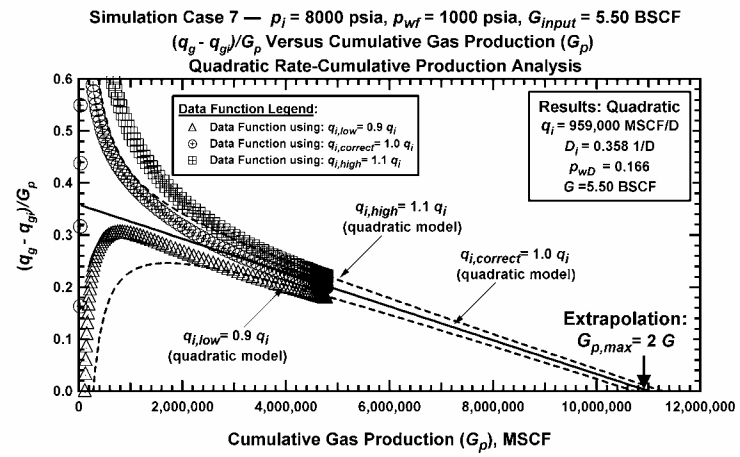


**Figure A-47 – Simulated Performance Case 7: $(q_{qi}-q_q)/G_p$ versus $G_p$ ($p_i$= 8000 psia, $p_{wf}$=1000 psia, $G_{input}$=5.50 BSCF) (Plotting Function 1 ($PF_1$)).**

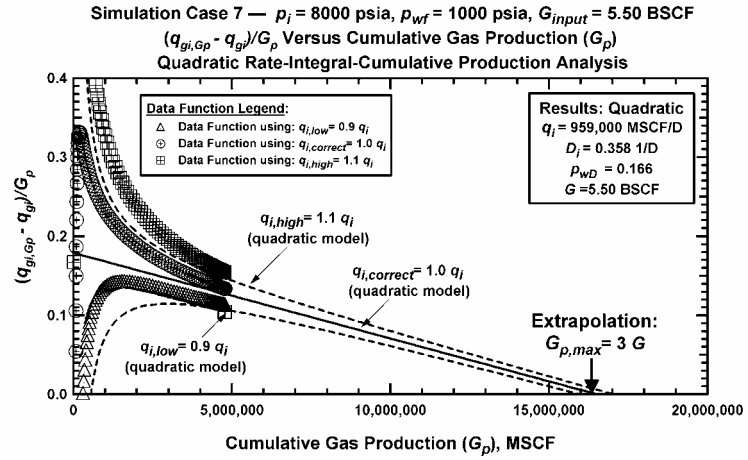


**Figure A-48 – Simulated Performance Case 7: $(q_{qi,Gp}-q_{qi})/G_p$ versus $G_p$ ($p_i$= 8000 psia, $p_{wf}$=1000 psia, $G_{input}$=5.50 BSCF) (Plotting Function 2 ($PF_2$)).**

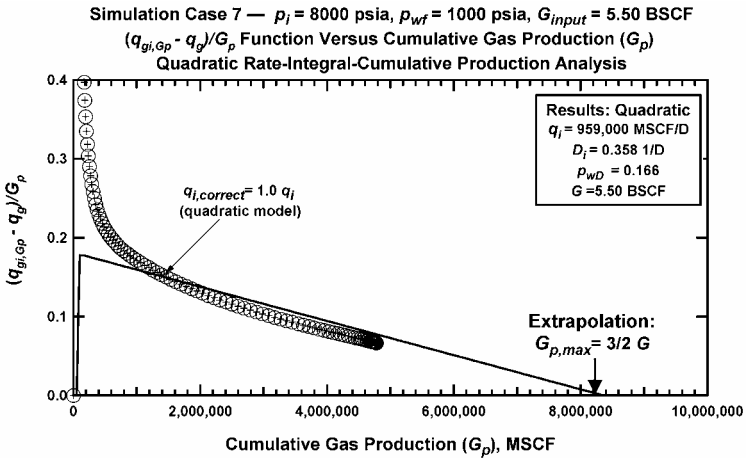


**Figure A-49 – Simulated Performance Case 7: $(q_{qi,Gp}-q_q)/G_p$ versus $G_p$ ($p_i$= 8000 psia, $p_{wf}$=1000 psia, $G_{input}$=5.50 BSCF) (Plotting Function 3 ($PF_3$)).**

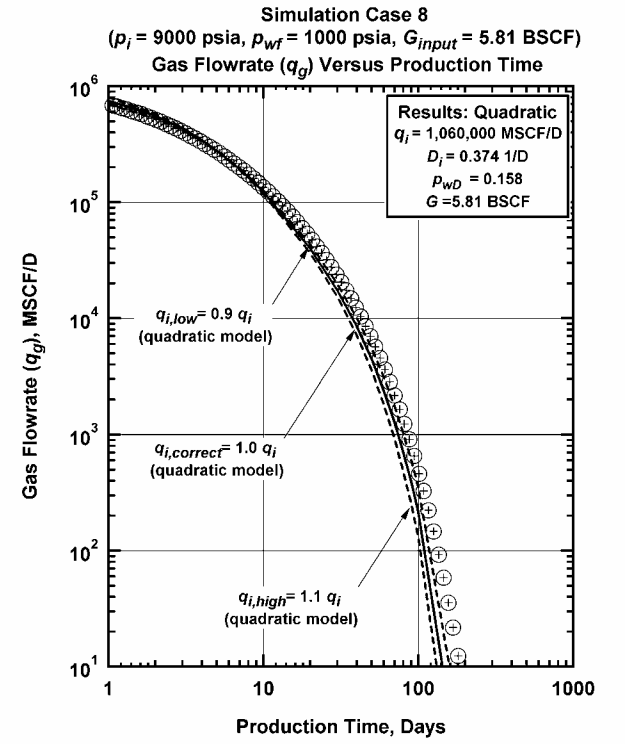


**Figure A-50 – Simulated Performance Case 8: $q_g$ versus $t$ ($p_i$=9000 psia, $p_{wf}$=1000 psia, $G_{input}$=5.81 BSCF).**

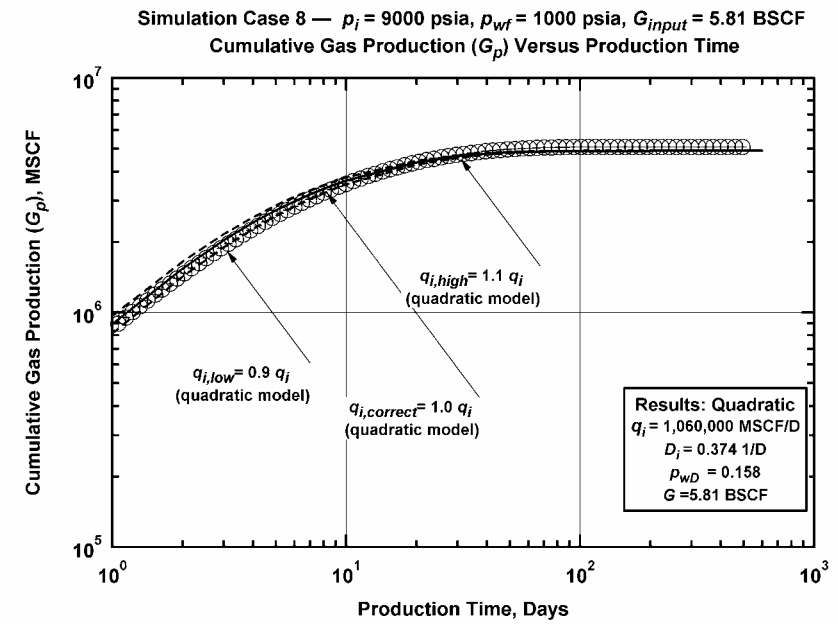


**Figure A-51 – Simulated Performance Case 8: $G_p$ versus $t$ ($p_i$=9000 psia, $p_{wf}$=1000 psia, $G_{input}$=5.81 BSCF).**

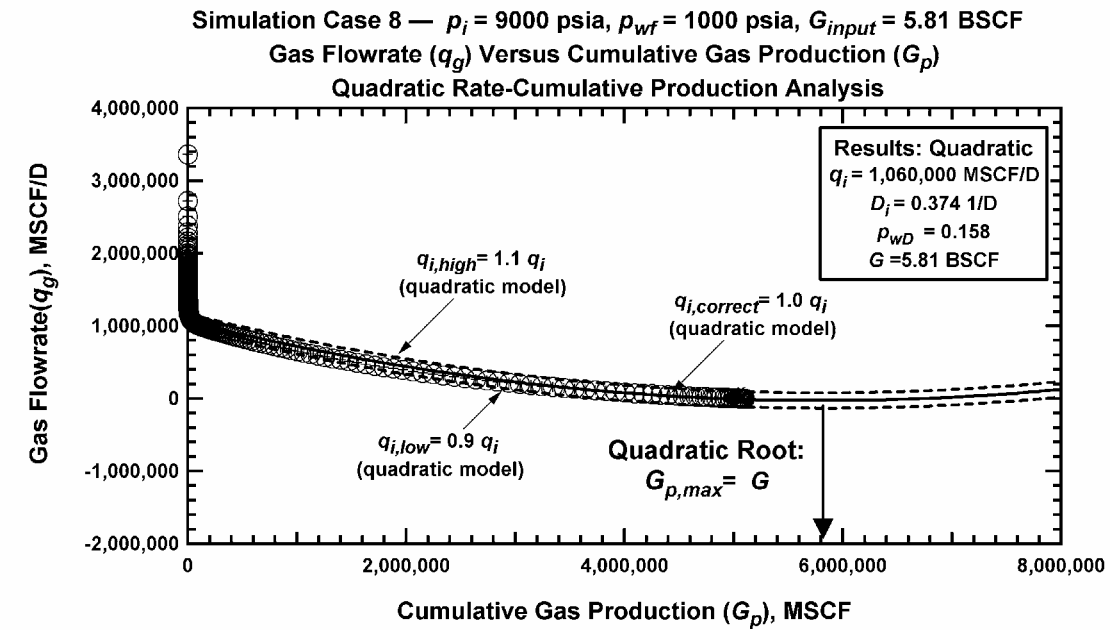


**Figure A-52 – Simulated Performance Case 8: $q_g$ versus $G_p$ ($p_i$=9000 psia, $p_{wf}$=1000 psia, $G_{input}$=5.81 BSCF).**

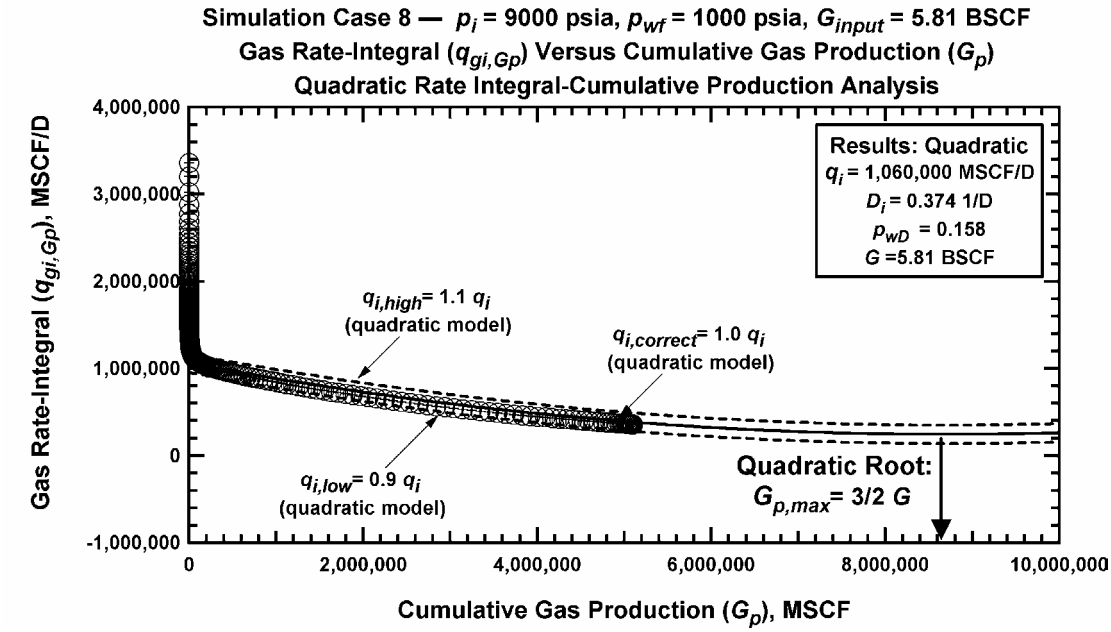


**Figure A-53 – Simulated Performance Case 8: $q_{qi,Gp}$ versus $G_p$ ($p_i$= 9000 psia, $p_{wf}$=1000 psia, $G_{input}$=5.81 BSCF).**

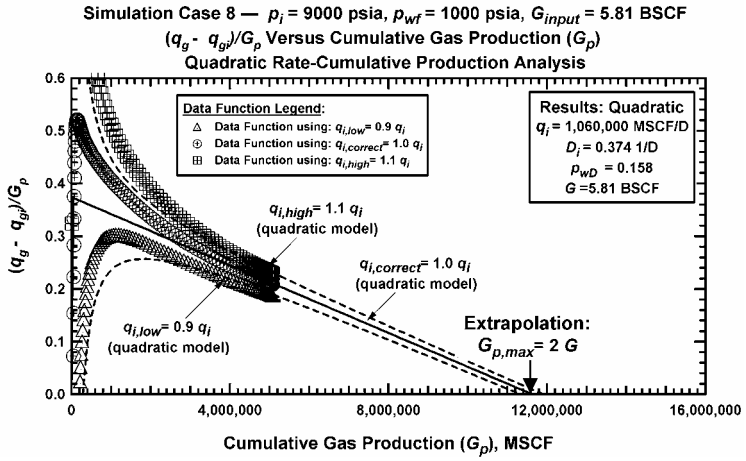


**Figure A-54 – Simulated Performance Case 8: $(q_{qi}-q_q)/G_p$ versus $G_p$ ($p_i$= 9000 psia, $p_{wf}$=1000 psia, $G_{input}$=5.81 BSCF) (Plotting Function 1 ($PF_1$)).**

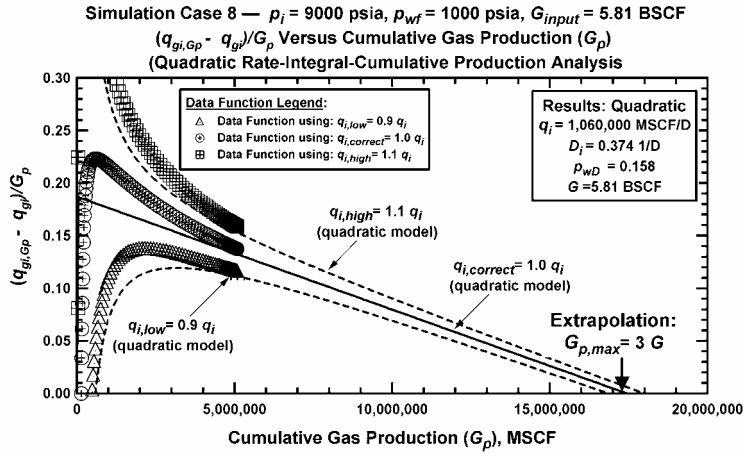


**Figure A-55 – Simulated Performance Case 8: $(q_{qi,Gp}-q_{qi})/G_p$ versus $G_p$ ($p_i$= 9000 psia, $p_{wf}$=1000 psia, $G_{input}$=5.81 BSCF) (Plotting Function 2 ($PF_2$)).**

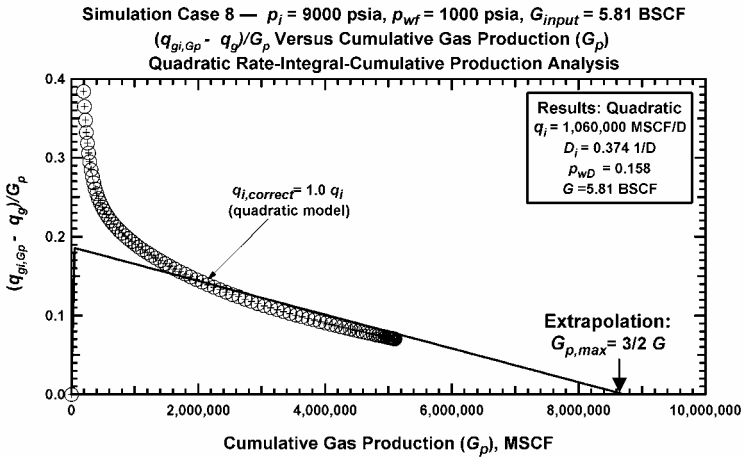


**Figure A-56 – Simulated Performance Case 8: $(q_{qi,Gp}-q_q)/G_p$ versus $G_p$ ($p_i$= 9000 psia, $p_{wf}$=1000 psia, $G_{input}$=5.81 BSCF) (Plotting Function 3 ($PF_3$)).**

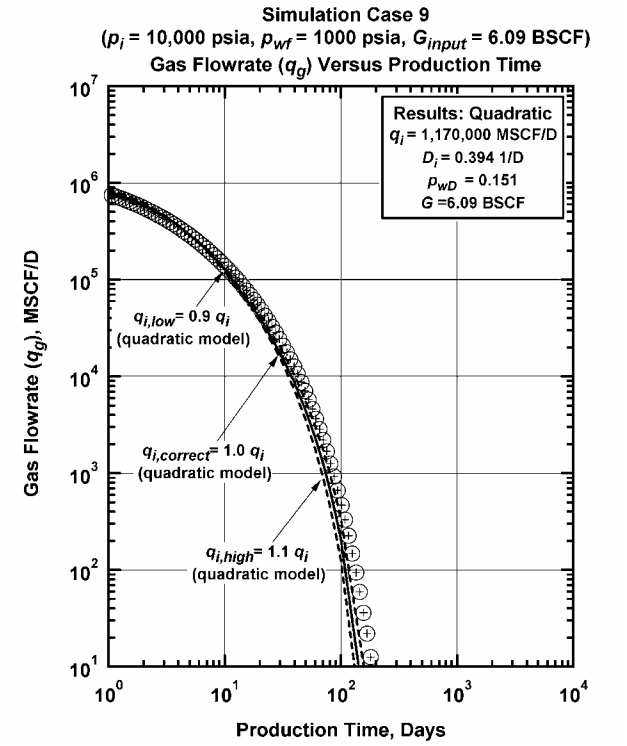


**Figure A-57 – Simulated Performance Case 9: $q_g$ versus $t$ ($p_i$=10,000 psia, $p_{wf}$=1000 psia, $G_{input}$=6.09 BSCF).**

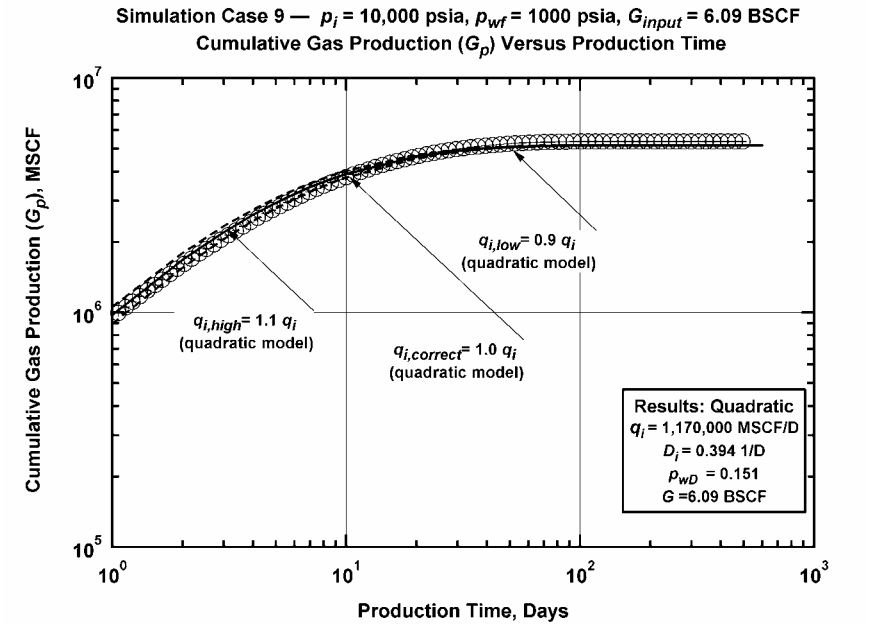


**Figure A-58 – Simulated Performance Case 9: $G_p$ versus $t$ ($p_i$=10,000 psia, $p_{wf}$=1000 psia, $G_{input}$=6.09BSCF).**

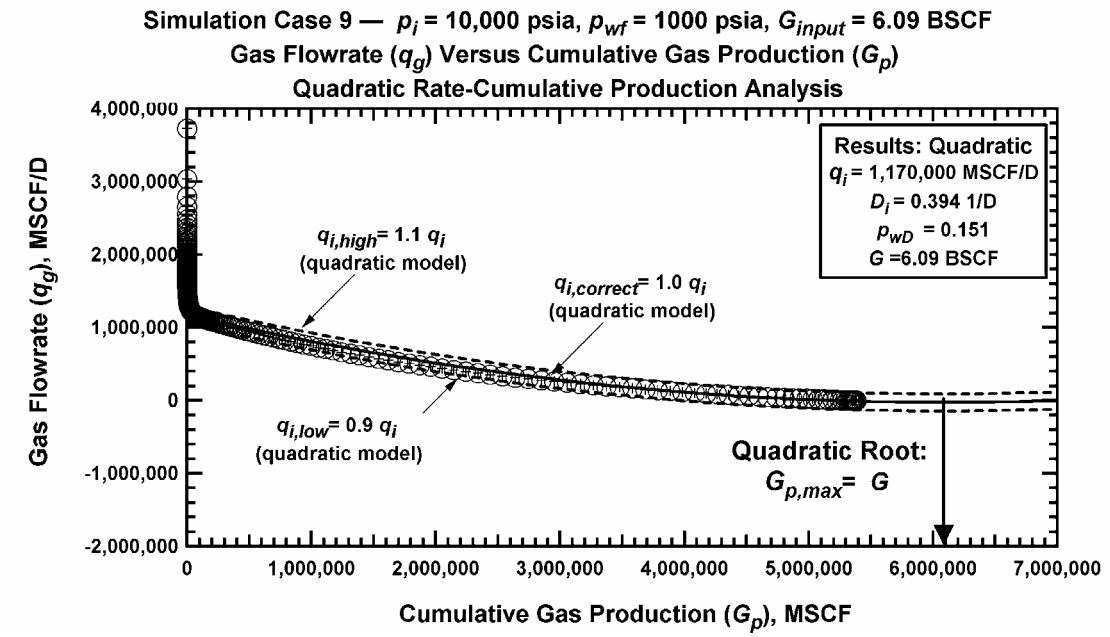


**Figure A-59 – Simulated Performance Case 9: $q_g$ versus $G_p$ ($p_i$=10,000 psia, $p_{wf}$=1000 psia, $G_{input}$=6.09 BSCF).**

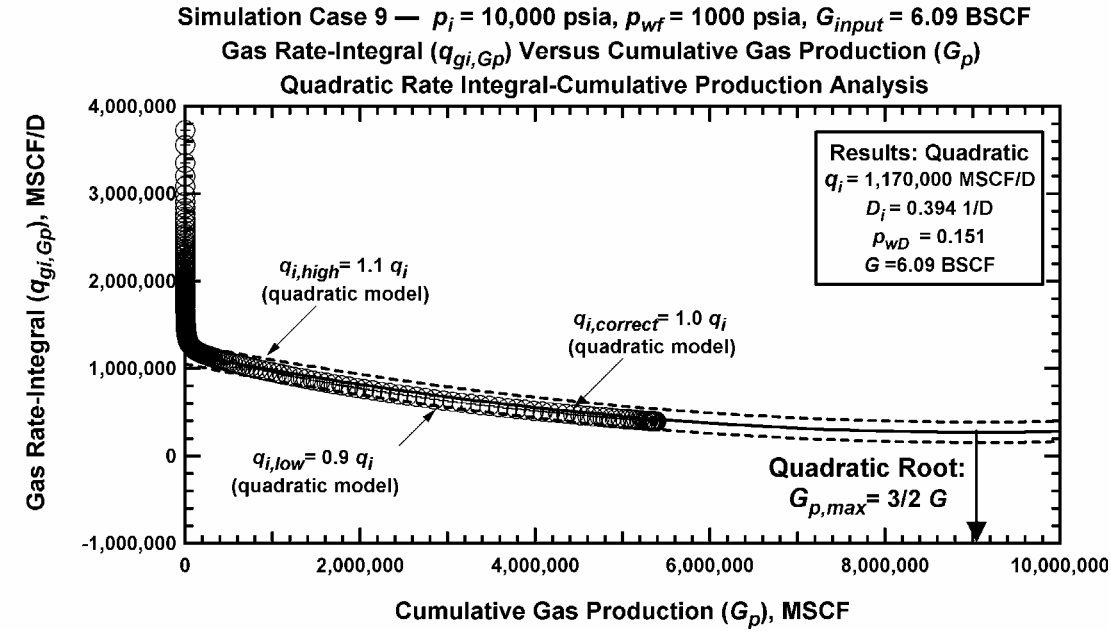


**Figure A-60 – Simulated Performance Case 9: $q_{qi,Gp}$ versus $G_p$ ($p_i$=10,000 psia, $p_{wf}$=1000 psia, $G_{input}$=6.09 BSCF).**

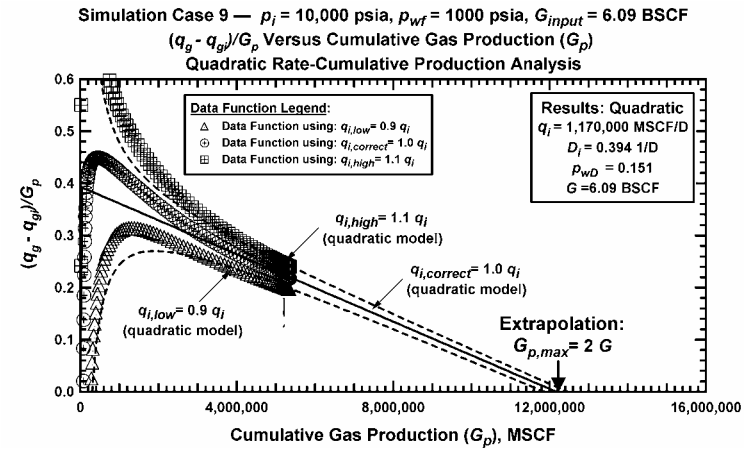


**Figure A-61 – Simulated Performance Case 9: $(q_{qi}-q_q)/G_p$ versus $G_p$ ($p_i$=10,000 psia, $p_{wf}$=1000 psia, $G_{input}$=6.09 BSCF). (Plotting Function 1 ($PF_1$)).**

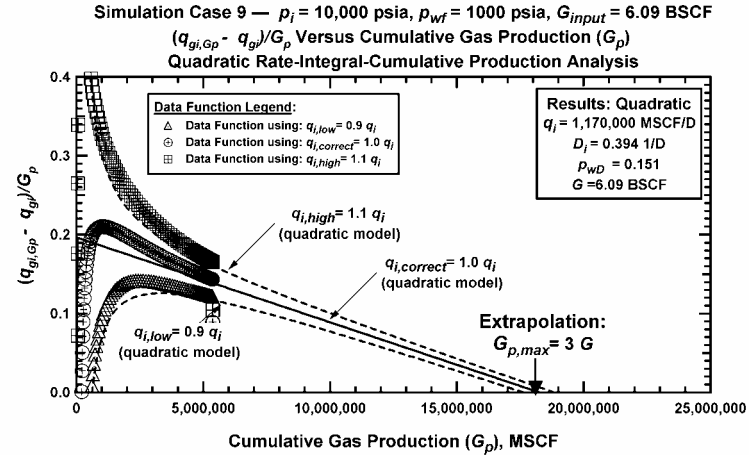


**Figure A-62 – Simulated Performance Case 9: $(q_{qi,Gp}-q_{qi})/G_p$ versus $G_p$ ($p_i$=10,000 psia, $p_{wf}$=1000 psia, $G_{input}$=6.09 BSCF). (Plotting Function 2 ($PF_2$)).**

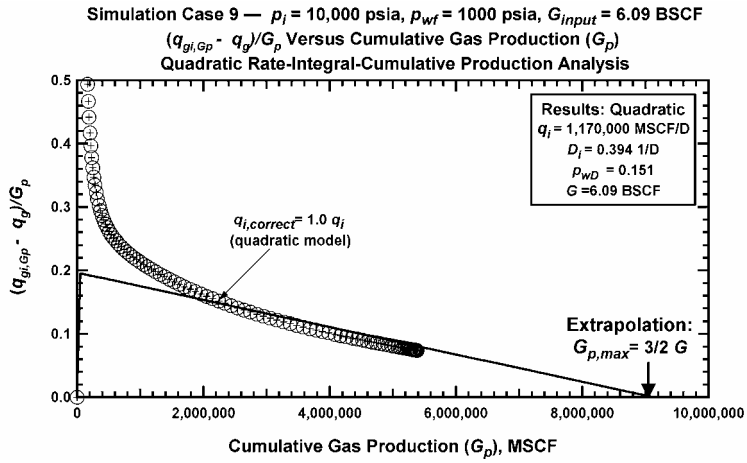


**Figure A-63 – Simulated Performance Case 9: $(q_{qi,Gp}-q_q)/G_p$ versus $G_p$ ($p_i$=10,000 psia, $p_{wf}$=1000 psia, $G_{input}$=6.09 BSCF). (Plotting Function 3 ($PF_3$)).**

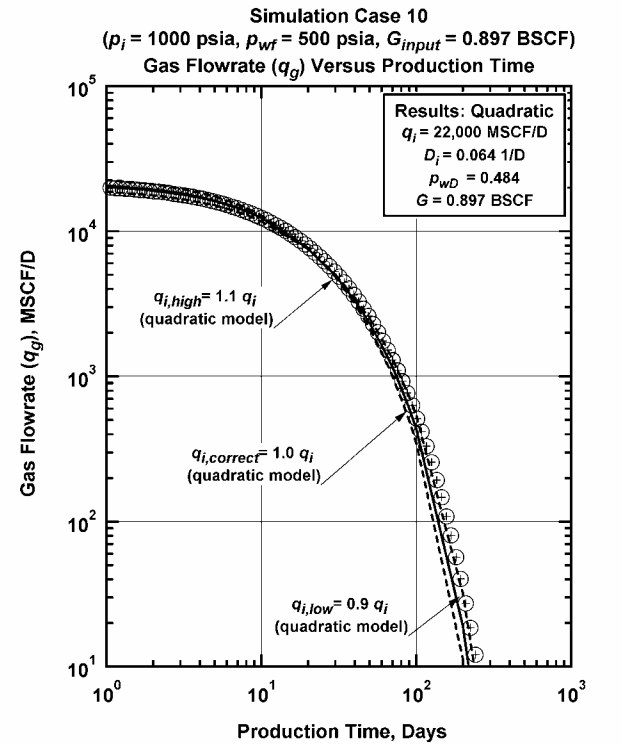


**Figure A-64 – Simulated Performance Case 10: $q_g$ versus $t$ ($p_i$=1000 psia, $p_{wf}$=500 psia, $G_{input}$=0.897 BSCF).**

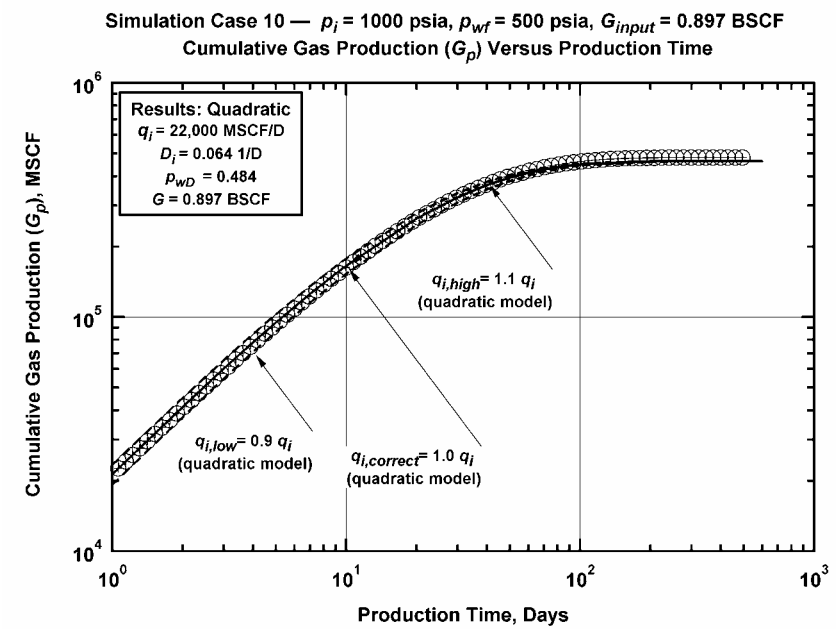


**Figure A-65 – Simulated Performance Case 10: $G_p$ versus $t$ ($p_i$=1000 psia, $p_{wf}$=500 psia, $G_{input}$=0.897 BSCF).**

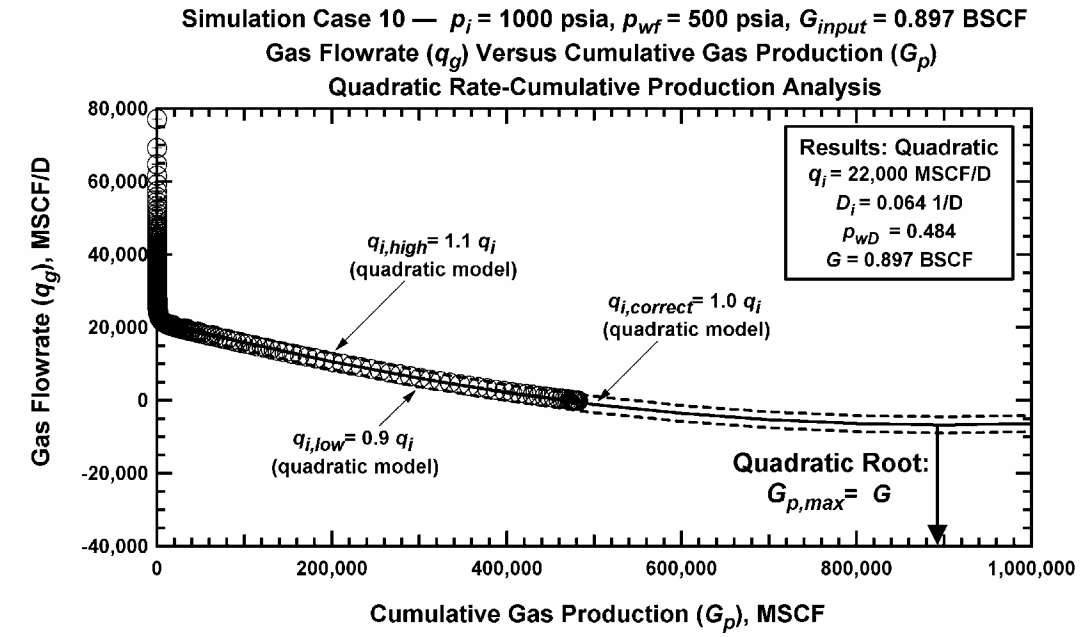


**Figure A-66 – Simulated Performance Case 10: $q_g$ versus $G_p$ ($p_i$=1000 psia, $p_{wf}$=500 psia, $G_{input}$=0.897 BSCF).**

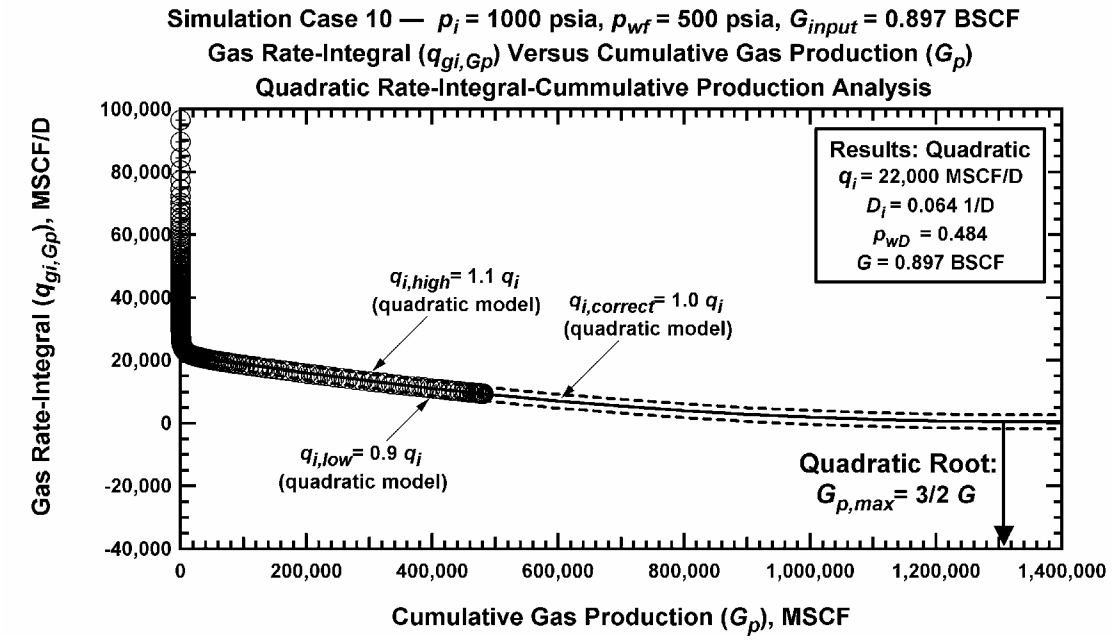


**Figure A-67 – Simulated Performance Case 10: $q_{qi,Gp}$ versus $G_p$ ($p_i$=1000 psia, $p_{wf}$=500 psia, $G_{input}$=0.897 BSCF).**

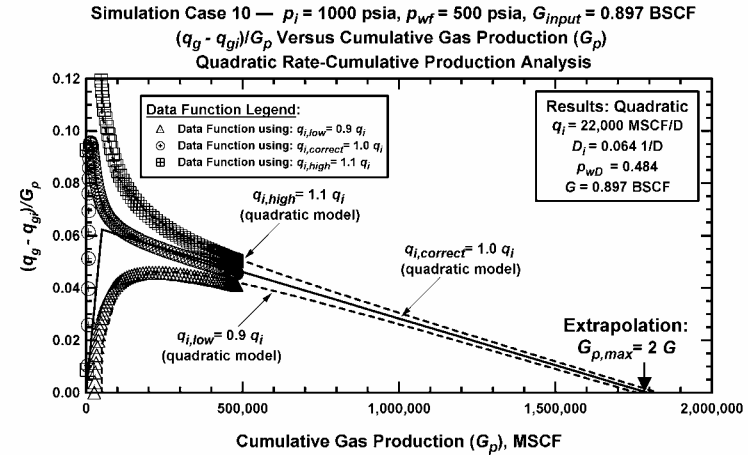


**Figure A-68 – Simulated Performance Case 10: $(q_{qi}-q_q)/G_p$ versus $G_p$ ($p_i$=1000 psia, $p_{wf}$=500 psia, $G_{input}$=0.897 BSCF). (Plotting Function 1 ($PF_1$)).**

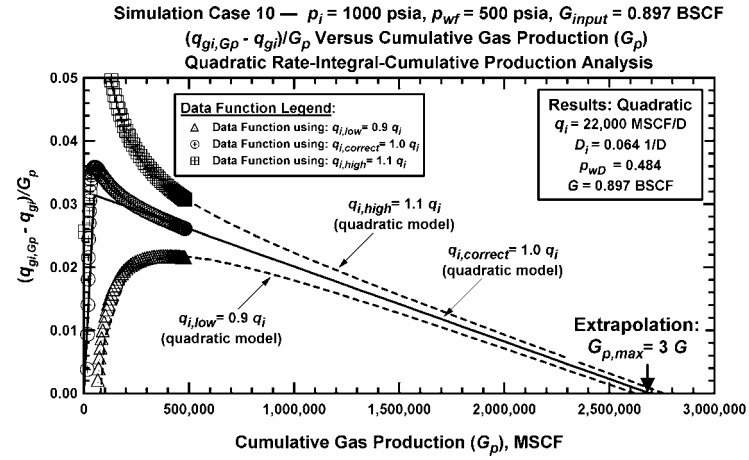


**Figure A-69 – Simulated Performance Case 10: $(q_{qi}-q_{qi})/G_p$ versus $G_p$ ($p_i$=1000 psia, $p_{wf}$=500 psia, $G_{input}$=0.897 BSCF) (Plotting Function 2 ($PF_2$)).**

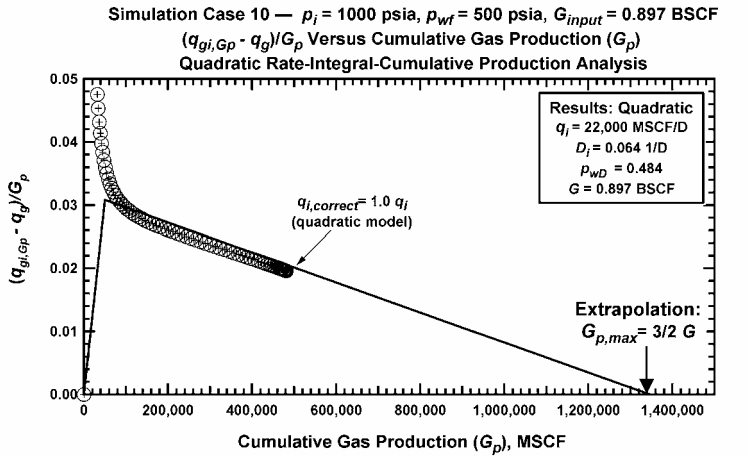


**Figure A-70 – Simulated Performance Case 10: $(q_{qi,Gp}-q_q)/G_p$ versus $G_p$ ($p_i$=1000 psia, $p_{wf}$=500 psia, $G_{input}$=0.897 BSCF) (Plotting Function 3 ($PF_3$)).**

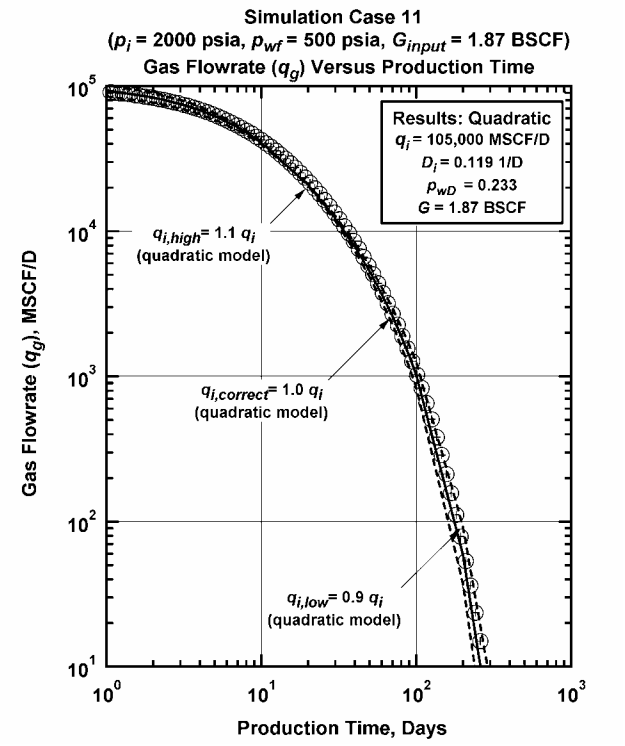


**Figure A-71 – Simulated Performance Case 11: $q_g$ versus $t$ ($p_i$=2000 psia, $p_{wf}$=500 psia, $G_{input}$=1.87 BSCF).**

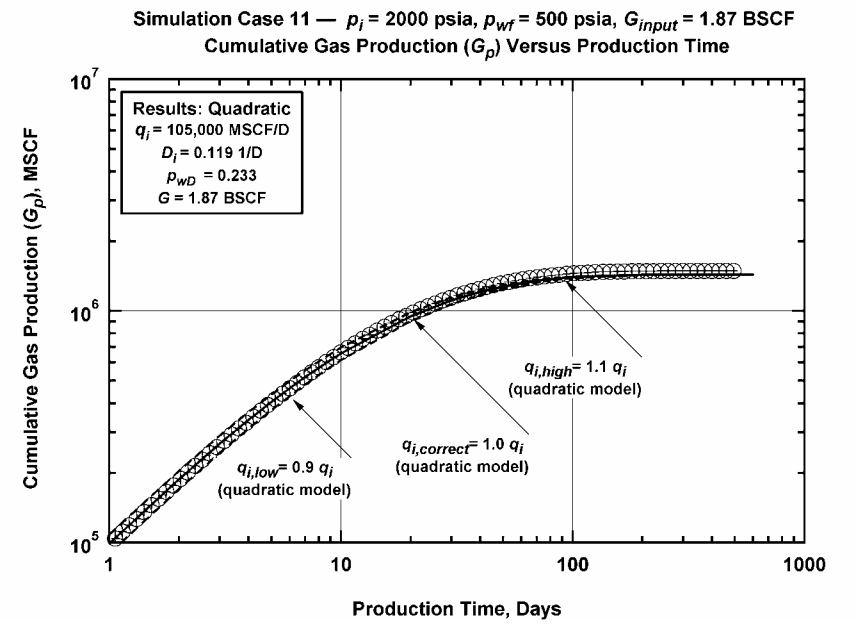


**Figure A-72 – Simulated Performance Case 11: $G_p$ versus $t$ ($p_i$=2000 psia, $p_{wf}$=500 psia, $G_{input}$=1.87 BSCF).**

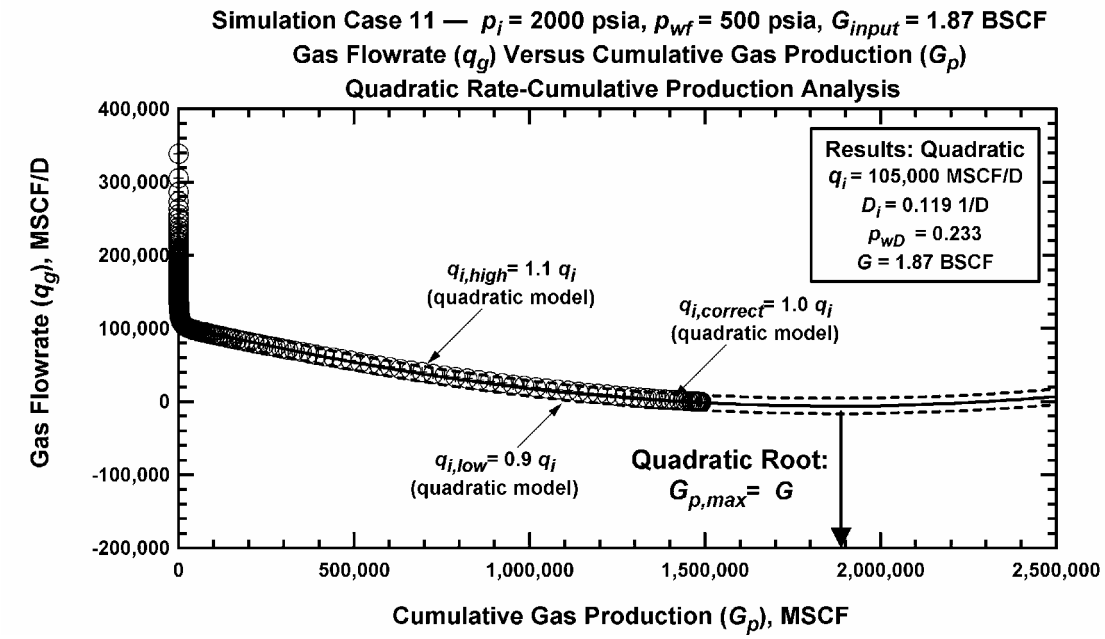


**Figure A-73 – Simulated Performance Case 11: $q_g$ versus $G_p$ ($p_i$=2000 psia, $p_{wf}$=500 psia, $G_{input}$=1.87 BSCF).**

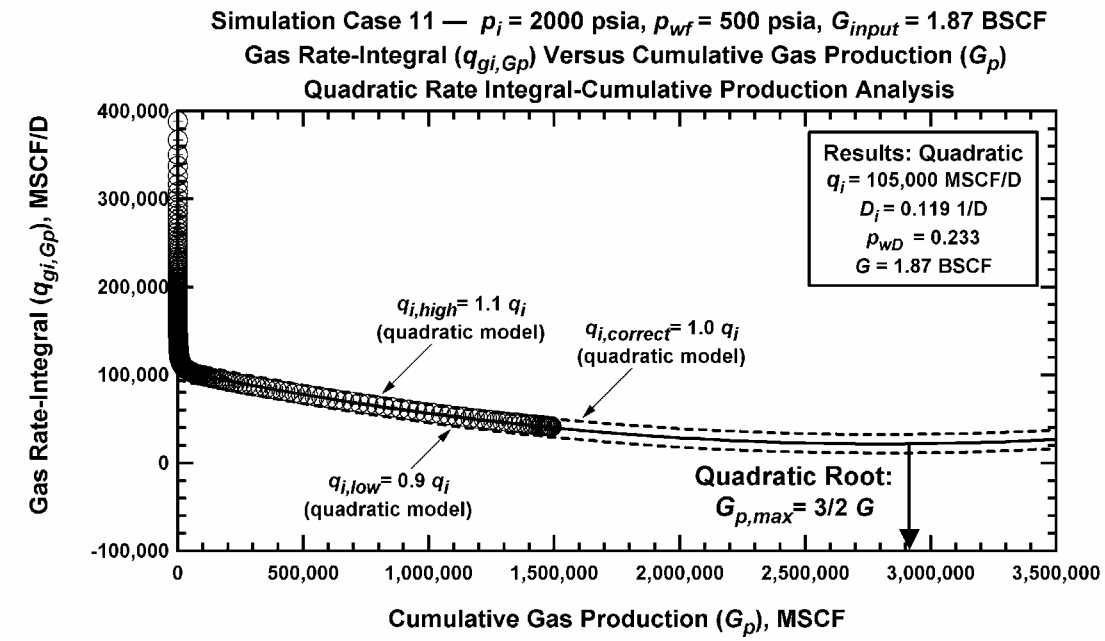


**Figure A-74 – Simulated Performance Case 11: $q_{qi,Gp}$ versus $G_p$ ($p_i$=2000 psia, $p_{wf}$=500 psia, $G_{input}$=1.87 BSCF).**

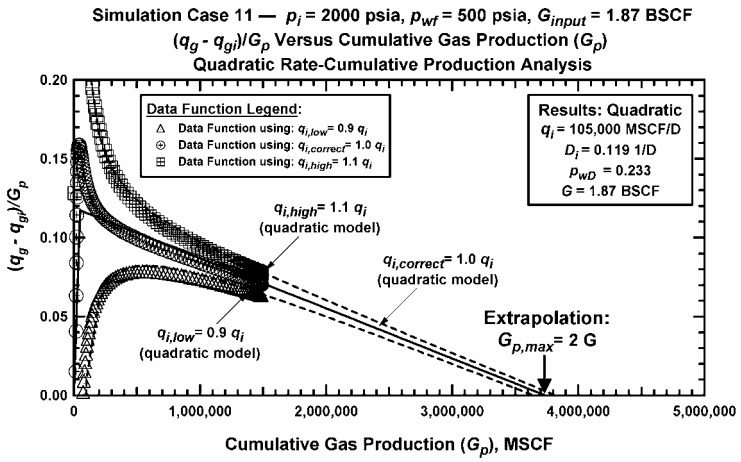


**Figure A-75 – Simulated Performance Case 11: $(q_{qi}-q_q)/G_p$ versus $G_p$ ($p_i$=2000 psia, $p_{wf}$=500 psia, $G_{input}$=1.87 BSCF). (Plotting Function 1 ($PF_1$)).**

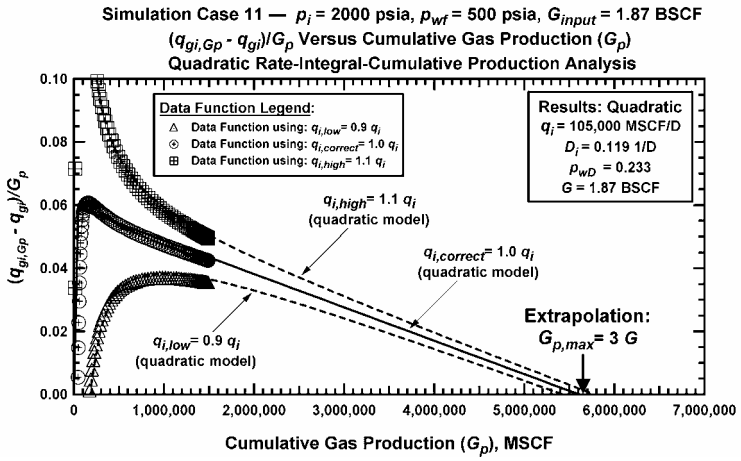


**Figure A-76 – Simulated Performance Case 11: $(q_{qi,Gp}-q_{qi})/G_p$ versus $G_p$ ($p_i$=2000 psia, $p_{wf}$=500 psia, $G_{input}$=1.87 BSCF). (Plotting Function 2 ($PF_2$)).**

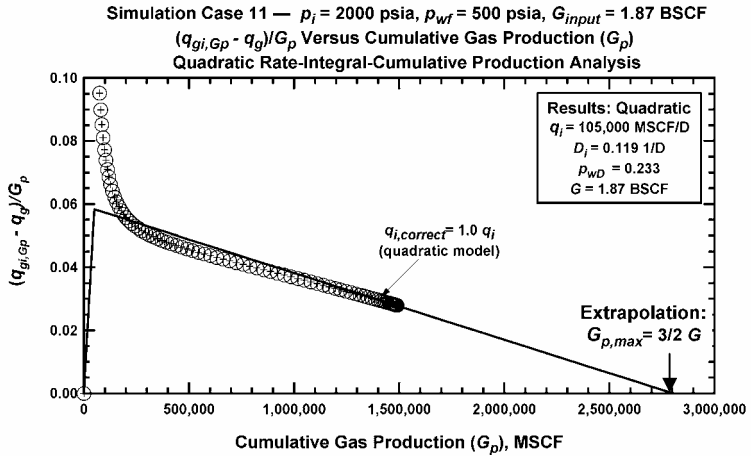


**Figure A-77 – Simulated Performance Case 11: $(q_{qi,Gp}-q_q)/G_p$ versus $G_p$ ($p_i$=2000 psia, $p_{wf}$=500 psia, $G_{input}$=1.87 BSCF). (Plotting Function 3 ($PF_3$)).**

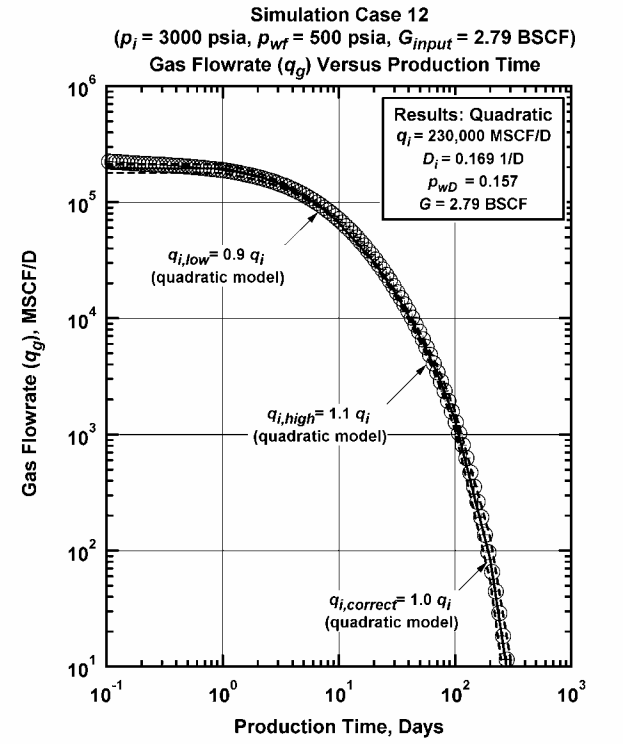


**Figure A-78 – Simulated Performance Case 12: $q_g$ versus $t$ ($p_i$=3000 psia, $p_{wf}$=500 psia, $G_{input}$=2.79 BSCF).**

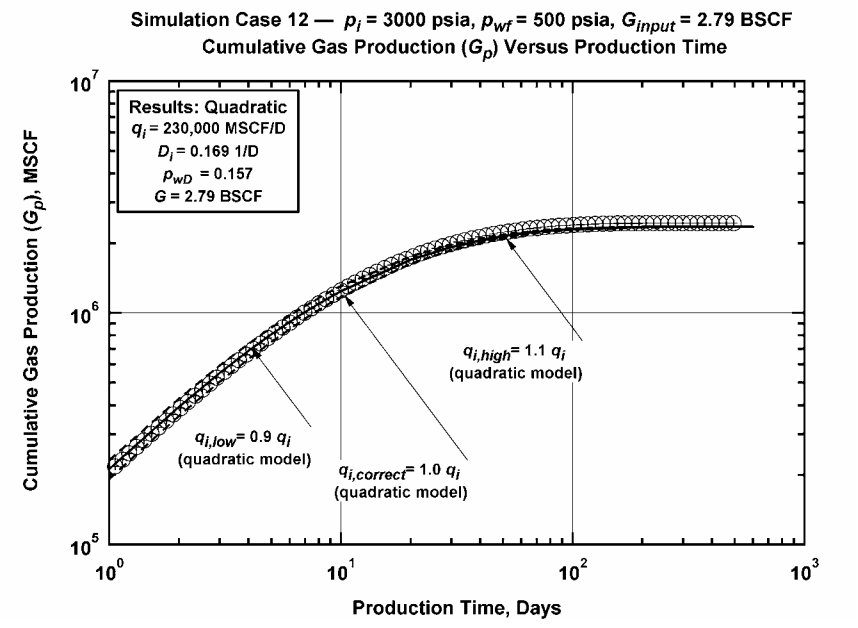


**Figure A-79 – Simulated Performance Case 12: $G_p$ versus $t$ ($p_i$=3000 psia, $p_{wf}$=500 psia, $G_{input}$=2.79 BSCF).**

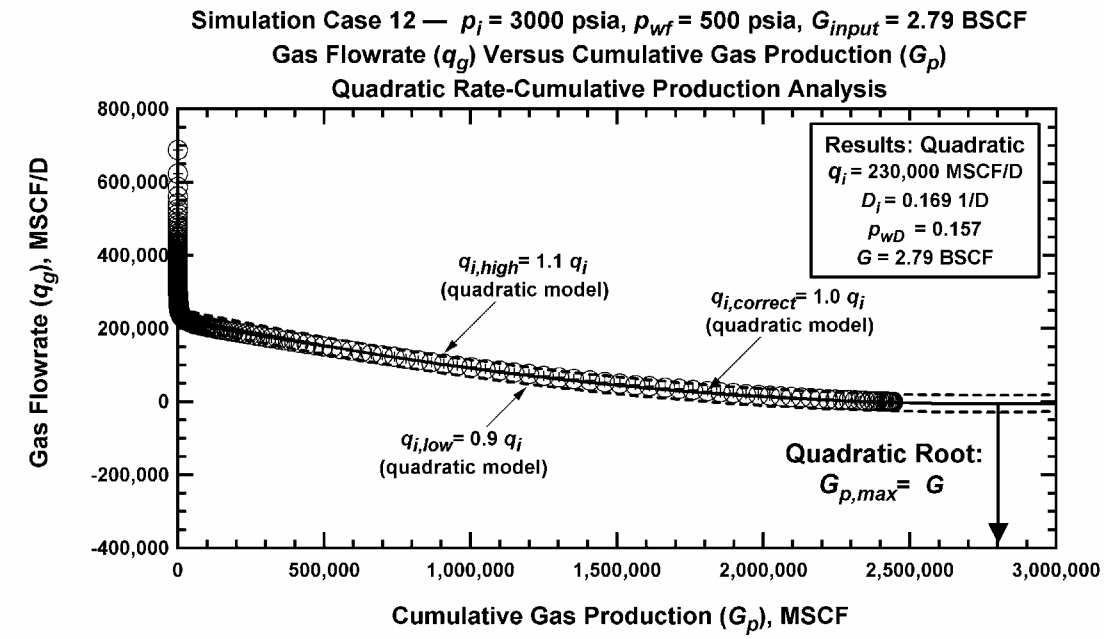


**Figure A-80 – Simulated Performance Case 12: $q_g$ versus $G_p$ ($p_i$=3000 psia, $p_{wf}$=500 psia, $G_{input}$=2.79 BSCF).**

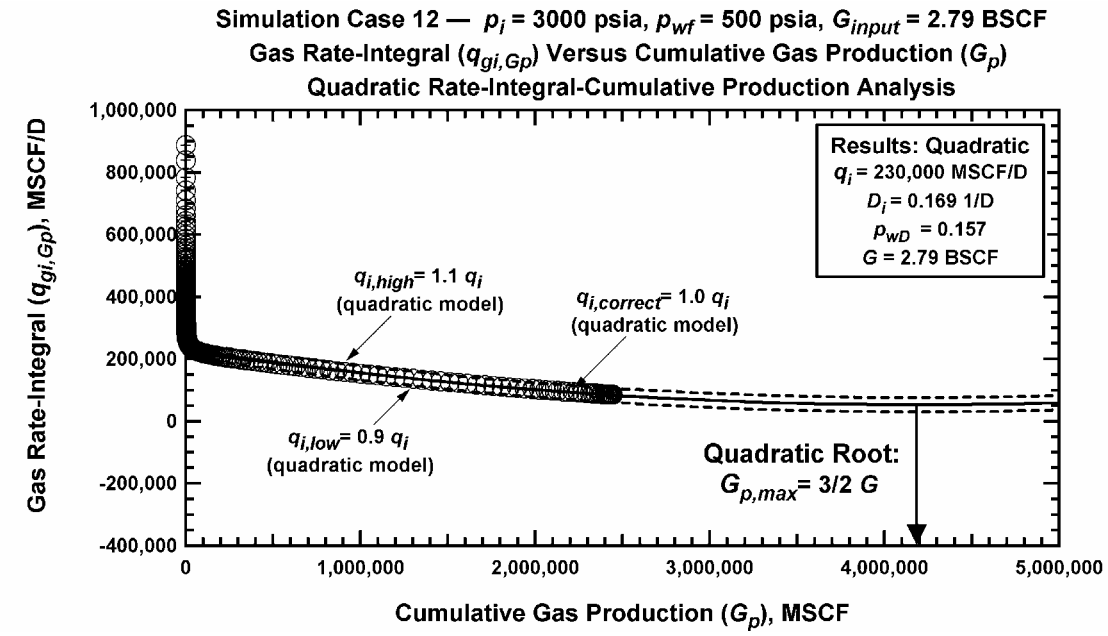


**Figure A-81 – Simulated Performance Case 12: $q_{qi,Gp}$ versus $G_p$ ($p_i$=3000 psia, $p_{wf}$=500 psia, $G_{input}$=2.79 BSCF).**

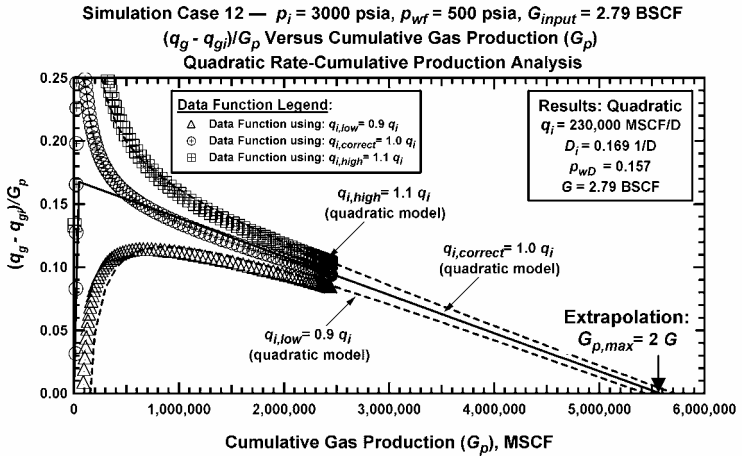


**Figure A-82 – Simulated Performance Case 12: $(q_{qi}-q_q)/G_p$ versus $G_p$ ($p_i$=3000 psia, $p_{wf}$=500 psia, $G_{input}$=2.79 BSCF). (Plotting Function 1 ($PF_1$)).**

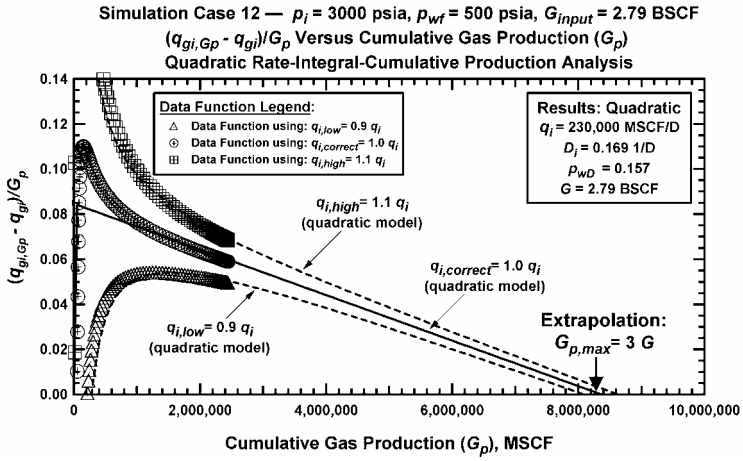


**Figure A-83 – Simulated Performance Case 12: $(q_{qi,Gp}-q_{qi})/G_p$ versus $G_p$ ($p_i$=3000 psia, $p_{wf}$=500 psia, $G_{input}$=2.79 BSCF). (Plotting Function 2 ($PF_2$)).**

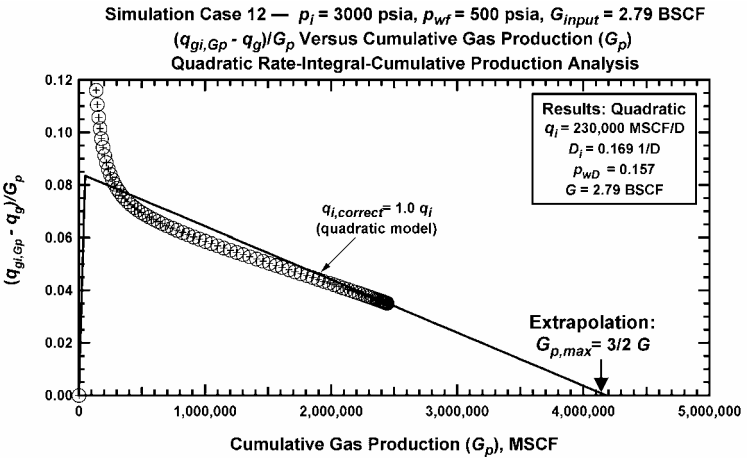


**Figure A-84 – Simulated Performance Case 12: $(q_{qi,Gp}-q_q)/G_p$ versus $G_p$ ($p_i$=3000 psia, $p_{wf}$=500 psia, $G_{input}$=2.79 BSCF). (Plotting Function 3 ($PF_3$)).**

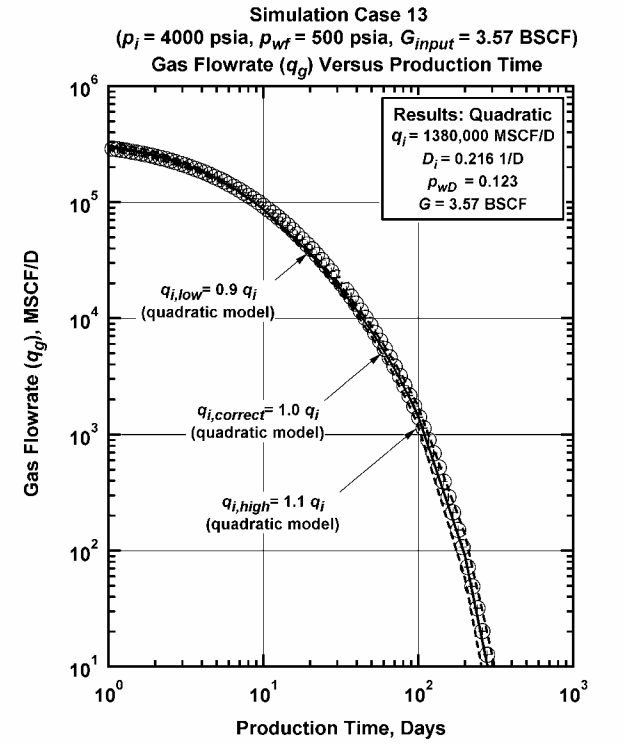


**Figure A-85 – Simulated Performance Case 13: $q_g$ versus $t$ ($p_i$=4000 psia, $p_{wf}$=500 psia, $G_{input}$=3.57 BSCF).**

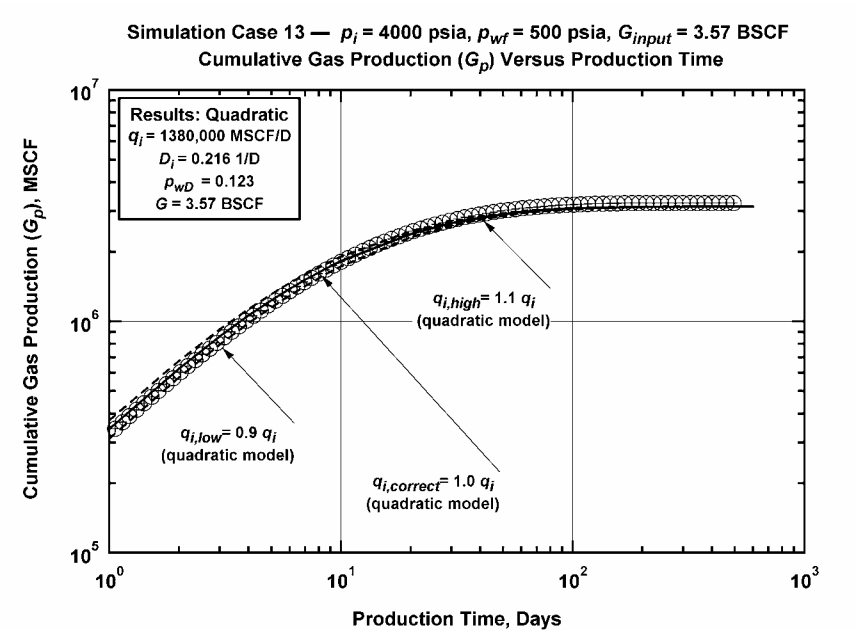


**Figure A-86 – Simulated Performance Case 13: $G_p$ versus $t$ ($p_i$=4000 psia, $p_{wf}$=500 psia, $G_{input}$=3.57 BSCF).**

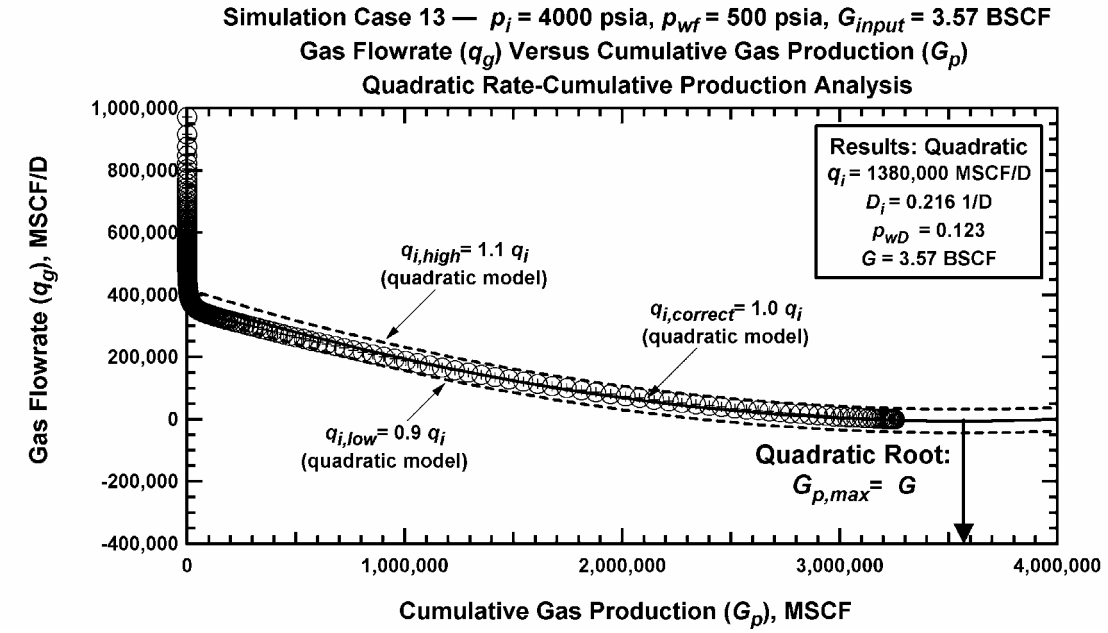


**Figure A-87 – Simulated Performance Case 13: $q_g$ versus $G_p$ ($p_i$=4000 psia, $p_{wf}$=500 psia, $G_{input}$=3.57 BSCF).**

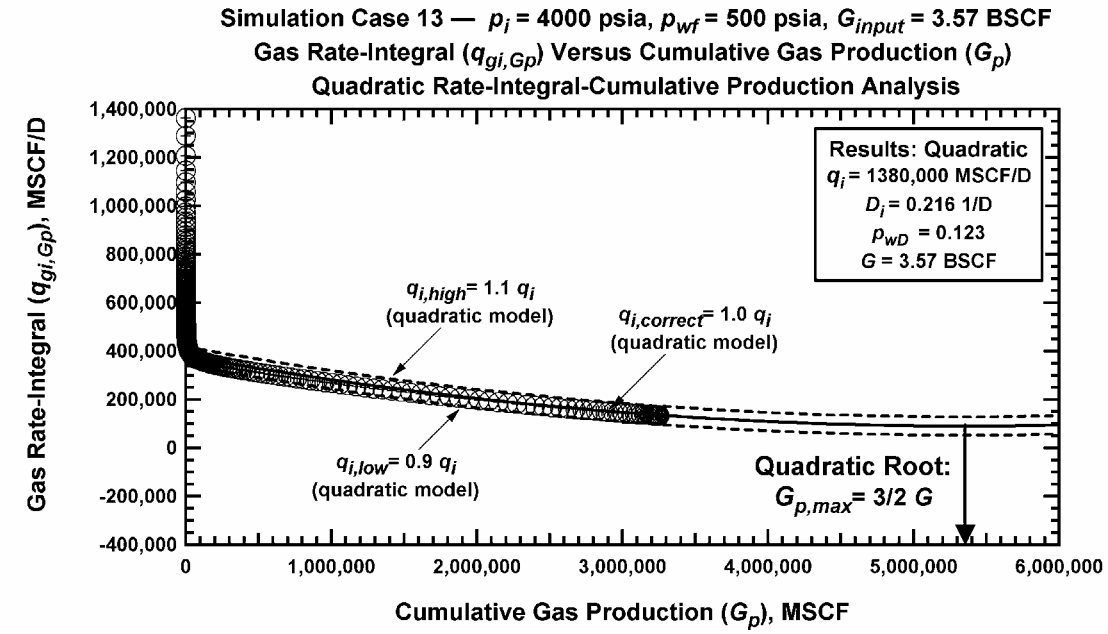


**Figure A-88 – Simulated Performance Case 13: $q_{qi,Gp}$ versus $G_p$ ($p_i$=4000 psia, $p_{wf}$=500 psia, $G_{input}$=3.57 BSCF).**

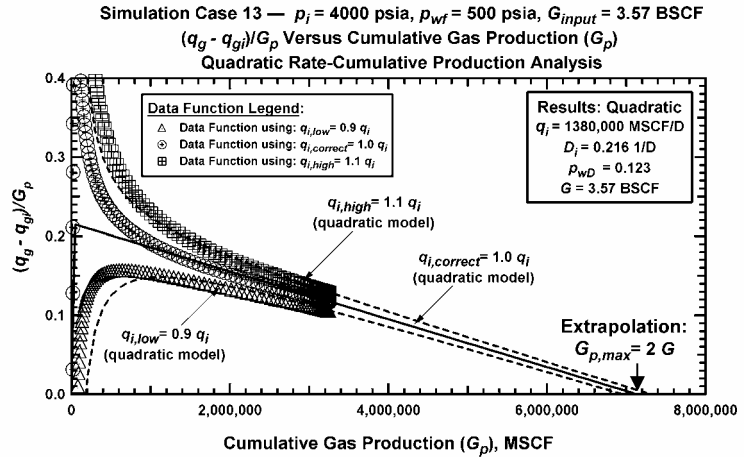


**Figure A-89 – Simulated Performance Case 13: $(q_{qi}-q_q)/G_p$ versus $G_p$ ($p_i$=4000 psia, $p_{wf}$=500 psia, $G_{input}$=3.57 BSCF). (Plotting Function 1 ($PF_1$)).**

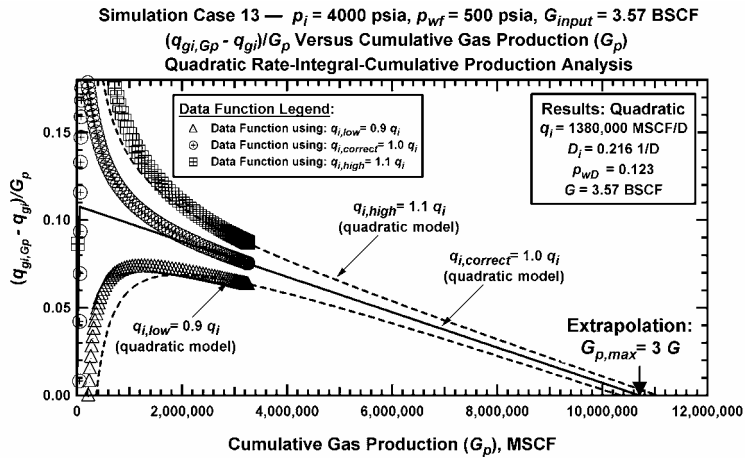


**Figure A-90 – Simulated Performance Case 13: $(q_{qi,Gp}-q_{qi})/G_p$ versus $G_p$ ($p_i$=4000 psia, $p_{wf}$=500 psia, $G_{input}$=3.57 BSCF). (Plotting Function 2 ($PF_2$)).**

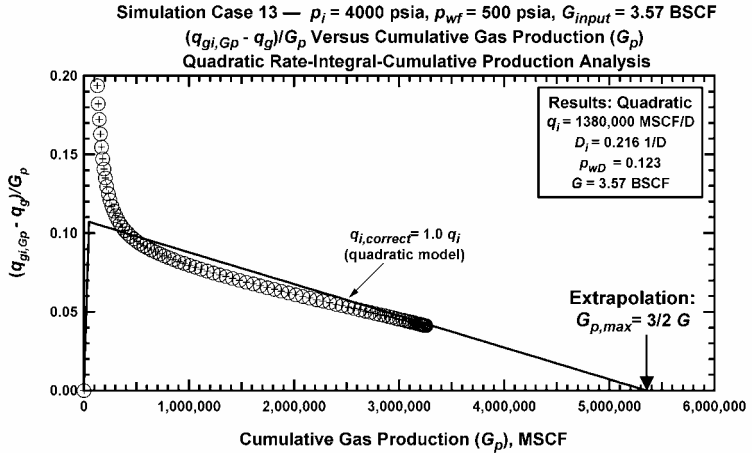


Figure A-91 – Simulated Performance Case 3: $(q_{qi,Gp}-q_q)/G_p$ versus $G_p$ ($p_i$=4000 psia, $p_{wf}$=500 psia, $G_{input}$=3.57 BSCF). (Plotting Function 3 ($PF_3$)).

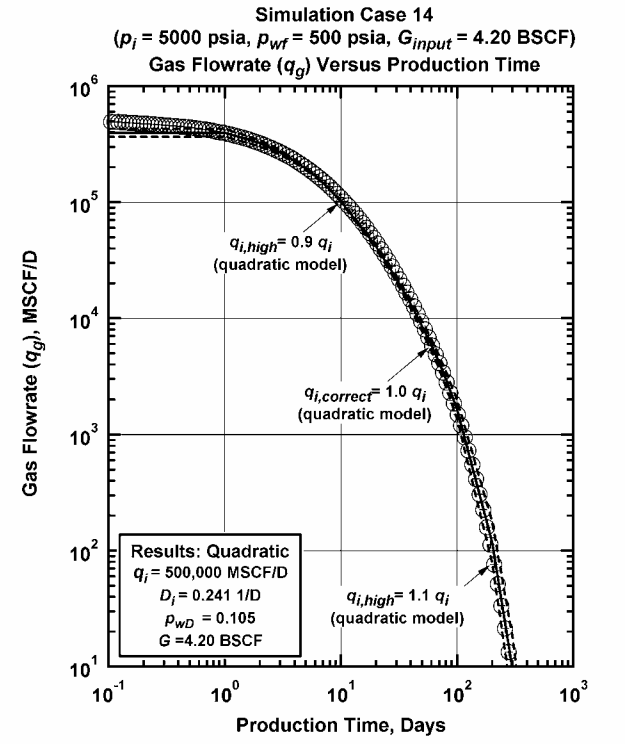


**Figure A-92 – Simulated Performance Case 14: $q_g$ versus $t$ ($p_i$=5000 psia, $p_{wf}$=500 psia, $G_{input}$=4.20 BSCF).**

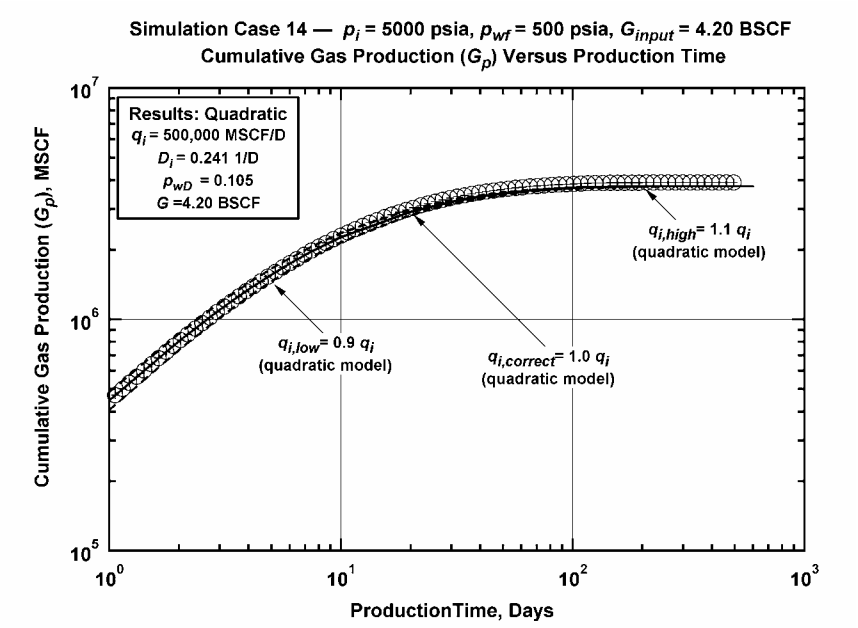


**Figure A-93 – Simulated Performance Case 14: $G_p$ versus $t$ ($p_i$=5000 psia, $p_{wf}$=500 psia, $G_{input}$=4.20 BSCF).**

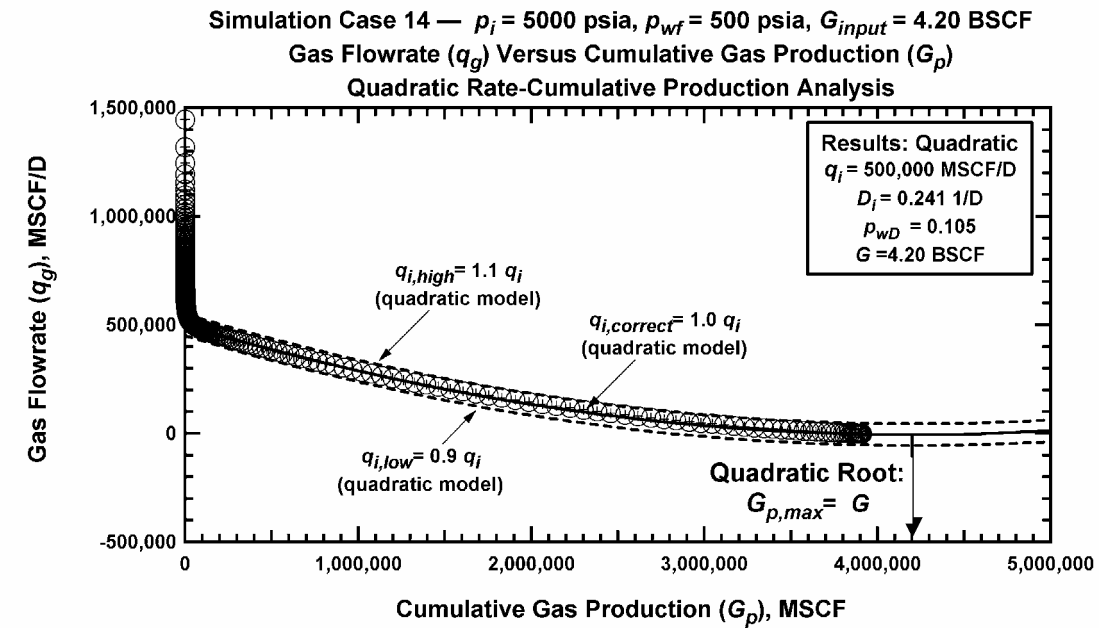


**Figure A-94 – Simulated Performance Case 14: $q_g$ versus $G_p$ ($p_i$=5000 psia, $p_{wf}$=500 psia, $G_{input}$=4.20 BSCF).**

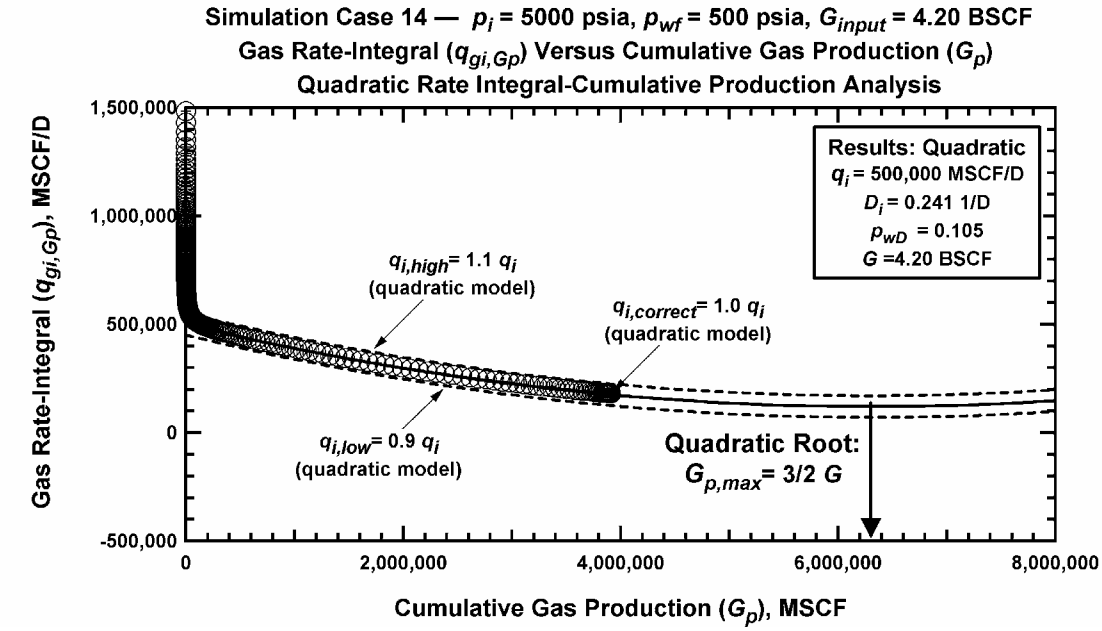


**Figure A-95 – Simulated Performance Case 14: $q_{qi,Gp}$ versus $G_p$ ($p_i$=5000 psia, $p_{wf}$=500 psia, $G_{input}$=4.20 BSCF).**

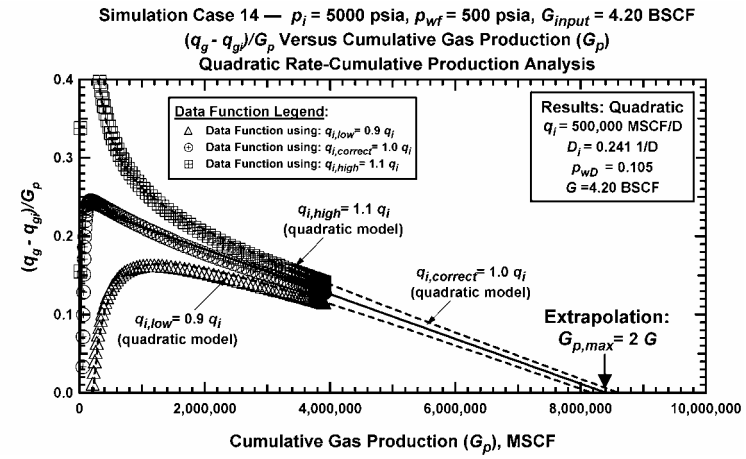


**Figure A-96 – Simulated Performance Case 14: $(q_{qi}-q_q)/G_p$ versus $G_p$ ($p_i$=5000 psia, $p_{wf}$=500 psia, $G_{input}$=4.20 BSCF). (Plotting Function 1 ($PF_1$)).**

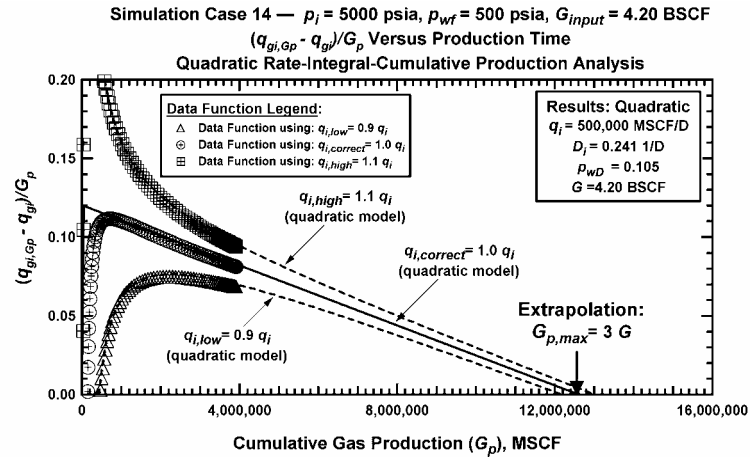


**Figure A-97 – Simulated Performance Case 14: $(q_{qi,Gp}-q_{qi})/G_p$ versus $G_p$ ($p_i$=5000 psia, $p_{wf}$=500 psia, $G_{input}$=4.20 BSCF). (Plotting Function 2 ($PF_2$)).**

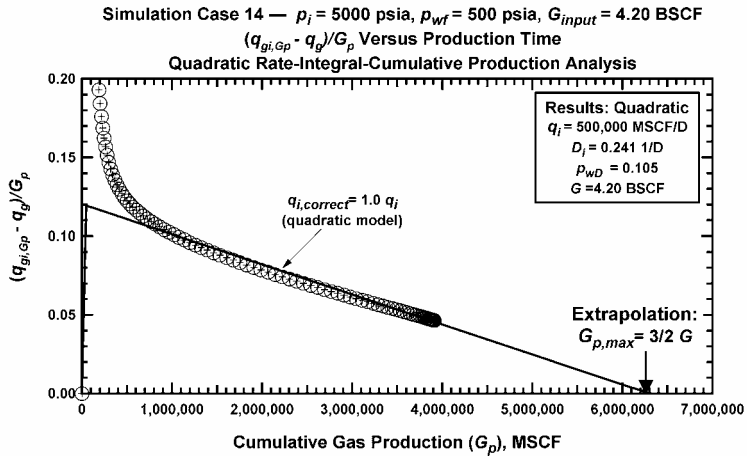


**Figure A-98 – Simulated Performance Case 14: $(q_{qi,Gp}-q_q)/G_p$ versus $G_p$ ($p_i$= 5000 psia, $p_{wf}$=500 psia, $G_{input}$=4.20 BSCF) (Plotting Function 3 ($PF_3$)).**

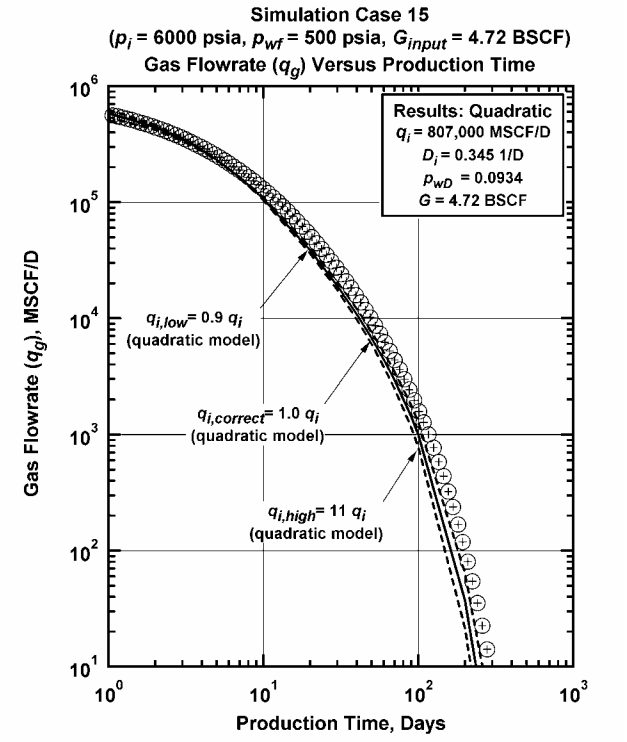


**Figure A-99 – Simulated Performance Case 15: $q_g$ versus $t$ ($p_i$=6000 psia, $p_{wf}$=500 psia, $G_{input}$=4.72 BSCF).**

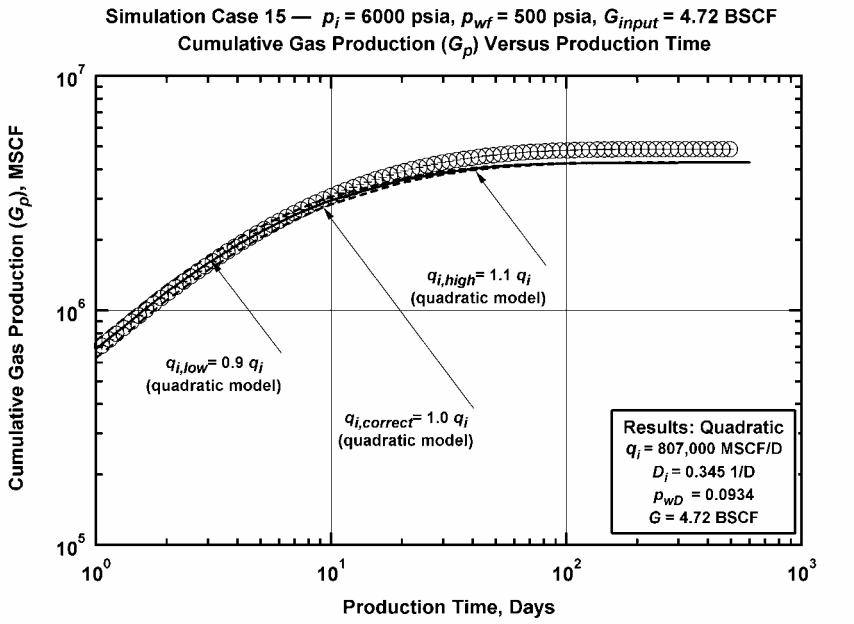


**Figure A-100 – Simulated Performance Case 15: $G_p$ versus $t$ ($p_i$=6000 psia, $p_{wf}$=500 psia, $G_{input}$=4.72 BSCF).**

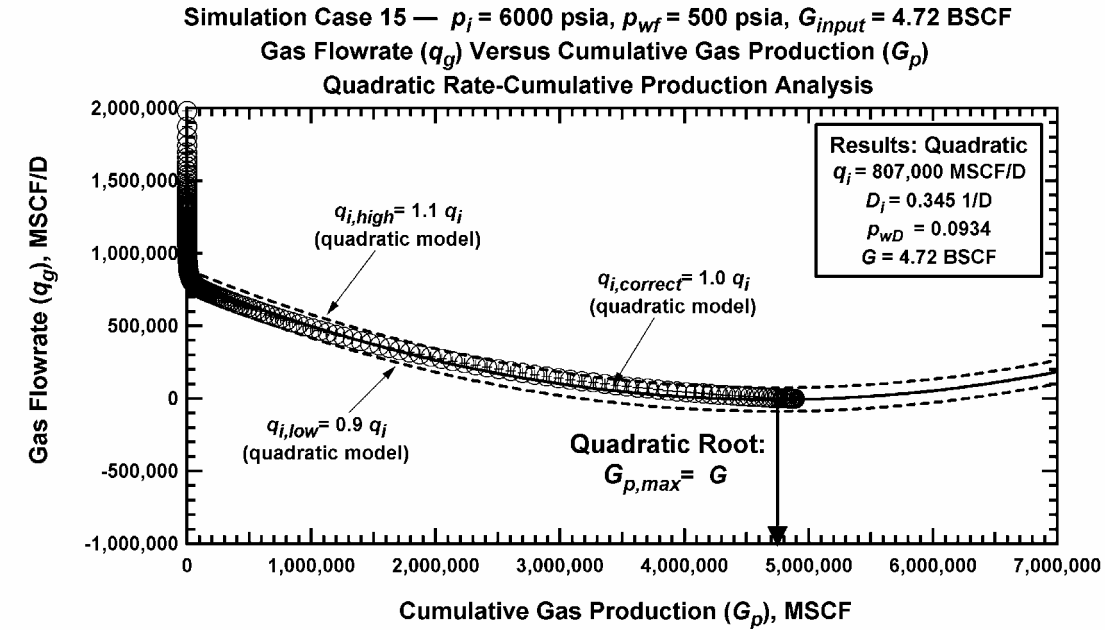


**Figure A-101 – Simulated Performance Case 15: $q_g$ versus $G_p$ ($p_i$=6000 psia, $p_{wf}$=500 psia, $G_{input}$=4.72 BSCF).**

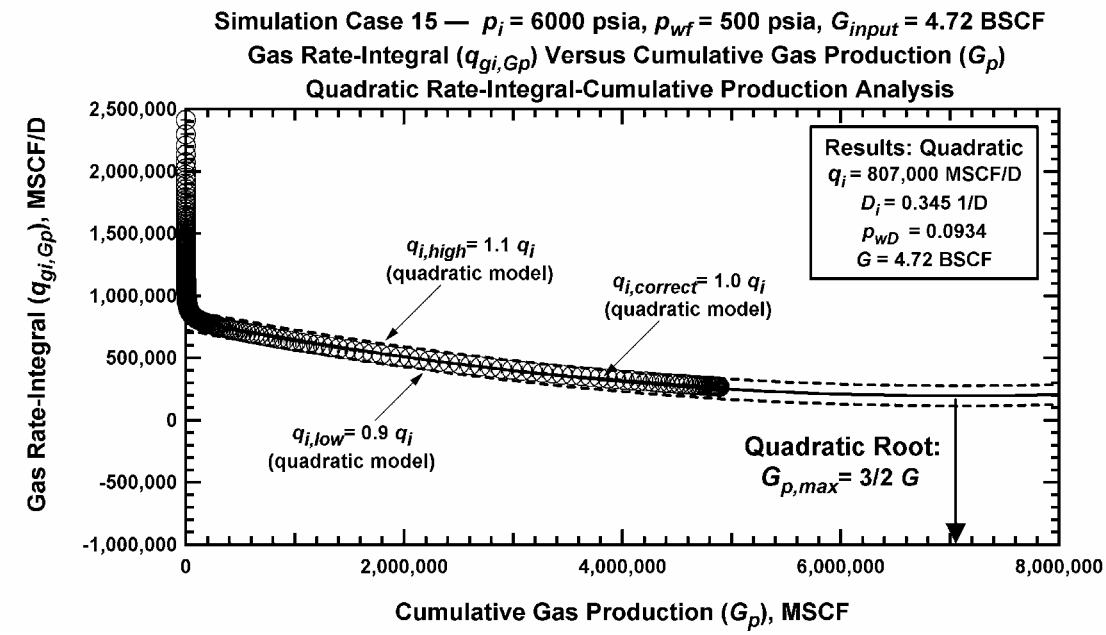


**Figure A-102 – Simulated Performance Case 15: $q_{qi,Gp}$ versus $G_p$ ($p_i$=6000 psia, $p_{wf}$=500 psia, $G_{input}$=4.72 BSCF).**

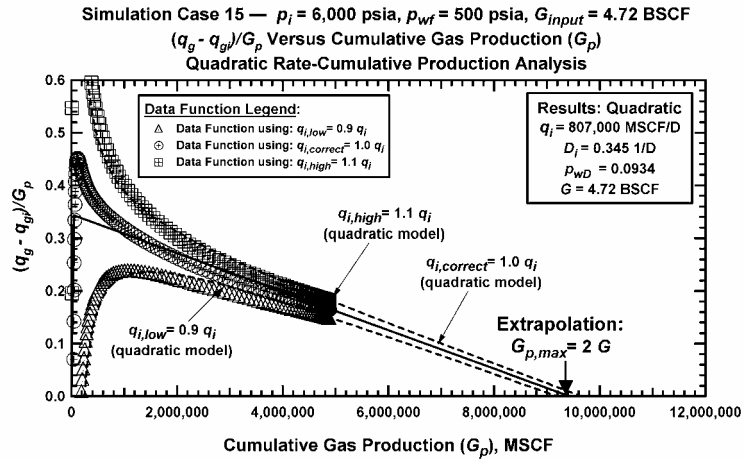


**Figure A-103 – Simulated Performance Case 15: $(q_{qi}-q_q)/G_p$ versus $G_p$ ($p_i$=6000 psia, $p_{wf}$=500 psia, $G_{input}$=4.72 BSCF). (Plotting Function 1 ($PF_1$)).**

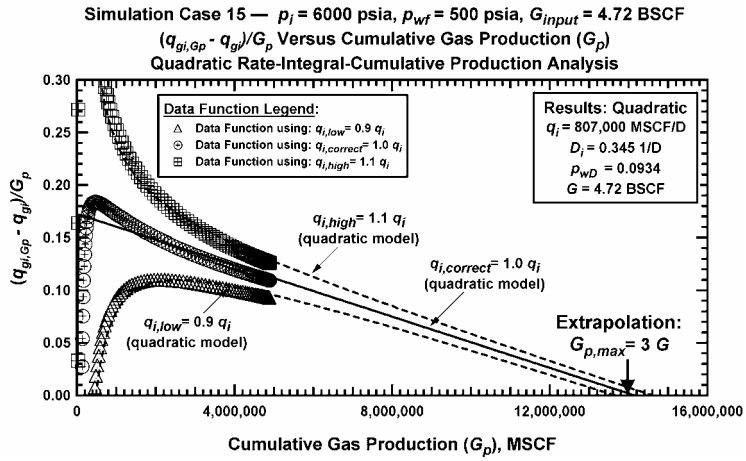


**Figure A-104 – Simulated Performance Case 15: $(q_{qi,Gp}-q_{qi})/G_p$ versus $G_p$ ($p_i$=6000 psia, $p_{wf}$=500 psia, $G_{input}$=4.72 BSCF). (Plotting Function 2 ($PF_2$)).**

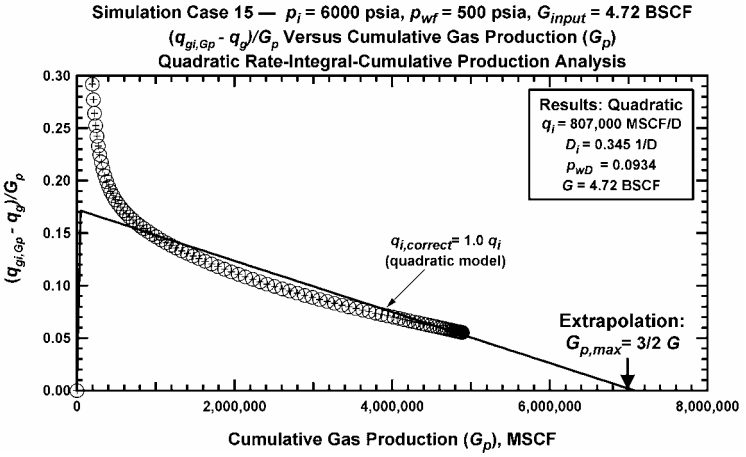


**Figure A-105 – Simulated Performance Case 15: $(q_{qi,Gp}-q_q)/G_p$ versus $G_p$ ($p_i$=6000 psia, $p_{wf}$=500 psia, $G_{input}$=4.72 BSCF). (Plotting Function 3 ($PF_3$)).**

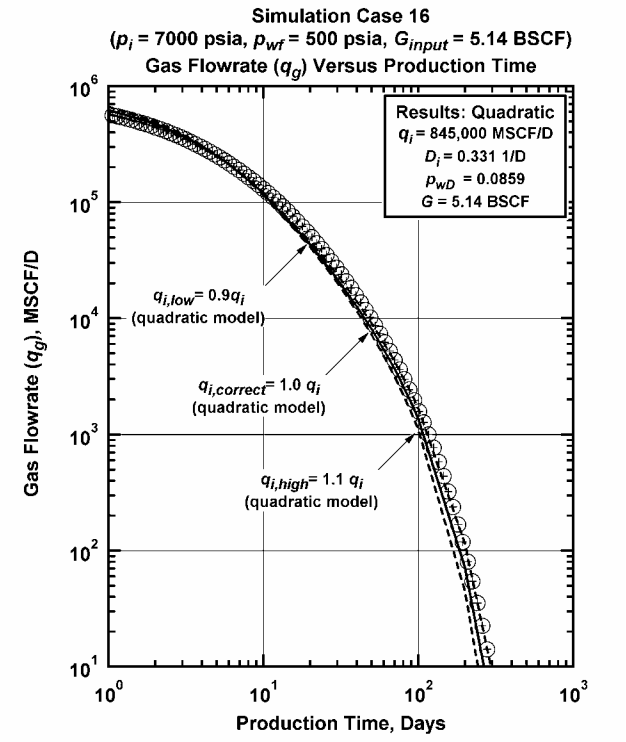


**Figure A-106 – Simulated Performance Case 16: $q_g$ versus $t$ ($p_i$=7000 psia, $p_{wf}$=500 psia, $G_{input}$=5.14 BSCF).**

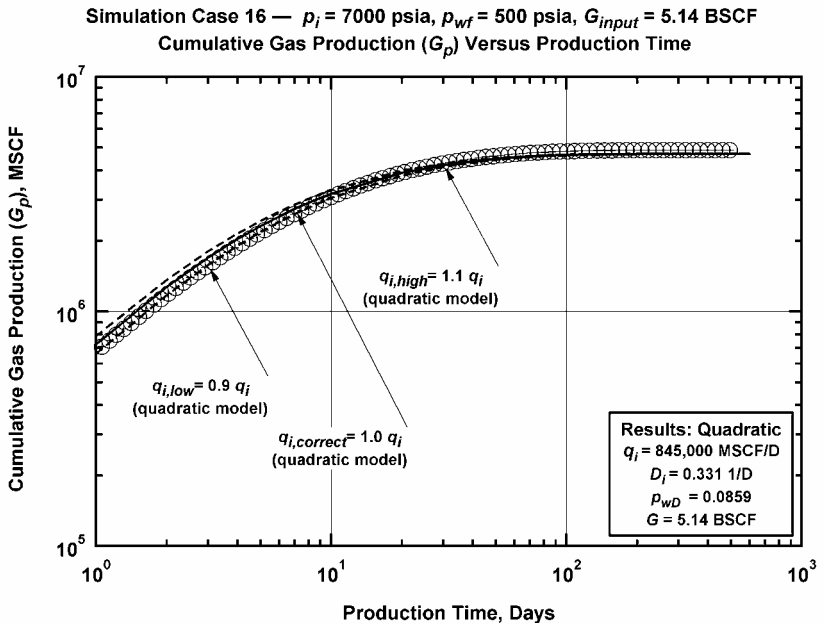


**Figure A-107 – Simulated Performance Case 16: $G_p$ versus $t$ ($p_i$=7000 psia, $p_{wf}$=500 psia, $G_{input}$=5.14 BSCF).**

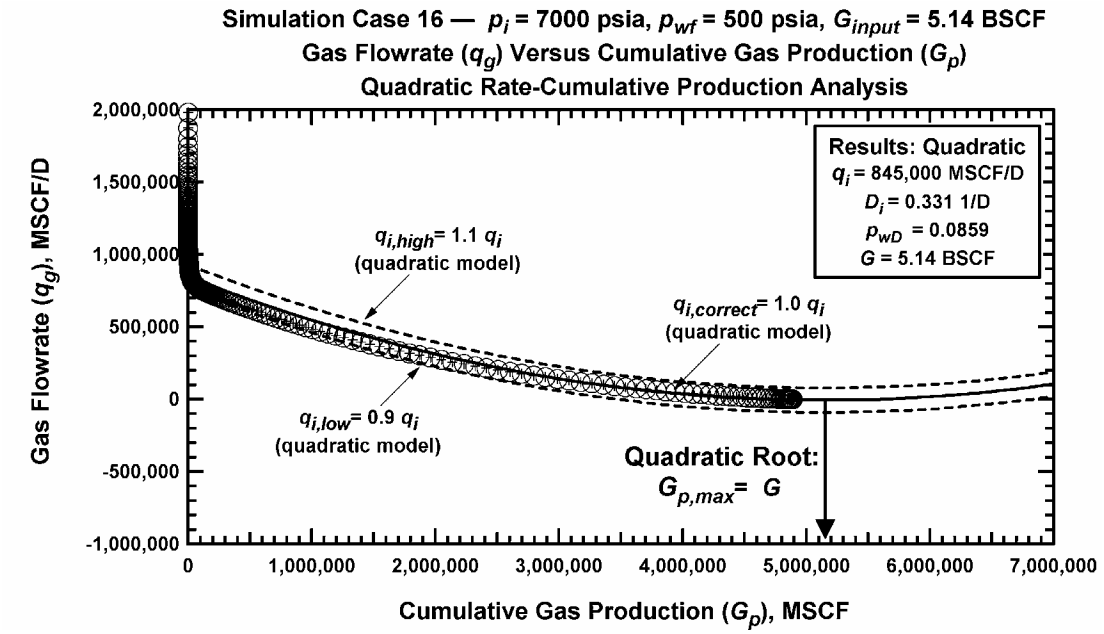


**Figure A-108 – Simulated Performance Case 16: $q_g$ versus $G_p$ ($p_i$=7000 psia, $p_{wf}$=500 psia, $G_{input}$=5.14 BSCF).**

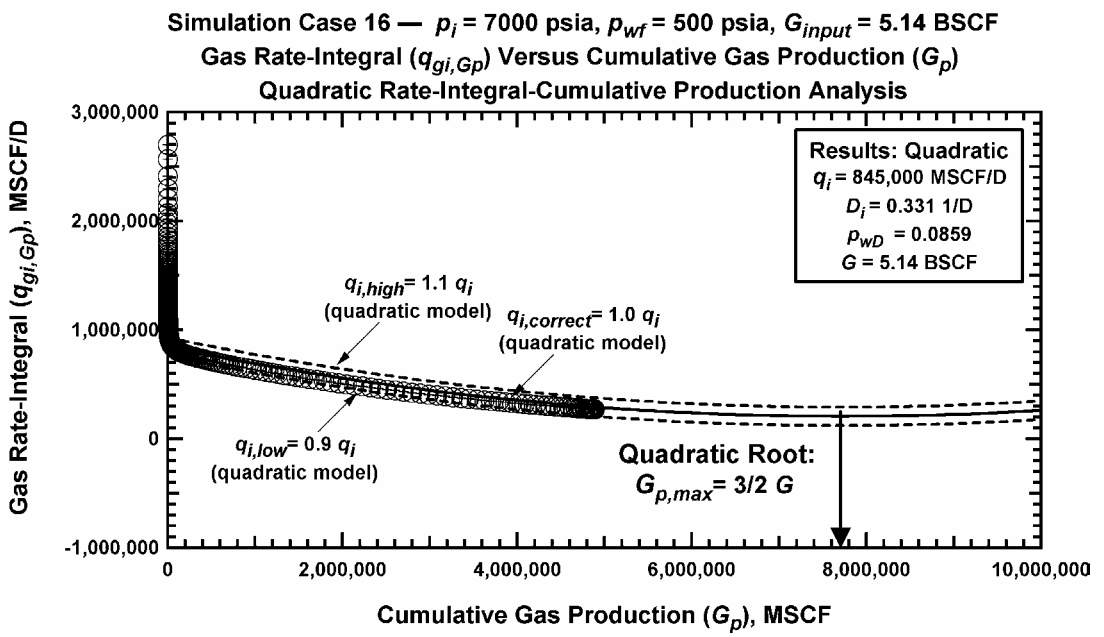


**Figure A-109 – Simulated Performance Case 16: $q_{qi,Gp}$ versus $G_p$ (($p_i$=7000 psia, $p_{wf}$=500 psia, $G_{input}$=5.14 BSCF).**

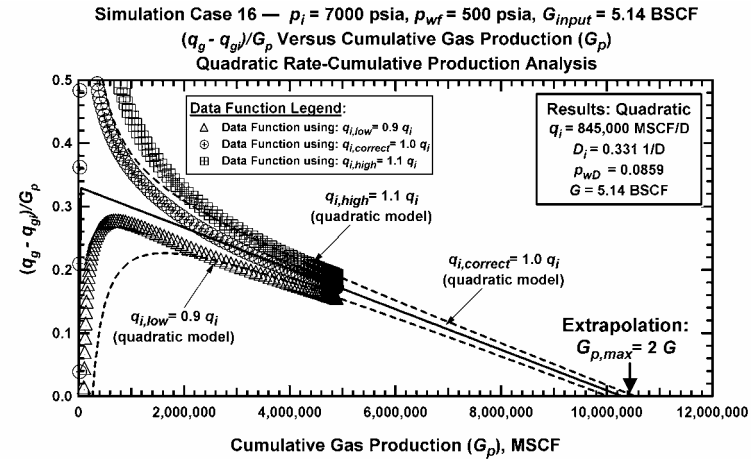


**Figure A-110 – Simulated Performance Case 16: $(q_{qi}-q_q)/G_p$ versus $G_p$ ($p_i$=7000 psia, $p_{wf}$=500 psia, $G_{input}$=5.14 BSCF). (Plotting Function 1 ($PF_1$)).**

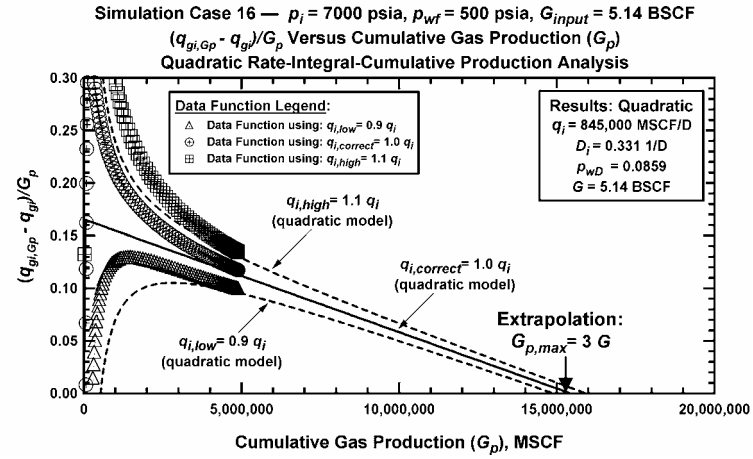


**Figure A-111 – Simulated Performance Case 16: $(q_{qi,Gp}-q_{qi})/G_p$ versus $G_p$ ($p_i$=7000 psia, $p_{wf}$=500 psia, $G_{input}$=5.14 BSCF). (Plotting Function 2 ($PF_2$)).**

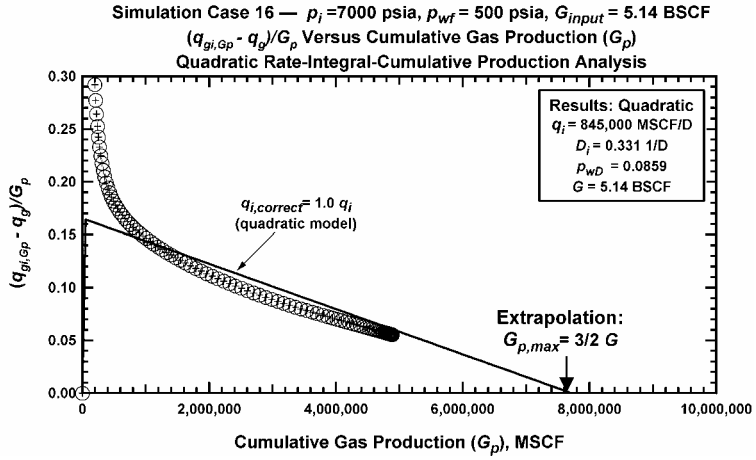


**Figure A-112 – Simulated Performance Case 16: $(q_{qi,Gp}-q_q)/G_p$ versus $G_p$ ($p_i$=7000 psia, $p_{wf}$=500 psia, $G_{input}$=5.14 BSCF). (Plotting Function 3 ($PF_3$)).**

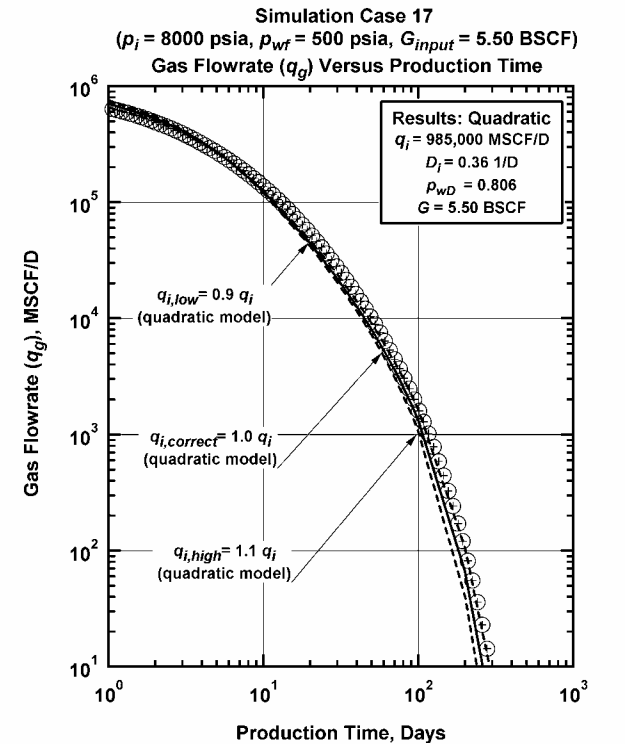


**Figure A-113 – Simulated Performance Case 17: $q_g$ versus $t$ ($p_i$=8000 psia, $p_{wf}$=500 psia, $G_{input}$=5.50 BSCF).**

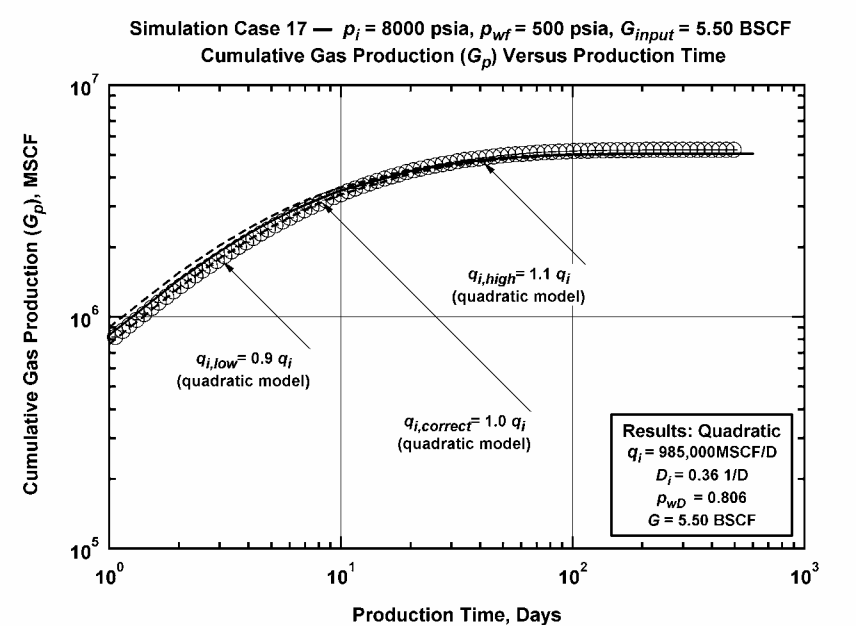


**Figure A-114 – Simulated Performance Case 17: $G_p$ versus $t$ ($p_i$=8000 psia, $p_{wf}$=500 psia, $G_{input}$=5.50 BSCF).**

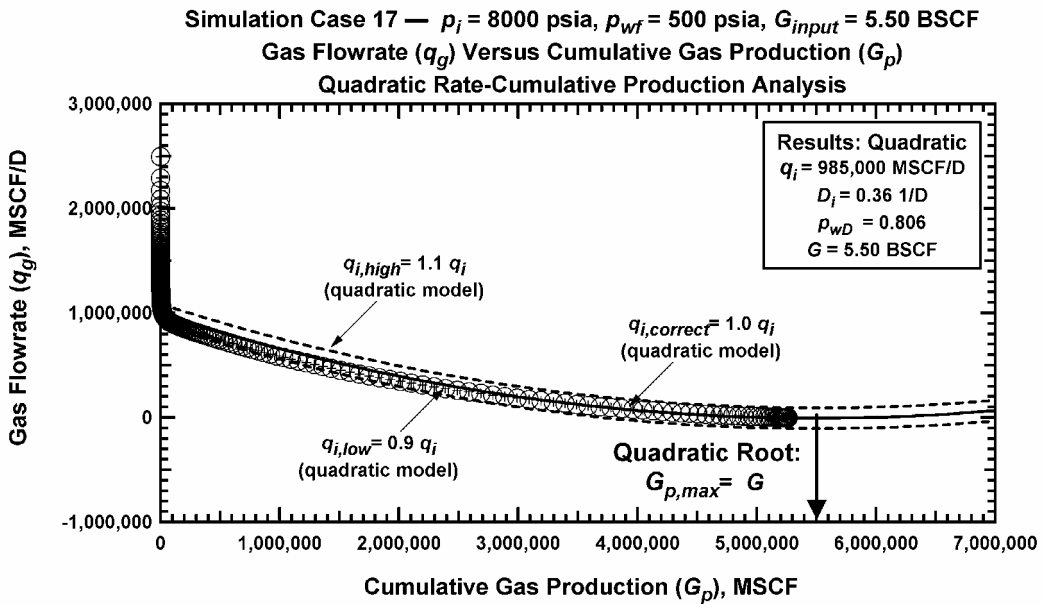


**Figure A-115 – Simulated Performance Case 17: $q_g$ versus $G_p$ ($p_i$=8000 psia, $p_{wf}$=500 psia, $G_{input}$=5.50 BSCF).**

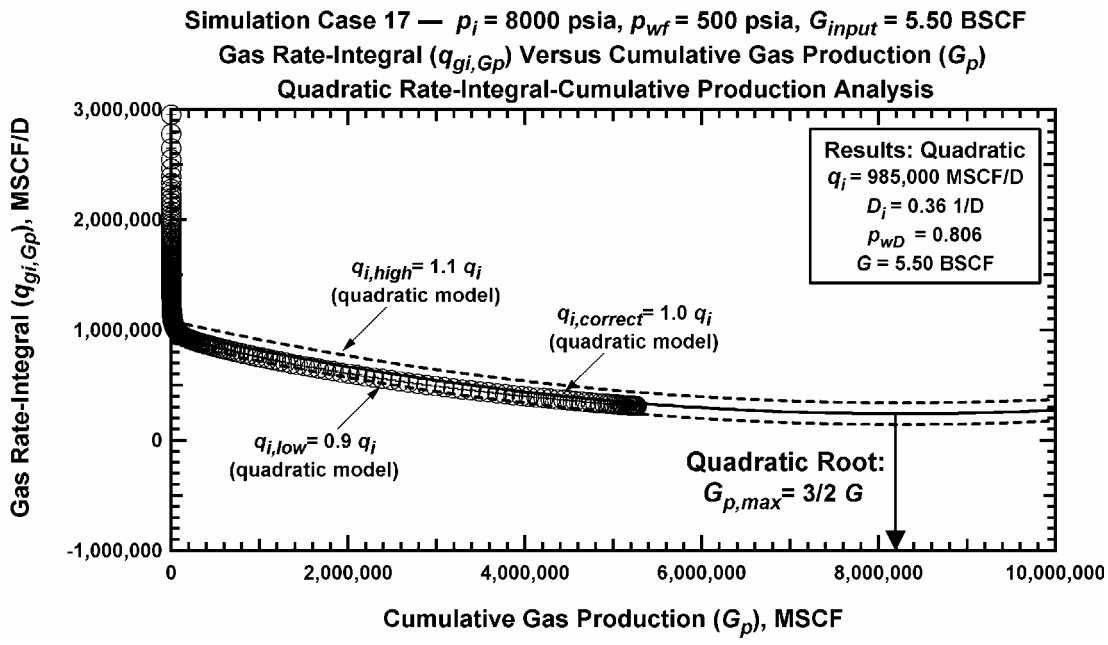


**Figure A-116 – Simulated Performance Case 17: $q_{qi,Gp}$ versus $G_p$ ($p_i$=8000 psia, $p_{wf}$=500 psia, $G_{input}$=5.50 BSCF).**

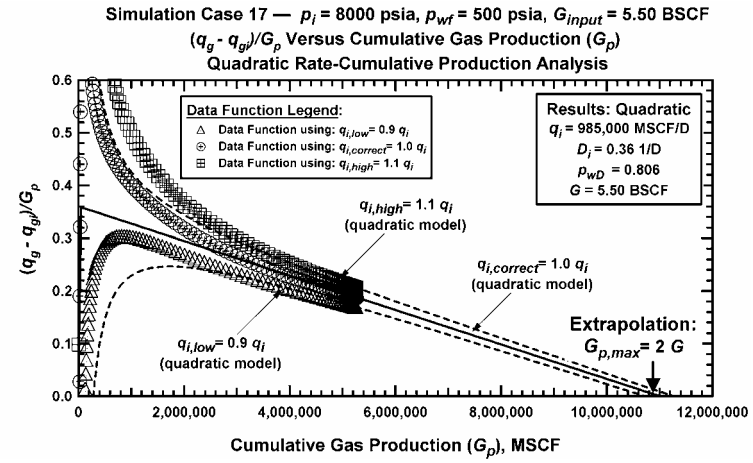


**Figure A-117 – Simulated Performance Case 17: $(q_{qi}-q_q)/G_p$ versus $G_p$ ($p_i$=8000 psia, $p_{wf}$=500 psia, $G_{input}$=5.50 BSCF). (Plotting Function 1 ($PF_1$)).**

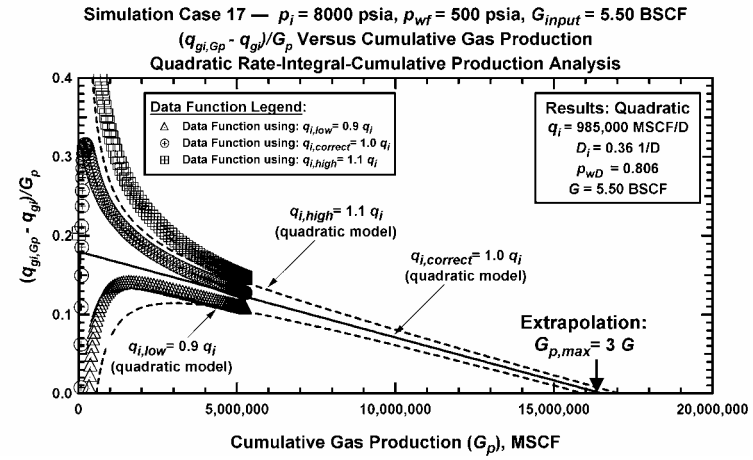


**Figure A-118 – Simulated Performance Case 17: $(q_{qi,Gp}-q_{qi})/G_p$ versus $G_p$ ($p_i$=8000 psia, $p_{wf}$=500 psia, $G_{input}$=5.50 BSCF). (Plotting Function 2 ($PF_2$)).**

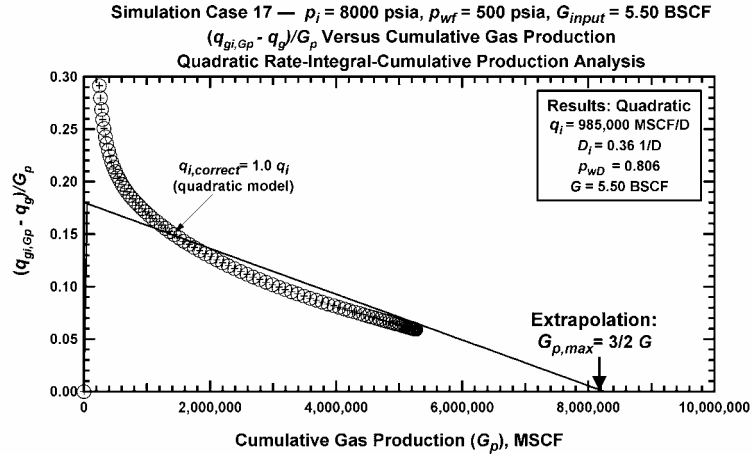


**Figure A-119 – Simulated Performance Case 17: $(q_{qi,Gp}-q_q)/G_p$ versus $G_p$ ($p_i$=8000 psia, $p_{wf}$=500 psia, $G_{input}$=5.50 BSCF). (Plotting Function 3 ($PF_3$)).**

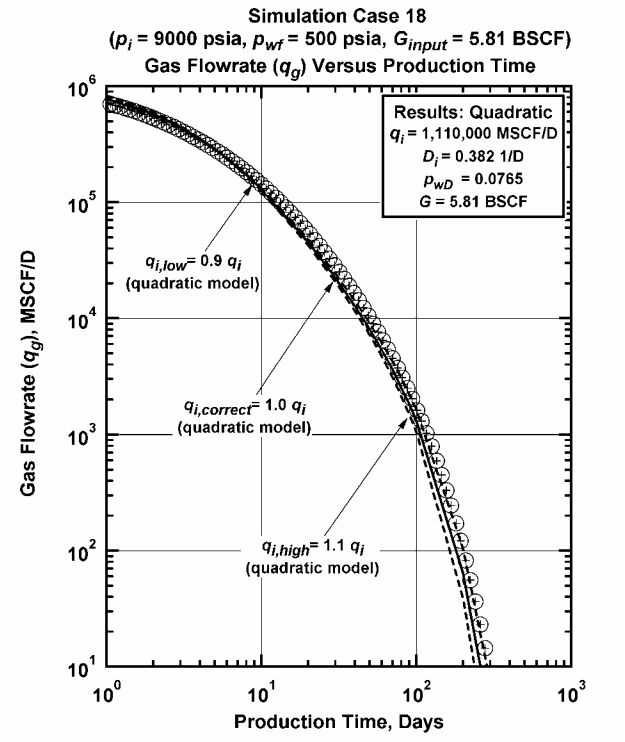


**Figure A-120 – Simulated Performance Case 18: $q_g$ versus $t$ ($p_i$=9000 psia, $p_{wf}$=500 psia, $G_{input}$=5.81 BSCF).**

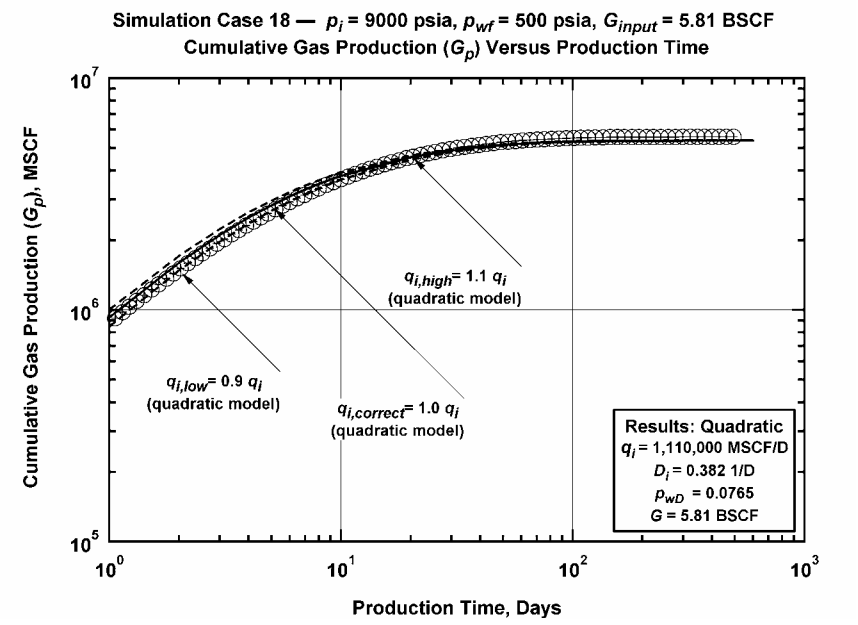


**Figure A-121 – Simulated Performance Case 18: $G_p$ versus $t$ (($p_i$=9000 psia, $p_{wf}$=500 psia, $G_{input}$=5.81 BSCF).**

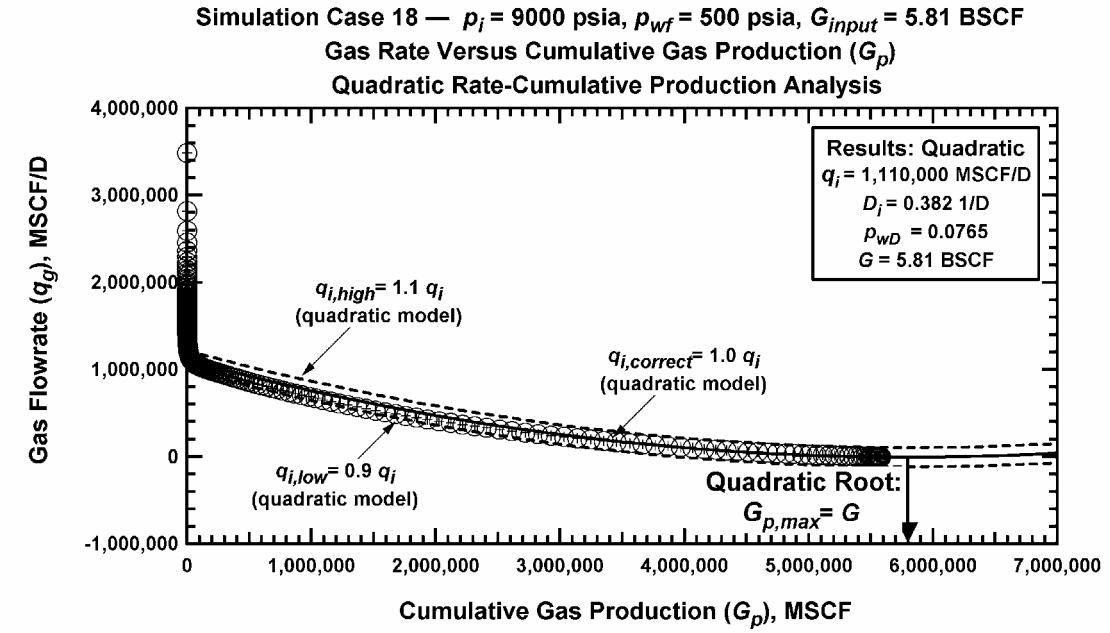


**Figure A-122 – Simulated Performance Case 18: $q_g$ versus $G_p$ ($p_i$=9000 psia, $p_{wf}$=500 psia, $G_{input}$=5.81 BSCF).**

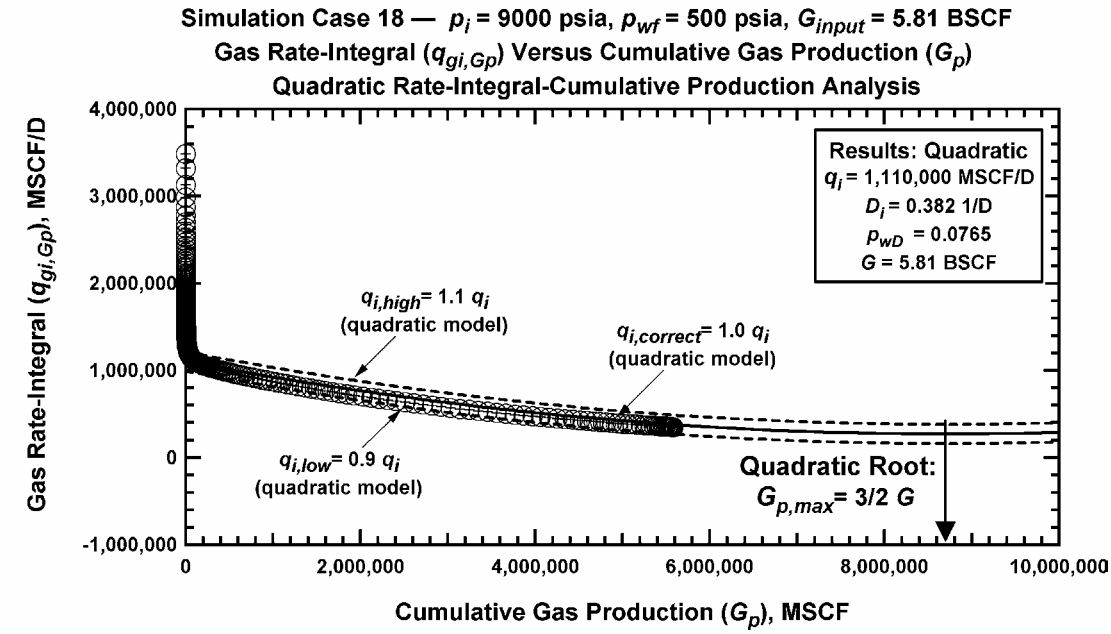


**Figure A-123 – Simulated Performance Case 18: $q_{qi,Gp}$ versus $G_p$ ($p_i$=9000 psia, $p_{wf}$=500 psia, $G_{input}$=5.81 BSCF).**

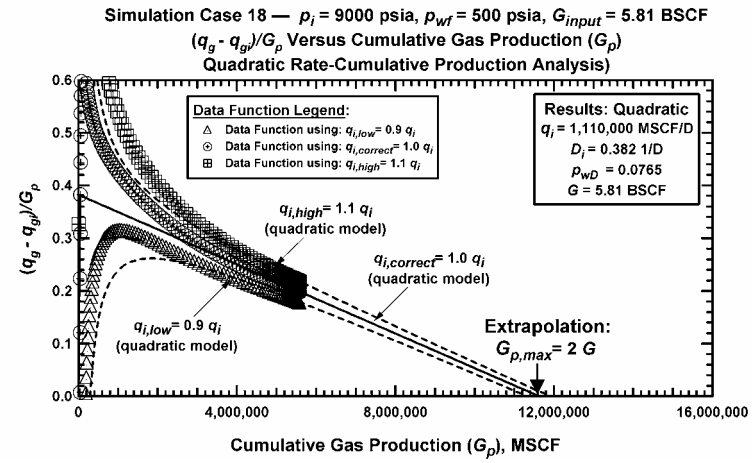


**Figure A-124 – Simulated Performance Case 18: $(q_{qi}-q_q)/G_p$ versus $G_p$ ($p_i$=9000 psia, $p_{wf}$=500 psia, $G_{input}$=5.81 BSCF). (Plotting Function 1 ($PF_1$)).**

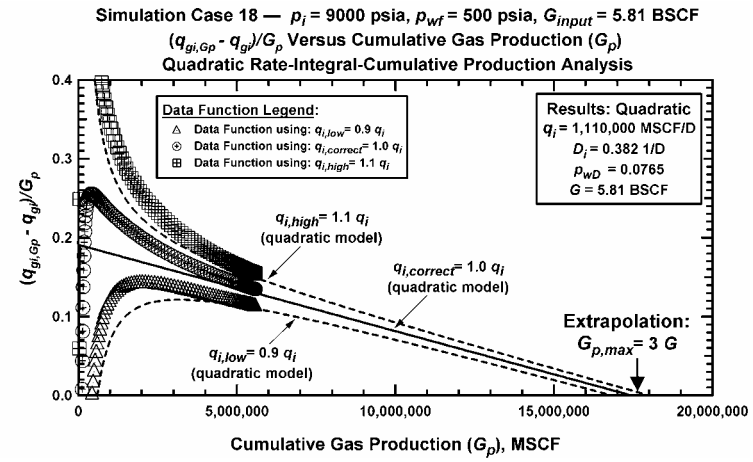


**Figure A-125 – Simulated Performance Case 18: $(q_{qi,Gp}-q_{qi})/G_p$ versus $G_p$ ($p_i$=9000 psia, $p_{wf}$=500 psia, $G_{input}$=5.81 BSCF). (Plotting Function 2 ($PF_2$)).**

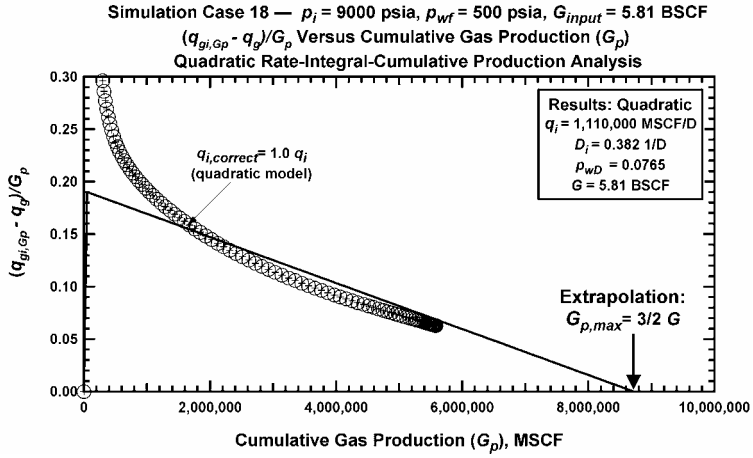


**Figure A-126 – Simulated Performance Case 18: $(q_{qi,Gp}-q_q)/G_p$ versus $G_p$ ($p_i$=9000 psia, $p_{wf}$=500 psia, $G_{input}$=5.81 BSCF). (Plotting Function 3 ($PF_3$)).**

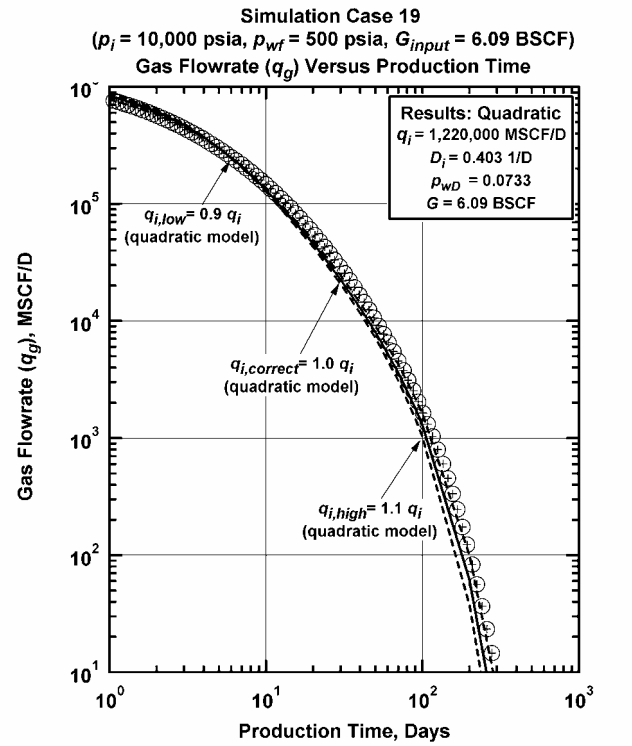


**Figure A-127 – Simulated Performance Case 19: $q_g$ versus $t$ ($p_i$=10,000 psia, $p_{wf}$=500 psia, $G_{input}$=6.09 BSCF).**

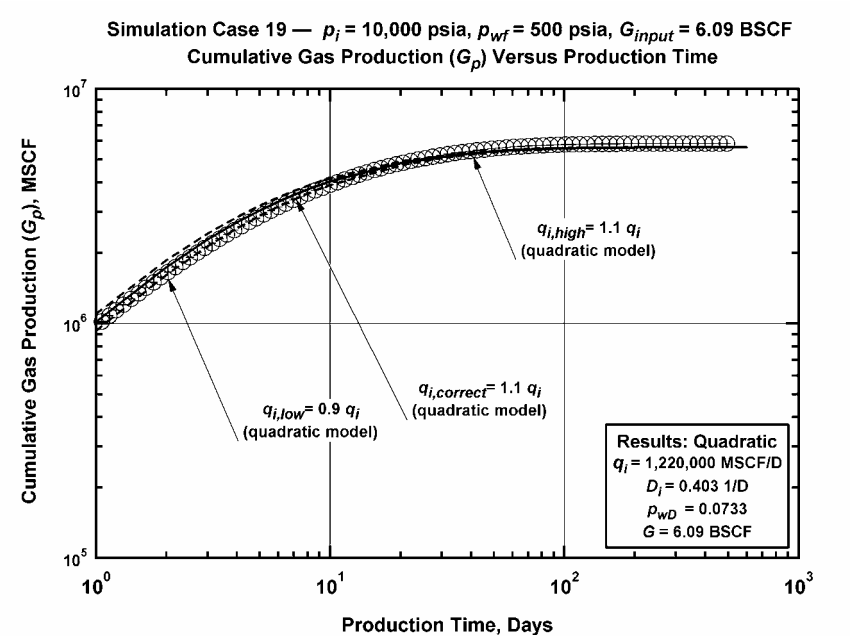


**Figure A-128 – Simulated Performance Case 19: $G_p$ versus $t$ ($p_i$=10,000 psia, $p_{wf}$=500 psia, $G_{input}$=6.09 BSCF).**

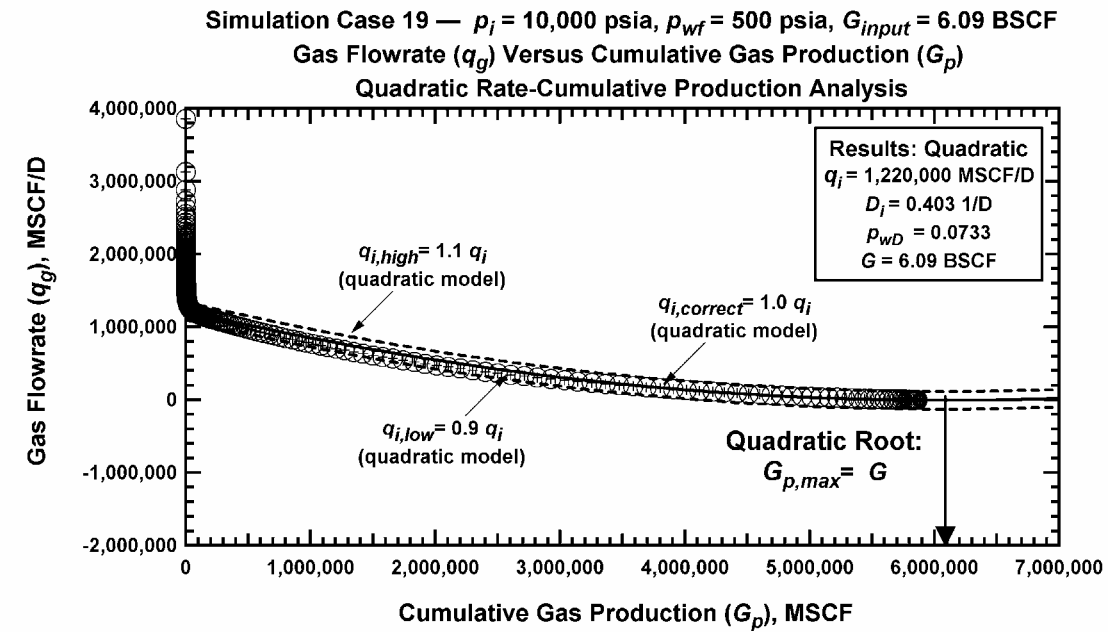


**Figure A-129 – Simulated Performance Case 19: $q_g$ versus $G_p$ ($p_i$=10,000 psia, $p_{wf}$=500 psia, $G_{input}$=6.09 BSCF).**

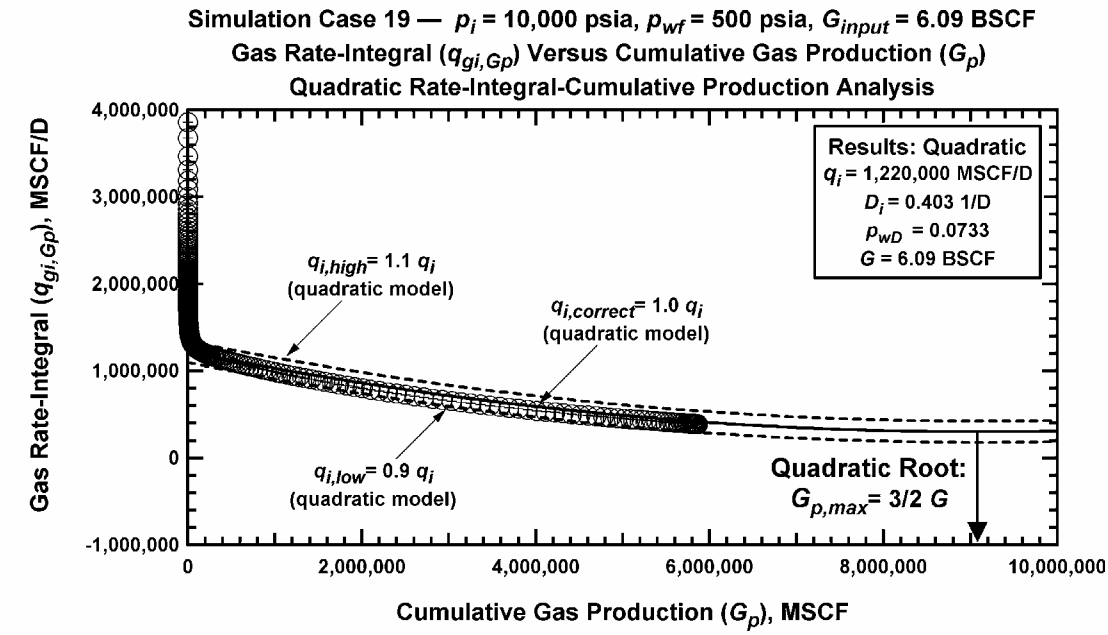


**Figure A-130 – Simulated Performance Case 19: $q_{qi,Gp}$ versus $G_p$ ($p_i$=10,000 psia, $p_{wf}$=500 psia, $G_{input}$=6.09 BSCF).**

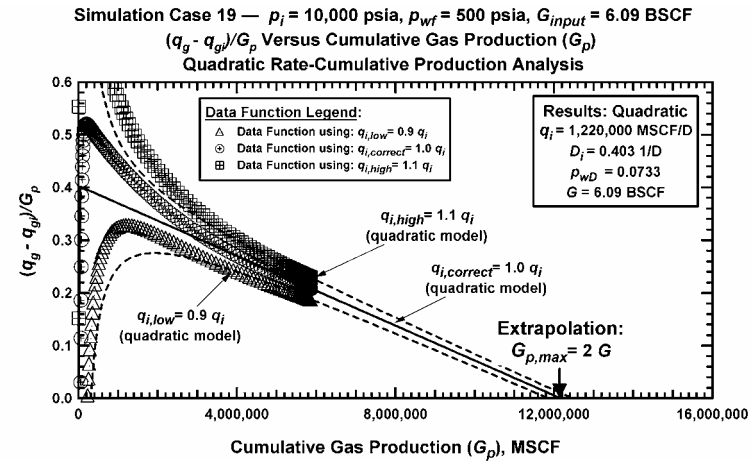


**Figure A-131 – Simulated Performance Case 19: $(q_{qi}-q_q)/G_p$ versus $G_p$ ($p_i$=10,000 psia, $p_{wf}$=500 psia, $G_{input}$=6.09 BSCF). (Plotting Function 1 ($PF_1$)).**

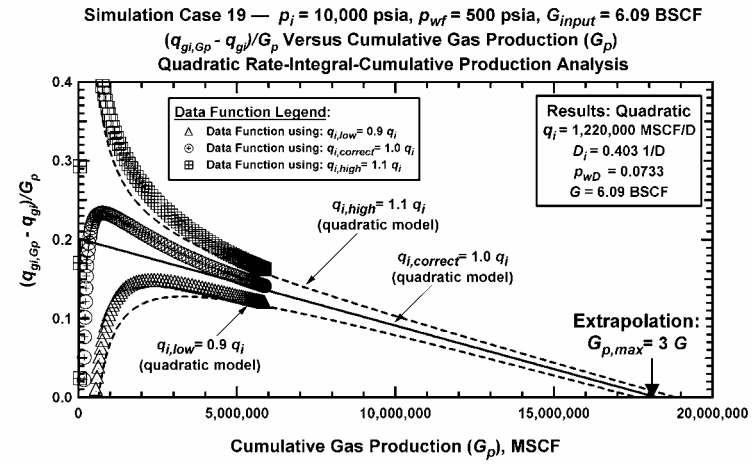


**Figure A-132 – Simulated Performance Case 19: $(q_{qi,Gp}-q_{qi})/G_p$ versus $G_p$ ($p_i$=10,000 psia, $p_{wf}$=500 psia, $G_{input}$=6.09 BSCF). (Plotting Function 2 ($PF_2$)).**

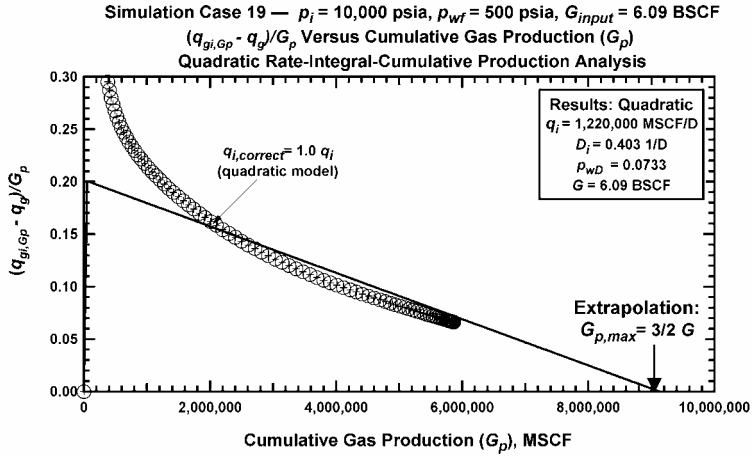


**Figure A-133 – Simulated Performance Case 19: $(q_{qi,Gp}-q_q)/G_p$ versus $G_p$ ($p_i$=10,000 psia, $p_{wf}$=500 psia, $G_{input}$=6.09 BSCF). (Plotting Function 3 ($PF_3$)).**

# APPENDIX B
# ANALYSIS OF FIELD EXAMPLES OBTAINED FROM THE PETROLEUM LITERATURE AND INDUSTRY SOURCES

This Appendix is a compilation of analyses results obtained using our new analysis methodology on a variety of field data cases. The following field data cases are evaluated:

| Case | Source | Comment |
|---|---|---|
| 1 | Literature | "Standard" literature case. |
| 2 | Industry | High reservoir pressure, formation compressibility not negligible. |
| 3 | Industry | High reservoir pressure, horizontal well completion. |
| 4 | Industry | Very high reservoir pressure, no reservoir description. |
| 5 | Industry | Moderate reservoir pressure, example of a "typical" well. |
| 6 | Industry | High reservoir pressure, another example of a "typical" well. |
| 7 | Industry | Very high reservoir pressure, no reservoir description (same as Case 4). |
| 8 | Industry | Low permeability reservoir, daily rate and surface pressure taken. |
| 9 | Industry | Source requests anonymity. |

**Case 1: Fetkovich *et al.*[8] — West Virginia Well A**

This case is the standard literature example given by Fetkovich *et al*. (ref. 8) and is known as "West Virginia Well A." This case represents a somewhat typical low permeability reservoir case where the rate history is considered accurate, but only a single, constant wellbore flowing pressure is reported.

**Case 1: (input data) Fetkovich *et al.*[8] — West Virginia Well A**

Reservoir Properties:

| | |
|---|---|
| Average net pay thickness, $h$ | = 70 ft |
| Average porosity, $\phi$ | = 0.06 (fraction) |
| Average formation permeability, $k$* | = 0.07 md |
| Irreducible water saturation, $S_{wi}$ | = 0.35 (fraction) |
| Initial reservoir pressure, $p_i$ | = 4175 psia |

Fluid properties:

| | |
|---|---|
| Gas specific gravity, $\gamma_g$ | = 0.57 (air=1) |
| Reservoir temperature, $T$ | = 160 deg F |

Production parameters:

| | |
|---|---|
| Bottomhole flowing pressure, $p_{wf}$ | = 710 psia |

* Permeability estimate obtained from pressure transient test analysis.

**Case 1: (results) Fetkovich *et al.*[8] — West Virginia Well A**

New "quadratic analysis" methods:

| | |
|---|---|
| Initial gas production rate, $q_{gi}$ | = 1920 MSCF/D |
| Decline constant, $D_i$ | = 0.00133 1/D |
| Dimensionless pressure, $p_{wD}$ | = 0.35 |
| Gas-in-place, $G$ | = 3.29 BSCF |

Material balance decline type curve analysis: (methods of ref. 16)

| | |
|---|---|
| Gas-in-place, $G$ | = 2.79 BSCF |
| Gas permeability, $k_g$ ($r_{eD}$=18) | = 0.0524 md |
| Near-well skin factor, $s$ ($r_{eD}$=18) | = -5.19 (dim-less) |

Fetkovich, *et al.*: (ref. 8)

| | |
|---|---|
| Gas-in-place, $G$ | = 3.36 BSCF |
| Gas permeability, $k_g$ ($r_{eD}$=20) | = 0.0524 md |
| Near-well skin factor, $s$ ($r_{eD}$=20) | = -5.17 (dim-less) |

Fraim and Wattenbarger: (ref. 14)

| | |
|---|---|
| Gas-in-place, $G$ | = 3.035 BSCF |
| Gas permeability, $k_g$ ($r_{eD}$=24) | = 0.077 md |
| Near-well skin factor, $s$ ($r_{eD}$=24) | = -5.08 (dim-less) |

McCray, *et al.*: (ref. 17)

| | |
|---|---|
| Gas-in-place, $G$ ($r_{eD}$=20) | = 2.62 BSCF |
| Gas permeability, $k_g$ ($r_{eD}$=20) | = 0.054 md |
| Near-well skin factor, $s$ ($r_{eD}$=20) | = -4.71 (dim-less) |

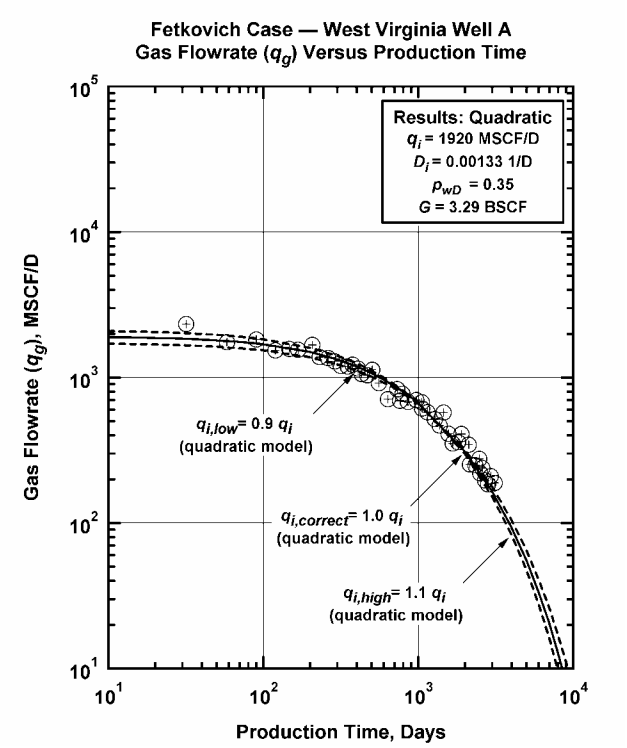


**Figure B-1 – West Virginia Well A (Fetkovich, *et al.*[8]): $q_g$ versus $t$.**

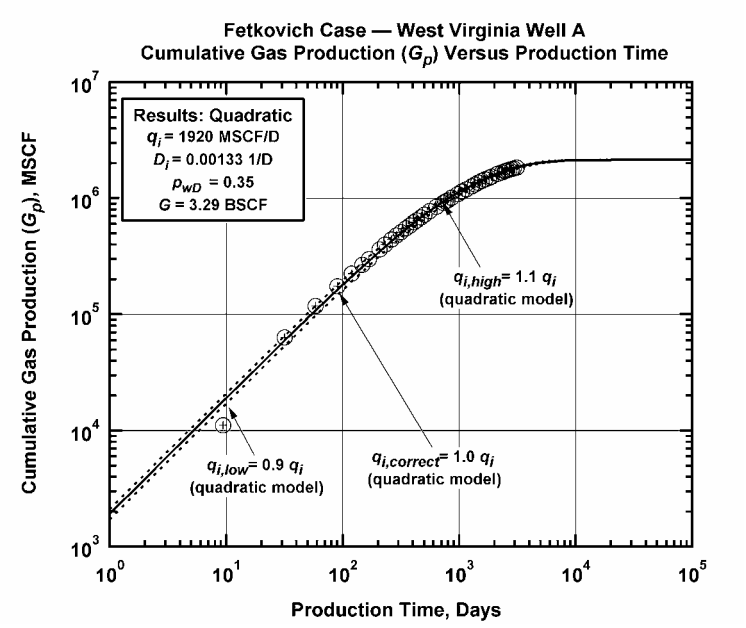


**Figure B-2 – West Virginia Well A (Fetkovich, *et al.*[8]): $G_p$ versus $t$.**

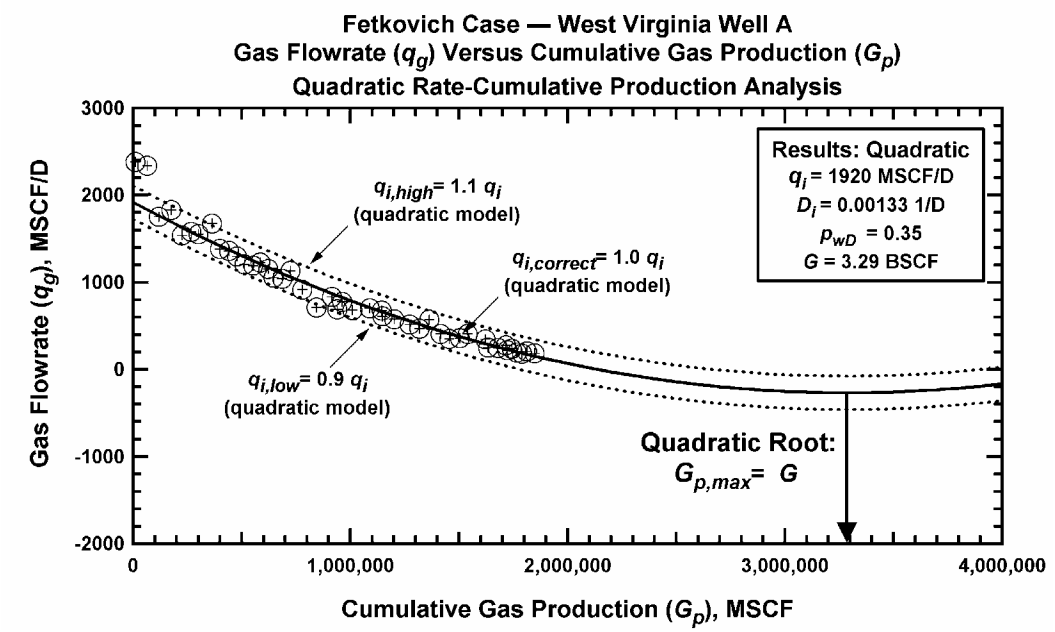


**Figure B-3 – West Virginia Well A (Fetkovich, *et al.*[8]): $q_g$ versus $G_p$.**

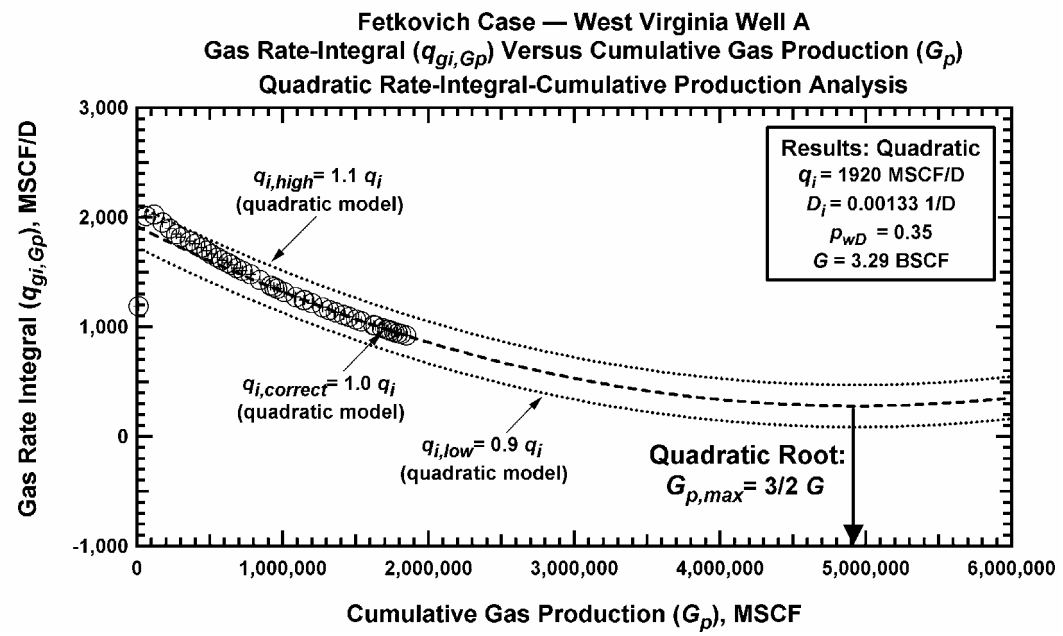


**Figure B-4 – West Virginia Well A (Fetkovich, *et al.*[8]): $q_{qi,Gp}$ versus $G_p$.**

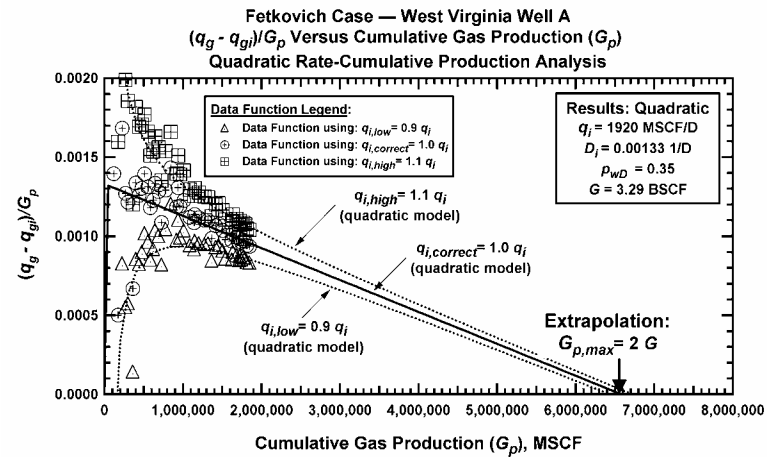


**Figure B-5 – West Virginia Well A (Fetkovich, *et al.*[8]): $(q_{qi}-q_q)/G_p$ versus $G_p$ (Plotting Function 1 ($PF_1$)).**

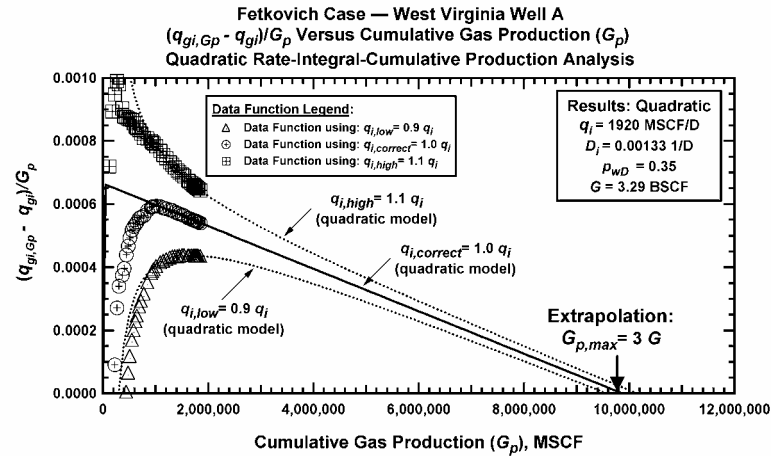


**Figure B-6 – West Virginia Well A (Fetkovich, *et al.*[8]): $(q_{qi}-q_q)/G_p$ versus $G_p$ (Plotting Function 2 ($PF_2$)).**

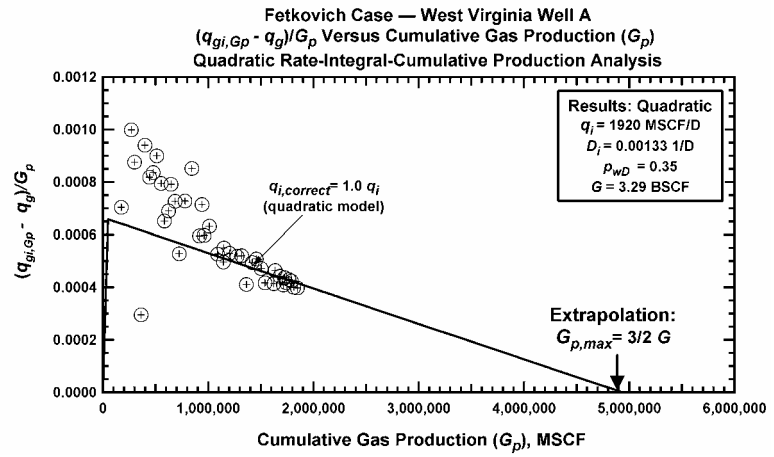


**Figure B-7 – West Virginia Well A (Fetkovich, *et al.*[8]): $(q_{qi,Gp}-q_q)/G_p$ versus $G_p$ (Plotting Function 3 ($PF_3$)).**

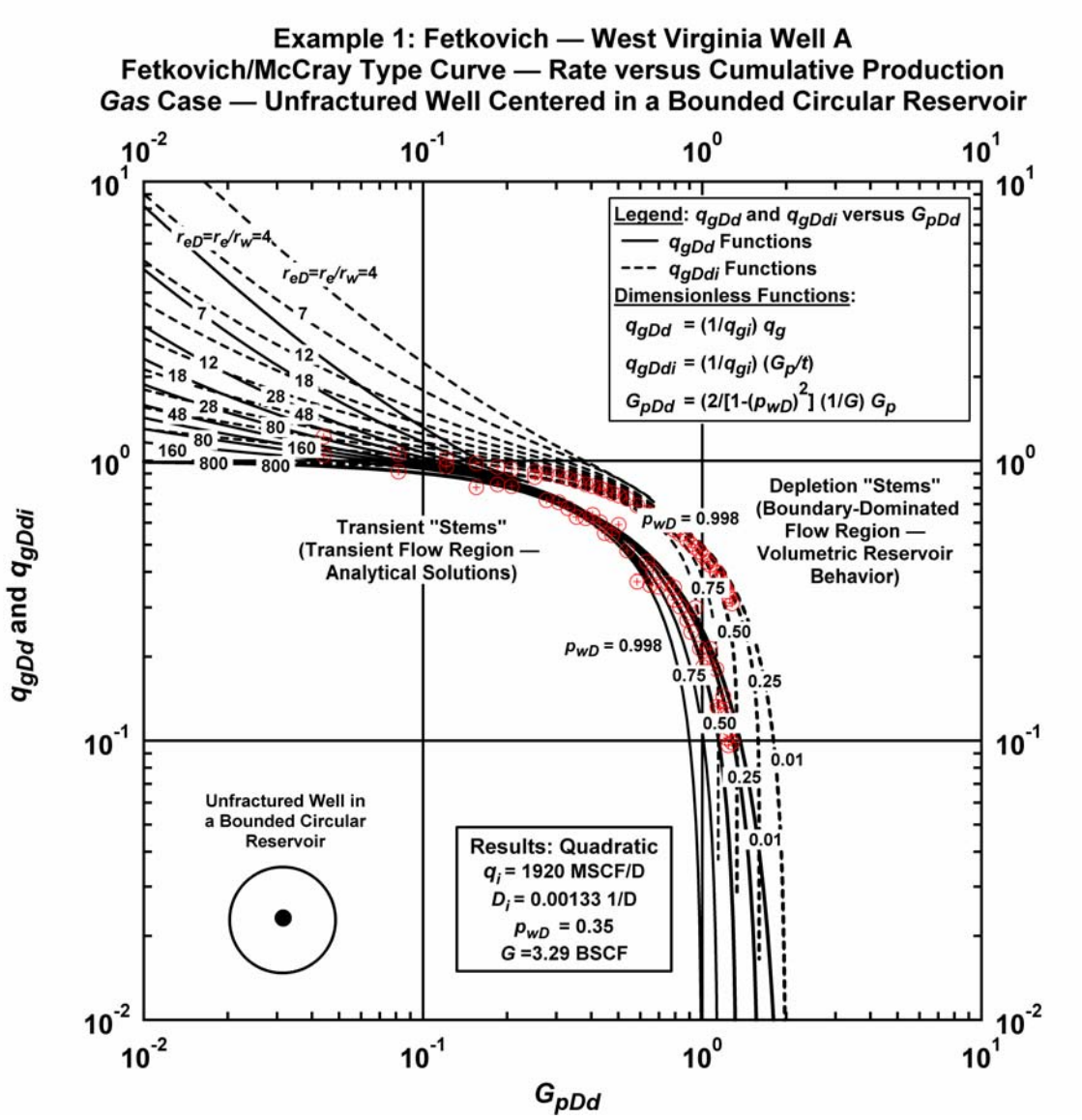


**Figure B-8 – West Virginia Well A (Fetkovich, *et al.*[8]): "Quadratic" Rate-Cumulative De-cline Type Curve Analysis.**

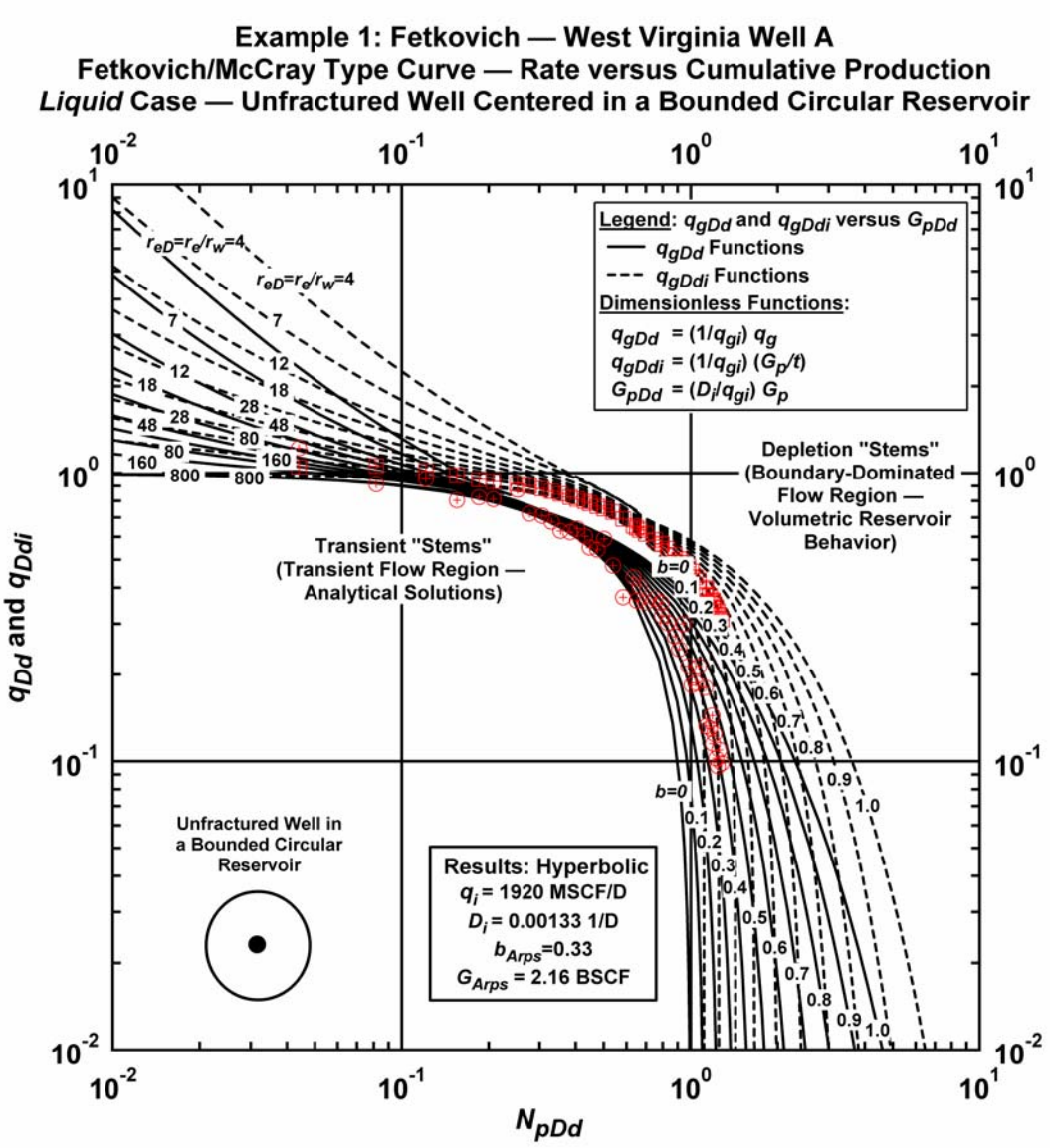


**Figure B-9 – West Virginia Well A (Fetkovich, *et al.*[8])): "Hyperbolic" Rate-Cumulative Decline Type Curve Analysis.**

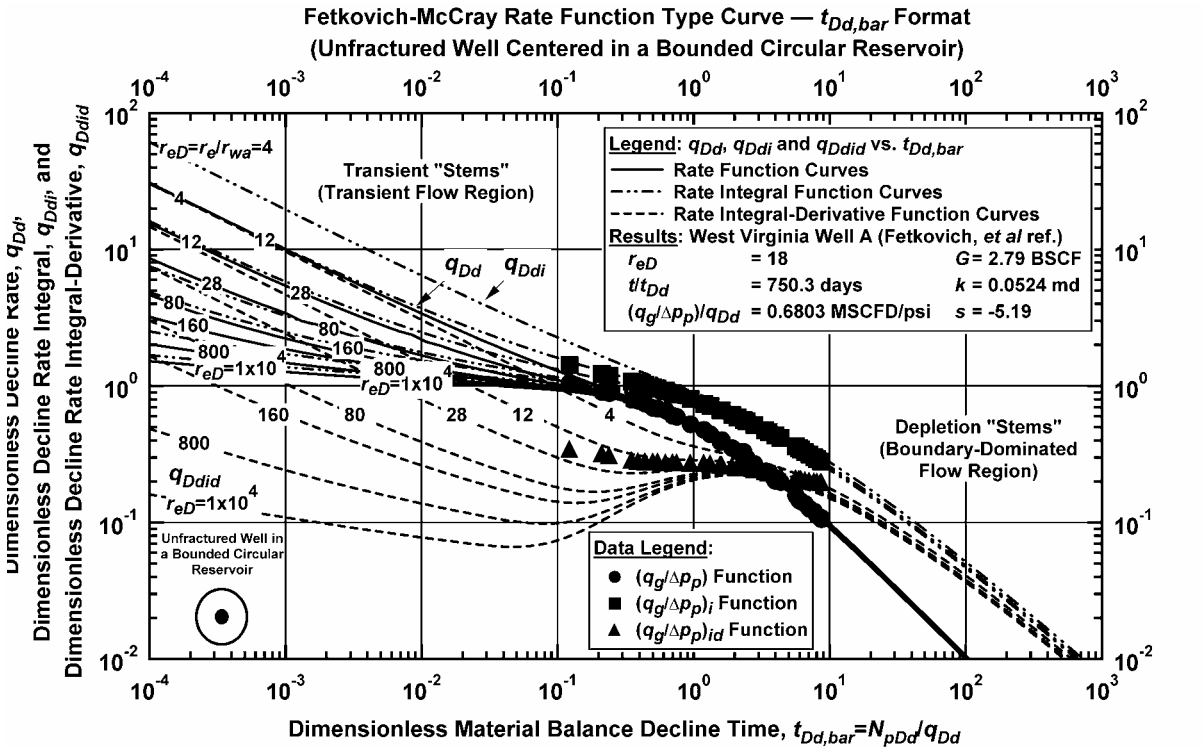


**Figure B-10 – West Virginia Well A (Fetkovich, *et al.*[8])): Decline Type Curve Analysis.**

**Case 2: Cox and Perkins Exploration — Well Porche 2**

This case is for a relatively high pressure reservoir ($p_i$=8578 psia) where the surface pressure varies continuously and the formation compressibility is estimated to be $c_f$=10x10$^{-6}$ psi$^{-1}$ (where the formation compressibility can not be neglected).

**Case 2: (input data) Cox and Perkins Exploration — Well Porche 2**

Reservoir Properties:

| | |
|---|---|
| Wellbore radius, $r_w$ | = 0.25 ft |
| Average net pay thickness, $h$ | = 25 ft |
| Average porosity, $\phi$ | = 0.20 (fraction) |
| Irreducible water saturation, $S_{wi}$ | = 0.50 (fraction) |
| Formation compressibility, $c_f$ | = 10x10$^{-6}$ psi$^{-1}$ |
| Initial reservoir pressure, $p_i$ | = 8578 psia |

Fluid properties:

| | |
|---|---|
| Gas specific gravity, $\gamma_g$ | = 0.695 (air=1) |
| Mole percent $CO_2$ | = 2.655 percent |
| Reservoir Temperature, $T$ | = 274 deg F |

Production parameters:

| | |
|---|---|
| Tubing length, $L$ | = 10,385 ft |
| Inside tubing diameter, $d_i$ | = 2.441 in |
| Bottomhole flowing pressure, $p_{wf}$ | = varies |

**Case 2: (results) Cox and Perkins Exploration — Well Porche 2**

New "quadratic analysis" methods:

| | |
|---|---|
| Initial gas production rate, $q_{gi}$ | = 3375 MSCF/D |
| Decline constant, $D_i$ | = 0.005 1/D |
| Dimensionless pressure, $p_{wD}$ | = 0.50 |
| Gas-in-place, $G$ | = 1.80 BSCF |

Material balance decline type curve analysis: (methods of ref. 16)

| | |
|---|---|
| Gas-in-place, $G$ | = 1.68 BSCF |
| Gas permeability, $k_g$ ($r_{eD}$=48) | = 0.5941 md |
| Near-well skin factor, $s$ ($r_{eD}$=48) | = -4.05 (dim-less) |

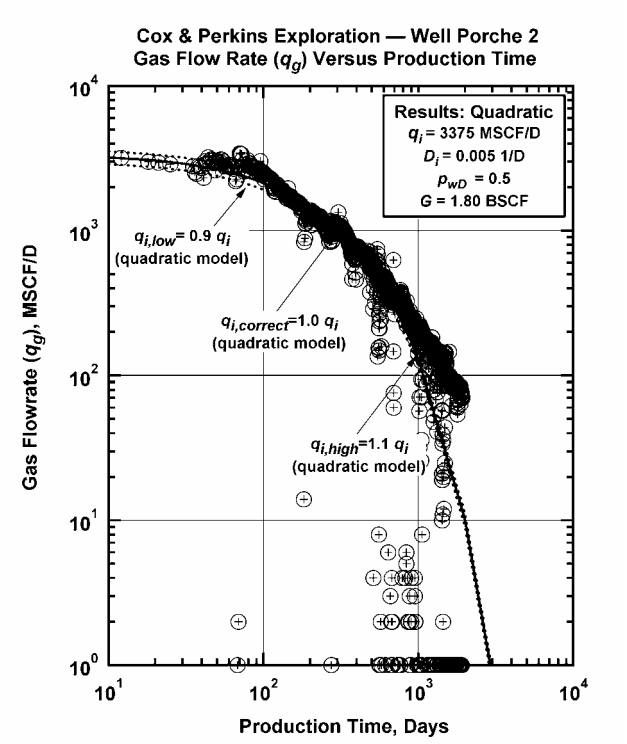


**Figure B-11 – Well Porche 2 (Cox and Perkins Exploration): $q_g$ versus $t$.**

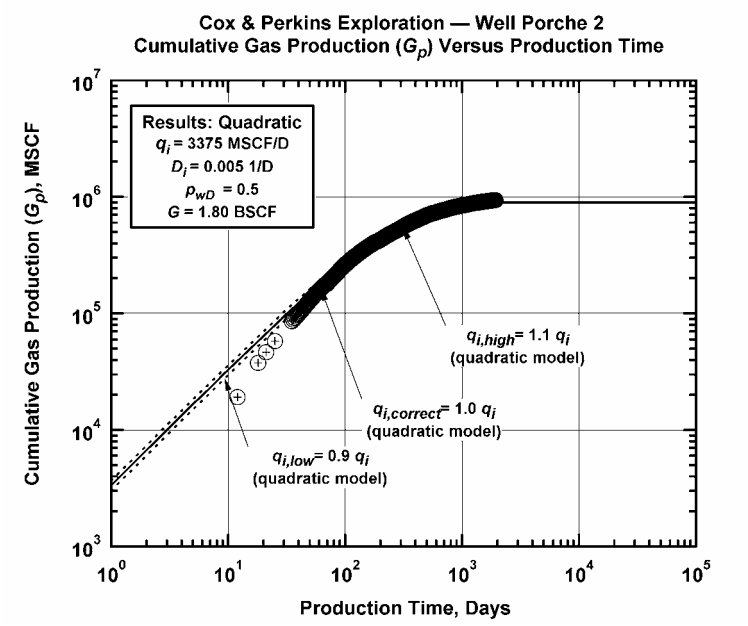


**Figure B-12 – Well Porche 2 (Cox and Perkins Exploration): $G_p$ versus $t$.**

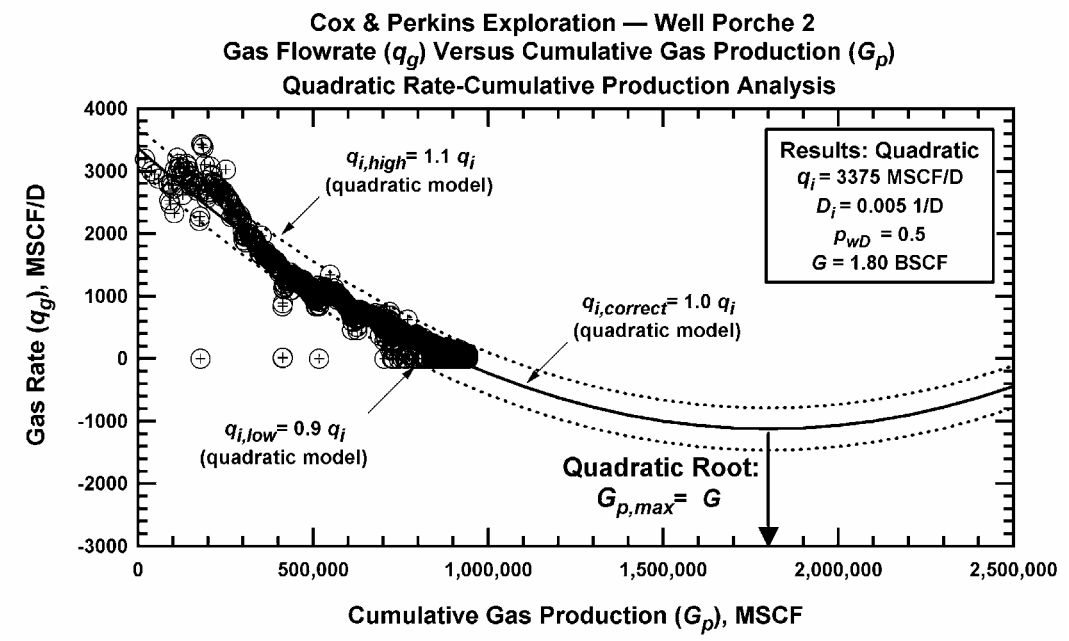


**Figure B-13 – Well Porche 2 (Cox and Perkins Exploration): $q_g$ versus $G_p$.**

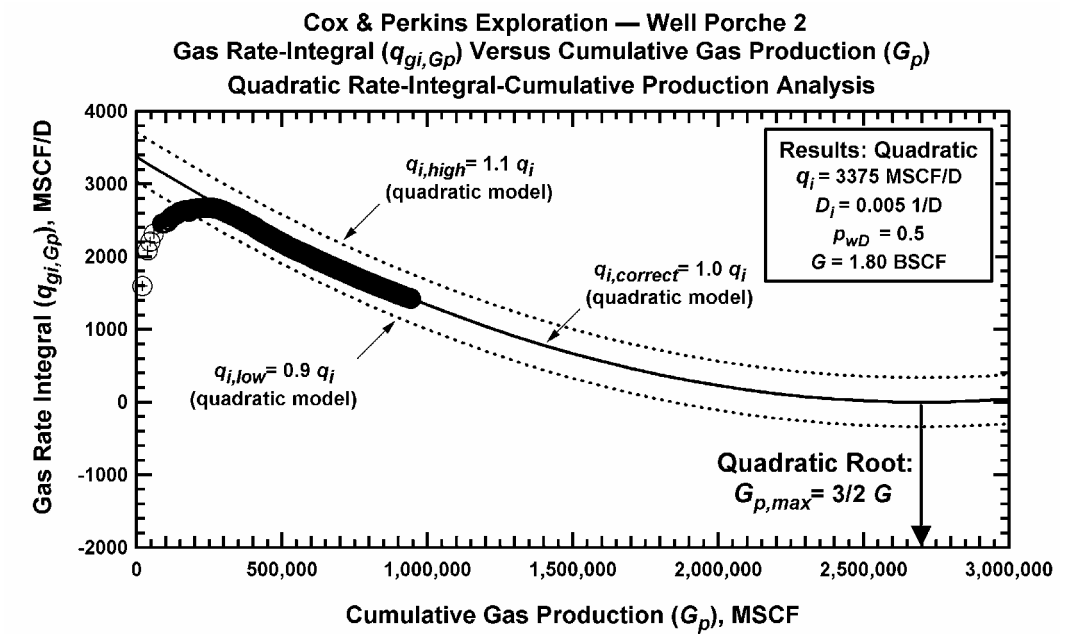


**Figure B-14 – Well Porche 2 (Cox and Perkins Exploration): $q_{qi,Gp}$ versus $G_p$.**

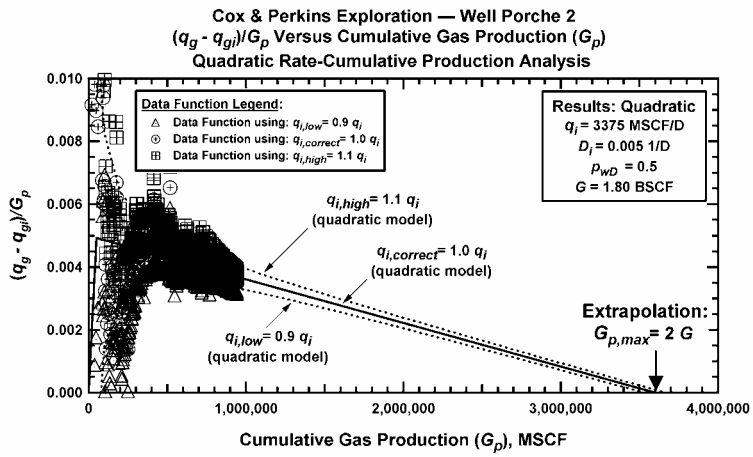


**Figure B-15 – Well Porche 2 (Cox and Perkins Exploration): $(q_{qi}-q_q)/G_p$ versus $G_p$. (Plotting Function 1 ($PF_1$)).**

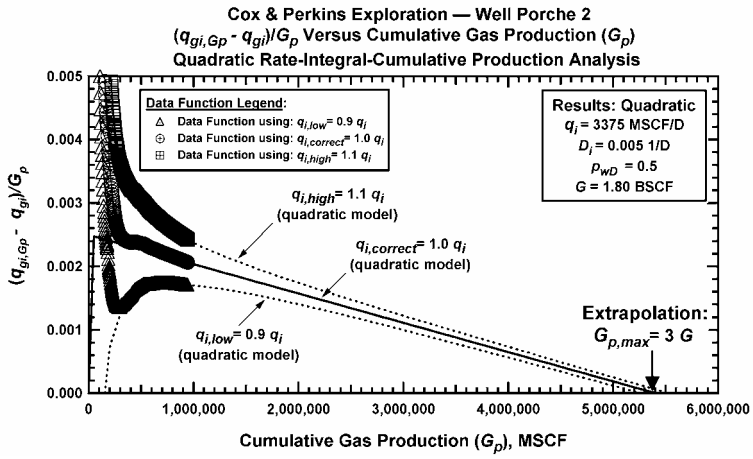


**Figure B-16 – Well Porche 2 (Cox and Perkins Exploration): $(q_{qi,Gp}-q_q)/G_p$ versus $G_p$ (Plotting Function 2 ($PF_2$)).**

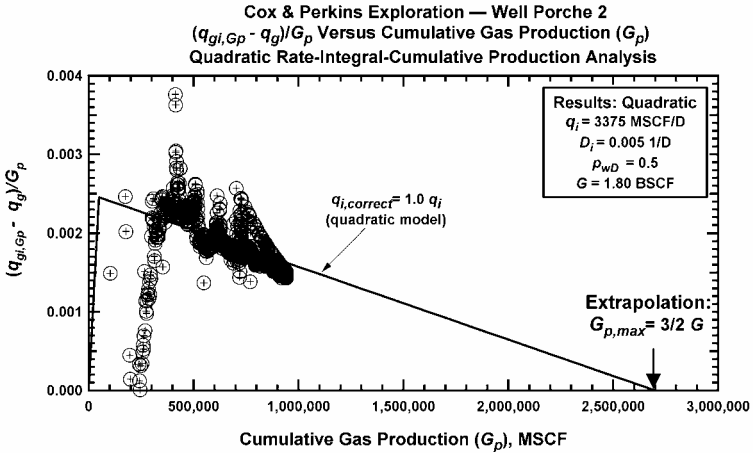


**Figure B-17 – Well Porche 2 (Cox and Perkins Exploration): $(q_{qi,Gp}-q_q)/G_p$ versus $G_p$ (Plotting Function 3 ($PF_3$)).**

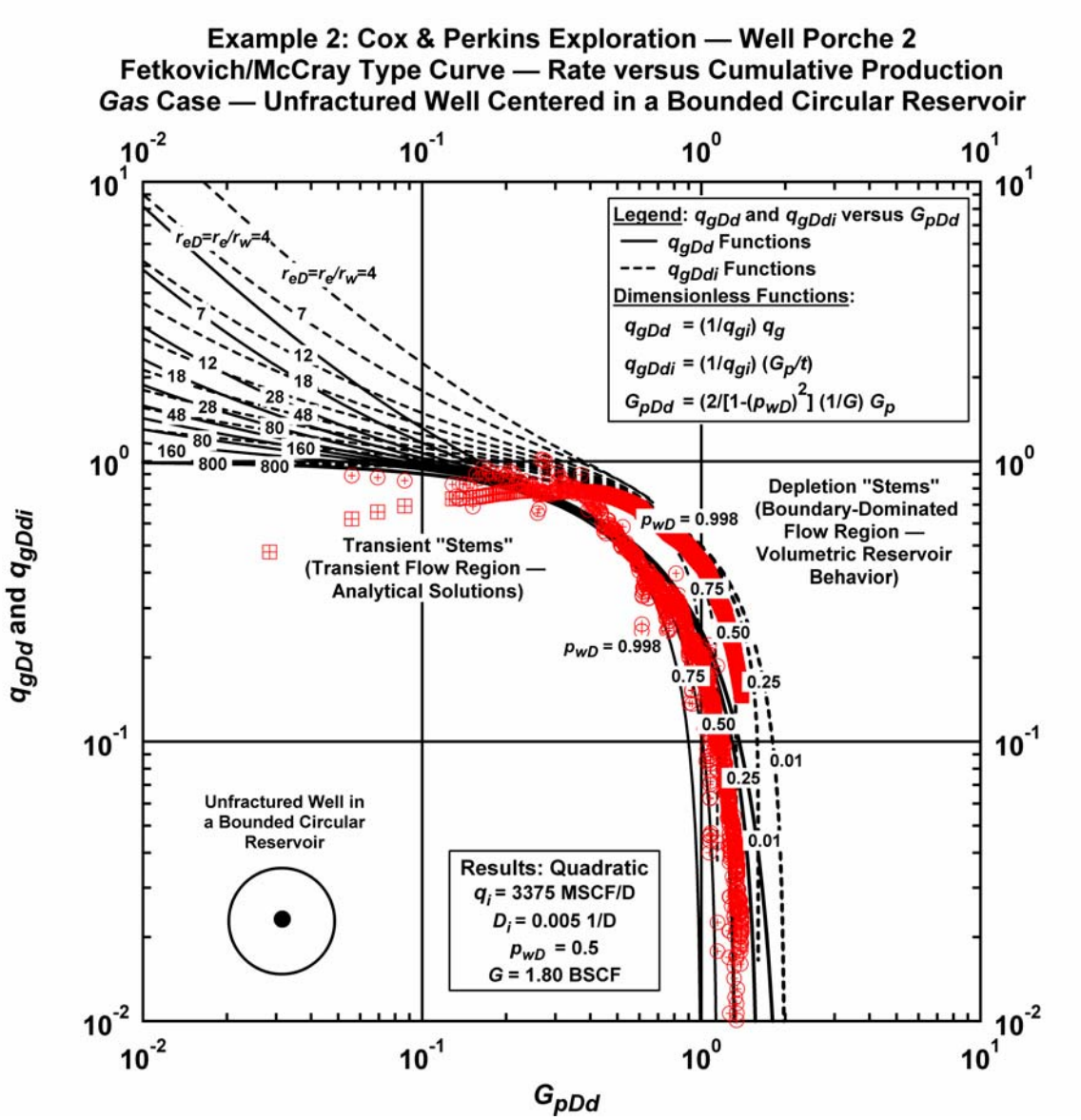


**Figure B-18 – Well Porche 2 (Cox and Perkins Exploration): "Quadratic" Rate-Cumulative Decline Type Curve Analysis.**

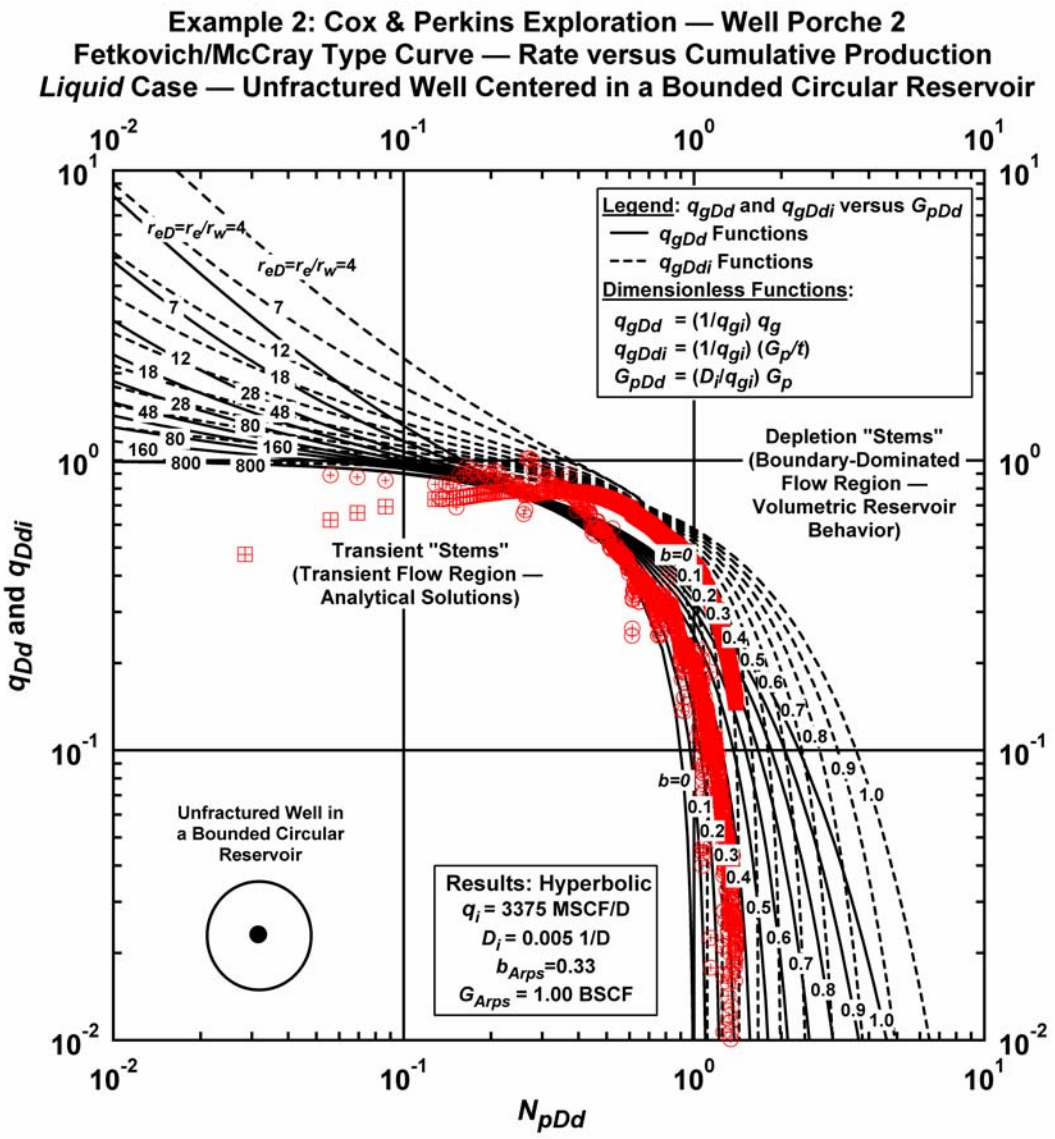


**Figure B-19 – Well Porche 2 (Cox and Perkins Exploration): "Hyperbolic" Rate-Cumulative Decline Type Curve Analysis.**

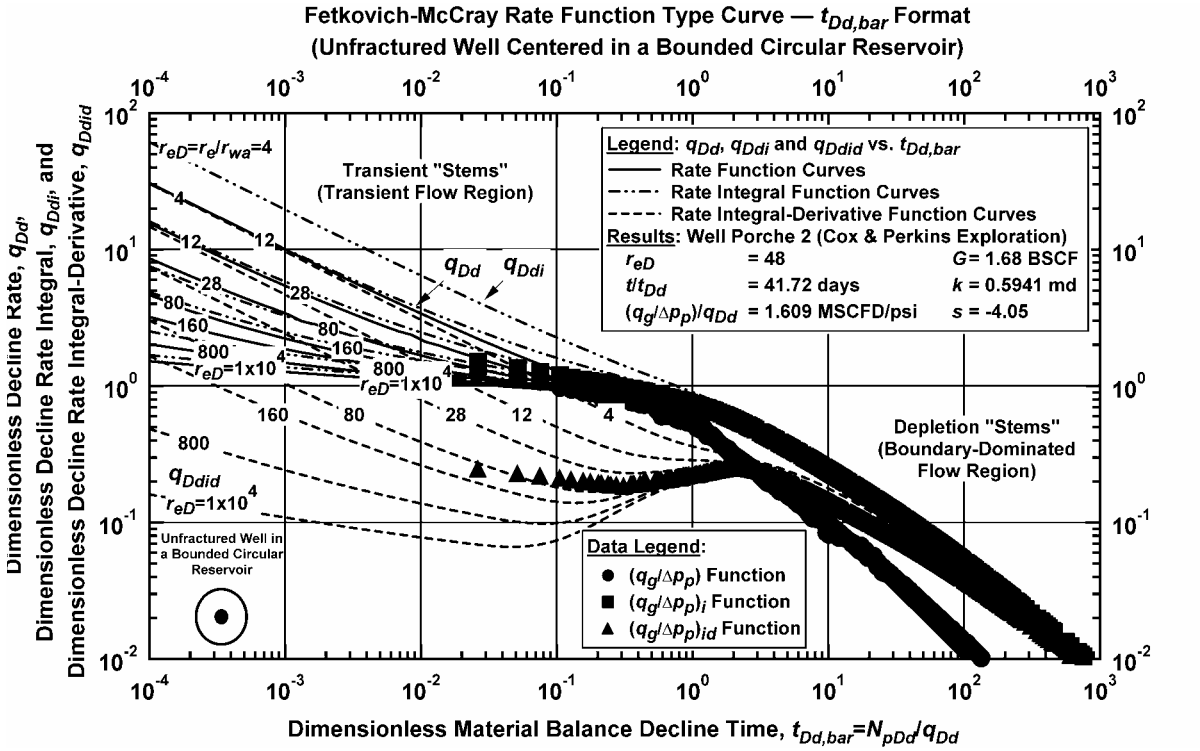


**Figure B-20 – Well Porche 2 (Cox and Perkins Exploration): Decline Type Curve Analysis.**

**Case 3: Anadarko Petroleum Corporation — Well Heckman 1**

The Heckmann 1 Well is a horizontal well completed in a gas zone within the Austin Chalk ($p_i \approx 9000$ psia). The surface pressure varies continuously and the formation compressibility is presumed to be negligible.

**Case 3: (input data) Anadarko Petroleum Corporation — Well Heckman 1**

Reservoir Properties:

| | |
|---|---|
| Wellbore radius, $r_w$ | = 0.33 ft |
| Average net pay thickness, $h$ | ≈ 100 ft |
| Average porosity, $\phi$ | = 0.25 (fraction) |
| Irreducible water saturation, $S_{wi}$ | = 0.20 (fraction) |
| Initial reservoir pressure, $p_i$ | ≈ 9000 psia |

Fluid properties:

| | |
|---|---|
| Gas specific gravity, $\gamma_g$ | = 0.64 (air=1) |
| Reservoir Temperature, $T$ | = 317 deg F |

Production parameters:

| | |
|---|---|
| Tubing length, $L$ | = 13,500 ft |
| Inside tubing diameter, $d_i$ | = 2.441 in |
| Bottomhole flowing pressure, $p_{wf}$ | = varies |

**Case 3: (results) Anadarko Petroleum Corporation — Well Heckman 1**

New "quadratic analysis" methods:

| | |
|---|---|
| Initial gas production rate, $q_{gi}$ | = 21,850 MSCF/D |
| Decline constant, $D_i$ | = 0.008 1/D |
| Dimensionless pressure, $p_{wD}$ | = 0.20 |
| Gas-in-place, $G$ | = 5.69 BSCF |

Material balance decline type curve analysis: (methods of refs. 16 and 23)
(horizontal well model (see ref. 23))

| | |
|---|---|
| Gas-in-place, $G$ | = 5.014 BSCF |
| Gas permeability, $k_g$ ($L_D$=100) | = 0.0975 md |

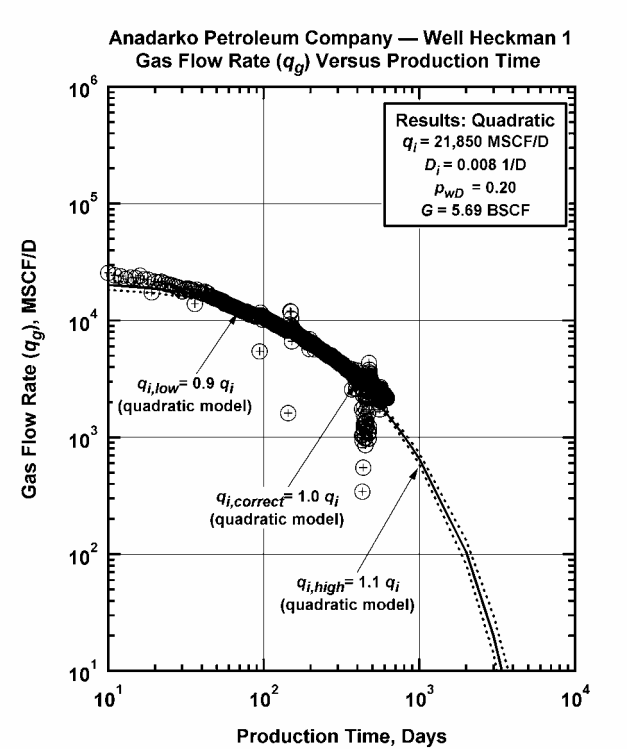


**Figure B-21 – Well Heckman 1 (Anadarko Petroleum Corporation): $q_g$ versus $t$.**

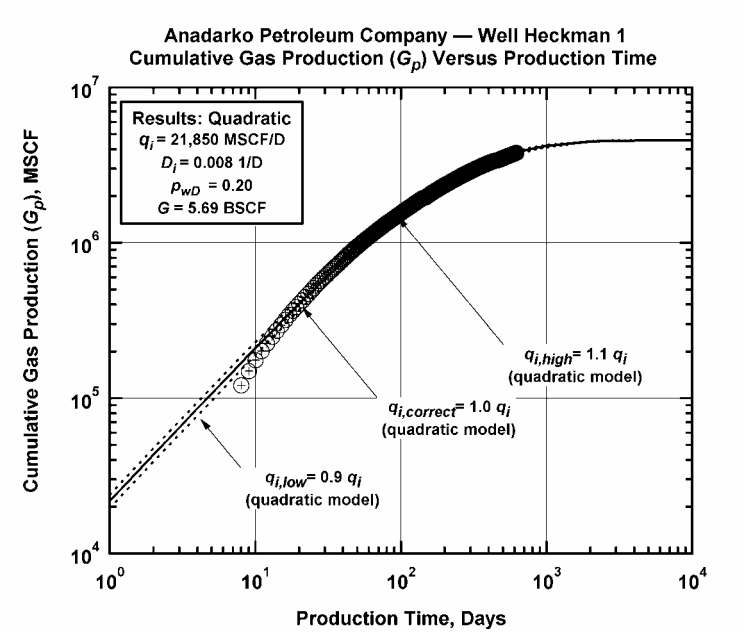


**Figure B-22 – Well Heckman 1 (Anadarko Petroleum Corporation): $G_p$ versus $t$.**

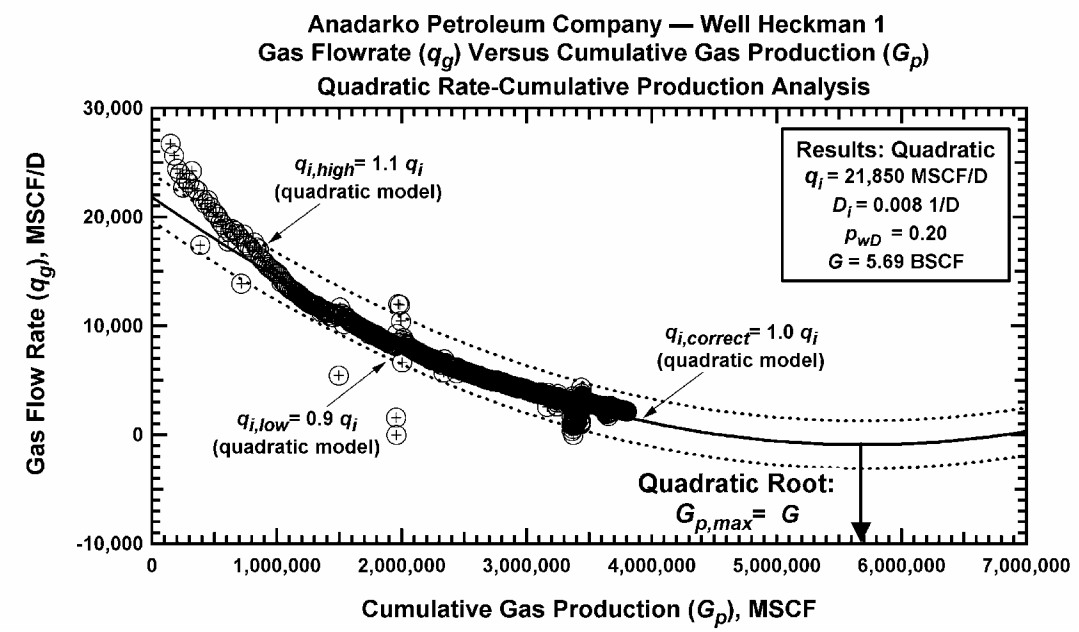


**Figure B-23 – Well Heckman 1 (Anadarko Petroleum Corporation): $q_g$ versus $G_p$.**

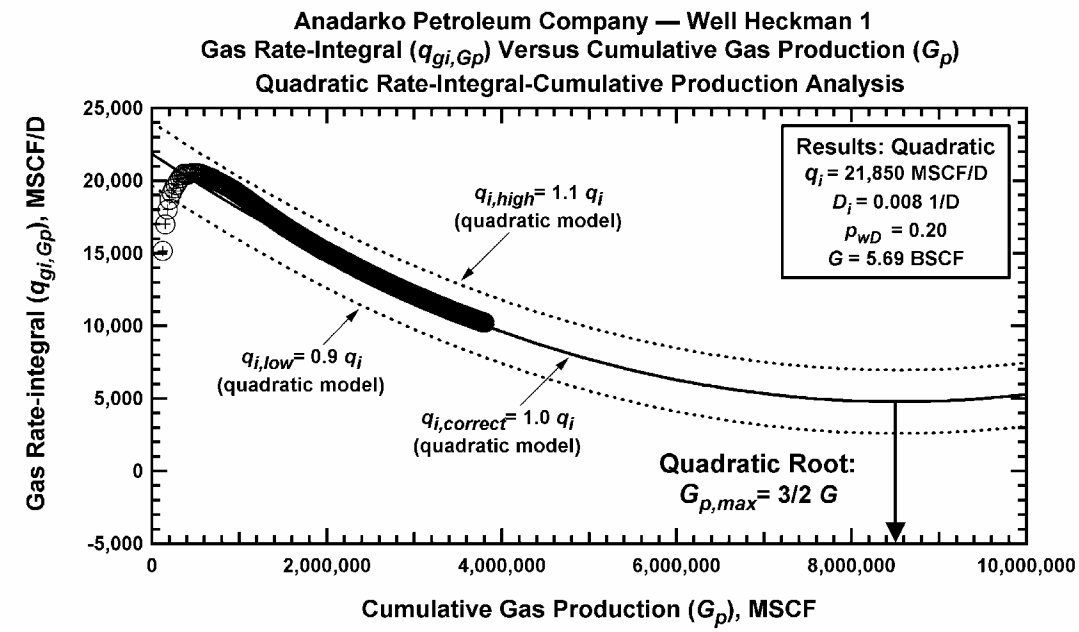


**Figure B-24 – Well Heckman 1 (Anadarko Petroleum Corporation): $q_{qi,Gp}$ versus $G_p$.**

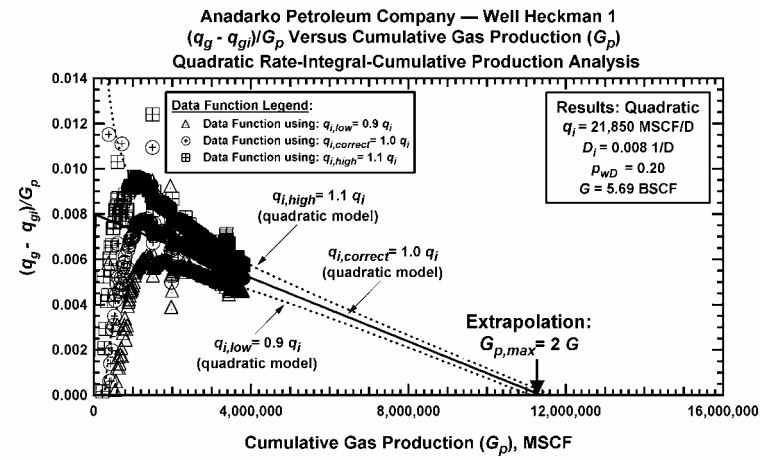


**Figure B-25 – Well Heckman 1 (Anadarko Petroleum Corporation): $(q_{qi}-q_q)/G_p$ versus $G_p$ (Plot-ting Function 1 ($PF_1$)).**

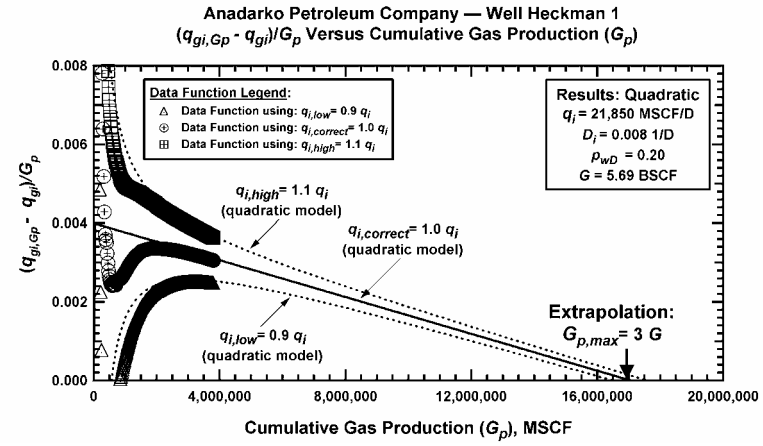


**Figure B-26 – Well Heckman 1 (Anadarko Petroleum Corporation): $(q_{qi}-q_q)/G_p$ versus $G_p$ (Plot-ting Function 2 ($PF_2$)).**

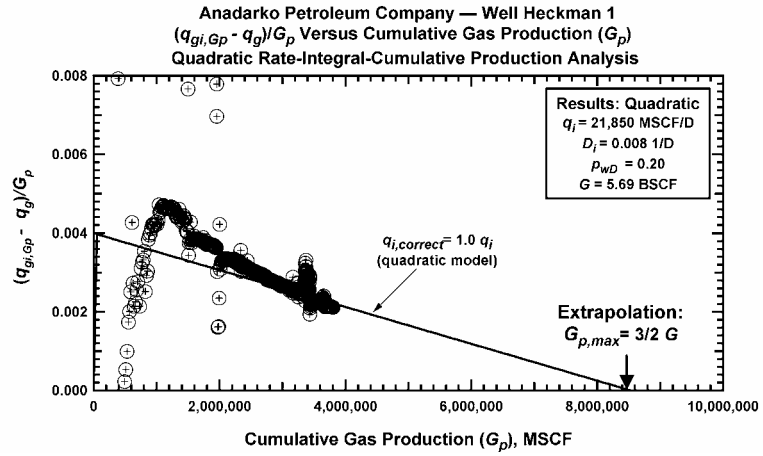


**Figure B-27 – Well Heckman 1 (Anadarko Petroleum Corporation): $(q_{qi,Gp}-q_q)/G_p$ versus $G_p$ (Plotting Function 3 ($PF_3$)).**

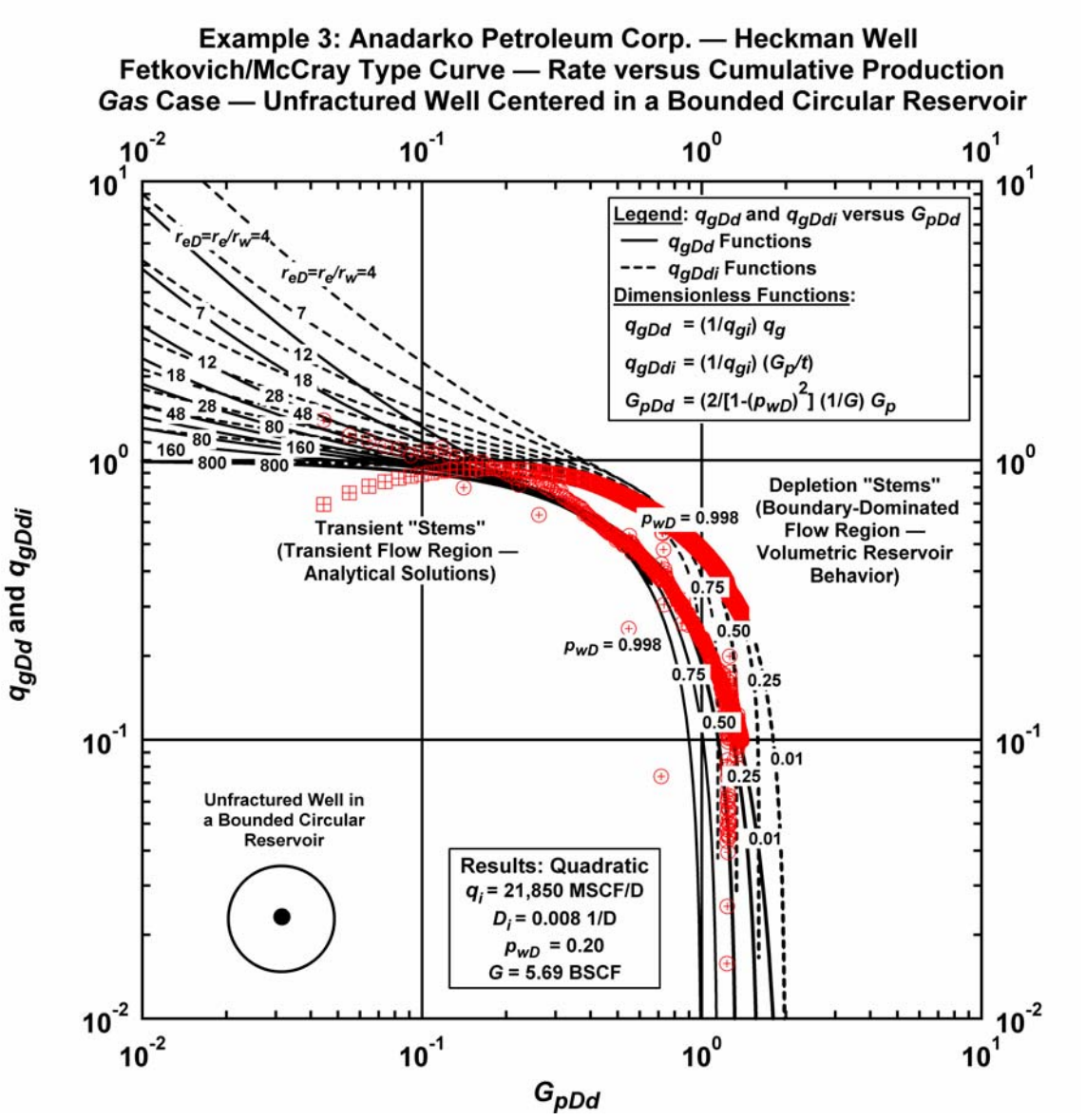


**Figure B-28 – Well Heckman 1 (Anadarko Petroleum Corporation): "Quadratic" Rate-Cumulative Decline Type Curve Analysis.**

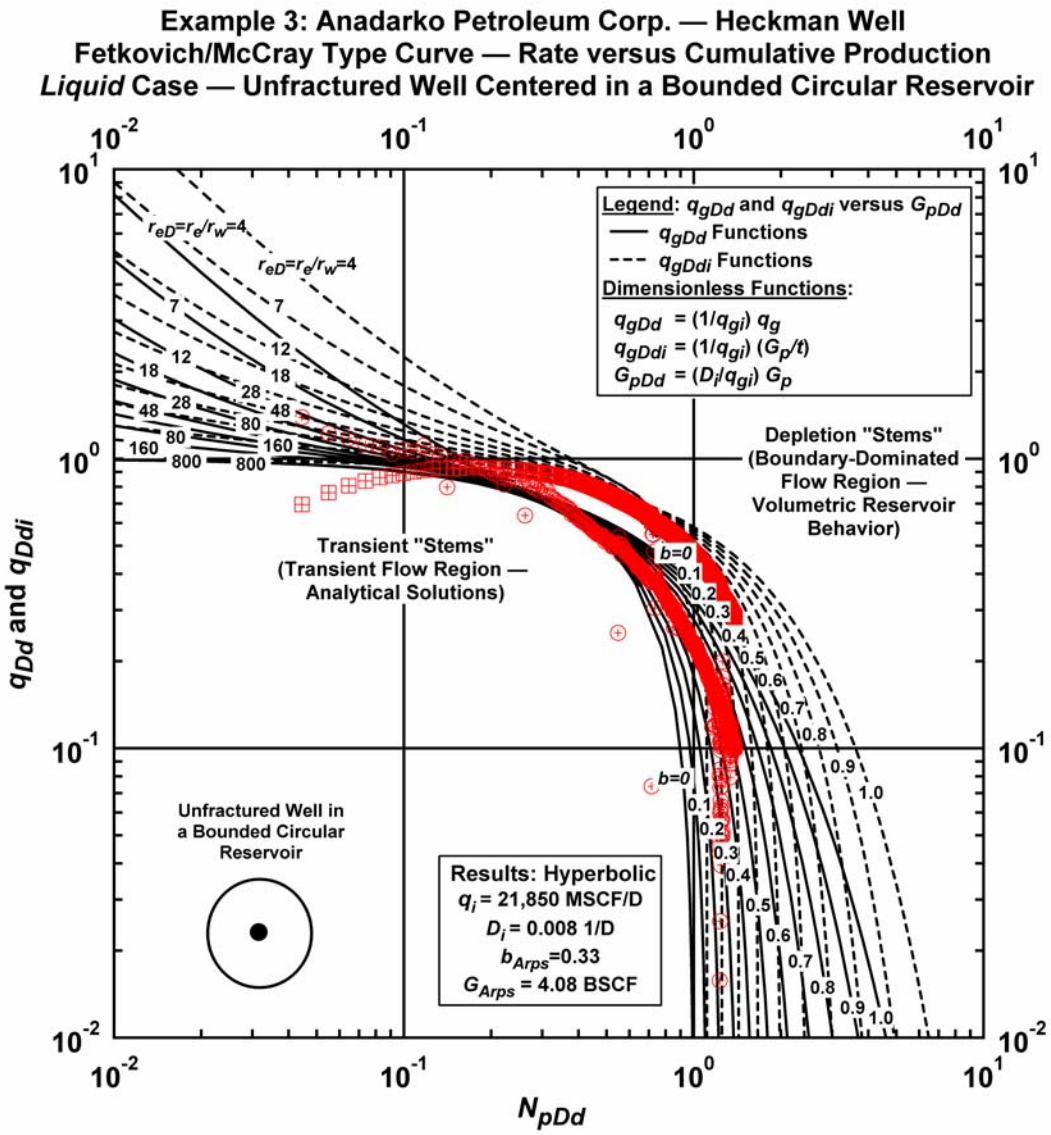


**Figure B-29 – Well Heckman 1 (Anadarko Petroleum Corporation): "Hyperbolic" Rate-Cumulative Decline Type Curve Analysis.**

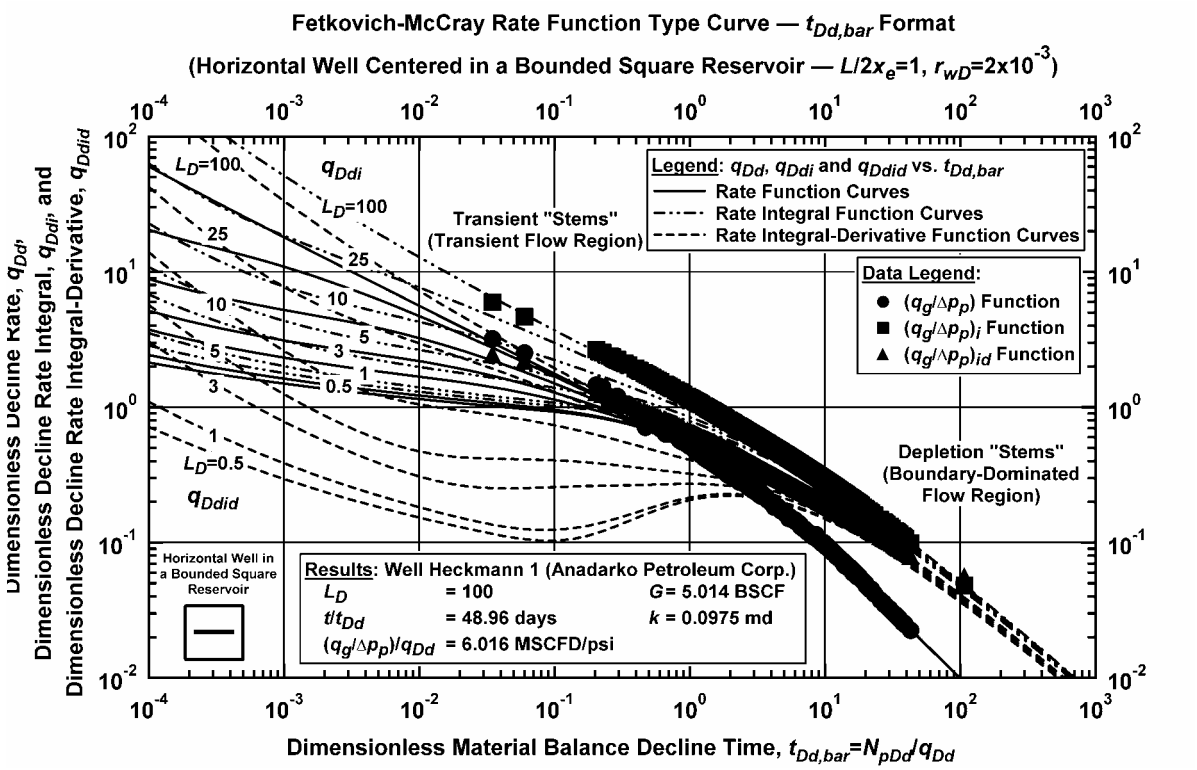


**Figure B-30 – Well Heckman 1 (Anadarko Petroleum Corporation): Decline Type Curve Analysis.**

**Case 4: Anadarko Petroleum Corporation — Well DV4**

No reservoir description is available for this case — we do note that all relevant properties are available and that the initial reservoir pressure is quite high ($p_i$=12,200 psia).

**Case 4: (input data) Anadarko Petroleum Corporation — Well DV4**

Reservoir Properties:

| | |
|---|---|
| Wellbore radius, $r_w$ | = 0.333 ft |
| Average net pay thickness, $h$ | = 180 ft |
| Average Porosity, $\phi$ | = 0.08 (fraction) |
| Irreducible water saturation, $S_{wi}$ | = 0.25 (fraction) |
| Initial reservoir pressure, $p_i$ | = 12,200 psia |

Fluid properties:

| | |
|---|---|
| Gas specific gravity, $\gamma_g$ | = 0.625 (air=1) |
| Mole Percent $CO_2$ | = 2.0 percent |
| Reservoir Temperature | = 380 deg F |

Production parameters:

| | |
|---|---|
| Tubing length, $L$ | = 14,000 ft |
| Inside tubing diameter, $d_i$ | = 1.995 in |
| Bottomhole flowing pressure, $p_{wf}$ | = varies |

**Case 4: (results) Anadarko Petroleum Corporation — Well DV4**

New "quadratic analysis" methods:

| | |
|---|---|
| Initial gas production rate, $q_{gi}$ | = 4000 MSCF/D |
| Decline constant, $D_i$ | = 0.0026 1/D |
| Dimensionless pressure, $p_{wD}$ | = 0.15 |
| Gas-in-place, $G$ | = 3.15 BSCF |

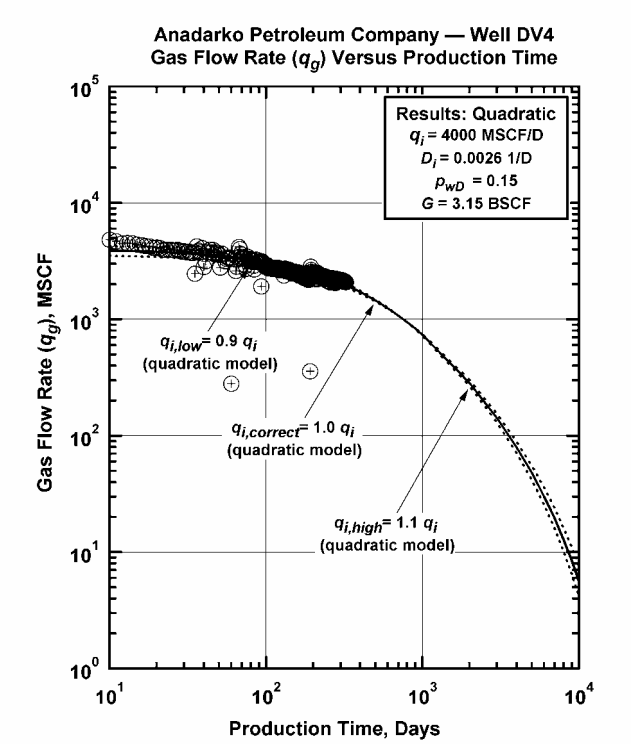


**Figure B-31 – Well DV4 (Anadarko Petroleum Corporation): $q_g$ versus $t$.**

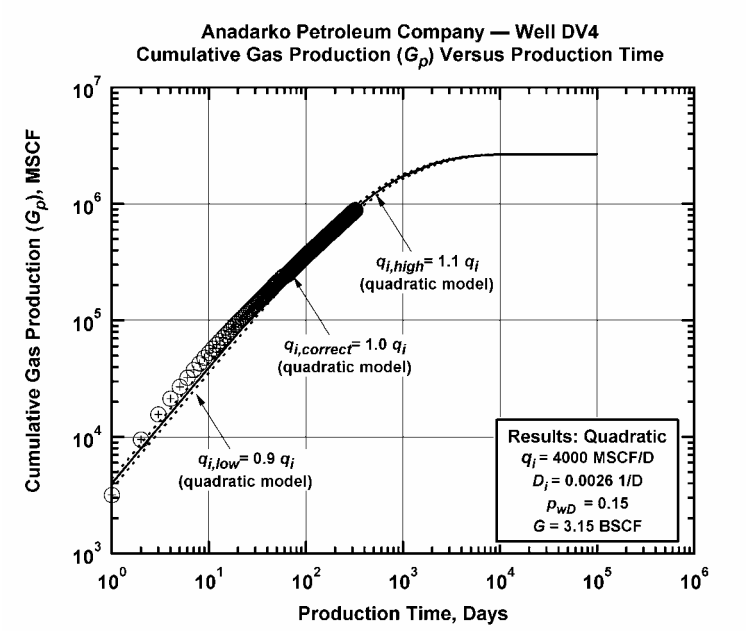


**Figure B-32 – Well DV4 (Anadarko Petroleum Corporation): $G_p$ versus $t$.**

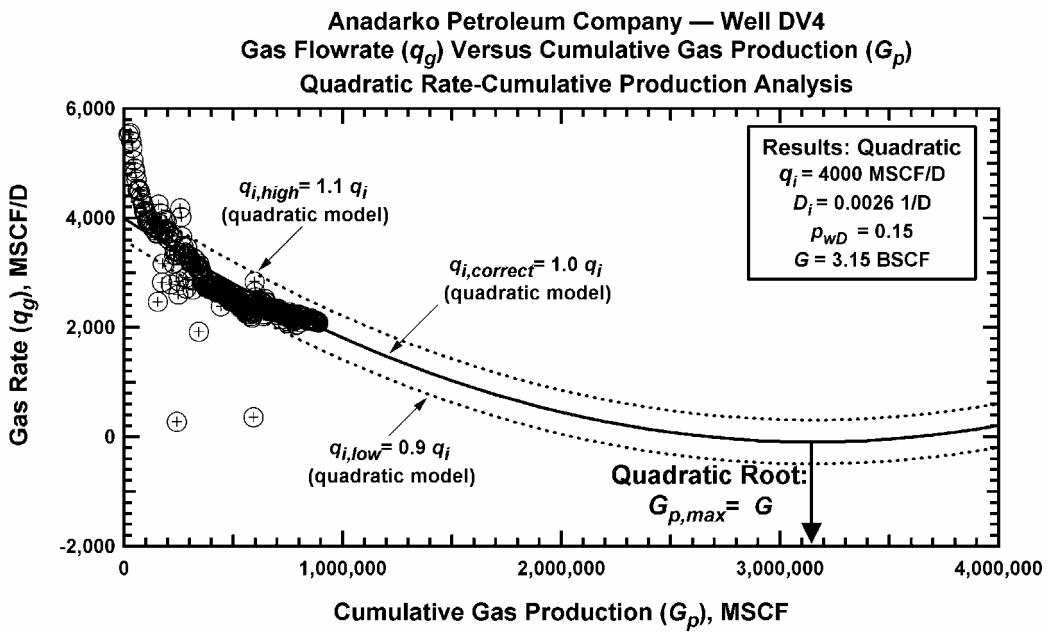


**Figure B-33 – Well DV4 (Anadarko Petroleum Corporation): $q_g$ versus $G_p$.**

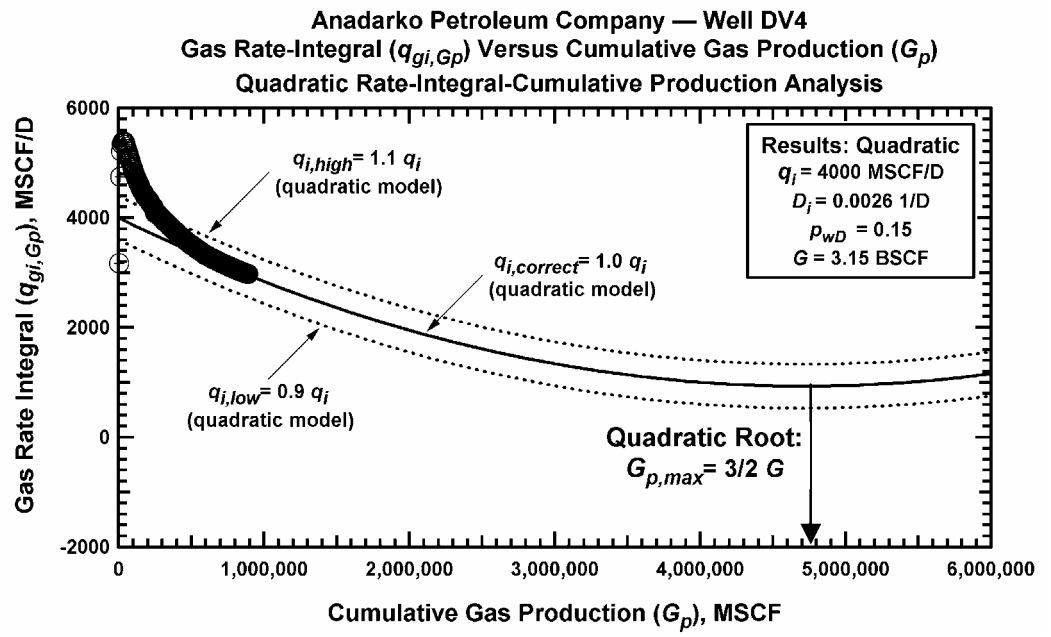


**Figure B-34 – Well DV4 (Anadarko Petroleum Corporation): $q_{qi,Gp}$ versus $G_p$.**

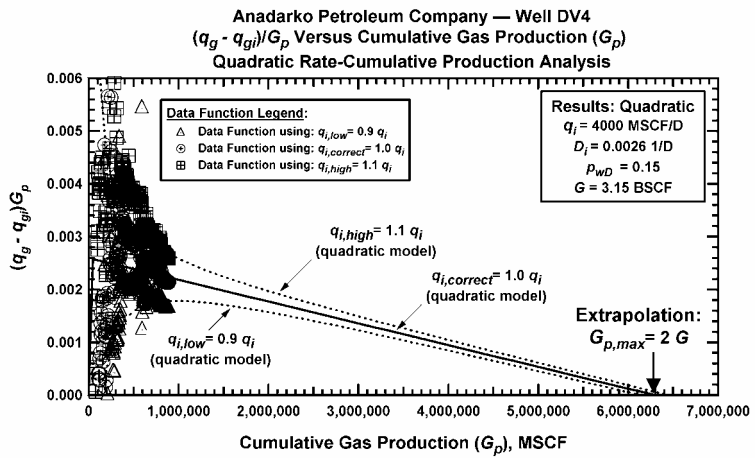


**Figure B-35 – Well DV4 (Anadarko Petroleum Corporation): $(q_{qi}-q_q)/G_p$ versus $G_p$ (Plotting Function 1 ($PF_1$)).**

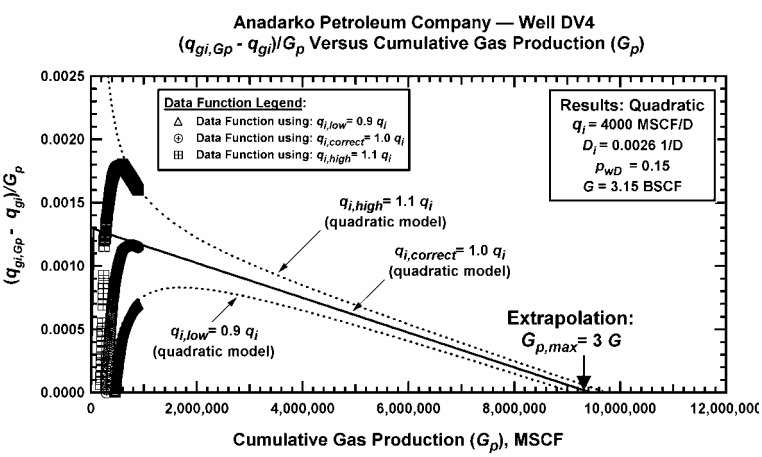


**Figure B-36 – Well DV4 (Anadarko Petroleum Corporation): $(q_{qi}-q_q)/G_p$ versus $G_p$ (Plotting Function 2 ($PF_2$)).**

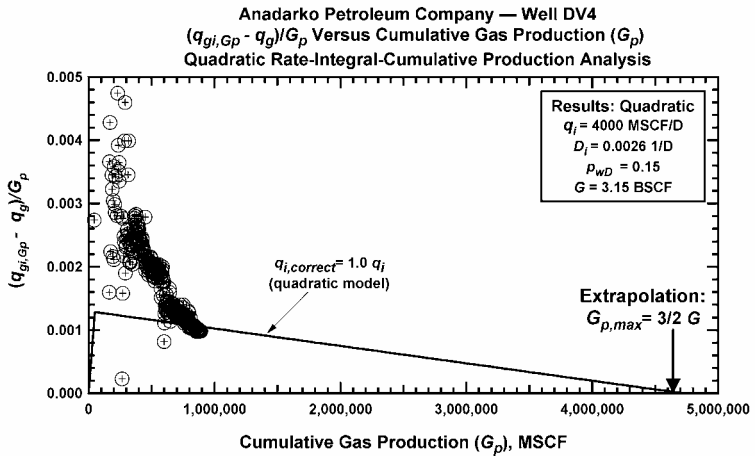


**Figure B-37 – Well DV4 (Anadarko Petroleum Corporation): $(q_{qi,Gp}-q_q)/G_p$ versus $G_p$ (Plotting Function 3 ($PF_3$)).**

**Case 5: Anadarko Petroleum Corporation — Well ELA**

As with some of the other field cases, no reservoir description is available for this case. The data and results suggest a relatively low permeability reservoir. As an example Well ELA provides a good demonstration for a "typical" moderate productivity case.

**Case 5: (input data) Anadarko Petroleum Corporation — Well ELA**

Reservoir Properties:

| | |
|---|---|
| Wellbore radius, $r_w$ | = 0.1875 ft |
| Average net pay thickness, $h$ | = 50 ft |
| Average Porosity, $\phi$ | = 0.10 (fraction) |
| Irreducible water saturation, $S_{wi}$ | = 0.00 (fraction) |
| Initial reservoir pressure, $p_i$ | = 3165 psia |

Fluid properties:

| | |
|---|---|
| Gas specific gravity, $\gamma_g$ | = 0.71 (air=1) |
| Reservoir Temperature | = 165 deg F |

Production parameters:

| | |
|---|---|
| Tubing length, $L$ | = 7820 ft |
| Inside tubing diameter, $d_i$ | = 1.995 in |
| Bottomhole flowing pressure, $p_{wf}$ | = varies |

**Case 5: (results) Anadarko Petroleum Corporation — Well ELA**

New "quadratic analysis" methods:

| | |
|---|---|
| Initial gas production rate, $q_{gi}$ | = 225 MSCF/D |
| Decline constant, $D_i$ | = 0.000495 1/D |
| Dimensionless pressure, $p_{wD}$ | = 0.07 |
| Gas-in-place, $G$ | = 0.914 BSCF |

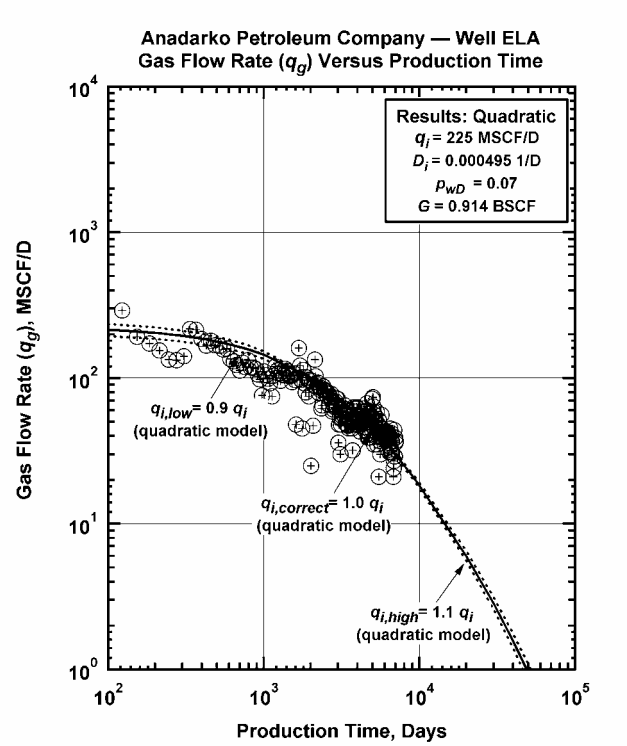


**Figure B-38 – Well ELA (Anadarko Petroleum Corporation): $q_g$ versus $t$.**

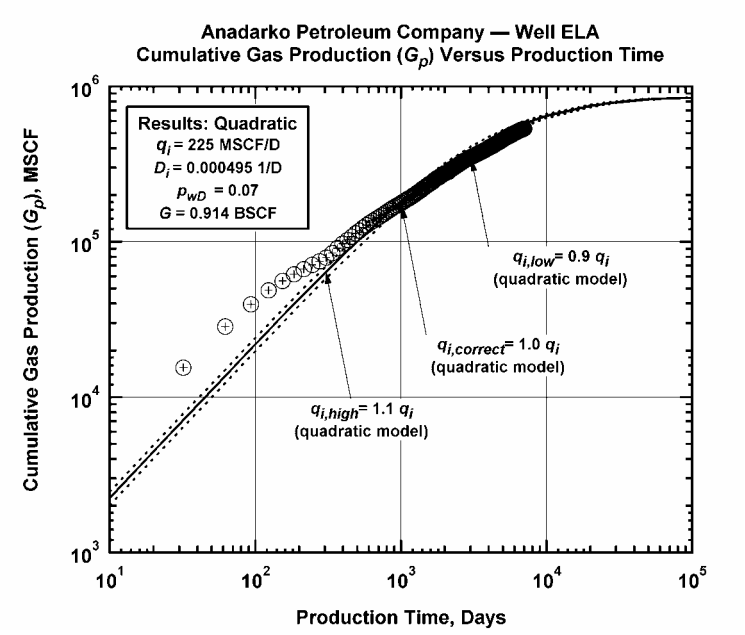


**Figure B-39 – Well ELA (Anadarko Petroleum Corporation): $G_p$ versus $t$.**

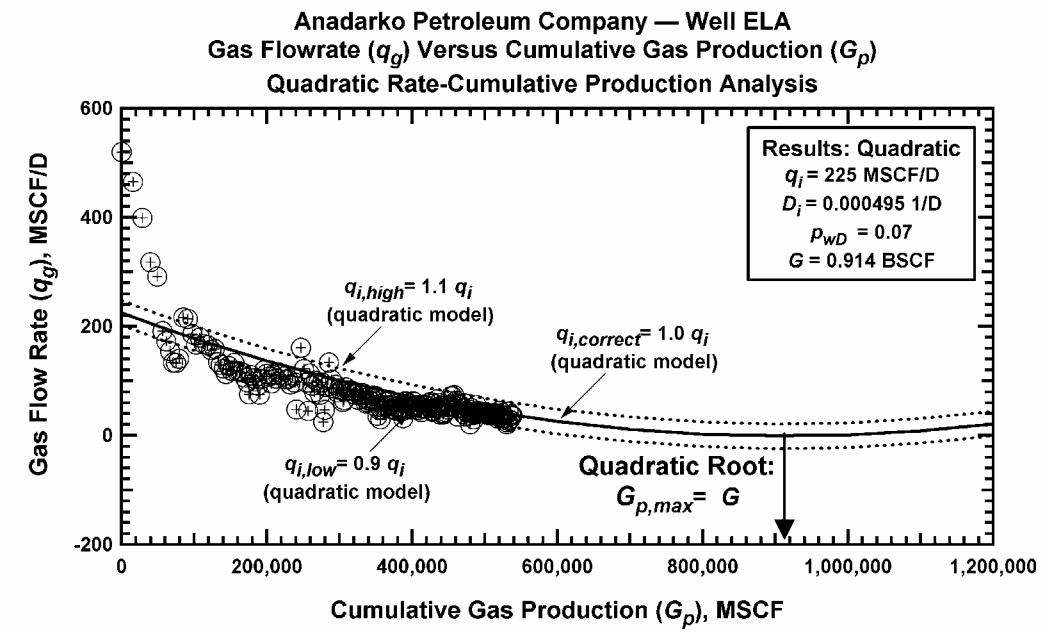


**Figure B-40 – Well ELA (Anadarko Petroleum Corporation): $q_g$ versus $G_p$.**

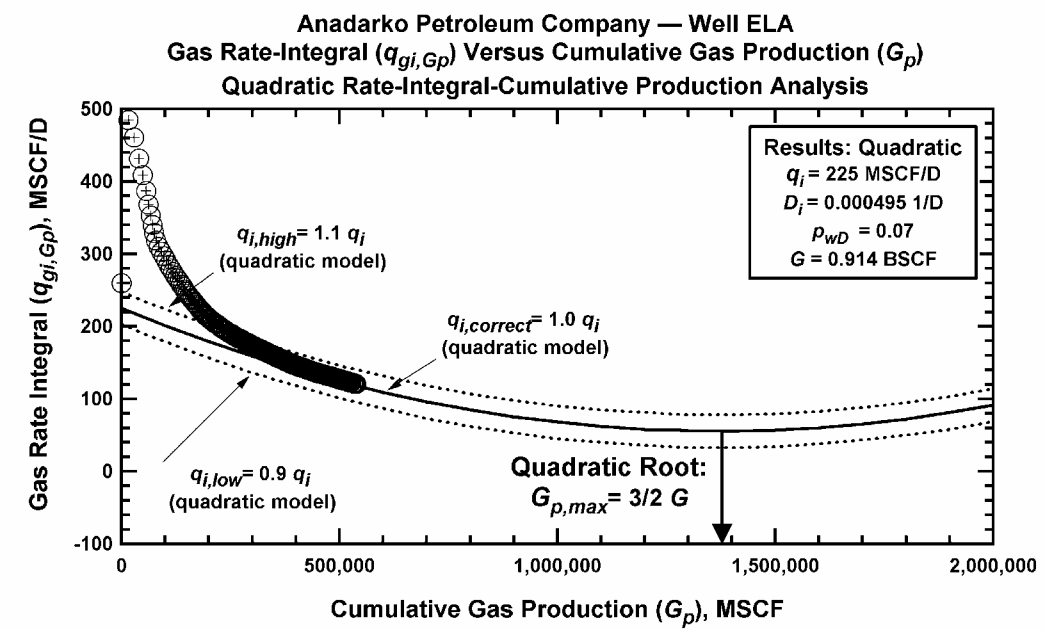


**Figure B-41 – Well ELA (Anadarko Petroleum Corporation): $q_{qi,Gp}$ versus $G_p$.**

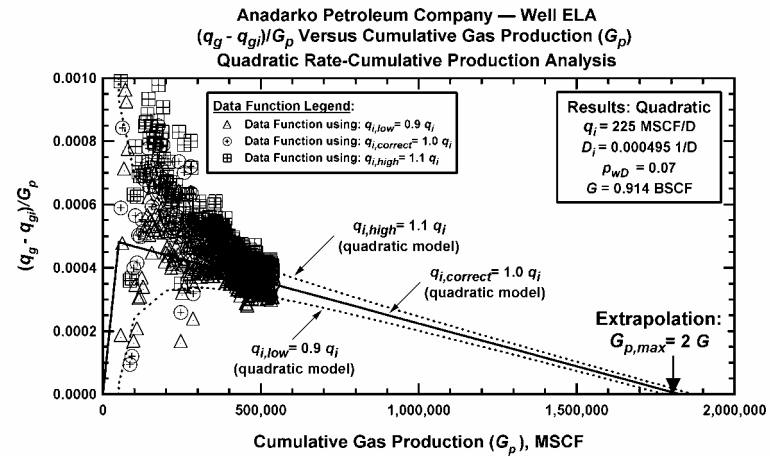


**Figure B-42 – Well ELA (Anadarko Petroleum Corporation): $(q_{qi}-q_q)/G_p$ versus $G_p$ (Plotting Function 1 ($PF_1$)).**

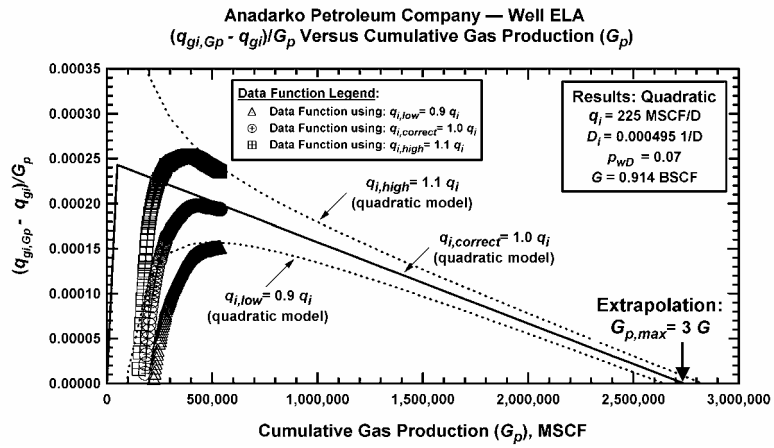


**Figure B-43 – Well ELA (Anadarko Petroleum Corporation): $(q_{qi}-q_q)/G_p$ versus $G_p$ (Plotting Function 2 ($PF_2$)).**

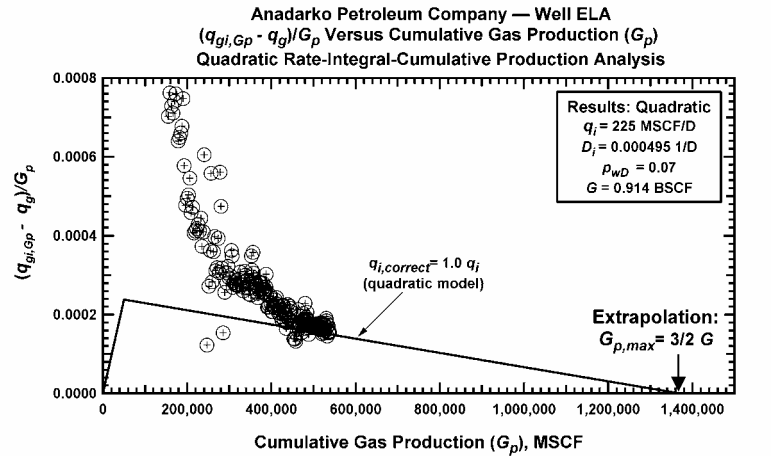


**Figure B-44 – Well ELA (Anadarko Petroleum Corporation): $(q_{qi,Gp}-q_q)/G_p$ versus $G_p$ (Plotting Function 3 ($PF_3$)).**

**Case 6: Anadarko Petroleum Corporation — Well EN1**

No reservoir description is available for this case. The initial reservoir pressure is about 7800 psia and the reservoir fluid can be described as a dry gas.

**Case 6: (input data) Anadarko Petroleum Corporation — Well EN1**

Reservoir Properties:

| | |
|---|---|
| Wellbore radius, $r_w$ | = 0.333 ft |
| Average net pay thickness, $h$ | = 78 ft |
| Average Porosity, $\phi$ | = 0.10 (fraction) |
| Irreducible water saturation, $S_{wi}$ | = 0.20 (fraction) |
| Initial reservoir pressure, $p_i$ | = 7800 psia |

Fluid properties:

| | |
|---|---|
| Gas specific gravity, $\gamma_g$ | = 0.635 (air=1) |
| Reservoir Temperature | = 285 deg F |

Production parameters:

| | |
|---|---|
| Tubing length, $L$ | = 12,500 ft |
| Inside tubing diameter, $d_i$ | = 2.441 in |
| Bottomhole flowing pressure, $p_{wf}$ | = varies |

**Case 6: (results) Anadarko Petroleum Corporation — Well EN1**

New "quadratic analysis" methods:

| | |
|---|---|
| Initial gas production rate, $q_{gi}$ | = 7200 MSCF/D |
| Decline constant, $D_i$ | = 0.007 1/D |
| Dimensionless pressure, $p_{wD}$ | = 0.05 |
| Gas-in-place, $G$ | = 2.06 BSCF |

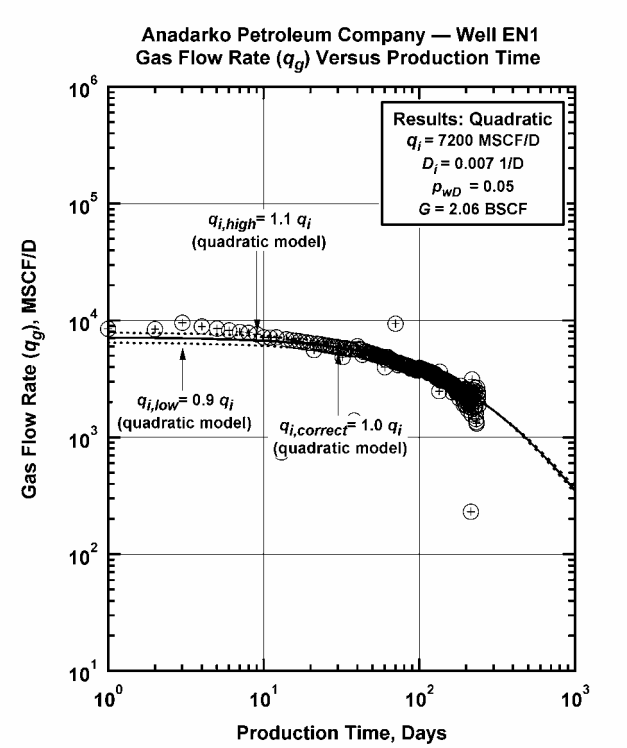


**Figure B-45 – Well EN1 (Anadarko Petroleum Corporation): $q_g$ versus $t$.**

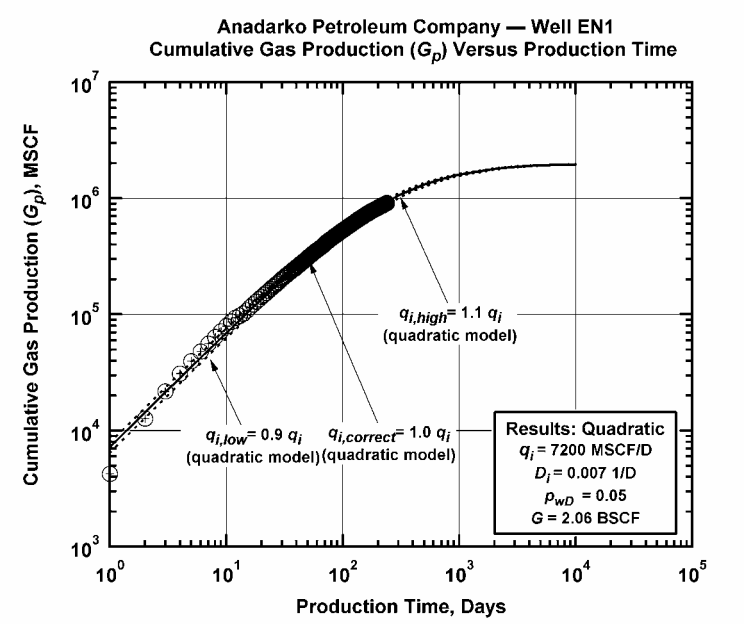


**Figure B-46 – Well EN1 (Anadarko Petroleum Corporation): $G_p$ versus $t$.**

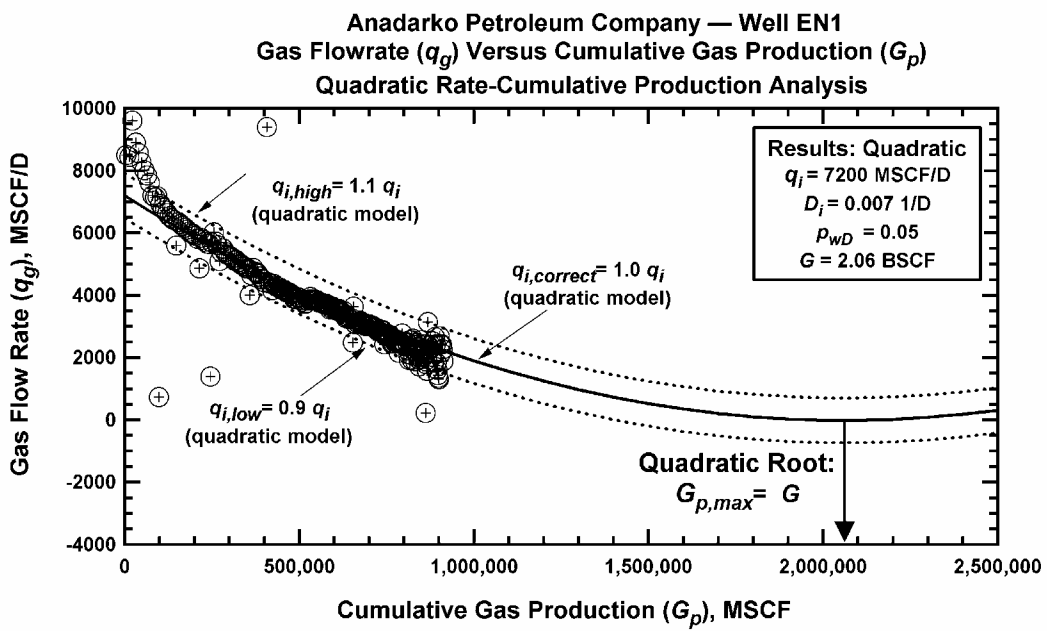


**Figure B-47 – Well EN1 (Anadarko Petroleum Corporation): $q_g$ versus $G_p$.**

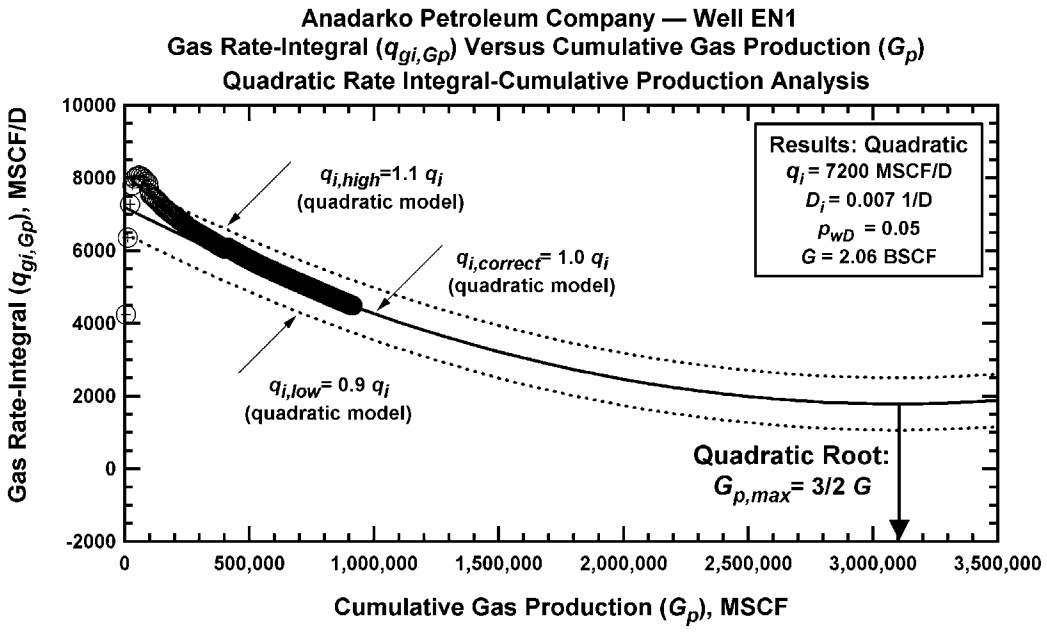


**Figure B-48 – Well EN1 (Anadarko Petroleum Corporation): $q_{qi,Gp}$ versus $G_p$.**

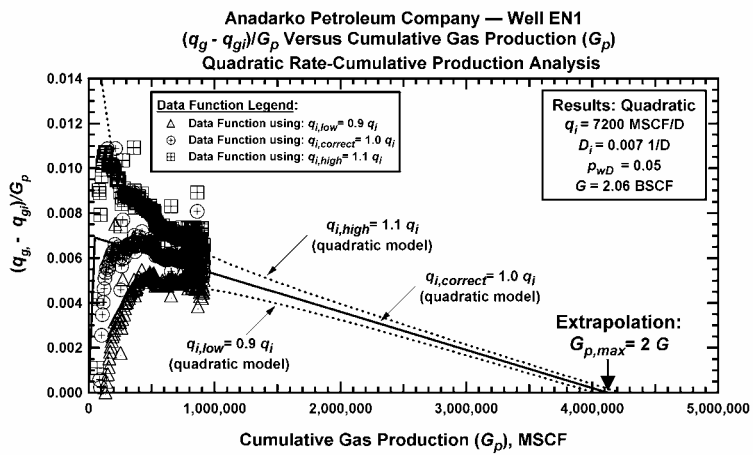


**Figure B-49 – Well EN1 (Anadarko Petroleum Corporation): $(q_{qi}-q_q)/G_p$ versus $G_p$ (Plotting Function 1 ($PF_1$)).**

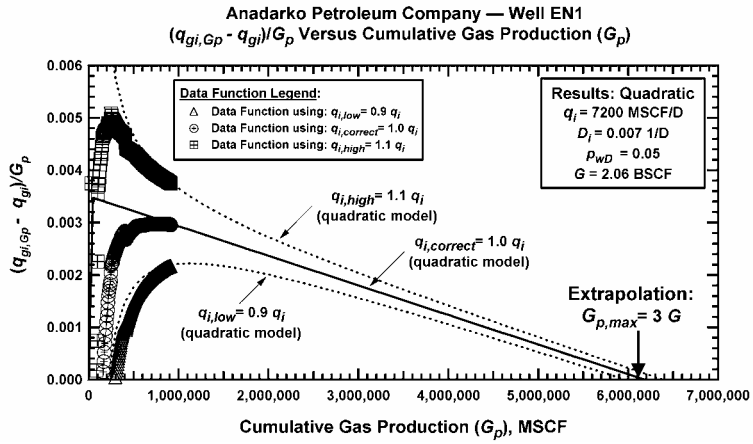


**Figure B-50 – Well EN1 (Anadarko Petroleum Corporation): $(q_{qi}-q_q)/G_p$ versus $G_p$ (Plotting Function 2 ($PF_2$)).**

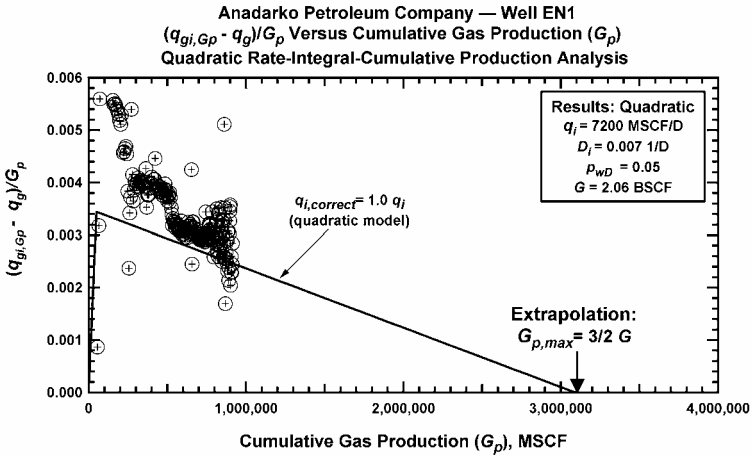


**Figure B-51 – Well EN1 (Anadarko Petroleum Corporation): $(q_{qi,Gp}-q_q)/G_p$ versus $G_p$ (Plotting Function 3 ($PF_3$)).**

**Case 7: Anadarko Petroleum Corporation — Well Rogers**

This case is taken from the same reservoir as case 4 (*i.e.*, Anadarko Well DV4) — no reservoir description is available for this case. Comparison of the results for Well Rogers and Well DV4 suggests that Well Rogers is either located in a much smaller "compartment" of the reservoir or the well completion for Well Rogers is much less efficient that that for Well DV4 — or both.

**Case 7: (input data) Anadarko Petroleum Corporation — Well Rogers**

Reservoir Properties:

| | |
|---|---|
| Wellbore radius, $r_w$ | = 0.333 ft |
| Average net pay thickness, $h$ | = 180 ft |
| Average Porosity, $\phi$ | = 0.08 (fraction) |
| Irreducible water saturation, $S_{wi}$ | = 0.25 (fraction) |
| Initial reservoir pressure, $p_i$ | = 12,200 psia |

Fluid properties:

| | |
|---|---|
| Gas specific gravity, $\gamma_g$ | = 0.625 (air=1) |
| Mole Percent $CO_2$ | = 2.0 percent |
| Reservoir Temperature | = 380 deg F |

Production parameters:

| | |
|---|---|
| Tubing length, $L$ | = 14,000 ft |
| Inside tubing diameter, $d_i$ | = 1.995 in |
| Bottomhole flowing pressure, $p_{wf}$ | = 500 psia (constant) |

**Case 7: (results) Anadarko Petroleum Corporation — Well Rogers**

New "quadratic analysis" methods:

| | |
|---|---|
| Initial gas production rate, $q_{gi}$ | = 300 MSCF/D |
| Decline constant, $D_i$ | = 0.0023 1/D |
| Dimensionless pressure, $p_{wD}$ | = 0.05 |
| Gas-in-place, $G$ | = 0.262 BSCF |

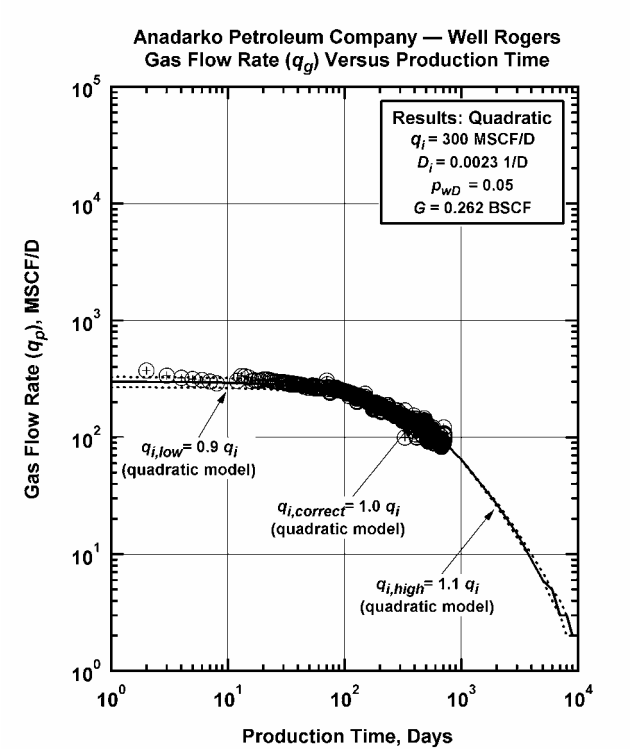


**Figure B-52 – Well Rogers (Anadarko Petroleum Corporation): $q_g$ versus $t$.**

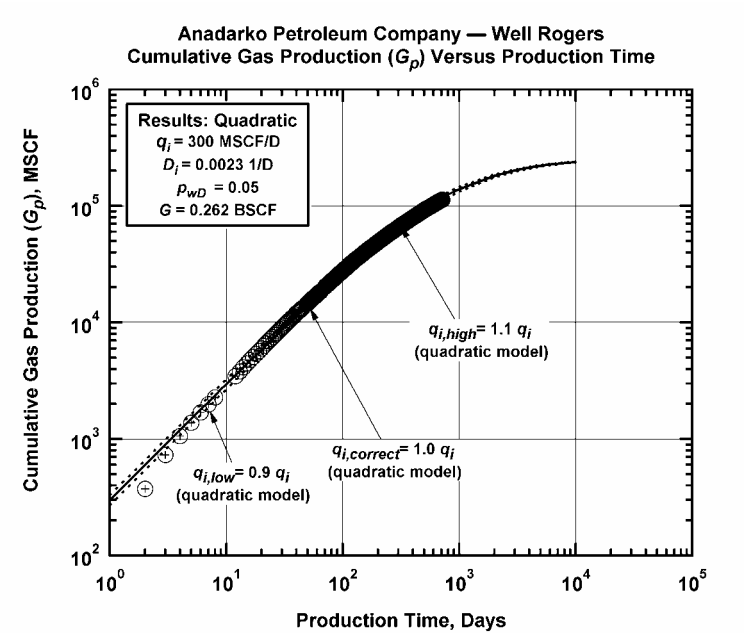


**Figure B-53 – Well Rogers (Anadarko Petroleum Corporation): $G_p$ versus $t$.**

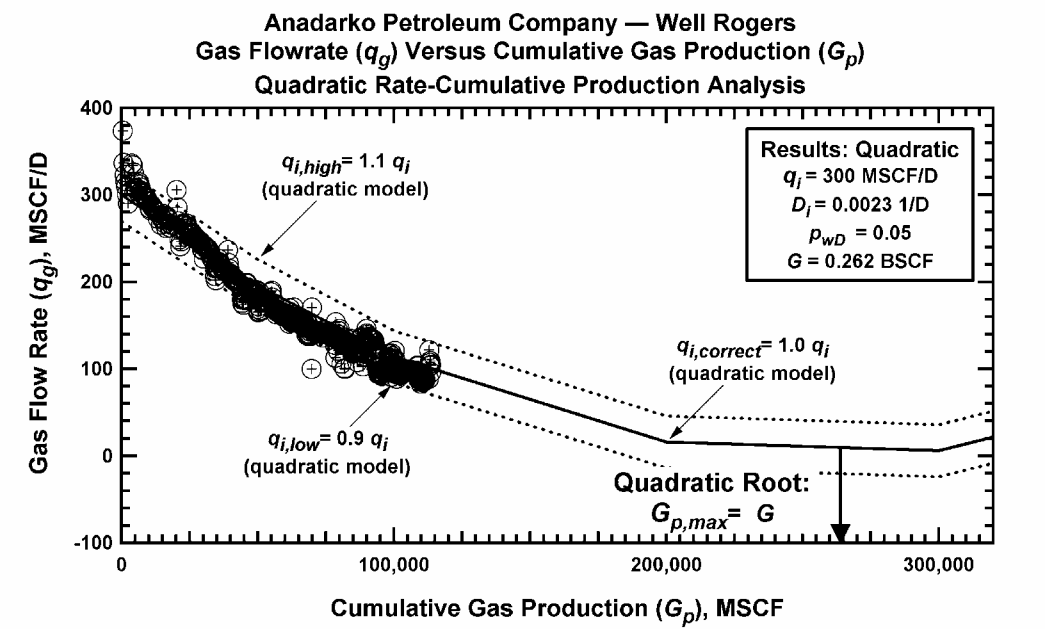


**Figure B-54 – Well Rogers (Anadarko Petroleum Corporation): $q_g$ versus $G_p$.**

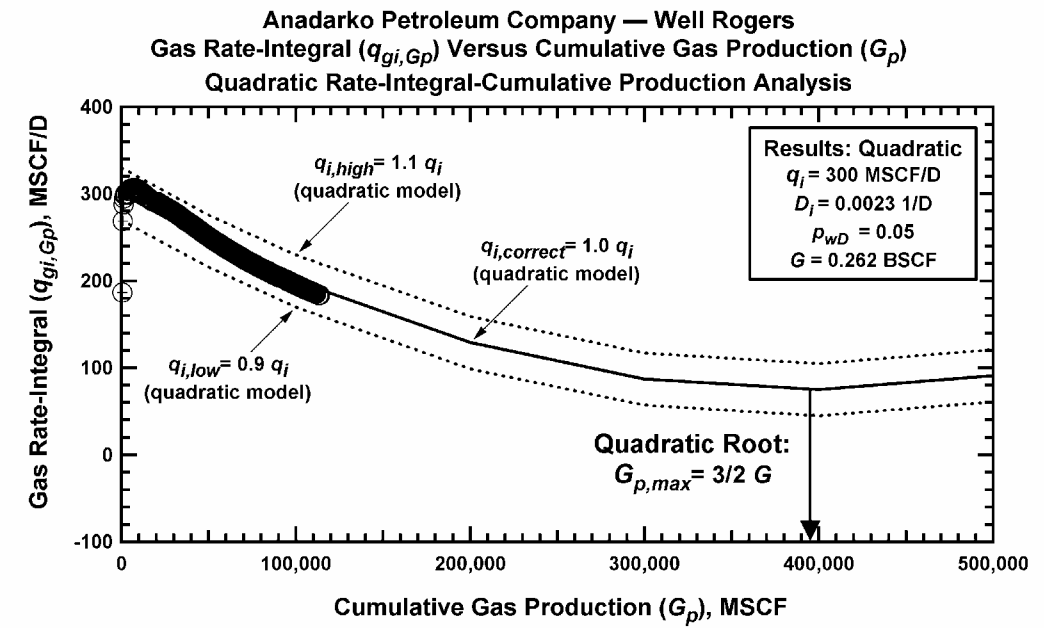


**Figure B-55 – Well Rogers (Anadarko Petroleum Corporation): $q_{qi,Gp}$ versus $G_p$.**

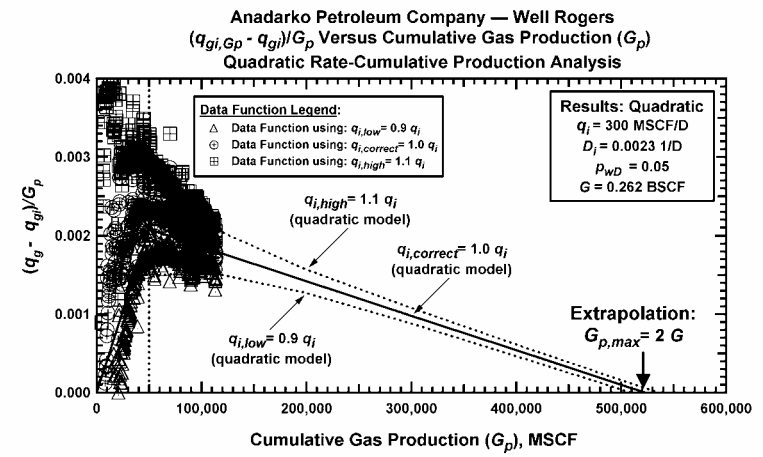


**Figure B-56 – Well Rogers (Anadarko Petroleum Corporation): $(q_{qi}-q_q)/G_p$ versus $G_p$ (Plotting Function 1 ($PF_1$)).**

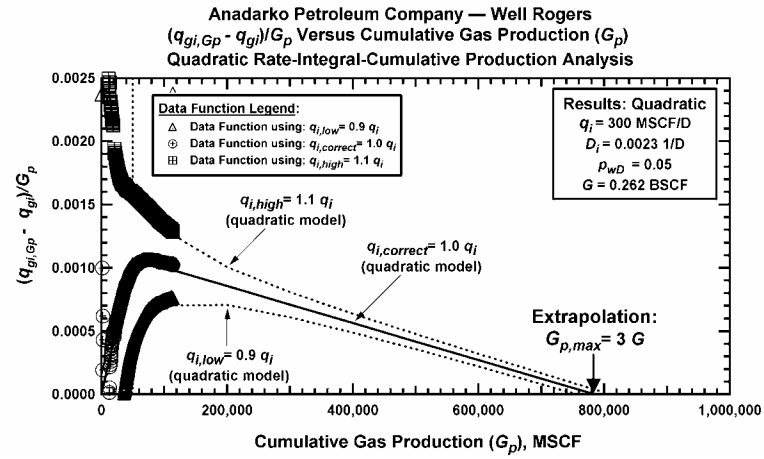


**Figure B-57 – Well Rogers (Anadarko Petroleum Corporation): $(q_{qi}-q_q)/G_p$ versus $G_p$ (Plotting Function 2 ($PF_2$)).**

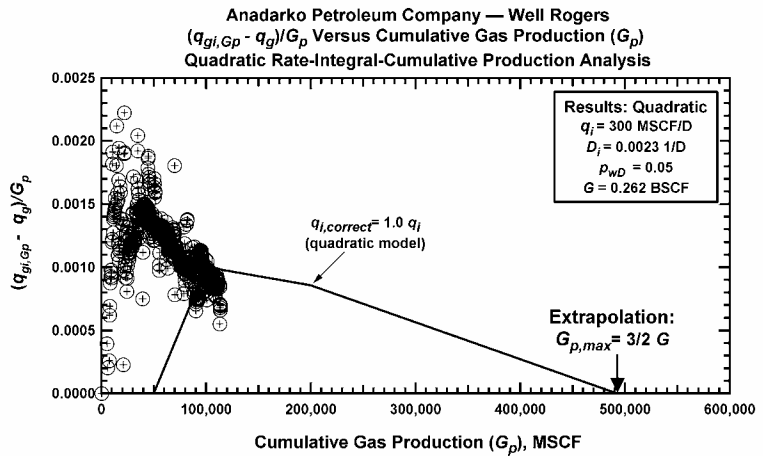


**Figure B-58 – Well Rogers (Anadarko Petroleum Corporation): $(q_{qi,Gp}-q_q)/G_p$ versus $G_p$ (Plotting Function 3 ($PF_3$)).**

**Case 8: Santos — Well SNBL**

This case is taken from the same reservoir as case 4 (*i.e.*, Anadarko Well DV4) — no reservoir description is available for this case.

**Case 8: (input data) Santos — Well SNBL**

Reservoir Properties:

| | |
|---|---|
| Wellbore radius, $r_w$ | = 0.333 ft |
| Average net pay thickness, $h$ | = 55 ft |
| Average Porosity, $\phi$ | = 0.118 (fraction) |
| Irreducible water saturation, $S_{wi}$ | = 0.252 (fraction) |
| Initial reservoir pressure, $p_i$ | = 4620 psia |

Fluid properties:

| | |
|---|---|
| Gas specific gravity, $\gamma_g$ | = 0.85 (air=1) |
| Mole Percent $CO_2$ | = 25 percent |
| Mole Percent $H_2S$ | = 0.7 percent |
| Reservoir Temperature | = 286 deg F |

Production parameters:

| | |
|---|---|
| Tubing length, $L$ | = 10,351 ft |
| Inside tubing diameter, $d_i$ | = 2.441 in |
| Bottomhole flowing pressure, $p_{wf}$ | = varies |

**Case 8: (results) Santos — Well SNBL**

New "quadratic analysis" methods:

| | |
|---|---|
| Initial gas production rate, $q_{gi}$ | = 1800 MSCF/D |
| Decline constant, $D_i$ | = 0.0055 1/D |
| Dimensionless pressure, $p_{wD}$ | = 0.13 |
| Gas-in-place, $G$ | = 0.67 BSCF |

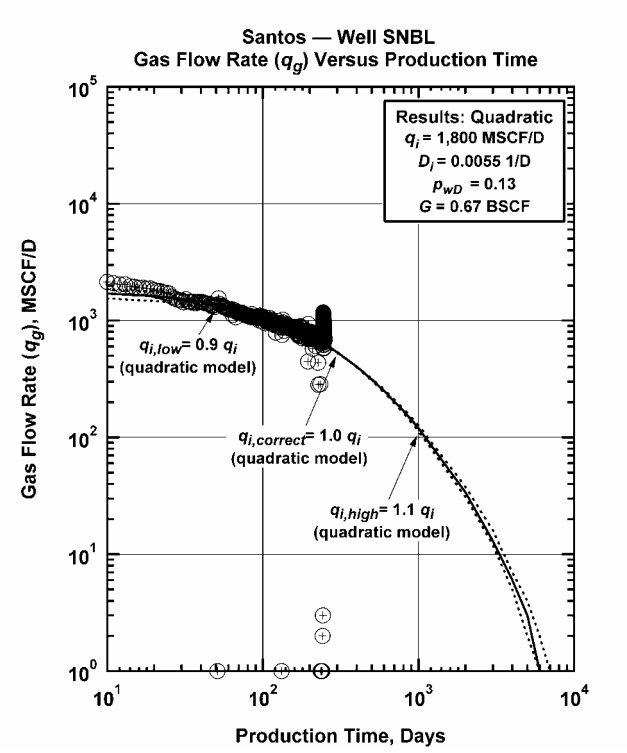


**Figure B-59 – Well SNBL (Santos): $q_g$ versus $t$.**

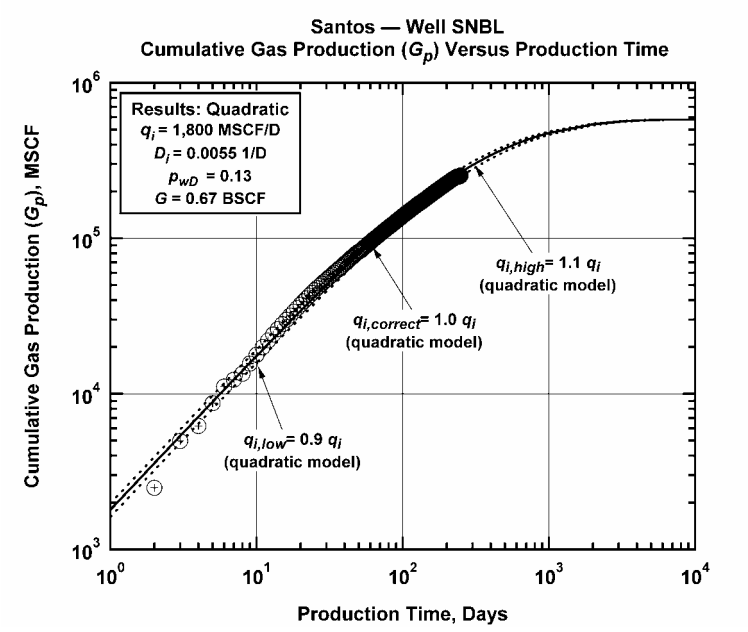


**Figure B-60 – Well SNBL (Santos): $G_p$ versus $t$.**

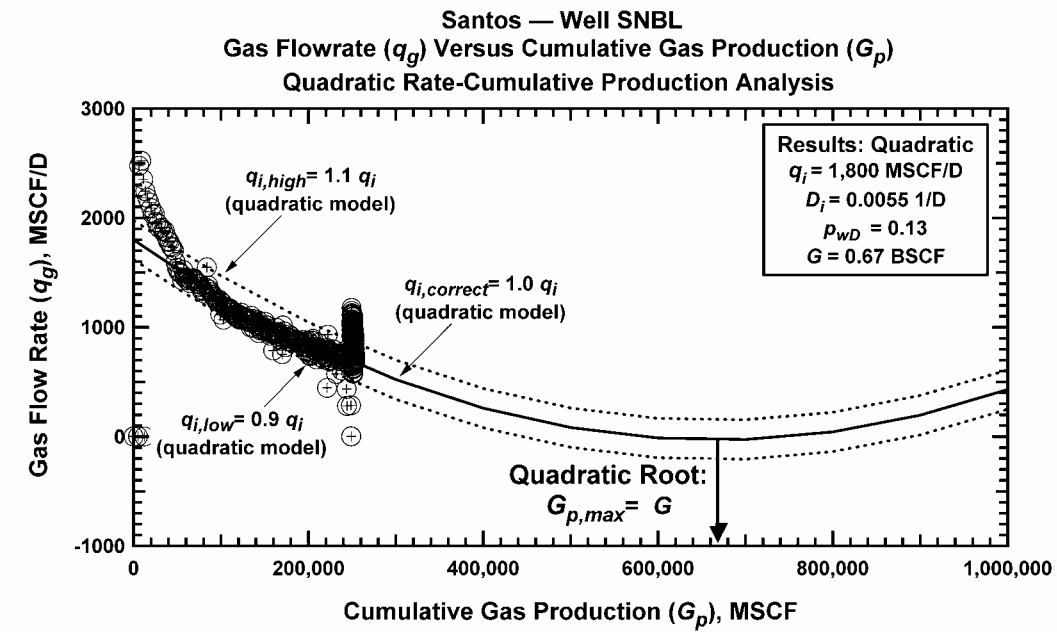


**Figure B-61 – Well SNBL (Santos): $q_g$ versus $G_p$.**

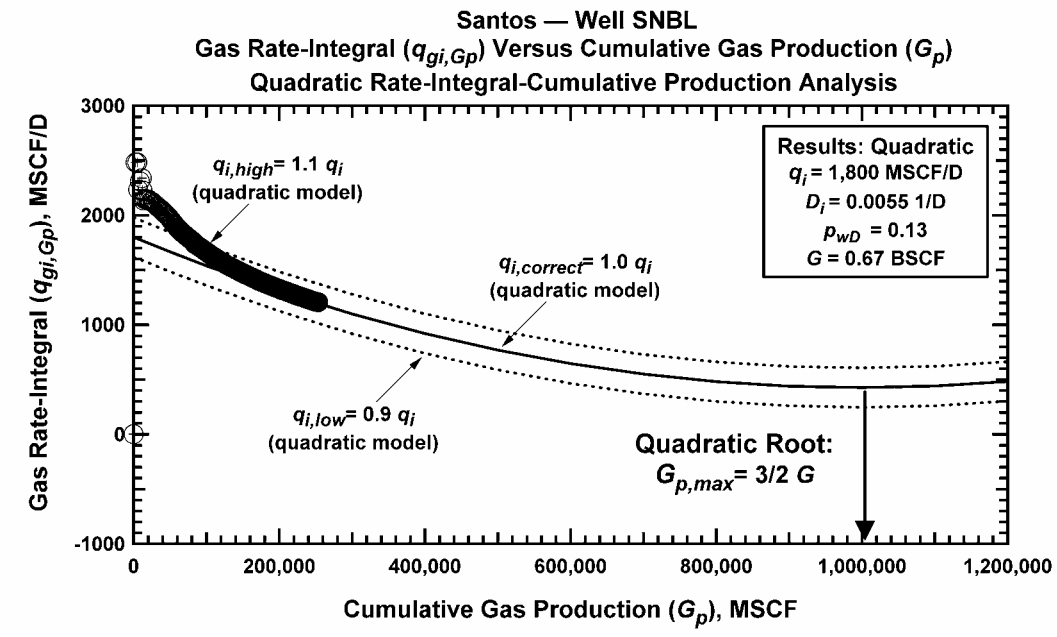


**Figure B-62 – Well SNBL (Santos): $q_{qi,Gp}$ versus $G_p$.**

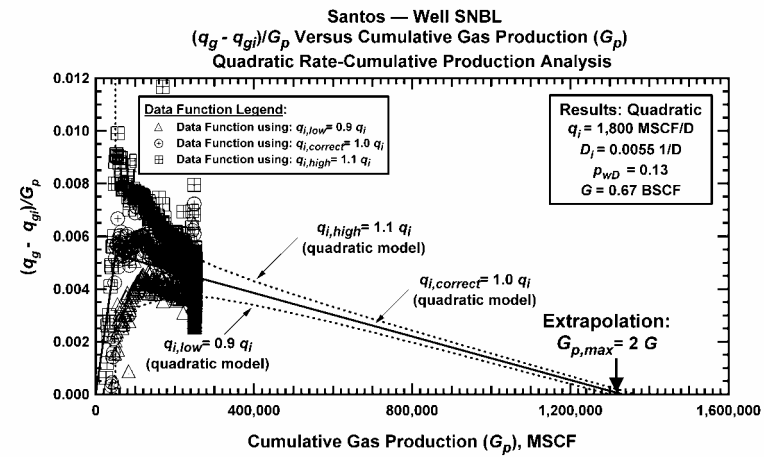


**Figure B-63 – Well SNBL (Santos): $(q_{qi}-q_q)/G_p$ versus $G_p$ (Plotting Function 1 ($PF_1$)).**

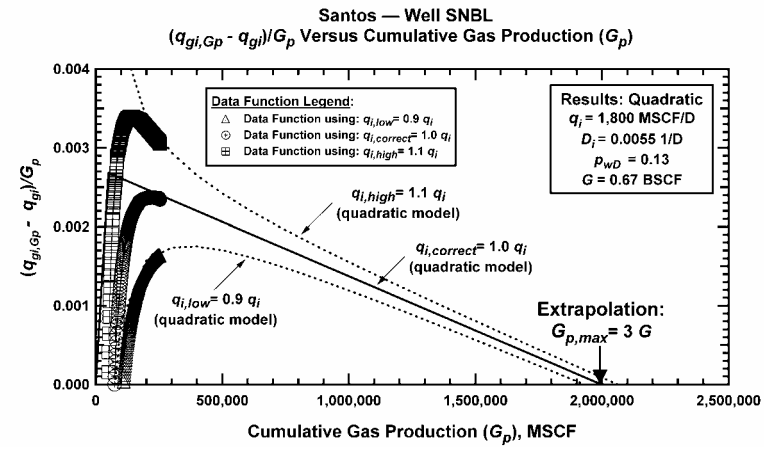


**Figure B-64 – Well SNBL (Santos): $(q_{qi}-q_q)/G_p$ versus $G_p$ (Plotting Function 2 ($PF_2$)).**

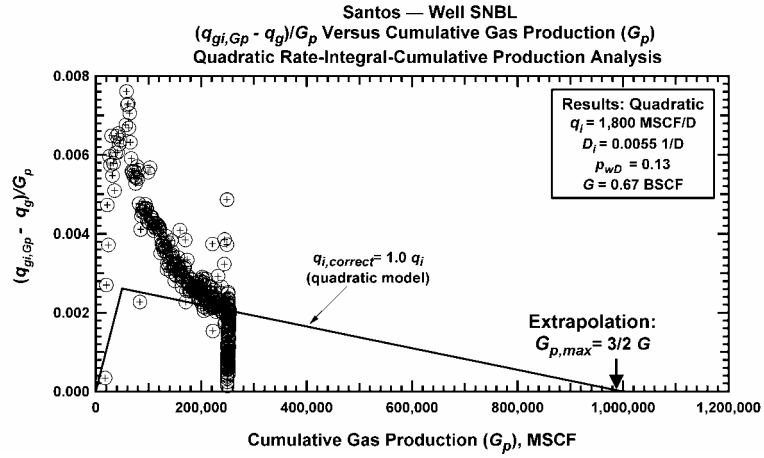


**Figure B-65 – Well SNBL (Santos): $(q_{qi,Gp}-q_q)/G_p$ versus $G_p$ (Plotting Function 3 ($PF_3$)).**

**Case 9: Company X — Well X**

The operator of this field has requested anonymity — we are permitted to describe this as a low permeability "sand-shale" reservoir with several hundred active wells. We have used this example to illustrate the utility of our proposed method on a "poor" quality reservoir case.

**Case 9: (input data) Company X — Well X**

Reservoir Properties:

| | |
|---|---|
| Wellbore radius, $r_w$ | = 0.333 ft |
| Average net pay thickness, $h$ | = 100 ft |
| Average Porosity, $\phi$ | = 0.25 (fraction) |
| Irreducible water saturation, $S_{wi}$ | = 0.20 (fraction) |
| Initial reservoir pressure, $p_i$ | = 4000 psia |

Fluid properties:

| | |
|---|---|
| Gas specific gravity, $\gamma_g$ | = 0.65 (air=1) |
| Reservoir Temperature | = 200 deg F |

Production parameters:

| | |
|---|---|
| Tubing length, $L$ | = 5000 ft |
| Inside tubing diameter, $d_i$ | = 2.441 in |
| Bottomhole flowing pressure, $p_{wf}$ | = varies |

**Case 9: (results) Company X — Well X**

New "quadratic analysis" methods:

| | |
|---|---|
| Initial gas production rate, $q_{gi}$ | = 535 MSCF/D |
| Decline constant, $D_i$ | = 0.00082 1/D |
| Dimensionless pressure, $p_{wD}$ | = 0.05 |
| Gas-in-place, $G$ | = 1.31 BSCF |

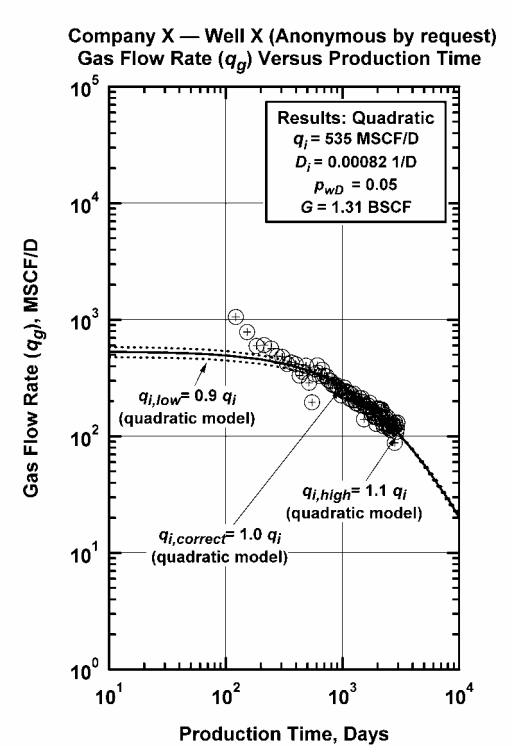


**Figure B-66 – Well X (Company X): $q_g$ versus $t$.**

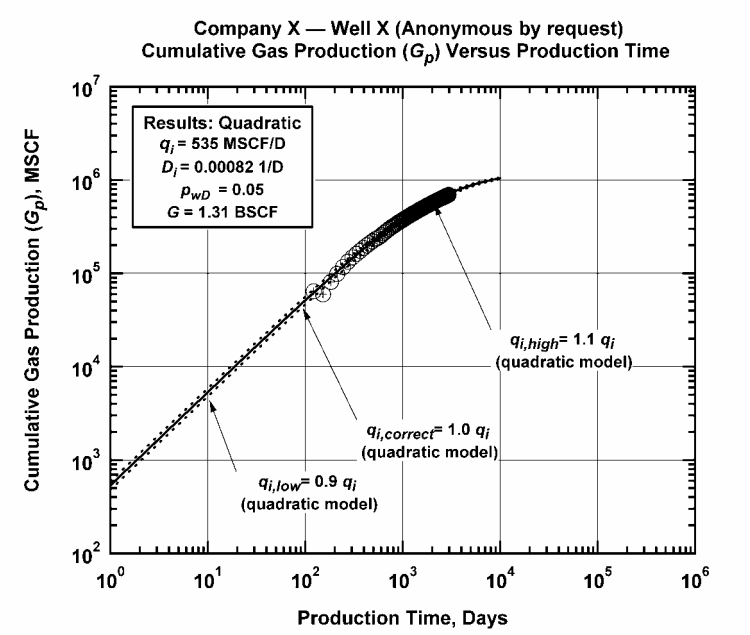


**Figure B-67 – Well X (Company X): $G_p$ versus $t$.**

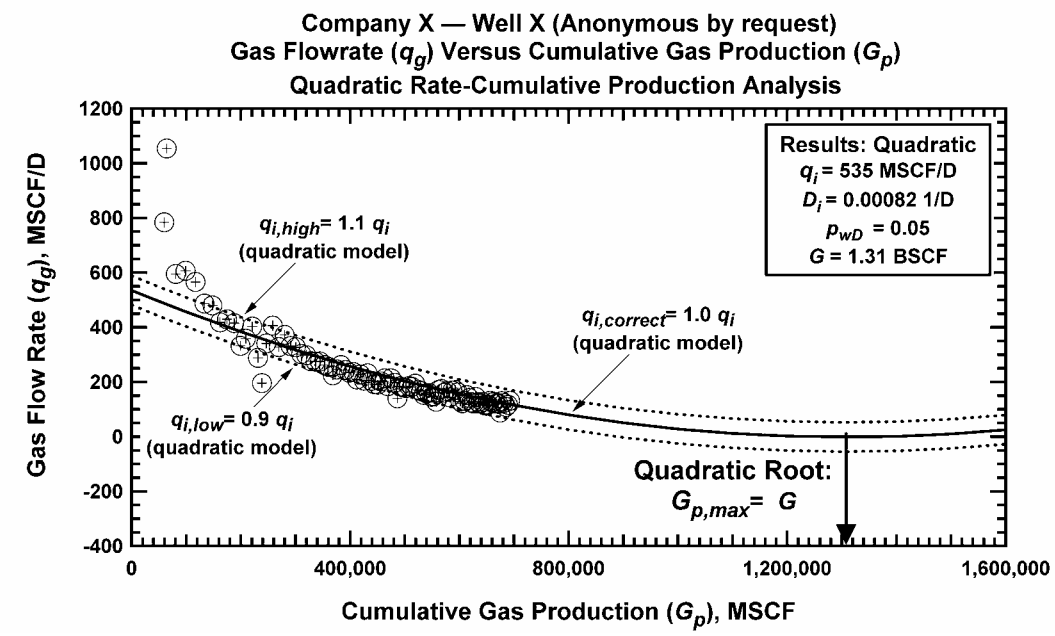


**Figure B-68 – Well X (Company X): $G_p$ versus $t$.**

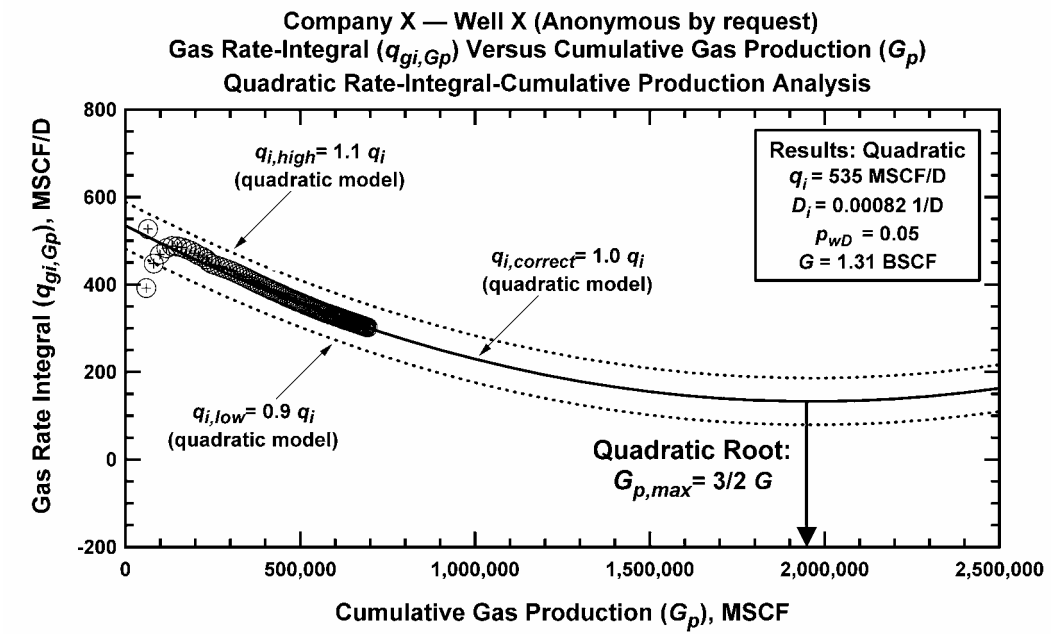


**Figure B-69 – Well X (Company X): $q_{qi,Gp}$ versus $G_p$.**

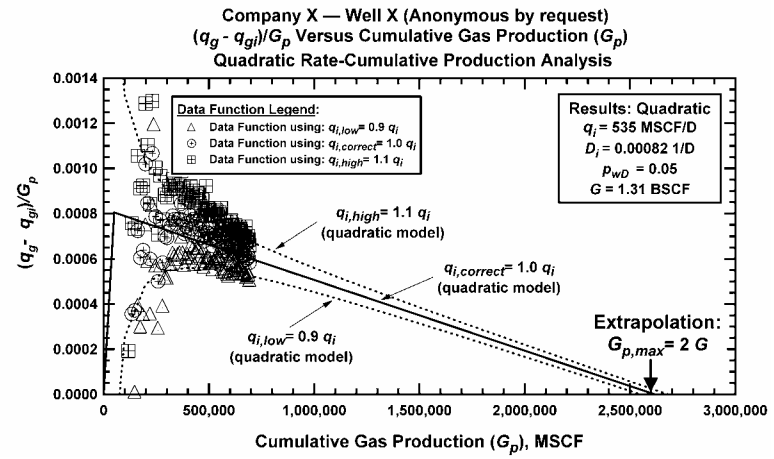


**Figure B-70 – Well X (Company X): $(q_{qi}-q_q)/G_p$ versus $G_p$ (Plotting Function 1 ($PF_1$)).**

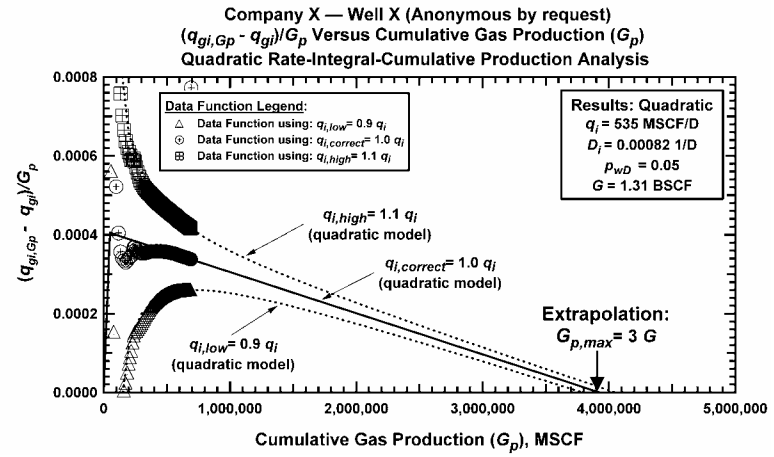


**Figure B-71 – Well X (Company X): $(q_{qi}-q_q)/G_p$ versus $G_p$ (Plotting Function 2 ($PF_2$)).**

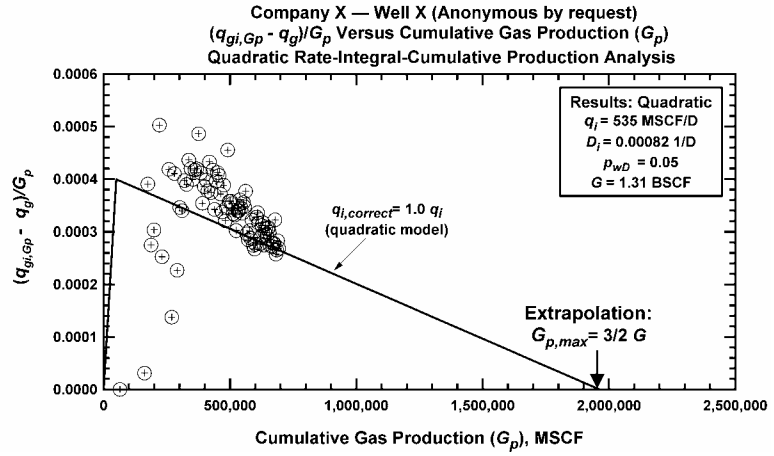


**Figure B-72 – Well X (Company X): $(q_{qi,Gp}-q_q)/G_p$ versus $G_p$ (Plotting Function 3 ($PF_3$)).**

# APPENDIX C
# DERIVATION OF THE "QUADRATIC" PLOTTING FUNCTIONS FOR THE ANALYSIS OF PRODUCTION DATA

Starting from the Knowles[1] results (*i.e.*, the generalized dimensionless rate-time and pressure-time relations) we have:

$$p_D = p_{wD}\left[\frac{1+\left[\frac{1-p_{wD}}{1+p_{wD}}\right]\exp(-p_{wD}\,t_{Dd})}{1-\left[\frac{1-p_{wD}}{1+p_{wD}}\right]\exp(-p_{wD}\,t_{Dd})}\right] \quad \text{.....(C-1)}$$

$$q_{Dd} = \frac{p_{wD}^{\,2}}{(1-p_{wD}^{\,2})}\left[\left[\frac{1+\left[\frac{1-p_{wD}}{1+p_{wD}}\right]\exp(-p_{wD}\,t_{Dd})}{1-\left[\frac{1-p_{wD}}{1+p_{wD}}\right]\exp(-p_{wD}\,t_{Dd})}\right]^2 - 1\right] \quad \text{.....(C-2)}$$

Where the dimensionless pressure is defined as

$$p_{wD} = \frac{\bar{p}/\bar{z}}{p_i/z_i} \quad \text{..... (C-3)}$$

And the dimensionless time for the rate-time relation for ($p_{wf} \neq 0$) is given as

$$t_{Dd} = \frac{2\,q_i t}{(1-p_{wD}^{\,2})G} \quad \text{.....(C-4)}$$

The definition of dimensionless rate is given as

$$q_{Dd} = \frac{q_g}{q_{gi}} \quad \text{.....(C-5)}$$

Where the "initial rate" estimated is: (using the $p^2$ case)

$$q_{gi} = 0.7026\frac{kh}{T}\frac{1}{\left[\ln\left[\frac{r_e}{r_{wa}}\right]-\frac{3}{4}\right]}\left[\frac{z_i}{p_i\,\mu_{gi}\,c_{gi}}\right]\left[\left[\frac{p_i}{z_i}\right]^2-\left[\frac{p_{wf}}{z_{wf}}\right]^2\right] \quad \text{.....(C-6)}$$

The material balance relation for this case is given as:

$$\frac{\bar{p}}{\bar{z}} = \frac{p_i}{z_i}\left[1-\frac{G_p}{G}\right] \quad \text{.....(C-7)}$$

Defining the dimensionless cumulative production:

$$G_{pDd} = \frac{G_p}{G} \quad \text{.....(C-8)}$$

Substituting the dimensionless pressure relation (Eq. C-3) into the material balance expression (Eq. C-7) and correlating with the definition of dimensionless cumulative production (Eq. C-8), we have:

$$G_{pDd} = 1 - p_D \quad \text{.....(C-9)}$$

Recalling the Knowles generalized dimensionless pressure relation (Eq. C-1) and substituting this relation into Eq. C-9, we have:

$$G_{PDd} = 1 - p_D = 1 - p_{wD}\left[\frac{1+\left[\frac{1-p_{wD}}{1+p_{wD}}\right]\exp(-p_{wD}\,t_{Dd})}{1-\left[\frac{1-p_{wD}}{1+p_{wD}}\right]\exp(-p_{wD}\,t_{Dd})}\right] \quad \text{.....(C-10)}$$

Defining a temporary parameter, $\alpha$, we can simplify the expression for the dimensionless cumulative production (Eq. C-10), shown above:

$$\alpha = \left[\frac{1+\left[\frac{1-p_{wD}}{1+p_{wD}}\right]\exp(-p_{wD}\,t_{Dd})}{1-\left[\frac{1-p_{wD}}{1+p_{wD}}\right]\exp(-p_{wD}\,t_{Dd})}\right] \quad \text{.....(C-11)}$$

Substituting the definition of $\alpha$ into Eq. C-11, then solving for the $\alpha$ parameter yields:

$$\alpha = \frac{1}{p_{wD}}(1 - G_{pDd}) \quad \text{.....(C-12)}$$

Substituting the definition of the $\alpha$ coefficient (Eq. C-11) into Eq. C-2,

$$q_{Dd} = \frac{{p_{wD}}^2}{(1-{p_{wD}}^2)}(\alpha^2 - 1) \quad \text{.....(C-13)}$$

Squaring Eq. C-12 — i.e., to yield the $\alpha^2$-term, we have

$$\alpha^2 = \frac{1}{{p_{wD}}^2}(1 - 2G_{pDd} + G_{pDd}^2) \quad \text{.....(C-14)}$$

Substituting Eq. (C-14) into Eq. C-13 and simplifying, the final form of the dimensionless rate-cumulative production quadratic expression is given by:

$$q_{Dd} = \frac{{p_{wD}}^2}{(1-{p_{wD}}^2)}\left[\frac{1}{{p_{wD}}^2}(1 - 2G_{pDd} + {G_{pDd}}^2) - 1\right]$$

$$= \frac{1}{(1-{p_{wD}}^2)}\left[(1-{p_{wD}}^2) - 2G_{pDd} + {G_{pDd}}^2\right]$$

Or, finally, we have:

$$q_{Dd} = 1 - \frac{2}{(1-{p_{wD}}^2)}G_{pDd} + \frac{1}{(1-{p_{wD}}^2)}{G_{pDd}}^2 \quad \text{.....(C-15)}$$

Substituting the definition of $q_{Dd}$ and $G_{pDd}$ (Eqs. C-5 and C-8) (respectively) into Eq. C-15, we obtain:

$$q_g = q_{gi} - \frac{2q_i}{(1-{p_{wD}}^2)G}G_p + \frac{q_i}{(1-{p_{wD}}^2)G^2}{G_p}^2 \quad \text{.....(C-16)}$$

Substituting the definition of $p_{wD}$ into Eq. (C-15) yields

$$q_g = q_{gi} - \frac{2q_{gi}}{\left[1-\left[\frac{p_{wf}/z_{wf}}{p_i/z_i}\right]^2\right]G}G_p + \frac{q_{gi}}{\left[1-\left[\frac{p_{wf}/z_{wf}}{p_i/z_i}\right]^2\right]G^2}G_p^2 \quad \text{.....(C-17)}$$

For convenience, we define the dimensionless "decline constant," $D_i$, as:

$$D_i = \frac{2q_{gi}}{\left[1-\left[\frac{p_{wf}/z_{wf}}{p_i/z_i}\right]^2\right]G} \quad \text{.....(C-18)}$$

Substitution of the definition of the dimensionless "decline constant," $D_i$, into Eq. C-18 yields:

$$q = q_{gi} - D_i G_p + \frac{1}{2}\frac{D_i}{G}{G_p}^2 \quad \text{.....(C-19)}$$

Dividing Eq. (C-19) through by $G_p$ and rearranging this results into a straight-line formulation yields our definition of "Plotting Function 1" (or $PF_1$). This result is given as:

$$\frac{q_{gi}-q_g}{G_p} = D_i - \frac{1}{2}\frac{D_i}{G}G_p \quad \text{.....(C-20)}$$

Recalling the definition of the "cumulative production aver-aged rate function," $(q_g)_{i,\,Gp}$, we have:

$$(q_g)_{i,Gp} \equiv \frac{1}{G_p}\int_0^{G_p} q_g\, dG_p \quad \text{.....(C-21)}$$

Integrating Eq. C-19 with respect to $G_p$, then dividing through by $G_p$, yields:

$$(q_g)_{i,G_p} \equiv q_{gi} - \frac{D_i}{2}G_p + \frac{1}{6}\frac{D_i}{G}{G_p}^2 \quad \text{.....(C-22)}$$

Subtracting $q_{gi}$ from both sides of Eq. C-22 and dividing through by $G_p$ yields:

$$\frac{(q_g)_{i,Gp}-q_{gi}}{G_p} = \frac{1}{2}D_i - \frac{1}{6}\frac{D_i}{G}G_p \quad \text{.....(C-23)}$$

Where Eq. C-23 provides our definition of "Plotting Function 2" (or $PF_2$). We immediately note the similarities in Eqs. C-20 and C-23 ($PF_1$ and $PF_2$, respectively), and comment that both are linear trends, and only differ by the "slope" and "intercept" terms.

Specifically, the extrapolation of Eq. C-20 to $(q_{gi}-q_g)/G_p = 0$ yields $G_{p,ext}=2\,G$. Similarly, the extrapolation of Eq. C-23 to $((q_g)_{i,\,Gp}-q_{gi})/G_p = 0$ yields $G_{p,ext}=3\,G$.

We can also construct a final plotting function — Plotting Function 3" (or $PF_3$), which is defined using the $(q_g)_{i,\,Gp}$ and the $q_g$ data functions.

The advantage of $PF_3$ is that it does not require knowledge of $q_{gi}$ — however, a disadvantage of this approach is that since the $q_g$ data function is used, the $PF_3$ trend mimics any erroneous behavior in the $q_g$ data function.

Subtracting Eq. C-21 from C-22 yields $PF_3$:

$$\frac{(q_g)_{i,Gp} - q_g}{G_p} = \frac{1}{2} D_i - \frac{1}{3} \frac{D_i}{G} G_p \quad \text{.....(C-24)}$$

The extrapolation of Eq. C-24 to $((q_g)_{i,\,Gp}\text{-}q_g)/G_p = 0$ yields $G_{p,ext}=3/2\,G$.

# VITA


| | |
|---|---|
| Name: | Ibrahim Muhammad Buba |
| Born: | 31 August 1976<br>Gwoza, Nigeria |
| Permanent Address: | 4 "Marais" Bolton Road<br>Grove Park, Chiswick<br>London W43TE<br>United Kingdom<br>(i_buba@hotmail.com) |
| Education: | University of Bath, Bath (UK)<br>Bachelor of Engineering Degree in Chemical Engineering<br>July 1999 |
| | Texas A&M University, College Station, Texas, USA<br>Master of Science Degree in Petroleum Engineering<br>August 2003 |